# DEVELOPMENT OF LARVAL PHOTOBEHAVIOUR AS A PARADIGM TO IDENTIFY MUTATIONS THAT AFFECT NERVOUS SYSTEM DEVELOPMENT AND FUNCTION

By

Balaji G. Iyengar

A Thesis

Submitted to the School of Graduate Studies

in Partial Fulfilment of the Requirements for the Degree

Doctor of Philosophy

McMaster University

# *DROSOPHILA* LARVAL PHOTOBEHAVIOUR – A NEUROGENETIC PLATFORM

**Doctor of Philosophy (2002)**

**(Biology)**

**McMaster University, Hamilton, Ontario**

**Title: DEVELOPMENT OF LARVAL PHOTOBEHAVIOUR AS A PARADIGM TO IDENTIFY MUTATIONS THAT AFFECT NERVOUS SYSTEM DEVELOPMENT AND FUNCTION**

**Author:** Balaji G. Iyengar

**Supervisor:** Dr. Ana Regina Campos

**Number of Pages:** xvii, 227

**Abbreviations:** CNS – Central nervous system, PNS – peripheral nervous system, mtDNA - mitochondrial DNA, PolG or *pol* $\gamma$-$\alpha$ - mitochondrial DNA polymerase $\gamma$-$\alpha$, *pol* $\gamma$-$\beta$ - mitochondrial DNA polymerase $\gamma$-$\beta$, UAS – Upstream activation sequence.

## Abstract

In *Drosophila* neurogenetics, one uses mutational approaches to dissect the function and development of the nervous system. This approach has been very successful in the isolation of many single gene mutations that affect adult fly behaviour. However, it has been estimated that 30-50% of all genes in *Drosophila* mutate to result in adult inviability. This encouraged us to consider the larval stage as a platform for identifying mutations that affect the nervous system through the use of larval behaviour assays.

A part of this thesis describes the design, standardization and demonstration of behaviour assays. The assays employed both a population of animals and individual larva to study their response to light. Using these assays we screened a collection of mutagenized recessive lethal strains to identify new genes that affect nervous system function. The development of these assays enabled the demonstration that larval visual system uses many of the same genes that participate in the transduction of light in the adults. Lack of response to light after genetic ablation of larval photoreceptors was also demonstrated.

A partial automation of one of the individual larval assays was also established. Using this, an expeditious screening of 50 mutant lines was carried out. This pilot screen

resulted in the isolation of candidate lines that show defects in larval photo-response and locomotion.

This study also focused on a single behavioural mutant line and called *tamas*. Through genetic analysis and direct sequencing of pre-existing alleles that belong to this locus it was determined that the *tamas* gene codes for mitochondrial DNA polymerase catalytic subunit (*tamas/pol* $\gamma$-$\alpha$/POLG). Mutations in this gene caused defects in nervous system development and locomotory behaviour. We also carried out phenotypic analysis of mutants with lesion in the gene that codes the accessory subunit of the mtDNA polymerase (*pol* $\gamma$-$\beta$). Pre-existing alleles in this gene were identified first through genetic analysis, next, through direct sequencing the mutations in this gene were confirmed. These experiments constituted the first phenotypic analysis of mutants in the mitochondrial DNA polymerase for any metazoan.

## Acknowledgements

Long before I underwent delamination to Canada, I remember and appreciate the patterning effort that was spent on me by my dad. For example, one day he demonstrated the consequence of asymmetrical aerodynamic forces with the help of a housefly. After deftly trapping a housefly, he clipped one of the housefly wings at its distal tip and placed it on the ground. The poor beast would flip over every time it attempted a take-off. Next, he grabbed it again and carefully made a similar clip on the other intact wing, and voila! it vanished into thin air!! As I near the completion of this dissertation towards a Ph.D. degree, I wonder if he knew how much I appreciate his influence on me.

How I wish he was around...

There are several other personalities whom I wish to thank. Call them maternal contribution, numerous long-range and short-range diffusible signals and some crucial cellular neighbours whose inputs among other signals kept me transcriptionally active.

First, my journey towards a possible neural fate continues through my mom's care and support. Without her, I would have drifted away and taken part in the head involution process and be destined to become a part of the boring foregut.

Next, my supervisor Dr. Ana Regina Campos, has been singularly crucial in my further specification, consistent with the role of *ana* in suppressing neuroblast

proliferation perhaps! Without her continued Wng signal as well on the antero-posterior axis, or in other words allowing me to pursue the study of larval behaviour, none of this work would have been possible. I thank her for the opportunity, for everything she has contributed towards my progress in academia and for helping me adjust to life in a new country.

I also thank Roger Jacobs, Dick Morton and Colin Nurse for valuable discussions and advice throughout the course. Perhaps, their inputs were of the Spitz and EGFR class, along the dorso-ventral axis. This I suppose completes the basic "positional information" that I think has been vital to my differentiation tragectory.

I would like to thank my ex-domain mates Mahua Mukhopadhyay for showing me the ropes when I started and Peter Pelka for the technical tips, discussions and many intense chess games. Thanks "desousd" for being a great friend both academically and otherwise, interactions with Dorothy Desousa made many an experimental rut transient. I was also delighted to have interacted with so many other "Fly-Pushers" who passed by the 5$^{th}$ floor, of note Maria Papaconstantinou. They gave me the opportunity to discuss science of the lighter kind. During the many years we also covered almost every aspect of life in the universe through sometimes serious and often entertaining discussions.

Finally, I thank my wife for being equivalent to the extra-cellular matrix, arranging all the "signalosomes" in 3-D space is so much easier and meaningful with her in my life.

Last but not the least, I appreciate all the support I have received from my relatives in taking care of my parents when they needed it most.

## Table of contents

## List of Figures:

### Chapter 1.



### Chapter 4.

## Chapter 5 A.

## Chapter 5 B.

**List of tables:**

# Chapter 1

## Introduction - Genes, development and behaviour

## Introduction

Perception of external sensory stimuli and generation of a physiological or organismal response is a unifying feature of all cellular life forms. Unraveling the molecular underpinnings of the machinery that receives, processes and responds to sensory or extracellular information is a common theme in modern biology. In studying metazoans this theme has become central to embryonic development and nervous system function.

In the last two decades both the aforementioned areas have benefited greatly by adopting molecular genetic strategies. These include approaches that begin from a mutant phenotype and reveal the nature of the underlying mutation using genetic analysis. Alternatively, one can also start with a known gene and ask what phenotype will ensue when the gene is mutated or misexpressed. As an example, these methods of analysis have been especially effective towards dissecting the complex genetic interactions that govern embryonic development in *Drosophila*. The knowledge gained from this model system has been particularly useful in identifying similar developmental pathways that use homologous molecular entities in the development of diverse body plans in the animal kingdom (Veraksa et al. 2000, Thomas and Wasserman 1999).

As we enter the new millennium we have amassed databases comprised of the almost complete genomic sequences of many model eukaryotes (URL: http://iubio.bio.indiana.edu/eugenes/). We have also begun to assemble and compare proteomes of various eukaryotes. Such an integrated approach will allow us to identify many molecules that control the regulation of common eukaryotic cellular behaviours (Weng et al. 1999, Rubin et al. 2000). For example, it is now possible to define a "core proteome" as a set of non-redundant protein families that are shared between various organisms like yeast, *C. elegans* and the *Drosophila.* Although the core proteome comparison between flies and *C. elegans* does not reveal significant differences, the number of multidomain proteins in *Drosophila* has been reported to be greater in number and more varied than that of the *C. elegans* (Rubin et al. 2000). This perhaps is indicative of the developmental complexity of *Drosophila* as compared to *C. elegans*.

Our understanding of embryonic development of various tissues in *Drosophila* has rapidly progressed in the last decade. This will be accelerated further with the use of genome databases. How can we use this knowledge to dissect the role of neuronal networks that generate various behaviours? I attempt to address this question in this introduction.

**Fixed action patterns and genes**

How does a nervous system mediate behavioural adaptation to an environmental niche after its embryonic development is accomplished? In order to appreciate this question it is useful to consider the following quote: *"One fundamental task of the nervous system is to carry out an adaptive perceptual categorization in an unlabelled world – one in which the macroscopic order and arrangement of objects and events cannot be prefigured for an organism"* – Edelman 1989. In comparison, during the development of the nervous system, most of the connectivity is orchestrated by a genetic program that responds to extracellular molecular cues (Goodman & Shatz 1993). The behavioural outcome of this relatively invariant developmental process can result in stereotypic motor patterns that do not require an environmental trigger. Fixed-action patterns can also be triggered by an external stimulus to result in a species-specific behaviour pattern, for example, courtship behaviour of *Drosophila*, brooding behaviour in birds triggered by eggs. Hence, innate behaviours like locomotion, prey avoidance and courtship behaviours are considered to be "hardwired" into the nervous system through the genetic and developmental programme (Haverkamp 1986; Haverkamp & Oppenheim 1986). These behaviours and their genetic basis must have been reinforced through selection due to their absolute requirement for survival.

The *nonA* gene in *Drosophila* is a good example to further elaborate this point. This gene codes for an RNA binding protein and mutations in this gene produces visual deficit and an abnormal courtship song (Rendahl et al. 1992). Demonstrating the species-specific function of this gene, a transgenic *D. melanogaster* expressing a *nonA* gene of *D. virilis* has been shown to result in a courtship song resembling that of *D. virilis* (Campesan *et al.* 2001). Similar modification of species specific circadian behaviour has also been demonstrated using the *period* gene between *D. simulans* and *D. melanogaster* (Wheeler et al. 1991).

An important aspect of the development of behaviour is that they can be influenced by environment. This property can also be viewed as the ability of the nervous system to allow sensory input to alter neural circuits and effect its maturation or modify an earlier pattern. It is important to note that the categorization of innate and learned behaviour is not a strict one. For example, synaptic plasticity has been reported in motor circuits that generate fixed action patterns (Nadim and Manor 2000) and in the development of bird song. Species-specific bird songs are formed in young birds through auditory feedback during a critical period. This process becomes refractory only gradually (reviewed in Brainard and Doupe 2000, Brainard and Doupe 2001). The molecular mechanisms involved in such activity dependent processes are also thought to be the basis of learning and memory (Bailey 1999).

In summary, most fixed action patterns are an immediate outcome of the nervous system development that are unique to various species. Such patterns of species-specific behaviour can be considered to have been established through natural selection. Thus such robust behavioural outputs offer us a platform to describe the behavioural codes in terms of genetic programs.

**Organization of function**

From a functional perspective, how can behavioural codes be organized in a nervous system? Towards answering this question, the nervous system has been described as being organized in a distributed, dedicated or modular network (Dickinson, 1995). In a distributed network, many and the same neurons will participate in the generation of different kinds of behaviour by adopting a different configuration (activity patterns) for each behaviour. For example, it has been shown in *Aplysia* that a distributed form of network generates reflex withdrawal of gills, respiratory pumping, and spontaneous gill contractions (Wu et al. 1994). The authors reported that 70-90% of approximately 300 neurons observed participate in these three behaviours and very few neurons participate exclusively in any one behaviour. The firing patterns of neurons participating in these behaviours are characteristic for each behaviour.

In the dedicated network configuration, each circuit will be responsible for the generation of only one specific kind of behaviour. For example the siphon withdrawal reflex in *Aplysia* has been described to be controlled by a dedicated neural network in the abdominal ganglia (Frost and Kandel 1995). The inhibitory interneuronal connectivities in the abdominal ganglia have been reported to be configured so as to block other inhibitory inputs that can alter the activity of this ganglia. Also very few excitatory inputs were found to enter the abdominal ganglia from other centers.

A global influence on network function or generation of different activity patterns from specific neural assemblies may also be mediated by neuromodulatory factors like neuropeptides and steroid hormones. These factors can alter the synaptic strengths within motor circuits or change ion conductances of neurons to bring about variations in network outputs. For example, the stomatogastric ganglion of lobster undergo extensive alterations in synaptic organization in response to neuromodulatory factors like serotonin (Peck et al. 2001).

Is the behaviour code represented in the nervous system's connectivity pattern? From a connectionist point of view the functional capability of nervous systems may be mainly attributed to its wiring scheme. One of the central problems of developmental neurobiology is to understand how neurons form connections with each other and with other targets in a stereotypic manner. Many studies have concluded that this "ground-

plan" is largely encoded in the genome of the organism. This is apparent through numerous reports that have dissected the formation of neuronal connectivity using a mutational approach (Klambt et al. 1991, Vactor et al. 1993, Tear et al. 1993, Seeger et al. 1993, Salzberg et al. 1994, Taniguchi et al. 1997, Saueressig et al. 1999, Beattie et al. 2000, Kraut et al. 2001). The *Drosophila* model system has been at the forefront of such efforts.

**Genetic analysis of nervous system development and connectivity formation**

The embryonic nervous system can be considered to be designed primarily in *Drosophila* to mediate the burrowing and feeding lifestyle of the larva. At the morphological level the mature larval nervous system consists of the ventral cord and the central brain hemisphere regions that consists of numerous sensory and motor projections (**Figure 1**).

During embryonic development the cells that give rise to this nervous system arise from the ventral neurogenic region and the procephalic neurogenic region. The formation of the embryonic central nervous system situated in the ventral midline of the embryo has been extensively studied in *Drosophila* (Thomas et al. 1988, Goodman and Doe 1993, Menne and Klambt 1994, Udolph et al. 1995, Campos-ortega and Hartenstein 1997, Hummel et al. 1999). The ventral cord CNS develops out of segmentally iterated groups of neuronal precursors that delaminate from the ventral ectodermal region

(Bossing et al. 1994, Bossing et al. 1996). In *Drosophila,* many molecular components that are involved in determining neuronal cell fate have been identified . The genetic interactions that determine these cells to differentiate into neurons have been well characterized (Skeath and Carroll 1992, Skeath and Carroll 1994, reviewed in Skeath 1999). Simplistically, two classes of genes namely the proneural genes and neurogenic genes function as binary switches in a competent group of approximately 2000 cells in the ventral ectoderm. Cells from this competent group undergo delamination and specification as neuroblasts in a non-autonomous manner (Berger et al. 2001). These neuroblasts are programmed to undergo stereotypic divisions that give rise to glia and neurons in a segment specific manner to construct the ventral cord region of the CNS. As a result of cell-cell interactions and clonally stereotypic cell divisions ~30 cells per hemi-segment are designated (Doe, 1992; Udolph et. al., 1993, Schmid et al. 1999).

Mutations in genes that control neuronal specification can create abnormal cell lineages, and defects in connectivity. A number of studies have described the genetic basis of the midline neuronal-glial architecture (reviewed in Tear 1999; reviewed in Jacobs 2000). For example, a screen for structural abnormalities in the midline nervous system pattern revealed genes such as *commisureless* (*comm*) and *roundabout* (*robo*) (Seeger et al. 1993). These mutants show severe pathfinding defects with phenotypes that include absence of commisures and nerve misrouting. The *comm* gene is required for

axonal projections to cross the midline and maintain the commisure (Seeger et al. 1995). This gene product has been reported to be synthesized mainly in midline glia. Upon axonal crossover it is transferred from the glia to the commissural axons (Tear et al. 1996). Mutations in the *robo* gene misroutes axonal pathways in the midline such that tracts that do not cross the midline are now attracted to cross the same (reviewed in Thomas 1998).

*comm*, *singleminded* (*sim*), *spitz* (*spi*) group of genes are also involved in the development of the descending pathways of the embryonic brain (Therianos et. al. 1995). Mutations that affect nervous system patterning at the embryonic stage result in lethality. However many hypomorphic mutations can allow larval survival. This can allow the study of the behavioural consequences of such defects. Unfortunately, such studies have not been undertaken yet perhaps due to lack of larval behavioural paradigms. It will be interesting to correlate nervous system abnormality with the degree of behavioural impairment using such mutations. A comparison along these lines is possible using the Zebrafish model system. For example, a screen of 400 morphologically mutant lines that were previously characterized were used to test optomotor response. Surprisingly, none of the mutants that showed abnormal connectivity showed optomotor defects (Neuhauss et al. 1999). This study suggests that a perhaps a minimal circuitry may be sufficient for motor response.

In *Drosophila*, many other single-gene mutations that affect adult brain morphology have been tested for adult behaviour. Genes like *minibrain, ogre, lobula plateless, no bridge, central body defect, central brain deranged, ellipsoid body, body open, mushroom bodies deranged* remove specific regions of the central complex and the mushroom body and the optic lobe regions of the adult *Drosophila* brain (Heisenberg and Bohl 1979). While the mushroom body is involved in olfactory associative memory, the central complex has been implicated in regulation of locomotory behaviour (Zars 2000, Dubnau and Tully 2001). The central complex mutants are defective in walking behaviour such as speed of walking, leg coordination and decay of motor pattern during walking (Strauss and Heisenberg 1993). Once again, these studies noted that the severity of the structural defect did not always positively co-relate with the locomotory phenotype. This suggests that a minimal circuitry may exist for a basic locomotory pattern. A similar analysis of locomotory behaviour using targeted silencing of central complex structures using the tetanus toxin and the GAL4 binary expression system corroborated conclusions reached using the mutant approach (Martin et al. 1999). These authors also determined that the maintenance and not the initiation of walking is affected due to disruption of central complex structures.

More recently, genetic screens have used an enhancer-trap approach to successfully generate lesions in the adult brain structures. For example, a screen for

structural abnormalities in 104 strains identified 5 strains that showed morphologically-defective central complex and mushroom body structures (Boquet et al. 2000).

These studies demonstrate that approaches to study structure-function relationships in *Drosophila* nervous system are highly amenable through a genetic approach. One other point that is also valid from such studies is the modularization of the brain. Morphologically distinct structures in the *Drosophila* brain may parallel that of vertebrate nervous system design (Hirth et al. 1995).

**Genetic analysis of adult *Drosophila* behaviours**

The *Drosophila* adult stage has been successfully used for genetic dissection of the visual perception (Heisenberg 1971, Pak 1979, Hall and Greenspan 1979), circadian rhythms (Rosato et al. 1997, reviewed in Hall 1998), learning (Tully and Quinn 1985, Dubnau and Tully 1998), olfaction (Woodard et al. 1989, Carlson 1996), courtship behaviour (Hall 1979, Yamamoto 1999), foraging behaviour (Perriera and Sokolowski 1993), grooming behaviour (Phillis et. al. 1993).

One of the earliest reports of a genetic basis of behaviour in the fruit fly was made by Hadler in 1964 (Hadler 1964). He observed hereditary changes in phototactic behaviour through progressive selection. Hadler also described mass screening methods to study phototaxis (Hadler 1964). Single gene mutations and their consequence on

specific behaviour pattern was first demonstrated by Seymour Benzer. Benzer isolated phototactic mutants by exploiting for the first time in flies the use of a chemical mutagen to induce high mutation rates (Benzer 1967). Additionally, using genetic techniques that can generate chimeric flies Benzer was able to demonstrate that the mutant behaviour was due lack of gene function specifically in the eye and not due to its lack of function elsewhere (Benzer 1967). These events mark the origin of the study of neurogenetics in *Drosophila*.

Since the birth of *Drosophila* neurogenetics field hundreds of genes have been isolated using behaviour screens. Although to date only about 50 genes have been characterized in great detail with respect to their function in a specific behavioural paradigm (reviewed in Pfulgfelder 1997, reviewed in Heisenberg 1997). The majority identified were isolated using learning/memory, courtship, circadian rhythmicity, olfaction/gustation, optomotor response, jump response paradigms (reviewed in Pflugfelder, 1997). The mutagenesis approach has been very successful in the identification of many genes that affect sensory perception, central brain function and motor output, but only a minority of mutations have been reported to be highly specific in their disruption of behaviour. For example, the *optomotor blind* (*omb*) mutant was isolated through a paradigm that tests the ability of a fly to make yaw corrections in response to rotation of a visual field (Heisenberg 1971, Pflugfelder and Heisenberg

1995). Although a distinct behaviour deficit has been described for the allele isolated in the screen, other mutant alleles that map to this locus show pleitropic effects that range from larval lethality to defects in wing development and abnormal pigmentation in the abdomen (Grimm and Pflugfelder 1996).

Similarly, an olfactory Y-maze assay and an odour induced jump assay both of which measure the attraction or repulsion response of *Drosophila* to a variety of stimulants, helped identify a mutant allele that was named OlfC (Ayyub et al. 1990, Ayyub et al. 2000). Although some OlfC alleles are insensitive to acetate esters, other alleles are affected in many developmental stages. These range from abnormal gastrulation, defects in neuromuscular synaptic development, defects in myogenesis (Beumer et al. 1999). *Myospheroid* or *OlfC* gene codes for β-subunit of integrin.

Mutant alleles of the *fruitless* gene which encodes a zinc-finger domain containing transcription factor, consistently display courtship behaviour defects (Ryner et al. 1996). The *fruitless* gene is predominantly expressed in the CNS (Lee et al 2000). Various alleles of the *fruitless* gene disrupt the progression of the courtship fixed action pattern while not affecting other behaviours (Villlela et al. 1997). For example, in strains that contain weak alleles wing extension during courtship can be observed but wing vibrations that generates the courtship song is not produced. Additionally, morphological defects in *fruitless* mutants result in an abnormally small size of an

abdominal muscle group called the "muscle of Lawrence" (Ohshima et al. 1997). *fruitless* mutants also show reduced immunoreactivity against serotonergic projections in the abdominal ganglia (Lee and Hall 2001). Thus from our understanding of the function of the *fruitless* gene, it appears to be involved in a limited manner with respect to development within the context of courtship behaviour.

In summary, the majority of mutations that have been isolated based on a specific behaviour have also turned out to affect other developmental or physiological processes in a pleiotropic manner.

Only genes that code for the core circadian clock components (like *per* and *timeless*) appear to operate in a dedicated process that in turn affects behaviour in an exclusive manner (Konopka and Benzer 1971). Mutant alleles of these core component genes always result in defective circadian behaviour rhythms (Baylies et al. 1992). Genes like *per*, *tim* and *Clock* (a.k.a *jrk*) whose gene products form the core circadian mechanism do not appear to be required for the development nor cause premature lethality.

Do these observations invalidate the search for "behaviour genes"? It is indeed a very rare occurance when a single gene could be exclusively used by the organism for a behaviour pattern. Nevertheless, mutational strategies followed by testing for behaviour performance have other advantages. For example, such an approach can be used to dissect a behavioural pathway into three levels based on the effect of the lesion.

Mutations can disrupt the reception of sensory cues, processsing of sensory information (CNS) or the generation of motor output. Such an approach was fundamental in identifying components of the phototransduction pathway underlying the adult photobehaviour (Hotta and Benzer, 1969, Pak et al., 1969, Heisenberg M, 1971). Genetic screens not only aid in elucidating intracellular events but they may also help us understand how the nervous system is configured for various behavioural outputs. For example, *Drosophila* mutant strains lacking different subsets of adult photoreceptors were used to address the role of these photoreceptor cell types in the performance of different types of photobehaviours. The outer photoreceptors R1-6 in the fly ommatidia have been shown to mediate optomotor response while the inner R7 photoreceptors were demonstrated to be involved in fast phototaxis and some types of slow phototaxis (Heisenberg and Wolf, 1984).

Using a reverse genetic approach the identity and function of a gene can also be used to dissect behaviour. The *transformer* gene product participates in the sex determination cascade of *Drosophila*. Transgenic expression of *transformer* is sufficient to feminize somatic tissues of a male fly (O'Dell and Kaiser, 1995). Techniques to express *transformer* in a targeted manner within the nervous system has been used to observe the effect of feminizing specific part of the male brain (Ferveur et al. 1995). Such feminization of male brain results in altered courtship behaviours in males.

**Manipulating the genome and developmental programme to study behaviour**

Our ability to manipulate the genome of an organism and then study the consequence on development and behaviours has gained momentum in the last decade. This is mainly due to advancements in our understanding of gene regulation and the design/delivery of transgenic DNA constructs. This allows us to target expression or misexpression of genes in a spatial and temporal manner (reviews by Takahashi et al. 1994, Fetcho and Liu 1998, Tully 1996). Model organisms where this has been successfully applied include *Drosophila melanogaster*, *C. elegans*, *Danio Rio*, and *Mus musculus*. Once again the *Drosophila* model has played a pioneering role in the use of such techniques.

The very first attempt to misexpress cloned genes in specific compartments of the nervous system of *Drosophila* was carried out using the yeast transcription factor - GAL4 (the driver) and its DNA binding sequence (a control element for expression of cloned genes) (Brand and Perrimon 1993, reviewed in Brand and Doramand 1995). It allows us to misexpress any gene at any chosen locations in the fly, limited only by the number of tissue specific enhancers and promoters in the genome. Although this exogenous control system has been used extensively to study developmental processes its use in the study of behaviour has continued to gather pace. For example, as mentioned earlier, this system was used to demonstrate that the feminizing gene *transformer* can modify sexual

behaviour of the male fly when misexpressed in a specific compartment of a neural structure called the mushroom body (O'Dell and Kaiser 1995 ; Ferveur et al., 1995). Using a similar approach, the role of sex peptides in reducing female mating behaviour has also been ascertained (Nakayama et. al.1997).

Mapping the areas in the adult fly brain for regions that are involved in generating sexually dimorphic locomotory behaviour has been attempted more recently using the Gal4/UAS binary system (Sylvain et al. 2000). The locomotory pattern in male and female are noticeably different, with males exhibiting fewer pauses during locomotory bouts than the females. In such a study, a group of neurons in the pars intercerbralis region was feminized in the male brain using a transgenic construct that contained the *transformer* gene. Expression of this transgene in the aforementioned region was sufficient to alter the male locomotory behaviour to resemble that of the female locomotory pattern (Sylvain et al. 2000).

Similarly, the role of visual input in conditioning males not to mate premated females was investigated. Males are not successful in mating females that exhibit a refractory behaviour soon after mating. Males learn this and continue to avoid premated females. Using this behavioural pattern it was demonstrated that conditioning in the absence of visual input can be disrupted through the inhibition of calcium/calmodulin kinase-II (CaMKII) in the mushroom body. In the presence of

visual input such an inhibition by the ectopic expression of an inhibitory peptide against CaMKII does not affect memory formation (Joiner and Griffith 1999, Joiner and Griffith 2000). These studies support the hypothesis that memory formation using different sensory modalities in *Drosophila* may involve distinct biochemical pathways or a separate input circuitry for each sensory modality.

The Gal4/UAS system has also been used to ablate or silence neuronal activity in specific parts of the nervous system in a targetted manner. This can be conducted by misexpressing pro-apoptosis genes like *reaper*, *hid* (head involution defective), *bax*, or expression of genes like TeTLx (tetanus toxin light chain) and ask whether a specific set of behaviour is affected (Busto et al. 1999, Blanchardon, et al. 2001, Silvain et al. 2000, McBride et. al. 1999, Heimbeck et al. 1999). TeTLx abrogates synaptic transmission by cleaving synaptobrevin that is essential for exocytosis (Sweeney et al. 1995).

The GAL4/UAS technique in this situation suffers from one major problem. One cannot control the expression of cloned deleterious genes temporally, since the expression of the GAL4 driver is under the influence of the endogenous enhancer. Thus it is likely that expression of a transgene under the control of Gal4 can impede developmental processes thus precluding the study of nervous system function.

This problem can be overcome by using the dominant temperature sensitive allele of *shibire*$^{ts1}$ (*shi*$^{ts1}$). In this instance temperature can be used to control the stability

of the Shibire protein. *shibire*$^{ts1}$ codes for Dynamin, and at restrictive temperature (> 29° C) can inactivate synaptic transmission due to disruption of endocytosis and synaptic vesicle recycling (reviewed in De Camilli et al. 1995). Expression of this gene under the control of a photoreceptor specific promoter (*nina E*, rhodopsin 1) or a nervous system specific promoter (*Choline acetyl transferase*) has been reported to result in disruption of visual behaviour and paralysis, respectively (Kitamoto 2001).

Another method for regulating transgenes in both time and space is using the tetracycline based transactivator (tTA) (Gossen and Bujard 1992). This form of regulation takes place through binding an operator (tetO) DNA sequence by tTA in the absence of tetracycline. There also exists a reverse version of this transactivator (rtTA) where transcription can be triggered in the presence of tetracycline (Gossen et al 1995). This has been applied in *Drosophila*, where a tetracycline analog called doxycycline was used to show eye-specific expression of the *Lac-Z* gene, upon withdrawal of doxycycline (Bieschke et.al. 1998, Stebbins et. al 2001). This approach can also be used for behavioural studies with due caution owing to its toxic side effects and relatively slow induction.

More recently, the GAL4/UAS system has been modified further to allow the control of expression of a cloned gene in a temporal manner, this technique is called the GeneSwitch or P{Switch} system (Osterwalder et. al 2001, Roman et. al. 2001). Here, a

chimeric transcription factor that contains the Gal4 DNA binding domain, the ligand binding domain of human progesterone receptor and a p65 transactivation domain (Roman et. al. 2001). This hybrid protein can be induced to enter the nucleus in the presence of a ligand, antiprogestin or RU486 to trigger expression of a UAS-transgene. This expression system is very responsive, the induction takes place in ~2.5 hours. In this seminal study, neuron and muscle specific promoters were used to drive a gene-switch expression construct. This induced the expression of a UAS-GFP transgene in RU-486 dependent manner in the respective tissues (Osterwalder et. al. 2001). These new tools are very promising and in the future will allow us to dissect the central neuronal networks in order to identify the behavioural codes encoded in the CNS.

**Molecular complexity in nervous systems**

As one of the earliest estimates of molecular diversity in the mammalian brain, 20,000 – 40,000 mRNA's were reported to be expressed in brain specific manner (reviewed in Sutcliffe, 1988). More recently, the cDNA microarray technique has been used to compare the genetic differences in the brain of two inbred mice strains (Sandberg et al. 2000). This study attempted to correlate the behavioural differences in these two strains of mice with the difference in gene expression profile of various regions in the brain. Initially, a microarray consisting of ~13, 000 genes/EST's was used

to estimate the degree of heterogeniety in various parts of the mouse brain. This resulted in an estimation of 0.54% (~70 genes) of the total genes sampled to be differentially expressed. In another experiment a similar comparison yielded the identification of 73 genes out of 7, 169. This suggests that although the pattern of gene expression is diverse within the mouse brain, the behavioural differences between two strains of mice may be due to only a minority of genes.

In yet another study, ~34,000 genes were examined using a microarray and *in situ* hybridization. Once again, it was found that 0.3% of genes were expressed in a region specific manner within a brain, with majority of these being restricted to the amygdala (Zirlinger et al. 2001).

Towards similar analysis, brain specific transcript isolation in *Drosophila* are currently underway (Posey et al. 2001).

A comparison using genes coding for ion channels has been reported using the *Drosophila* and the *C. elegans* genomes (Littleton and Ganetzky 2000). This study concluded that every kind of ligand-gated and the voltage-gated channels, with the exception of voltage gated sodium channels are found in both fruit fly and the worm. More noticeable differences were only seen at the quantitative level. For example, when comparing12 categories of $K^+$ channels (including genes coding for the various subunits), it was observed that the *C. elegans* contains ~90 $K^+$ channels while *Drosophila* contains ~30

$K^+$ channels. Comparisons among other kinds of ion channels do not support the notion that differences in behaviour repertoires exhibited by the worm and the fly may be correlated with the ion channel differences. The differences must stem from the number of neurons used in each of these animals. *C. elegans* consists of only 302 neurons while the *Drosophila* nervous system is made up of ~250, 000 neurons.

**_C. elegans_ and _Drosophila_ as models to study molecular and cellular components of behaviour**

*C. elegans* is a soil dwelling nematode that survives by feeding on bacteria. This model system has been favoured to study various behaviours due to its clonal and hardwired developmental programme and a short life cycle of 3 days. The cell lineages and the connectivity of 302 neurons with 118 neuronal cell types and ~5000 synapses and ~2000 neuromuscular junctions in the adult have been elucidated in great detail (White et al. 1986, Sulston and Horvitz 1977, Kimble and Hirsh 1979, Sulston et al. 1983, Hall and Russell 1991).

Genetic dissection of sensory and motor behaviours have been very successful in *C. elegans*. These include mechanosensory (reviewed in Garcia-Anoveros and Corey 1996), chemical senses and thermosensation (reviewed in Mori 1999) and motor behaviours like reflexive reversals and defecation (reviewed in Mori and Ohshima 1997,

reviewed in Bargman 1993). Similar to methods used in *Drosophila* neurogenetics, C. *elegans* behaviours have been dissected using mutagenesis, followed by genetic analysis and molecular techniques (reviewed in Bargman 1993). For example, the molecular machinery that is involved in mechanosensation was elucidated through this approach. 13 mutants were identified in a mutagenesis screen based on the development or function of six touch sensitive neurons (Chalfie and Sulston 1981, Chalfie and Au 1989). Mutations that did not appear to affect the development of these neurons were then investigated further at molecular level. This led to the identification of proteins called "Degenerins" encoded by the *mec-4* and *mec-10* genes (Driscoll and Chalfie 1991). Gain-of-function mutations in these two genes lead to defects in ion transport that lead to cell swelling and degeneration (Driscoll and Chalfie 1991). Several genes have also been identified through mutational screens that enhance or suppress this phenotype (Huang and Chalfie 1994). Such studies have been very successful in the identification of many components that make a mechanoreceptor channel in C. *elegans*.

The clonally hardwired developmental programme and a transparent cuticle allows one to identify and ablate specific cells using lasers (Bargman and Avery 1995). For example, this technique has been used to study the neural circuit that mediates a mostly backward locomotion and rare occurrences of forward locomotion in response to a mechanical tap stimulus that is subjected to the side of a petri dish. This motor

behaviour has been described as the "tap withdrawal response" (Rankin et al. 1990). Seven sensory neurons, nine interneurons two motorneuron pools forming two sub-circuits have been understood to participate in this behaviour (Wicks and Rankin 1995). Each sub-circuit is thought to compete with the other to produce a backward or forward locomotion. Laser ablation of sensory inputs into each of the two sub-circuits showed that habituation kinetics of this response are distinct for each circuit. The circuit mediating forward locomotion habituated slower than the reverse locomotion mediating circuit and the intact animal habituating even faster than each circuit operating alone (Wicks and Rankin 1996). This suggests that the habituation response of the intact animal is not dependant on any one of the circuits but is an integration of their characteristics.

These examples demonstrate that the *C. elegans* model is a powerful platform to gain insights at both the molecular and network level to understand behaviour. This model has also gained recent momentum through the use of inhibitory RNA technique that can be used to silence the expression of target genes (Fire et al. 1998, Grishok et al. 2000). Thus a variety of genes that may participate in nervous system function in the post genomic period of this organism will now be open to analysis.

Compared to *C. elegans*, the *Drosophila* nervous system consists of ~250, 000 neurons (Kei Ito pers. comm.). *Drosophila* offers a halfway point in terms of the

complexity and diversity of behaviours exhibited in comparison to higher vertebrates. These include 3 different kinds of locomotion, courtship behaviour and a platform to study learning and memory. *Drosophila* offers almost 100 years of knowledge about its genome and various visible phenotypes. This wealth of information coupled to modern genetic and molecular tools like suppressor and enhancer interaction screens, epistatic analysis, enhancer trapping, Gal4 system, mosaic analysis using FLP recombinase, modular overexpression screens and neuroanatomical techniques makes this an ideal platform to dissect nervous system at various levels.

Subtractive hybridization experiments suggests that *Drosophila* neural tissue prepared from the head contains 11,000 different RNA species, coded by at least a few thousand genes (Levy and Manning. 1981). While the forward genetic approaches have been very successful in the discovery of genes, recently developed transgenic approaches will specifically allow us to manipulate the development of nervous system and its function in a targeted manner and study the consequences in terms of behaviour.

Novel genetic tools together with our knowledge of nervous system development will be crucial in answering fundamental questions regarding behaviour. For instance, what are the elements of a behavioural "code" that resides in a simple nervous system? Let us consider a fixed action pattern in a foraging third instar *Drosophila* larva. Larvae at this stage show an aversion to light by exhibiting a well co-

ordinated movement away from light. How is this "avoid light" command represented in a nervous system? Although it is expected that central neural circuits process this sensory input, how can we identify these central neurons? After identification will it be possible to alter the electrical properties of the neurons? What are the neural mechanisms that change this orientation behaviour towards light in larval stage to a positively phototactic adult fly? Such questions have been central to understand neural basis of behaviour. A singular model where we can perform non-invasive modifications and then study the consequences in terms of behavioural output will be invaluable in the future.

A molecular genetic approach has been very successful in isolating key molecules that play recurring roles in the designing various systems of the fruit fly. It is possible that the answers to such cognitive questions may be fathomable by manipulating genetic networks in order to redesign or alter neural circuits during embryonic development in *Drosophila.*

**References:**

Ayyub, C., Paranjape, J., Rodrigues, V., Siddiqi, O. 1990. Genetics of olfactory behaviour in *Drosophila melanogaster*. *J Neurogenet* 6:243-62.

Bailey CH. 1999. Structural changes and the storage of long-term memory in *Aplysia*. Can J Physiol Pharmacol 1999 Sep;77(9):738-47.

Baylies, M. K., Vosshall, L. B., Sehgal, A., Young, M. W. 1992. New short period mutations of the *Drosophila* clock gene per. *Neuron* 9:575-81.

Bargmann, C. I. 1993. Genetic and cellular analysis of behaviour in *C. elegans*. *Annu. Rev. Neurosci*. 16:47-71.

Bargman, C. I. and Avery L. 1995. Laser killing of cells in *Caenorhabditis elegans*. *Methods Cell. Biol.* 48: 225-250.

Beattie, C. E. 2000. Control of motor axon guidance in the zebrafish embryo. *Brain Res Bull* 53:489-500.

Benzer, S. 1967. Behavioural mutants of *Drosophila* isolated by countercurrent distribution. *Proc. Natl. Acad. Sci. USA* 1967 58:1112--1119

Berger, C., Urban, J., Technau, G. M. 2001. Stage-specific inductive signals in the *Drosophila* neuroectoderm control the temporal sequence of neuroblast specification. *Development* 128:3243-51.

Beumer, K. J., Rohrbough, J., Prokop, A., Broadie, K. 1999. A role for PS integrins in morphological growth and synaptic function at the postembryonic neuromuscular junction of *Drosophila*. *Development* 126:5833-46.

Bieschke, E. T., Wheeler, J. C., Tower, J. 1998. Doxycycline-induced transgene expression during *Drosophila* development and aging. *Mol Gen Genet* 258:571-9.

Blanchardon, E., Grima, B., Klarsfeld, A., Chelot, E., Hardin, P. E., et al. 2001. Defining the role of *Drosophila* lateral neurons in the control of circadian rhythms in motor activity and eclosion by targeted genetic ablation and PERIOD protein overexpression. *Eur J Neurosci* 13:871-88.

Boquet, I., Hitier, R., Dumas, M., Chaminade, M., Preat, T. 2000. Central brain postembryonic development in *Drosophila*: implication of genes expressed at the interhemispheric junction. *J Neurobiol* 42:33-48.

Bossing, T., Technau, G. M. 1994. The fate of the CNS midline progenitors in *Drosophila* as revealed by a new method for single cell labelling. *Development* 120:1895-906.

Bossing, T., Udolph, G., Doe, C. Q., Technau, G. M. 1996. The embryonic central nervous system lineages of *Drosophila melanogaster*. I. Neuroblast lineages derived from the ventral half of the neuroectoderm. *Dev Biol* 179:41-64.

Brainard, M. S., Doupe, A. J. 2000. Auditory feedback in learning and maintenance of vocal behaviour. *Nat Rev Neurosci* 1:31-40.

Brainard, M. S., Doupe, A. J. 2001. Postlearning consolidation of birdsong: stabilizing effects of age and anterior forebrain lesions. *J Neurosci* 21:2501-17.

Brand, A. H., Dormand, E. L. 1995. The GAL4 system as a tool for unravelling the mysteries of the *Drosophila* nervous system. *Curr Opin Neurobiol* 5:572-8.

Brand, A. H., Perrimon, N. 1993. Targeted gene expression as a means of altering cell fates and generating dominant phenotypes. *Development* 118:401-15.

Busto, M., Iyengar, B., Campos, A. R. 1999. Genetic dissection of behaviour: modulation of locomotion by light in the *Drosophila melanogaster* larva requires genetically distinct visual system functions. *J Neurosci* 19:3337-44.

Campesan, S., Dubrova, Y., Hall, J. C., Kyriacou, C. P. 2001. The nonA gene in *Drosophila* conveys species-specific behavioural characteristics. *Genetics* 158:1535-43.

Carlson, J. R. 1996. Olfaction in *Drosophila*: from odor to behaviour. *Trends Genet* 12:175-80.

Chalfie, M., Au, M. 1989. Genetic control of differentiation of the *Caenorhabditis elegans* touch receptor neurons. *Science* 243:1027-33.

Chalfie M, Sulston J. 1981. Developmental genetics of the mechanosensory neurons of *Caenorhabditis elegans*. *Dev Biol*. Mar;82(2):358-70.

De Camilli, P., Takei, K., McPherson, P. S. 1995. The function of dynamin in endocytosis. *Curr Opin Neurobiol* 5:559-65.

Driscoll M, Chalfie M. 1991. The mec-4 gene is a member of a family of *Caenorhabditis elegans* genes that can mutate to induce neuronal degeneration. Nature. 1991 Feb 14; 349(6310) :588-93.

Dickinson, P. S. 1995. Interactions among neural networks for behaviour. *Curr Opin Neurobiol* 5:792-8.

Doe, C. Q. 1992. Molecular markers for identified neuroblasts and ganglion mother cells in the *Drosophila* central nervous system. *Development* 116:855-63

Dubnau, J., Tully, T. 1998. Gene discovery in *Drosophila*: new insights for learning and memory. *Annu Rev Neurosci* 21:407-44.

Fire A, Xu S, Montgomery MK, Kostas SA, Driver SE, Mello CC. 1998. Potent and specific genetic interference by double-stranded RNA in *Caenorhabditis elegans*. Nature. 1998 Feb 19;391(6669):806-11.

Ferree, T.C. and Lockery, S.R. (1999) Computational rules for chemotaxis in the nematode *C. elegans*. *J. Computat. Neurosci.* **6**:263-277.

Ferveur, J. F., Stortkuhl, K. F., Stocker, R. F., Greenspan, R. J. 1995. Genetic feminization of brain structures and changed sexual orientation in male *Drosophila*. *Science* 267:902-5.
Fetcho, J. R., Liu, K. S. 1998. Zebrafish as a model system for studying neuronal circuits and behaviour. *Ann N Y Acad Sci* 860:333-45.

Frost, W. N., Kandel, E. R. 1995. Structure of the network mediating siphon-elicited siphon withdrawal in *Aplysia*. *J Neurophysiol* 73:2413-27.

Garcia-Anoveros J, Corey DP. Touch at the molecular level. Mechanosensation. *Curr Biol.* 1996 May 1;6(5):541-3. Review.

Goodman, C. S., Shatz, C. J. 1993. Developmental mechanisms that generate precise patterns of neuronal connectivity. *Cell* 72 Suppl:77-98.

Gossen, M., Bujard, H. 1992. Tight control of gene expression in mammalian cells by tetracycline- responsive promoters. *Proc Natl Acad Sci U S A* 89:5547-51.

Gossen, M., Bujard, H. 1995. Efficacy of tetracycline-controlled gene expression is influenced by cell type: commentary. *Biotechniques* 19:213-6; discussion 216-7.

Grimm, S., Pflugfelder, G. O. 1996. Control of the gene optomotor-blind in *Drosophila* wing development by decapentaplegic and wingless. *Science* 271:1601-4.

Grishok A, Tabara H, Mello CC. 2000. Genetic requirements for inheritance of RNAi in *C. elegans*. Science. Mar 31;287(5462):2494-7.

Hall, J. C. 1979. Control of male reproductive behaviour by the central nervous system of *Drosophila*: dissection of a courtship pathway by genetic mosaics. *Genetics* 92:437-57.

Hall, J. C. 1998. Molecular neurogenetics of biological rhythms. *J Neurogenet* 12:115-81.

Hall, D.H. and Russell, R.L. (1991). The posterior nervous system of the nematode *Caenorhabditis elegans*: Serial reconstruction of identified neurons and complete pattern of synaptic interactions. *J. Neurosci.* 11, 1-22.

Hall, J. C., Greenspan, R. J. 1979. Genetic analysis of *Drosophila* neurobiology. *Annu Rev Genet* 13:127-95

Haverkamp, L. J. 1986. Anatomical and physiological development of the Xenopus embryonic motor system in the absence of neural activity. *J Neurosci* 6:1338-48.

Haverkamp, L. J., Oppenheim, R. W. 1986. Behavioural development in the absence of neural activity: effects of chronic immobilization on amphibian embryos. *J Neurosci* 6:1332-7.

Heimbeck, G., Bugnon, V., Gendre, N., Haberlin, C., Stocker, R. F. 1999. Smell and taste perception in *Drosophila melanogaster* larva: toxin expression studies in chemosensory neurons. *J Neurosci* 19:6599-609.

Heisenberg, M. 1971. Separation of receptor and lamina potentials in the electroretinogram of normal and mutant *Drosophila*. *J Exp Biol* 55:85-100.

Heisenberg, M. 1997. Genetic approaches to neuroethology. *Bioessays* 19:1065-73.

Heisenberg, M., Wolf, R. 1984. Vision in *Drosophila*. *Stud. Brain Function*.12:1--250

Hirth, F., Therianos, S., Loop, T., Gehring, W. J., Reichert, H., Furukubo-Tokunaga, K. 1995.

Developmental defects in brain segmentation caused by mutations of the homeobox genes orthodenticle and empty spiracles in *Drosophila*. *Neuron* 15:769-78.

Holmes, A. L., Raper, R. N., Heilig, J. S. 1998. Genetic analysis of *Drosophila* larval optic nerve development. *Genetics* 148:1189-201.

Hotta, Y., Benzer, S. 1969. Abnormal electroretinograms in visual mutants of *Drosophila*. *Nature* 222:354-6.

Hotta, Y., Benzer, S. 1970. Genetic dissection of the *Drosophila* nervous system by means of mosaics. *Proc Natl Acad Sci U S A* 67:1156-63.

Huang M, Chalfie M. 1994. Gene interactions affecting mechanosensory transduction in *Caenorhabditis elegans*. *Nature*. Feb 3;367(6462):467-70.

Hummel, T., Schimmelpfeng, K., Klambt, C. 1999. Commissure formation in the embryonic CNS of *Drosophila*. *Development* 126:771-9.

Jacobs, J. R. 2000. The midline glia of *Drosophila*: a molecular genetic model for the developmental functions of glia. *Prog Neurobiol* 62:475-508.

Jarecki, J., Keshishian, H. 1995. Role of neural activity during synaptogenesis in *Drosophila*. *J Neurosci* 15:8177-90.

Joiner, M. A., Griffith, L. C. 1999. Mapping of the anatomical circuit of CaM kinase-dependent courtship conditioning in *Drosophila*. *Learn Mem* 6:177-92.

Joiner, M. A., Griffith, L. C. 2000. Visual input regulates circuit configuration in courtship conditioning of *Drosophila melanogaster*. *Learn Mem* 7:32-42.

Kimble J, Hirsh D. The postembryonic cell lineages of the hermaphrodite and male gonads in *Caenorhabditis elegans*. Dev Biol. 1979 Jun;70(2):396-417.

Kitamoto, T. 2001. Conditional modification of behaviour in *Drosophila* by targeted expression of a temperature-sensitive *shibire* allele in defined neurons. *J Neurobiol* 47:81-92.

Klambt, C., Jacobs, J. R., Goodman, C. S. 1991. The midline of the *Drosophila* central nervous system: a model for the genetic analysis of cell fate, cell migration, and growth cone guidance. *Cell* 64:801-15.

Kraut, R., Menon, K., Zinn, K. 2001. A gain-of-function screen for genes controlling motor axon guidance and synaptogenesis in *Drosophila*. *Curr Biol* 11:417-30.

Lee, G., Foss, M., Goodwin, S. F., Carlo, T., Taylor, B. J., Hall, J. C. 2000. Spatial, temporal, and sexually dimorphic expression patterns of the fruitless gene in the *Drosophila* central nervous system. *J Neurobiol* 43:404-26.

Lee, G., Hall, J. C. 2001. Abnormalities of male-specific FRU protein and serotonin expression in the CNS of fruitless mutants in *Drosophila*. *J Neurosci* 21:513-26.

Levy, L. S., Manning, J. E. 1981. Messenger RNA sequence complexity and homology in developmental stages of *Drosophila*. *Dev Biol* 85:141-9.

Littleton, J. T., Ganetzky, B. 2000. Ion channels and synaptic organization: analysis of the *Drosophila* genome. *Neuron* 26:35-43.

Mori I. Genetics of chemotaxis and thermotaxis in the nematode *Caenorhabditis elegans*. Annu Rev Genet. 1999;33:399-422. Review.

Martin, J. R., Raabe, T., Heisenberg, M. 1999. Central complex substructures are required for the maintenance of locomotor activity in *Drosophila melanogaster*. *J Comp Physiol [A]* 185:277-88.

McBride, S. M., Giuliani, G., Choi, C., Krause, P., Correale, D., et al. 1999. Mushroom body ablation impairs short-term memory and long-term memory of courtship conditioning in *Drosophila melanogaster*. *Neuron* 24:967-77.

Mitchell, K. J., Doyle, J. L., Serafini, T., Kennedy, T. E., Tessier-Lavigne, M., et al. 1996. Genetic analysis of Netrin genes in *Drosophila*: Netrins guide CNS commissural axons and peripheral motor axons. *Neuron* 17:203-15.

Mori I, Ohshima Y. 1997. Molecular neurogenetics of chemotaxis and thermotaxis in the nematode *Caenorhabditis elegans*. Bioessays. Dec;19(12):1055-64. Review.

Muralidhar, M. G., Thomas, J. B. 1993. The *Drosophila* bendless gene encodes a neural protein related to ubiquitin-conjugating enzymes. *Neuron* 11:253-66.

Nadim, F., Manor, Y. 2000. The role of short-term synaptic dynamics in motor control. *Curr Opin Neurobiol* 10:683-90.

Nakayama, S., Kaiser, K., Aigaki, T. 1997. Ectopic expression of sex-peptide in a variety of tissues in *Drosophila* females using the P[GAL4] enhancer-trap system. *Mol Gen Genet* 254:449-55.

Neuhauss, S. C., Biehlmaier, O., Seeliger, M. W., Das, T., Kohler, K., et al. 1999. Genetic disorders of vision revealed by a behavioural screen of 400 essential loci in zebrafish. *J Neurosci* 19:8603-15.

Osterwalder, T., Yoon, K. S., White, B. H., Keshishian, H. 2001. A conditional tissue-specific transgene expression system using inducible GAL4. *Proc Natl Acad Sci U S A* 98:12596-601.

Parras, C., Garcia-Alonso, L. A., Rodriguez, I., Jimenez, F. 1996. Control of neural precursor specification by proneural proteins in the CNS of *Drosophila*. *Embo J* 15:6394-9.

Peck, J. H., Nakanishi, S. T., Yaple, R., Harris-Warrick, R. M. 2001. Amine modulation of the transient potassium current in identified cells of the lobster stomatogastric ganglion. *J Neurophysiol* 86:2957-65.

Pereira, H. S., Sokolowski, M. B. 1993. Mutations in the larval foraging gene affect adult locomotory behaviour after feeding in *Drosophila melanogaster*. *Proc Natl Acad Sci U S A* 90:5044-6.

Pflugfelder, G. O. 1998. Genetic lesions in *Drosophila* behavioural mutants. *Behav Brain Res* 95:3-15.

Phillis, R. W., Bramlage, A. T., Wotus, C., Whittaker, A., Gramates, L. S., et al. 1993. Isolation of mutations affecting neural circuitry required for grooming behaviour in *Drosophila melanogaster*. *Genetics* 133:581-92.

Posey, K. L., Jones, L. B., Cerda, R., Bajaj, M., Huynh, T., et al. 2001. Survey of transcripts in the adult *Drosophila* brain. *Genome Biol* 2

Rankin CH, Beck CD, Chiba CM. 1990. *Caenorhabditis elegans:* a new model system for the study of learning and memory. Behav Brain Res. Feb 12;37(1):89-92.

Rendahl, K. G., Jones, K. R., Kulkarni, S. J., Bagully, S. H., Hall, J. C. 1992. The dissonance mutation at the no-on-transient-A locus of D. melanogaster: genetic control of courtship song and visual behaviours by a protein with putative RNA-binding motifs. *J Neurosci* 12:390-407.

Roman, G., Endo, K., Zong, L., Davis, R. L. 2001. P[Switch], a system for spatial and temporal control of gene expression in *Drosophila melanogaster. Proc Natl Acad Sci U S A* 98:12602-7.

Rosato, E., Piccin, A., Kyriacou, C. P. 1997. Circadian rhythms: from behaviour to molecules. *Bioessays* 19:1075-82.

Rubin, G. M., Yandell, M. D., Wortman, J. R., Gabor Miklos, G. L., Nelson, C. R., et al. 2000. Comparative genomics of the eukaryotes. *Science* 287:2204-15.

Ryner, L. C., Goodwin, S. F., Castrillon, D. H., Anand, A., Villella, A., et al. 1996. Control of male sexual behaviour and sexual orientation in *Drosophila* by the fruitless gene. *Cell* 87:1079-89.

Salzberg, A., D'Evelyn, D., Schulze, K. L., Lee, J. K., Strumpf, D., et al. 1994. Mutations affecting the pattern of the PNS in *Drosophila* reveal novel aspects of neuronal development. *Neuron* 13:269-87.

Sandberg, R., Yasuda, R., Pankratz, D. G., Carter, T. A., Del Rio, J. A., et al. 2000. Regional and strain-specific gene expression mapping in the adult mouse brain. *Proc Natl Acad Sci U S A* 97:11038-43.

Saueressig, H., Burrill, J., Goulding, M. 1999. Engrailed-1 and netrin-1 regulate axon pathfinding by association interneurons that project to motor neurons. *Development* 126:4201-12.

Schmid, A., Chiba, A., Doe, C. Q. 1999. Clonal analysis of *Drosophila* embryonic neuroblasts: neural cell types, axon projections and muscle targets. *Development* 126:4653-89.

Seeger, M., Tear, G., Ferres-Marco, D., Goodman, C. S. 1993. Mutations affecting growth cone guidance in *Drosophila*: genes necessary for guidance toward or away from the midline. *Neuron* 10:409-26.

Sink, H., Whitington, P. M. 1991. Pathfinding in the central nervous system and periphery by identified embryonic *Drosophila* motor axons. *Development* 112:307-16.

Skeath, J. B. 1999. At the nexus between pattern formation and cell-type specification: the generation of individual neuroblast fates in the *Drosophila* embryonic central nervous system. *Bioessays* 21:922-31.

Skeath, J. B., Carroll, S. B. 1992. Regulation of proneural gene expression and cell fate during neuroblast segregation in the *Drosophila* embryo. *Development* 114:939-46.

Skeath, J. B., Carroll, S. B. 1994. The achaete-scute complex: generation of cellular pattern and fate within the *Drosophila* nervous system. *Faseb J* 8:714-21.

Stebbins, M. J., Urlinger, S., Byrne, G., Bello, B., Hillen, W., Yin, J. C. 2001. Tetracycline-inducible systems for *Drosophila*. *Proc Natl Acad Sci U S A* 98:10775-80.

Strauss, R., Heisenberg, M. 1993. A higher control center of locomotor behaviour in the Drosophila brain. *J Neurosci* 13:1852-61.

Sulston JE, Horvitz HR. Post-embryonic cell lineages of the nematode, *Caenorhabditis elegans*. *Dev Biol*. 1977 Mar;56(1):110-56.

Sulston JE, Schierenberg E, White JG, Thomson JN. The embryonic cell lineage of the nematode *Caenorhabditis elegans*. Dev Biol. 1983 Nov;100(1):64-119.

Sutcliffe, J. G. 1988. mRNA in the mammalian central nervous system. *Annu Rev Neurosci* 11:157-98

Sweeney, S. T., Broadie, K., Keane, J., Niemann, H., O'Kane, C. J. 1995. Targeted expression of tetanus toxin light chain in *Drosophila* specifically eliminates synaptic transmission and causes behavioural defects. *Neuron* 14:341-51.

Sylvain, G., Jean-Francois, G., Jean-Rene, F. 2000. Genetic identification of neurons controlling a sexually dimorphic behaviour. *Curr Biol* 10:667-70.

Takahashi, J. S., Pinto, L. H., Vitaterna, M. H. 1994. Forward and reverse genetic approaches to behaviour in the mouse. *Science* 264:1724-33.

Taniguchi, M., Yuasa, S., Fujisawa, H., Naruse, I., Saga, S., et al. 1997. Disruption of semaphorin III/D gene causes severe abnormality in peripheral nerve projection. *Neuron* 19:519-30.

Tear, G., Harris, R., Sutaria, S., Kilomanski, K., Goodman, C. S., Seeger, M. A. 1996. commissureless controls growth cone guidance across the CNS midline in *Drosophila* and encodes a novel membrane protein. *Neuron* 16:501-14.

Tear, G., Seeger, M., Goodman, C. S. 1993. To cross or not to cross: a genetic analysis of guidance at the midline. *Perspect Dev Neurobiol* 1:183-94

Therianos, S., Leuzinger, S., Hirth, F., Goodman, C. S., Reichert, H. 1995. Embryonic development of the *Drosophila* brain: formation of commissural and descending pathways. *Development* 121:3849-60.

Thomas, B. J., Wassarman, D. A. 1999. A fly's eye view of biology. *Trends Genet* 15:184-90.

Thomas, J. B. 1998. Axon guidance: crossing the midline. *Curr Biol* 8:R102-4.

Thomas, J. H., Birnby, D. A., Vowels, J. J. 1993. Evidence for parallel processing of sensory information controlling dauer formation in *Caenorhabditis elegans*. *Genetics* 134:1105-17.

Tully, T., Quinn, W. G. 1985. Classical conditioning and retention in normal and mutant *Drosophila melanogaster*. *J Comp Physiol [A]* 157:263-77.

Udolph, G., Luer, K., Bossing, T., Technau, G. M. 1995. Commitment of CNS progenitors along the dorsoventral axis of *Drosophila* neuroectoderm. *Science* 269:1278-81.

Udolph, G., Prokop, A., Bossing, T., Technau, G. M. 1993. A common precursor for glia and neurons in the embryonic CNS of *Drosophila* gives rise to segment-specific lineage variants. *Development* 118:765-75.

Vactor, D. V., Sink, H., Fambrough, D., Tsoo, R., Goodman, C. S. 1993. Genes that control neuromuscular specificity in *Drosophila*. *Cell* 73:1137-53.

Veraksa, A., Del Campo, M., McGinnis, W. 2000. Developmental patterning genes and their conserved functions: from model organisms to humans. *Mol Genet Metab* 69:85-100.

Villella, A., Gailey, D. A., Berwald, B., Ohshima, S., Barnes, P. T., Hall, J. C. 1997. Extended reproductive roles of the fruitless gene in *Drosophila melanogaster* revealed by behavioural analysis of new fru mutants. *Genetics* 147:1107-30.

Weng, G., Bhalla, U. S., Iyengar, R. 1999. Complexity in biological signaling systems. *Science* 284:92-6.

Wheeler, D. A., Kyriacou, C. P., Greenacre, M. L., Yu, Q., Rutila, J. E., et al. 1991. Molecular transfer of a species-specific behaviour from *Drosophila simulans* to *Drosophila melanogaster*. *Science* 251:1082-5.

White, B., Osterwalder, T., Keshishian, H. 2001a. Molecular genetic approaches to the targeted suppression of neuronal activity. *Curr Biol* 11:R1041-53.

White, B. H., Osterwalder, T. P., Yoon, K. S., Joiner, W. J., Whim, M. D., et al. 2001b. Targeted attenuation of electrical activity in *Drosophila* using a genetically modified K(+) channel. *Neuron* 31:699-711.

White JG, Southgate E, Thomson JN, Brenner S. The structure of the ventral nerve cord of *Caenorhabditis elegans. Philos Trans R Soc Lond B Biol Sci.* 1976 Aug 10;275(938):327-48.

Wicks SR, Rankin CH. 1995. Integration of mechanosensory stimuli in *Caenorhabditis elegans. J Neurosci.* Mar;15(3 Pt 2):2434-44.

Wicks SR, Roehrig CJ, Rankin CH. A dynamic network simulation of the nematode tap withdrawal circuit: predictions concerning synaptic function using behavioural criteria. J *Neurosci* 1996 Jun 15;16(12):4017-31.

Williams, D. W., Shepherd, D. 2002. Persistent larval sensory neurones are required for the normal development of the adult sensory afferent projections in *Drosophila. Development* 129:617-24.

Wilson, R., Ainscough, R., Anderson, K., Baynes, C., Berks, M., et al. 1994. 2.2 Mb of contiguous nucleotide sequence from chromosome III of *C. elegans. Nature* 368:32-8.

Woodard, C., Huang, T., Sun, H., Helfand, S. L., Carlson, J. 1989. Genetic analysis of olfactory behaviour in *Drosophila*: a new screen yields the ota mutants. *Genetics* 123:315-26.

Wu, J. Y., Cohen, L. B., Falk, C. X. 1994. Neuronal activity during different behaviours in Aplysia: a distributed organization? *Science* 263:820-3.

Yamamoto, D., Nakano, Y. 1999. Sexual behaviour mutants revisited: molecular and cellular basis of *Drosophila* mating. *Cell Mol Life Sci* 56:634-46.

Zars, T. 2000. Behavioural functions of the insect mushroom bodies. *Curr Opin Neurobiol* 10:790-5.

Zirlinger, M., Kreiman, G., Anderson, D. J. 2001. Amygdala-enriched genes identified by microarray technology are restricted to specific amygdaloid subnuclei. *Proc Natl Acad Sci U S A* 98:5270-5.

**Figure 1.**

The larval nervous system can be visualized in an intact living animal through the use of a transgene coding for the green fluorescent protein (GFP). In the figure the GFP is expressed under the control of a neuron specific promoter (*elav*). The larval specimen is visualized here from the dorsal side . Segments are numbered on the right. The central brain hemispheres and the ventral cord receive inputs from sensory nerves in the periphery and also send afferent projections that will control the motor apparatus. The musculature is arranged in a segmentally iterated manner.

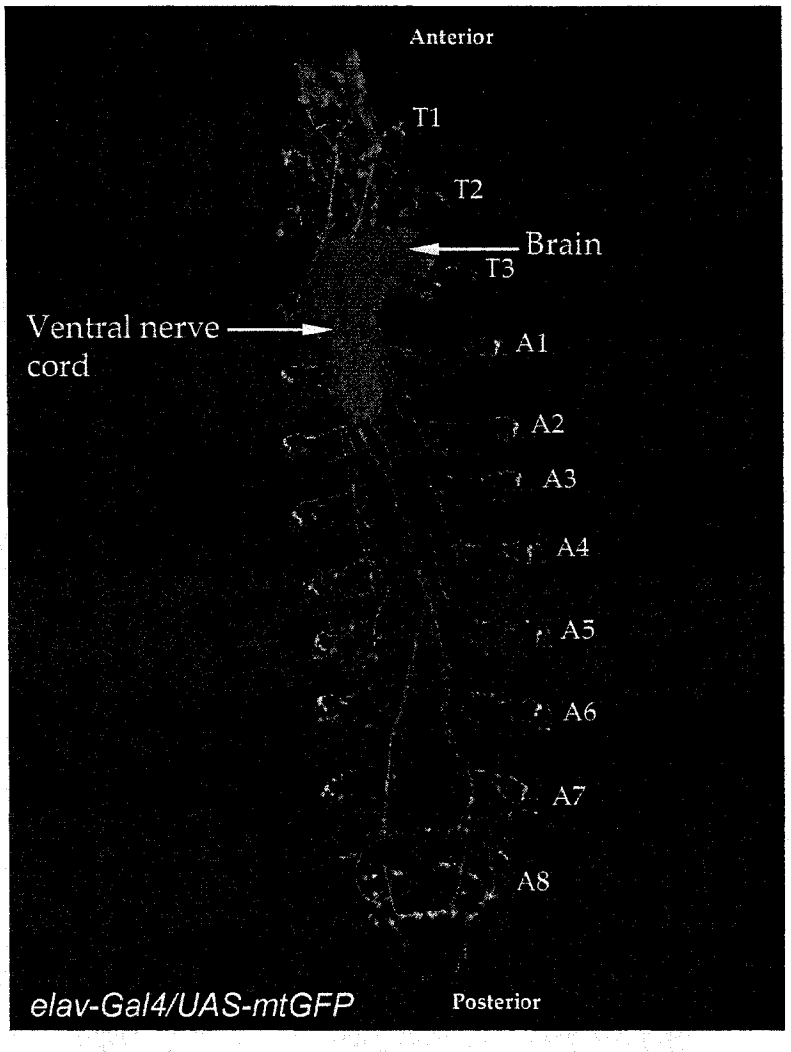
Anterior
T1
T2
Brain
T3
Ventral nerve cord
A1
A2
A3
A4
A5
A6
A7
A8
elav-Gal4/UAS-mtGFP
Posterior

# Chapter 2

# The Rationale

In this study we developed *Drosophila* larval photobehaviour as a model system to isolate genes that affect nervous system function. Genetic screens using the *Drosophila* third instar larva have validated this developmental stage as a good model for the identification of novel behavioural genes (Kernan et al. 1994).

Mutagenesis procedures which can generate single gene mutations have been an important tool in the study of developmental mechanisms (Nusslein-Volhard, 1994). The advantage of random mutational approach resides in the fact that when searching for mutations that, for example, disrupts embryonic pattern formation, or adult eye morphogenesis, one is simply asking the organism as a whole which one of its several thousand genes is required for proper function or development of a particular structure of interest. This unbiased approach does not require previous knowledge of the kinds of molecules that may be required for the process under consideration.

However, a requirement of a specific gene function for the viability of the organism at an earlier stage in development may preclude the availability of the mutation for analysis in the adult. This observation is of special significance to the nervous system in holometabolous insects where the larval nervous system is redesigned during pupation for adult function (reviewed in Weeks and Levine, 1990). While maternal genetic contribution may help build a nervous system for the larva, these molecules may not be available or be sufficient for the construction of the adult

nervous system. Hence, a subset of vital loci that may be involved in nervous system development or its function prior to pupation remains relatively unaccounted for in most screens that are based on identifying hypomorphic phenotypes in the adult.

One example of what can be gained by studying behaviour at larval stages comes from observations on behaviour of calmodulin null larvae (Heiman et al., 1996, Nelson et al. 1997). These larvae die at the end of $I^{st}$ instar. Prior to onset of lethality it is seen that the larvae show abnormal motor behaviours like higher incidence of spontaneous backward locomotion (an avoidance response), and increased head swinging behaviour. This suggests a critical role for calcium signalling in the CNS for generating motor behaviours.

A method by which one can study these mutations that otherwise pre-empt analysis in the adult is through mosaic techniques. Several genetic tools are available today that can produce homozygous mutant clones of cells in specific parts of the nervous system, that can be later studied in the adult (Xu and Rubin 1993, Xu and Harrison 1994, Perrimon 1998, Hotta and Benzer 1970, Janning 1978). Mosaic experiments to study the contribution of vital loci in the development of a complex structure like the adult eye has been very successful (Meyerowitz and Kankel 1978, Campos et al. 1985, Thaker and Kankel, 1992). One such example suggested that two-thirds of all vital genes may be required for the assembly of the adult eye and neuronal

connectivity therein (Thaker and Kankel, 1992). This is a large group of genes and a search for a functional role of each of these in nervous system function will yield interesting results.

A mosaic approach to study the role of vital loci in larval nervous system function has not been simple. This is due to unavailability of reliable visible markers until recently in the larvae and in theory even when the FRT-FLP system could be used with suitable internal markers, the time window available to induce mitotic recombination in the population of neuronal stem cells that make the larval brain is considerably narrow. Mosaic experiments also require good characterization of behaviour phenotypes at the resolution of a single larva.

We used a collection of late larval and pupal lethals for a behavioural screen using the plate assay for the following reasons. The basic methodology to study the photobehaviour of the foraging $3^{rd}$ instar larvae has been well established using this assay (Sawin-McCormak et al.1995). The 3rd instar has the longest period of 48 h between the second molt and the onset of wandering, this facilitates synchronization of larval development for behavioural assays.

Pupal lethal or 3rd instar larval lethal mutations are second largest class of mutations among all vital loci, they constitute in the range of 20% and 10-20%

respectively, of all lethal mutations, next to embryonic lethal mutations which constitute about 50% (Torok, et al. 1993., Ripoll, 1977., Bryant, and Zornetzer, 1973).

We considered the possibility that the class of mutations that we chose to study, may most often affect only processes that are involved in transforming the larva into an adult. And hence, one can argue, that the late larval and pupal lethal lethal class may not be the right sample of mutations to study for a role in an earlier phase in development. This skepticism can be cleared by asking whether most vital loci in the fly genome mutate only to embryonic lethality, larval lethality or pupal lethality? Or does their respective alleles suggest a developmental spread in terms of stage of lethality? These questions essentially are directed towards understanding how the information in a genome is managed by the organism during various stages in development. The answers to such questions will also suggest whether the sample of mutated genes that we considered is biased against our ideas. Unfortunately, a systematic study of all lethal mutations that are allelic to their respective essential genes and their lethal phases has not been conducted so far. But a look at a different "window" in ontogeny does give us some clues regarding the use of gene products in multiple times and places.

It is well established now that *Drosophila* embryogenesis (post-zygotic development) will be possible only if the maternal contribution has laid a primary design. This maternal process begins at oogenesis. To reinstate the earlier argument,

one can hypothesize that specific genes will be involved only in a specific developmental compartment. For instance one can consider oogenesis and embryogenesis to be two different developmental compartments that use unique subsets of gene products. What did we notice when one conducted a genetic screen hoping to find phenotypes strictly to one compartment?

As a case study, screens that were aimed at isolating female sterile mutations and embryonic lethality have been conducted in X chromosome extensively to 86% saturation (Perrimon et al., 1989). Such screens isolated genes that affect oogenesis and embryonic pattern formation (Perrimon et al. 1989, Perrimon et al., 1984). The genetic analysis of such loci and their respective alleles suggests that a number of genes that affect sterility can also mutate to cause zygotic (embryonic) lethality. Alternatively, many instances of embryonic lethality are due to mutations in maternally expressed genes. A closer look at expression patterns of some of these loci also shows pleiotropism of gene function, a few examples include *torpedo-* an EGF receptor, *toll-* (a transmembrane receptor ) that also plays a role in *Drosophila* immune system , *armadillo-* a cytoskeletal protein that is involved in maintaining cell-cell contact through adherance junctions, *dunce-* (cAMP phosphodiesterase) that is also involved in olfactory learning, *ultraspiracle-* (a steroid hormone receptor/transcription factor) and *broad* complex- (coding for Zinc finger and BTB domain transcription factors) that are required for

development through out the larval stages as well. These observations demonstrating genetic pleiotropy tell us that a finite number of gene products are reutilized by the organism in multiple developmental contexts. Within these premises, the percentages of lethals affecting a specific stage of larval development then do not necessarily indicate that identification of gene function at later stages will be in vain. Similarly, it is also highly likely that the same molecular players that played a part in the development of various systems in the embryo/larva will be redeployed for constructing the adult nervous system. This is supported by the observations that such a reconstruction is based on pre-existing larval nervous system (Williams and Shepherd 2002, Shepherd and Smith 1996).

A functional screen to investigate the role of a set of vital loci that when mutated causes late larval lethal or pupal lethal in the nervous system prior to the onset of lethality is hence justified. By using the larval photobehaviour as a model system one can ask whether this model system can diagnose nervous system abnormalities prior to occurrence of lethality.

In this study, we report our first steps towards the genetic dissection of larval photobehaviour in *Drosophila*. We first standardized an existing behavioural assay. Next, we use used a collection of 65 second chromosome pupal lethal mutations kindly provided by Drs. Hiliker and Sokolowski (Hiliker pers. comm.). We also improvised

and streamlined a behavioural paradigm for expeditious screening of mutant lines to isolate mutations that affect larval locomotion and response to light. The report also describes the genetic mapping and phenotype analysis of a previously identified loci *l(2)34Dc*, which we called "*tamas*" (Sanskrit - "dark inertia"). The characterization of this locus led towards first ever description of phenotypic consequences of mutations in the mitochondrial DNA polymerase and its accessory subunit.

## References

Bryant, P. J., Zornetzer, M. 1973. Mosaic analysis of lethal mutations in *Drosophila*. *Genetics* 75:623-37.

Heiman, R. G., Atkinson, R. C., Andruss, B. F., Bolduc, C., Kovalick, G. E., Beckingham, K. 1996. Spontaneous avoidance behaviour in *Drosophila* null for calmodulin expression. *Proc Natl Acad Sci U S A* 93:2420-5.

Hotta, Y., Benzer, S. 1970. Genetic dissection of the *Drosophila* nervous system by means of mosaics. *Proc Natl Acad Sci U S A* 67:1156-63.

Janning, W. 1978. Gynandromorph fate maps in *Drosophila*. *Results Probl Cell Differ* 9:1-28

Kernan, M., Cowan, D., Zuker, C. 1994. Genetic dissection of mechanosensory transduction: mechanoreception- defective mutations of *Drosophila*. *Neuron* 12:1195-206.

Meyerowitz, E. M., Kankel, D. R. 1978. A genetic analysis of visual system development in *Drosophilia melanogaster*. *Dev Biol* 62:112-142.

Nelson, H. B., Heiman, R. G., Bolduc, C., Kovalick, G. E., Whitley, P., et al. 1997. Calmodulin point mutations affect *Drosophila* development and behaviour. *Genetics* 147:1783-98.

Nusslein-Volhard, C. 1994. Of flies and fishes. *Science* 266:572-4.

Perrimon, N. 1998. Creating mosaics in *Drosophila*. *Int J Dev Biol* 42:243-7.

Perrimon, N., Engstrom, L., Mahowald, A. P. 1984. The effects of zygotic lethal mutations on female germ-line functions in *Drosophila*. *Dev Biol* 105:404-14.

Perrimon, N., Engstrom, L., Mahowald, A. P. 1989. Zygotic lethals with specific maternal effect phenotypes in *Drosophila melanogaster*. I. Loci on the X chromosome. *Genetics* 121:333-52.

Ripoll, P. 1977. Behaviour of somatic cells homozygous for zygotic lethals in *Drosophila melanogaster*. *Genetics* 86:357-76.

Sawin-McCormack, E. P., Sokolowski, M. B., Campos, A. R. 1995. Characterization and genetic analysis of *Drosophila melanogaster* photobehaviour during larval development. *J Neurogenet* 10:119-35.

Shepherd, D., Smith, S. A. 1996. Central projections of persistent larval sensory neurons prefigure adult sensory pathways in the CNS of *Drosophila*. *Development* 122:2375-84.

Torok, T., Tick, G., Alvarado, M., Kiss, I. 1993. P-lacW insertional mutagenesis on the second chromosome of *Drosophila melanogaster*: isolation of lethals with different overgrowth phenotypes. *Genetics* 135:71-80.

Weeks, J. C., Levine, R. B. 1990. Postembryonic neuronal plasticity and its hormonal control during insect metamorphosis. *Annu Rev Neurosci* 13:183-94

Williams W. D., Shepherd D. 2002. Persistent larval neurones are required for the normal development of the adult sensory afferent projections in *Drosophila*. *Development* 129, 617-624.

Xu, T., Harrison, S. D. 1994. Mosaic analysis using FLP recombinase. *Methods Cell Biol* 44:655-81

Xu, T., Rubin, G. M. 1993. Analysis of genetic mosaics in developing and adult *Drosophila* tissues. *Development* 117:1223-37.

# Chapter 3

# Materials and Methods

**Fly stocks used in this study.** Please see **Table 1**.

**Fly medium.** The normal fly medium contained the following ingredients: Water 800 ml, sucrose 100 g, Agar 16 g, potassium phosphate 1.0 g, potassium sodium tartrate 8.0 g, NaCl 0.5 g, megnesium chloride 0.5 g, calcium chloride 0.5 g, ferric sulphate 0.5 g, dry yeast 50 g. These ingredients were autoclaved and dissolved to make 1 liter of the fly culture medium. Acid mix solution (11 parts water:10 parts propionic acid:1 part phosphoric acid) was added to the medium upon cooling. 1.2 g of β-carotene (5000 IU, Jamieson Laboratories, Toronto) was added as a Vitamin A source.

**Sang's medium preparation.** 10.9 g of Sang's medium (gift from William Stark) was weighed and added to 100ml of boiling water and frequently stirred for 10 minutes. After the medium began to cool down 1ml (100 units/ml) of penicillin-G (0.22 g/ml) of streptomycin sulphate was added. Vitamin A supplemented Sang's medium was prepared separately by adding 0.125 g of β-carotene to 100 ml of Sang's medium synchronized eggs for this experiment were dechorionated using 5% bleach and washed with an antibiotic solution and transferred to a sterile plate containing Sang's medium (see **Appendix F** for ingredients) (Methods in Developmental Biology ed. F.H. Wilt, N. K. Wessels, NY: Thomas Y. Crowell Co. 1967, p. 234).

**Fly crosses for genetic analyses.** Fly crosses were set up using at least 5-10 pairs of male and virgin females in 100 x 25 mm plastic vials. Parents were allowed to lay eggs for 4-5 days. At least 100 progeny were scored for complementation or non-complementation tests.

**Larval egg collection for behaviour, culture preparation and growth conditions.** The egg collection involved 2-3 pre-collections of 2 hours each on a fresh plate. The last 1 hour collection was retained and incubated for 80-85 hours at 25°C before testing in the plate assay at between 80-90 hours AEL (after egg laying). For the pupal lethal screen we incubated the embryos for the first 36 hours at 30°C such that the heterozygous flies carrying the *CyO, l(2)DTS513*$^{1}$ (*CyO, DTS*) chromosome would die. The plates with larvae were placed at 25°C until 80-85 hours AEL. The balancer chromosomes in all stocks used for photobehaviour experiments were exchanged for *CyO, Dp(1;2)y*$^{+}$ (*CyO-y*$^{+}$) and the X chromosome was substituted for one carrying the mutations $y^{1}$ and $w^{1}$, to facilitate selection of larvae based on the *y* (*yellow*) phenotype of the larval mouth hooks. For the individual larval assays, eggs were collected for 1 hour and incubated at 25°C. At 20-22 hours AEL all newly hatched first instar larvae were cleared and after another one hour incubation period approximately 70 newly-hatched first instar larvae were collected and transferred to a fresh food plate coated with yeast paste. Larvae were

grown in a 12 hour L:D cycle. Third instar larvae were tested for photobehaviour at 84 hours AEL, a minimum of three hours into the dark cycle.

**Synchronization of larval age for the behaviour assays and for mitochondrial DNA quantification.** Experiments suggests that the 3rd instar larval negative photoresponse is dependent on the age the larvae. Wandering larvae show decay in photobehaviour (For example see **Figure 18**). This observation demands synchronization of larval hatching at the point of egg laying and hatching. The egg collection involved at least 3 pre-collection stages for 2hours each on a fresh egg collecting petri plate each time, the eggs collected in these pre-collection stages were discarded and the 4th collection for 1 hr were retained for the tests. The eggs from the last collection are incubated for 80 hrs at 25°C incubator and tested in the plate assay between 80-90 h. For single larval tests larvae of the right genotype were selected based on either the *yellow* mouth hook marker or the *Tubby* phenotype. Approximately 50 larvae were added into one food plate (60x15mm Fisher petri plates). The food plate was streaked with yeast paste and the surface was scraped to allow larvae to burrow easily.

For estimating mitochondrial DNA levels in appropriate genotypes of larvae were synchronized as described above. All mutant larvae that were harvested were 6-7 days old. 50 larvae from each food plate were washed with phosphate buffer saline

thoroughly. Washed larvae were dried using tissue paper and placed in a microfuge tube and preserved in -80° C until preparation for quantitative Southern analysis.

**Environmental scanning electron microscopy (ESEM) of adult compound eyes.** We used ESEM model 2020 manufactured by ElectroScan Corporation (now Philips ElectroScan). This technology does not require metal coating of the specimen that is to be visualized. Adult flies were etherized and placed on the ESEM mount. Flies were immobilized using water based colloidal carbon glue for proper orientation. The electroscan was performed at 20.0 kV and 3.9 Torr. Images are saved as TIFF files in the ESEM software.

**Larval brain immunohistochemistry.** Larval brains with the eye-antenna imaginal discs were dissected from third instar larvae in PBS (Phosphate Buffer Saline), and fixed in 4% paraformaldehyde (pH 7.4) for 45 minutes at room temperature. This was followed by 3-4 PBS washes. Brains were incubated in a blocking solution, which contained PBS with 0.3% Triton X-100 and 5% goat serum at room temperature for 1 hour, followed by addition of a fresh 100µl of blocking solution containing 2µl of 24B10 primary antibody (raised in mouse, DSHB, Univ. of Iowa). After 8-12 hours of incubation at 4°C the samples were washed with PBT (Phosphate buffer saline with 0.2% triton 100-X) for 4

hours, with changes every 10-20 minutes, incubated in a blocking solution as described above and finally incubated with a secondary antibody conjugated to horseradish peroxidase (Jackson Immunoresearch labs) for another 8-12 hours. Once again the specimens were washed thoroughly for 4 hours and stained with 0.5 ml of 3, 3′-diaminobenzidine (0.5 mg/ml, Sigma 72H3614) in the presence of hydrogen peroxide. The reaction was stopped by washing several times with PBS. The samples were mounted in 70% glycerol in PBS, and observed with a Zeiss axiophot microscope.

**Visualization of mitochondria in whole mount larval brains.** Individual brains after dissection in 1x Phosphate Buffered Saline (PBS) were immediately transferred to a glass tube containing Mitotracker CMX-Ros (Molecular probe) at 1μg/ml concentration. After 10 min, the brain was transferred to a glass tube containing 100ng/ml of DAPI in PBS (1:1000 dilution, stock soln 1mg/ml in 70% ethanol). The brain was stained in DAPI for 3-4 minutes followed by placing the brain for a dorsal view on a glass slide. The mitochondrial and nuclear profiles were characterized separately using the Texas red and DAPI filter sets. The images were captured using a SPOT CCD camera and the images were merged using the SPOT imaging software.

**Acridine orange staining.** Acridine Orange (Sigma, A-6014) staining was performed on the dissected larval CNS that included the eye-antennal disk. The dissection was performed in acridine orange solution (5µg/ml) made in PBS (Abrams *et al.* 1993). The samples were kept in acridine orange solution for 5 minutes, mounted in PBS and observed using fluorescein filters.

**BrdU staining protocol.** BrdU was dissolved in an injection buffer (0.1mM $NaPO_4$, 5mM KCl) for 1mg/ml concentration. Injection was carried out on late third instar larvae using a micro-manipulator setup and pulled glass needle. Larvae were first anaesthetized on a perforated $CO_2$ pad for a few minutes (this also relaxes the larval body thus allowing efficient injection). Approximately 1µl of BrDU solution was injected into the thoracic region of the larva. The larva was then placed in a petri dish with moist filter paper for 4 hours to allow incorporation of BrDU. The brains were further processed as described in (Winberg et al. 1992) using anti-BrDu antibody (BD Pharmingen, cat. no. 555627). After mounting on glass slides, the preparations were viewed using Normarski optics in a Zeiss Axioskop microscope. Images were captured using SPOT CCD camera.

**Genomic DNA preparation.** Genomic DNA was extracted from 80-100 larvae selected for the appropriate genotype - the *yellow* mouth hook marker. The larvae were washed with distilled water and frozen in liquid nitrogen prior to grinding using a mortar and pestle. The powdered larvae were resuspended (10µl/larvae) in homogenization buffer (0.1M Tris HCl, pH9.0; 0.1M EDTA; 1% SDS) for 30 minutes at 70°C. 14µl of 8M potassium phosphate per 100ml of homogenate were added and placed on ice for 30 minutes. The homogenate was centrifuged at 15,000 RPM, 4°C for 15 minutes. The supernatant was precipitated with 0.5 volumes of isopropanol. The precipitate was centrifuged at room temperature for 5 minutes, washed with 500µl of cold 70% absolute alcohol and again centrifuged at room temperature for 5 minutes at 15,000 RPM. The pellet was dried for 10 minutes at 37 °C and resuspended in 80-100µl of sterile water for 8-10 hours at 37 °C.

**PCR, sequencing and analysis.** To sequence mutations in *tamas* alleles the following oligonucleotides were designed and used for PCR amplification:

A. 5'-CCCCACCAACTTCCATAATG -3'; 3'-GTTACTACTTCCCCTGGTCCA-5'

B. 5'-GGTTGGACTTCAGTTGCCTTA-3'; 3'-CGTGTGGTGCAACAAAGTACT-5'

C. 5'-GAGGAGTTACTACTTCCCCTG-3'; 3'-CTGTGGAGCTTAAGGATTCTG-5'

D. 5'-TGTGGGTTCATCATTTTCATG-3'; 3'-ATCCCTAACAGCTACAGC-5'

E. 5'-GGGCGTAAGTAGTCACAAACC-3'; 3'-AAGGAGACTTGGAGGCTGTTA-5'

F. 5'-TAGAGGATGACGAAGAGCCGT-3'; 3'-GATGGAACCCACATGGATGAC-5'

G. 5'-CAGCGATATGCAACTCCATAAC-3'; 3'-GTGGACTTCCTTCATCTGATG-5'

The fragments generated by PCR amplification (using Platimum™ Taq DNA polymerase, Gibco BRL®) covered the whole gene including introns, beginning 354 bp upstream of the open reading frame start site and terminating 75 bp after the stop codon. The DNA fragments generated in the PCR reactions were purified using the QIAquick Gel Extraction kit (Cat. No. 28704). Automated sequencing was done using the cycle sequencing protocol with Taq-FS enzyme and BigDye terminator chemistry in a Perkin Elmer-ABI 373A Stretch machine. Each fragment was sequenced at least twice from two directions. The fly strain numbered as 2-68 (**see Table 1**) is the parental strain for *tam*$^{2}$ and *tam*$^{3}$ hence this strain was used for sequence alignments. Similarly, the fly strain numbered as 2-66 is the parental strain of *tam*$^{4}$ and this was used for sequence alignments for *tam*$^{4}$ allele. The sequence alignments were conducted using Clustal X (PPC). The mutation in the *tam*$^{9}$ allele was confirmed by amplification of *tam*$^{9}$ DNA using primer set-B and primer set-F which provide overlapping sequence data (*n=6).* The mutation in *tam*$^{2}$ was identified by overlapping sequence data obtained using the primer set-D (*n=4*). The mutation in *tam*$^{3}$ was identified using primer

set-E which also provides overlapping PCR product, ($n$=4).The lesion in *tam*$^{4}$ was identified using the primers in set-E, ($n$=6).

To sequence mutations in *pol* $\gamma$-$\beta$ alleles the following oligonucleotides were designed and used for PCR amplification: 5′- GAG AAT GTT GCG TCT GTT CA - 3′ and 5′- GAA GGT TCC GCT AGG CTG - 3′. This primer set amplified a 1.638 kb product that included 447 bp upstream sequence of the translational start site and 120 bp after the translational stop site. To sequence the whole 1.638 Kb product we used the above mentioned primers and the following primer 5′ - GGA AGA CAA TAA ACT GGA GC - 3′. This primer was designed from within open reading frame. Automated sequencing was done using the cycle sequencing protocol with Taq-FS enzyme and BigDye terminator chemistry in a Perkin Elmer ABI 373 stretch machine. Mutations were confirmed by sequencing two independent samples. The *pol* $\gamma$-$\beta^{1}$ mutation was further confirmed by sequencing the parental strain of this stock. Sequence alignments were performed using ClustalX software. (Thompson et al. 1997)

**Behaviour assay recording, measurements and statistical analysis.** All assays were conducted in the presence of "safe-light", which consisted of a 20 W incadescent lamp fitted with Kodak GBX-2 filter. This filter provides red light of wavelength above ~600

nm. Plate assays and Checker assays were conducted on a light box manufactured by Hall Productions, Model BL-1824 with 2 General Electric's fluorescent lamps at 15W each, "Cool White" type. Unlike the plate assay design described by Lily and Carlson (1991), the plate assays we used consisted of a template cast on a clear glass plate with electrical type insulation tape. Unless specified, all plate assays were conducted using ~100 larvae of 80-100 h age (AEL). The kinetic analysis of plate assay was recorded on to a video tape after capturing through a CCD video camera (Elmo 272s), and frames were frozen every 30 s to count and measure response index. A similar setup was used for recording the Checker assay and the On/Off assay.

For the Checker assays residence time was measured using the built-in VCR timer. Larvae were allowed 5 s in the start square after placement for recovery before the assay commenced. Larvae that did not move out of the start square within 90 s were not considered fit for measurement of response in this assay. Larvae were tracked in this assay by following the posterior end of the larva as they moved from one square to the other. The Checker assay was terminated at 3 min. While calculating response index equal number of dark and light squares visited by a larva were included.

In the all-manual mode of On/Off assay, the alternate pulses on light and dark were delivered using a voltage switcher that was previously designed for controlling an electrophoresis apparatus. This contraption was calibrated using a digital stop watch.

Movement tracks were sketched on a transparency sheet that was placed over a TV monitor while the pre-recorded assay was being played. A calibration was also performed for each session using a semi-log graphing paper. The tracks were then scanned using a flat-bed scanner and imported to an image analysis programme (NIH-image). Segmented-line measurement tool was used to measure path length in this program following calibration using the reference 1 cm length obtained from the graphing paper. All assays begin with a light stimulus and consisted of at least 2 pulses of light and 2 pulse of dark intervals. The response index calculation [(Distance traveled in the lights OFF pulse – Distance traveled in lights ON pulse) /Total distance traveled] always consisted of such even number of pulses with respect to light and dark phases. Unless specified all assays were conducted using 80-90 h old (AEL) foraging stage larvae.

The 30 s locomotory test were tracked and measured using a similar protocol using safe-light conditions.

All data were processed using Minitab 10.15 Xtra for the Macintosh platform. All response indices or distance traveled in centimeters/pixels were checked for normal distribution using the stem and leaf plot, suspended rootogram or Anderson-Darling normality test in Minitab. Following which a 2 sample T-tests were performed if the data distributed normally. Non-parametric, Mann-Whitney tests were used when data

was observed to depart from normality. Graphs were plotted using the mean values and standard error of the mean in Cricket Graph version III.

**References**

Thompson JD, Gibson TJ, Plewniak F, Jeanmougin F, Higgins DG. 1997. The CLUSTAL_X windows interface: flexible strategies for multiple sequence alignment aided by quality analysis tools. *Nucleic Acids Res*. 1997 Dec 15;25(24):4876-82.

Winberg ML, Perez SE, Steller H. 1992. Generation and early differentiation of glial cells in the first optic ganglion of *Drosophila melanogaster*. *Development*. Aug;115(4):903-11.

**TABLE 1**

**Fly stocks used in this study**

| Strains | Breakpoints/Cytology | Genetic Limits | Reference |
|---|---|---|---|
| **34D region:** | | | |
| *Df(2L)64j, Adh$^{n1}$ L2* | 34D1-34D2; 35B9-35C1 | *l(2)34Db-l(2)35Cf* | Ashburner *et al.* 1982 |
| *Df(2L)b87e25* | 34C1;35C1 | *kuz-vas* | Alexandrov and Alexandrova 1991 |
| *Df(2L)b80c1, b80c1 noc$^{Sco}$* | 34D3;34E2 | *l(2)34Db-Ance* | Ashburner *et al.* 1982 |
| *In(2LR)b81a2* | 34D5;34D8;41E1 | *b-tam* | Alexandrov and Alexandrova 1986 |
| *In(2L)b81l7* | 34D4;34D4-34D5;40F | *l(2)34Db-b* | Alexandrov and Alexandrova1986 |
| *Df(2L)b81a2$^{LA80R}$, cn bw* | 34D5;35A3.4 | *b-pu* | Unpublished results, John Roote |
| *In(2L)b82c44* | 34D4;34D4-34D5;40h | *Sos-b* | Alexandrov and Alexandrova 1986 |
| *Df(2L)b85b2* | 34D4;34D8 | *b-tam* | Alexandrov and Alexandrova 1986 |
| *Df(2L)b88b42* | 34D4-34D6;34D8 | *b-tam* | Alexandrov and Alexandrova 1991 |
| *In(2L)b83b22* | 34D4;34D4-34D6;35B10 | *b-tam* | Alexandrov and Alexandrova 1986 |
| *In(2L)b79h1A* | 34D4;34D8;40E | *l(2)34Db-tam* | Alexandrov and Alexandrova 1991 |
| *b$^{1}$ tam$^{2}$ Adh$^{n4}$* | 34D8-34D8 | | Woodruff and Ashburner 1979 |
| *b$^{1}$ tam$^{3}$ Adh$^{n4}$* | 34D8-34D8 | | Woodruff and Ashburner 1979 |
| *b$^{1}$ tam$^{4}$ Adh$^{n2}$ pr cn* | 34D8-34D8 | | Woodruff and Ashburner 1979 |
| *tam $^{9}$* | ---------- | | This study |
| *kuz$^{3}$* | 34C7-34C7 | | Unpublished data, John Roote |
| *l(2)34Db$^{3}$ b$^{1}$ Adh$^{n2}$ pr$^{1}$ cn$^{1}$* | 34D4-34D4 | | Woodruff and Ashburner 1979 |
| *l(2)Sop2 Adh$^{D}$ pr$^{1}$ cn$^{1}$* | 34D8-34E1 | | Gubb *et al.* 1984 |
| *In(2LR)Gla, Gla l(2)34De$^{2}$* | 34D8-34D8 | | Woodruff and Ashburner 1979 |
| *b$^{1}$ l(2)34Df$^{2}$ el rds pr$^{1}$ cn$^{1}$* | 34D8-34D8 | | Alexandrov and Alexandrova 1996 |
| *b$^{1}$ l(2)34Dg$^{1}$ Adh$^{n4}$* | 34D8-34D8 | | Ashburner *et al.* 1982 |
| *b$^{1}$ Sos$^{34Ea-6}$ Adh$^{n4}$* | 34D4-34D4 | | Woodruff and Ashburner 1979 |
| *l(2)34De$^{1}$ Adh$^{UF}$ rds* | 34D8-34D8 | | Woodruff and Ashburner 1979 |
| **35B region:** | | | |
| *Df(2L)TE35BC-24, b$^{1}$ pr$^{1}$ pk$^{1}$ cn$^{1}$ sp$^{1}$* | 35B4-B6;35E1-35E2 | | Gubb *et al.* 1984 |
| *In(2LR)Gla, Gla$^{1}$ l(2)34De$^{2}$ l(2)35Bb$^{6}$* | 35B4-35B4 | | Woodruff and Ashburner 1979 |
| *b $^{1}$ Adh$^{D}$ l(2)35Bc$^{2}$ pr$^{1}$ cn$^{1}$* | 35B4-35B4 | | Woodruff and Ashburner 1979 |
| *b$^{1}$ l(2)35Be$^{1}$ pr$^{1}$* | 35B4-35B4 | | Woodruff and Ashburner 1979 |
| *b$^{1}$ Adh$^{n4}$ l(2)35Bf$^{5}$* | 35B4-35B4 | | Woodruff and Ashburner 1979 |
| *Adh$^{D}$ l(2)35Bg$^{2}$ pr$^{1}$ cn$^{1}$* | 35B10-35B10 | | O'Donell *et al.* 1977 |
| *Adh$^{UF}$ Su(H)$^{8}$ cn$^{1}$* | 35B10-35B10 | | Woodruff and Ashburner 1979 |

Table 1 contd.

**Miscellaneous chromosomes**

| | |
|---|---|
| *b*$^{1}$ *pr*$^{1}$ *c*$^{1}$ *px*$^{1}$ *sp*$^{1}$<br>Stock Center | Bloomington |
| *CyO, l(2)DTS513*$^{1}$<br>Stock Center | Bloomington |
| *CyO, Dp(1;2)y*$^{+}$<br>1993 | Mardahl *et al.*, |
| *b Adh*$^{n2}$ *pr cn / (In (2LR)O, Cy dp*$^{1v1}$ *pr cn*$^{2}$)<br>Roote | Donor John |
| **#2-68** - *b Adh*$^{n4}$ *pr cn / (In (2LR)O, Cy dp*$^{1v1}$ *pr cn*$^{2}$)<br>Roote | Donor John |
| **#2-46** - *Adh*$^{uf3}$ *l(2)35Bd*$^{sf6}$ *rd*$^{s}$ *pr cn / In(2LR)O, Cy dp*$^{1v1}$ *pr cn*<br>Roote | Donor John |
| #23-42 *T(2;3)SM5a TM6B, al*$^{2}$ *Cy, Lt*$^{v}$ *cn*$^{2}$ *sp*$^{2}$ *Hu Tu e* (a.k.a TSTL)<br>Roote | Donor John |

# Chapter 4

## Development of larval photobehaviour paradigms and screening for mutations that affect larval response to light

**Abstract**

We are interested in unraveling the genetic basis of larval aversion response to light stimulus. In *Drosophila*, mutational approaches to identify individual genes that contribute to a behavioural trait have been very successful. Larval behavioural paradigms, especially photobehavioural assays at the time when we commenced this project were unreliable. This motivated us to standardize an existing population behaviour paradigm while we conceptualized and implemented individual larval assays. The individual larval assays were used in greater detail to examine larval photobehaviour using pre-existing mutants as well as other genetic tools. Finally, as an improvement of one such assay, we have developed a semi-automated tracking setup that can expedite screening of mutant larvae for studying response to light stimulation.

## Introduction

The *Drosophila* larva is a burrowing animal that completes its larva stages while feeding on rotting fruits in nature. During the larval stages digging and locomotory behaviours are essential for survival. Besides aiding in feeding the ability to dig and burrow also allows evasion from predators like *Leptopilina heterotoma* (Hymenoptera: Eucoilidae) which use the *Drosophila* larvae to incubate their eggs (Fleury et al. 1995).

The motor behaviours of the larva are mediated by the larval body wall that acts as a hydrostatic skeleton. This skeleton is reinforced by segmental iterated pattern of musculature (Casey 1991). The feeding behaviour involves rhythmic activity of pharyngeal muscles and the locomotory behaviour involves coordinated peristaltic muscular contractile waves along the body (Elder 1980, Gorczyca et al. 1991, Berrigan and Pepin 1995). In some species of fruit flies like the Medfly, the larva can also perform up to 12 cm jumps by generating an elastic strain by bending followed by release of this strain; this aids in dispersal for pupation (Maitland 1992).

One of the main source of propulsion and traction for a *D. melanogaster* larva during linear peristaltic locomotion comes from abdominal (A1-A7) segments. Each hemisegment consists of 30 muscles innervated by 34 motor neurons, whose development has been extensively studied (Akam 1987, Keshishian et al. 1994, Bate et al. 1999).

The *Drosophila* larval locomotory rhythm is generated at approximately 1Hz, one complete peristaltic wave per second during linear bout of locomotion (Berrigan and Pepin 1995). So far, the study of genetic basis of larval behaviours have involved selection strategies, quantitative trait loci (QTL) mapping techniques and mutagenesis approaches (Sewell et al. 1974, Godoy-Herrera 1978, Sokolowski 1980, Thompson et al. 1983, Kernan et .al 1994). One of the highlights of a QTL approach was the identification of a polymorphism in a single locus called *foraging*. This locus determines whether a larva will crawl farther in the presence of food source. The $for^{Rover}$ allele exhibits a longer tracks than the $for^{Sitter}$ allele ( Sokolowski 1980, Sokolowski and Hansell 1992).

Using a mutagenesis approach, single gene mutations have been isolated that severely affect linear locomotion of larva. For example, mutations in the *scribbler* gene induce abnormal turning behaviour in larvae (Yang et al. 2000). Interestingly, *scribbler* mutant larvae do not display this abnormal behaviour on a substrate that contains a thin layer of yeast paste. It was also demonstrated that *scribbler* gene product is required in the nervous system in order to rescue this behaviour deficit (Yang et al. 2000). More recently a mutagenesis approach has been used to screen a set of lethal mutants that showed sluggish locomotion. A single mutant named *turtle* was isolated that showed abnormal motor control in larvae. *turtle* mutant larvae displayed lower contractile

peristaltic waves per unit time during locomotion and marked abnormality in righting response of the larva in a roll over test (Bodily et al. 2001).

Mutations in genes that code for ion channels have been well studied at the nerve excitability level (Wu and Ganetsky 1992). Although many mutants of ion channels cause adult behavioural defects when challenged their role in locomotion has not been investigated. For example, mutations in the *paralytic* locus that codes for $Na^+$ channel causes paralysis of adult flies above 29° C (Suzuki et al. 1971, Loughney et al. 1989) and mutations in the *Hyperkinetic* gene that codes for $K^+$ channel β-subunit, causes adult leg shaking under anesthesia (Chounard 1995, Wang and Wu 1995). These two ion channel mutations appear to affect larval locomotory behaviour differently. *Hk* mutant displays longer bouts of linear locomotion and decreased change in direction as compared to *para* mutant larva, that shows shorter linear path interspersed with longer pauses (Wang et al. 1997). In a similar study a mutation in calcium calmodulin gene has been reported to result in larvae whose locomotion mostly consists of spontaneous reverse contractile waves that lead to backward locomotion (Nelson et al. 1997).

Many studies have also used the developing neuromuscular system to reveal genes that participate in building the motor apparatus (Bate et al. 1999, Landgraf et al. 1997). Recently, an in vitro preparation of the larval motor system was used to investigate the neural control of larval motor pattern generators. This study indicated

that the control of larval motor rhythmicity resided in the brain hemispheres and not in the ventral cord region. Further, using a pharmacological antagonists it was also demonstrated that the control is mediated through NMDA-like receptors (Cattaert and Birman 2001).

The study of larval sensory modalities and the response of the larva to sensory stimulations have also been exploited for identifying genes that affect nervous system function. For example, a mechanical touch stimulation on the anterior region of the larva will produce a reverse contractile wave along its body. This paradigm has been used very successfully to identify genes that are involved in mechanotransduction in the larva (Kernan et al. 1994). Such a screen isolated a mutant called *nompA* whose gene product is required for maintenance of contact between sensory nerve endings and cuticular structures (Chung et al. 2001). Larvae also respond to sensory modalities like odor and taste (Ayub et al. 1990, Miyakawa 1982, reviewed in Carlson 1996). The use of this paradigm has resulted in isolation of mutations that affect chemosensory behaviour (Rodrigues et al. 1991, Carlson 1996, Park et al. 1997,). For example, mutations in a gene named *Voila* was isolated as a transposon insert that showed expression in larval taste sensilla, and the pharynx. *Voila* mutant larvae do not exhibit a behavioural response to NaCl and sucrose (Balakireva et al. 1998). The subsets of sensory neurons that mediate

chemosensation have also been characterized in the larva through the use of *in vivo* ablation approaches (Heimbeck et al 1999).

In summary, these studies show the validity of this developmental stage to identify the genes that participate in both sensory and motor functions of the larva.

**Larval response to light in Diptera**

The very first study of a Dipteran larval response to light was conducted on *Lucilia caesar* by Pouchet, french biologist (Pouchet 1872). He observed that the larvae that infest rotting flesh surfaced during the night from their burrows. He then experimentally demonstrated that the larvae showed photonegative behaviour to light. Pouchet also conducted superficial ablation experiments at the anterior end of the larva using mercuric chloride application to investigate their photonegative response to light, although he was not successful in abrogating the response (Pouchet 1872).

The next historical use of larval photobehaviour appears to be central to the origins of the study of animal behaviour itself. This is substantiated by the theory of tropism as proposed by Jacques Loeb (1859-1924). This theory is considered to be central to the development of an objective and mechanistic approach to psychology and acceptance of animal behaviour (or "behaviourism") in the field of psychology. Thus was also born comparative psychology (Wozniak 1993).

The tropism theory proposed that observable behaviours of organisms "as a whole" are due to the influence of the activity of sensory receptors on organs of locomotion, which Loeb described as the basis of reflexes. He further elaborated that these aspects of behaviour are entirely grounded in the physicochemical nature of the system. A watershed proposal at the time that left behind the vague constructs of "free will" and tried to describe animal behaviour through mechanisms that generate forced movements. The basis of this theory stems from behavioural experiments that he designed using simpler animals like the Dipteran blowfly larva. Loeb's experiments used natural sunlight as stimulation on these larva to demonstrate a photonegative response. His experimental design consisted of subjecting the larva to sunlight as a source of stimulation. He placed a larva in front of a window that allowed natural sunlight at one end of a test tube and diffuse light from the sky at another, divided by a narrow beam of shadow cast by a window pane. In his own words – "When animals crossed the boundary from diffuse light into direct sunlight, the reaction caused by the increase in the intensity of the light did not take place until a half or a third of the body was in the sunlight (because all phenomena of stimulation some time elapses between the application of the stimulus and the reaction to it). The animal checked its movement and turned its head through an angle of 90 – 130 from side to side. If in so doing the head again and again came into the shade the animal returned to shade, but if this did

not happen, as was more usually the case, the animal continued its movement into the sunlight." (Loeb 1890, translated from German by Mast 1911). Thus Loeb summarized that the larva responds to change in intensity of light that is mediated by the anterior end of the larva. He also suggested that the net orientation response is due to increased activity on the side of the larva that receives higher light intensity. Although he alluded to directionality of stimulus being discernible by the animal he did not subscribe to the view that any single dedicated organ may be involved in this process.

Mast began studies based on Loeb's hypothesis by asking whether larval locomotory rate would increase when one increases light intensity laterally from both sides of the larva. The outcome of these experiments did not support Loeb's hypothesis that asymmetrical stimulation controls locomotory activity of the larva and the net orientation response. Mast, further described the larval orientation behaviour as sampling of light intensities in a temporal manner, which is aided by the articulation of larval head while it continued to crawl. He suggested that this behaviour can be explained through the assumption that the anterior end of the larva consists of "a small mass of substance located in the middle of the very tip of the anterior end". Further work on whether the larva can discern directionality of stimulus continued to be debated as the speculations about various anterior structures of the larva especially the dorsal papillae as light sensitive organs continued without any conclusions.

In 1946 Bolwig comprehensively reviewed the current knowledge of the larval response to light and also described the sense organs of the anterior end of the common housefly larva (Bolwig 1946). Bolwig adopted a systematic strategy to rule out other sensory structures that were speculated to be the larval photoreceptors. He performed microsurgical ablation of the cephalic lobes using a silk thread followed by a behaviour test to observe larval response to light. He discovered that the damage to the cephalopharyngeal skeleton (the mouth hook) caused failure to respond to light as well as dissection of regions immediately posterior to the mouth hook causes larval blindness. Further, using histological sections of the cephalopharyngeal region he was able to identify the location of a putative bilaterally-symmetrical visual organs. They resided "in a pair of pockets" anteriorly placed with respect to the cephalopharyngeal skeleton and appeared to project neuronal bundles posteriorly. Bolwig further demonstrated that the common housefly larvae showed peak behavioural sensitivity to green wavelengths (~520 nm) of the visible spectrum. As an acknowledgement of Bolwig's work, in *Drosophila* the larval visual system is named – The Bolwig's Organ (BO).

**Development of the Bolwig's Organ**

The morphology of the mature larval visual system is a simple one as compared to the adult. The larval photoreceptors are bilaterally symmetrical clusters made up of 12 photoreceptors on each side of the cephalopharyngeal skeleton. They form an individual neuronal bundle which connects to the larval brain hemispheres through a stereotypic projection pattern (Campos et al 1995). As one traces this simple projection from the photoreceptor cluster towards the posterior direction, the Bolwig's nerve bundle takes a characteristic route ventrally along the surface of the brain hemisphere. It enters the brain hemisphere through the optic lobe primordium to make synaptic connections with the hereto unidentified partners in the central brain (Green et al. 1993, Campos et al. 1995).

Two different aspects have been explored in studying the development of this visual system. The first one, mainly deals with elucidating the neuronal pathfinding events by the Bolwig's nerve in the developing embryo (Green et al. 1995, Campos et al. 1995, Schmucker et al. 1997). Another group of studies, more recently have focused on the genetic basis of cellular interactions among the developing larva photoreceptor clusters (Green et al. 1995, Daniel et al. 1999, Suzuki and Saigo 2000, Chang et al. 2001). Both directions of study have used mutations that affect the developmental processes very effectively.

**Morphogenesis and genetic control of BO formation**

Prior to the onset of gastrulation, the fly embryo is characterized by stereotypically positioned mitotic domains. These domains are defined by groups of cells that undergo cell division in synchrony (Foe 1989). One of these domains numbered as domain 20 resides in the procephalic neurogenic region and gives rise to the visual primordium (Namba and Minden 1999). Procephalic neurogenic region can also be further described by distinct morphogenetic movements and overlapping patterns of gene expression. Cells in the anterior region of the procephalic neurogenic region delaminates to give rise to the brain precusors.

The domain 20 which gives rise to optic placode is a tightly packed group of ~80 cells that is in the posterior part of this region **(Figure 2A)**. This region invaginates from the ectodermal layer to give rise to the optic lobe primordium. Two genes namely *sine oculis*(*so*) and *tailless*(*tll*) are expressed in this placode, both of which code for transcription factors (Cheyette 199, Rudolph 1997). This region can be identifiable by the expression of *fasciclinII* gene whose product codes for a cell adhesion molecule (Hartenstein and Campos Ortega 1985). The optic placode after invagination forms the optic lobe primordium. Lack of *so* gene product results in failure to invaginate (Cheyette et al. 1994).

Brain morphogenesis is completed before the invagination takes place. Thus the invagination places the optic lobe primordium in contact with the brain. The ventral most part of the optic placode contains a few cells that expresses the *atonal* gene even before the placode invagination takes place. *atonal* is a pro-neural gene that codes for bHLH transctiption factor (Daniel et al. 1999). These founder cells appear to recruit neighbouring cells to adopt BO fate, as the expression profile of this gene has been described to be dynamic until all the 12 cells express this gene (Daniel et al. 1999, Suzuki and Saigo 2000). In *so* and *eyes absent* (*eya*) mutant embryos *atonal* (*ato*) expression is absent. It was also demonstrated that ectopic expression of either *so* or *eya* does induce *atonal and Kruppel* expression in the head segment (Suzuki and Saigo 2000). *Kruppel* transcription factor is considered to be a late stage marker in BO development (Schmucker et al. 1992). *atonal* expression also precedes neuronal differentiation as indicated by *elav* immunoreactivity within this region. Thus *so* and *eya* appear to be necessary for *atonal* expression, which in turn defines the Bolwig's organ primordium (BOP).

The recruitment by founder cells of BO appears to be mediated by mediated by Rhomboid and Spitz (Daniel et al. 1999). This is inferred from *spi* and *rho* mutant embryos where only 3-4 photoreceptors are formed (Daniel et al. 1999). In the same study the *argos* and *pointed* gene were also shown to be expressed in all photoreceptor

cells at a later stage. Thus the EGFR pathway appears to be involved in recruitment of larval photoreceptors through perhaps suppression of cell death akin to cell number control described in midline glial cells (Lanoue and Jacobs 1999, Jacobs 2000).

Hegdgehog is a diffusible signal and cells that express this gene reside in an ocular stripe that lies antero-dorsally to the Bolwig's Organ precursors (BOP). *hedgehog* mutant embryos lack *ato* and *Kr* expression suggesting that Hh may induce cells in BOP to express *atonal* (Suzuki and Saigo 2000). Loss of *hh* expression also results in complete absence of visual primordium (Chang et al. 2001). Consistent with these results, misexpression of Hh in the head ectodermal results in supernumerary BO neurons (Suzuki and Saigo 2000).

*Dpp* is another diffusible signal that is involved in patterning of the head segment. The expression of *so* and *eya* in the visual primordium is dependent on *decapentaplegic* (*dpp*) expression (Chang et al. 2001). Inferences from these studies so far support a model in which *dpp* expression first patterns the visual primordium through *so* and *eya* expression. *Hh* expression from the adjacent ocular stripe induces *atonal* expression in a competent cluster of cells in the ventral tip of the primordium.

The Bolwig's organ primordium is also characterized by the absence of *tll* expression. In *tailless* mutant embryos the whole placode adopts the BO fate and the expression of *so* appears to be absent (Daniel et al. 1999). Consistent with this the

overexpression of *tll* using a heat shock promoter results in suppression of BO fate in the placode (Daniel et al. 1999). Thus *tll* expression counters the patterning signal initiated by the Hh signal.

Bolwig's organ development finally results in a contiguous group of 12 cells, organized in two tiers (7 upper cells in rosette pattern and 5 lower) (Green et al. 1993). This "dome-shaped" group of cells maintains contact with the head epithelium even during the head involution process and stays attached with what later becomes the dorsal pouch. Dorsal pouch is a thin epithelium that surrounds the pharyngeal muscles. Due to head involution the BO now is placed laterally with their apical end pointing the anterior. No support cells or pigment cells are seen in BO during the development of the optic placode (Green et al. 1993). As larval development proceeds the BO cluster is gradually pulled away from the optic lobe primordium while the BO axons continue to elongate while staying connected with the larval brain and thus a final morphology is established (**Figure 2 B**). This may perhaps be due to the anchoring of photoreceptor clusters on one end.

**Bolwig's nerve pathfinding in the developing brain:**

The uniqueness Bolwig's organ development is that while it extends its neurites towards the brain to connect with the target area, the whole nerve bundle also elongates

as morphogenesis of the head displaces the photoreceptor cluster (Steller et al. 1987, Green et al. 1993, Schmucker et al. 1997, Campos et al. 1995).

At the onset of differentiation the neurons of the BO are relatively close to their target area (Green et al 1993 ). One pioneer neuron undertakes the pathfinding journey first among the differentiating cluster, and is joined later by the others (Schmucker et al. 1997). During outgrowth, the pioneer neurons interact with identified cells in the optic lobe primordium that in turn appear to provide directional cues for reaching the target area (Tix et al. 1989, Campos et al. 1995). One such interaction occurs with optic lobe pioneer (OLP) neurons (Tix et al. 1989). A set of OLPs (corner OLPs) situated very close to attachment point of the optic stalk within the optic lobe primordium interacts with the pioneer neurons first. There also appears to be yet another set of OLPs called central OLPs that reside deeper in the brain. This cluster is characterized by a single neuron that expresses *brain-specific homeobox (bsh)* gene (Jones and McGinnis 1993, Campos et al. 1995, Schmucker 1997). LON fasciculates with the corner OLPs (Campos et al. 1995). Corner OLPs together with LON pioneers project medially towards the central OLPs (P2 in Schmucker et al. 1997) where they have been described to "stall" upon arrival. Authors describe that this stalling allows all the 12 photoreceptor neurons to arrive following which LON is directed to reach its terminus (Schmucker et al. 1997).

LON projection defects due to mutations in two genes provide us with further clues regarding guidance interactions. The *disconnected* (*disco*) and *Kruppel* (*Kr*) both genes encode transcriptional regulators (Schmucker et al. 1992, Steller et al. 1987). *Kr* is expressed in BO , while *disco* is expressed in the glial cells that are in close association with LON in the optic stalk, corner and central OLP cells (Campos et al. 1995). In *disco* mutants two different kinds of phenotypes called the "connected" and the "unconnected" are observed with respect to BO connectivity. In the connected category the Bolwig's nerve appears to connect with in its target area appropriately but after the head involution stage the connection is not maintained. In the unconnected category the nerve projects to an abnormal and ectopic location of the optic lobe (Steller et al. 1987). In *disco* mutant embryos the glial cells appear abnormal and the corner OLP cells cannot be visualized (Campos et al. 1995). This observation supports the notion that the corner OLPs guide the LON to the target area through perhaps a cell autonomous requirement of Disco function. A mutation in a photoreceptor specific gene called *glass* allow OLPs to develop normally, suggesting that OLP development is not dependent on LON projection (Campos et al. 1995).

Loss of function mutations in the *Kruppel* gene also causes severe defects in BO development (Schmucker et al. 1992). The majority of the embryos display photoreceptor clusters that contain only 6 cells with abnormal terminations. Also

embryos carrying weaker alleles contain ~8 photoreceptors, abnormal fasciculation and abnormal branching in the target area, suggesting that $Kr^{+}$ gene product functions in many aspects of BO connectivity and maintenance.

Two separate genetic screens have been undertaken so far to isolate mutations that disrupt this projection pattern (Schmucker et al. 1997, Holmes et al. 1998). Schmucker and colleagues used a collection of 2800 of EMS generated mutations and a collection of 300 chromosome P-transposon mediated insertional mutations. Although mutations were identified that affected photoreceptor numbers, 13 mutations were studied that belonged to two categories with respect to their BO phenotype. In one category the integrity and projection of BO was affected and in the other category only the projection pattern was disrupted. For example, in *alf* mutant embryos a subset of photoreceptor cluster is not held together and projects abnormally. As another example in the latter category, in *pkl* mutants the projection does not stop at the normal terminus but goes further beyond. Defasiculation of the nerve bundle was a consistent feature in all mutations isolated. In yet another independent screen Holmes and colleagues identified 11 mutations in the second and 13 mutations in the X chromosome that affect BO development. These mutations similarly affect larval photoreceptor cluster differentiation and integrity, projection defects, fasciculation and LON elongation. The

molecular identity of these mutations together with the their expression pattern will allow us to unravel the molecular interactions that control Bolwig's organ development.

**Genetic dissection of larval response to light**

At the time when we began to consider using larval photobehaviour assays for a genetic screen, few studies had explored its genetic basis. However it was also recognized that genes which were previously isolated in screens that used adult visual system through behaviour paradigms and electroretinogram may also function in the larva. One of the first attempts that tried to address this issue began with a categorization of genes (Hotta and Keng 1984). The three categories considered were: mutations the affected only the adult visual system function, mutations that affected larval visual system function while also affect the adult and finally mutations that only affected larval visual behaviour. For example, *norpA* gene that codes for phospholipase C, *rdgA* and *rdgB* genes that cause retinal degeneration were reported to affect both visual systems, while *tanA, so, sev, ora* appeared to affect only adult visual function. In the same study, an X-linked gene named *lph* or larval non-phototactic was shown to affect only larval visual behaviour (Hotta and Keng 1984).

Besides the above study one other genetic screen is of note. An X-linked mutant called *lphA* was isolated that showed larval stage specific abnormal photoresponse

(Gordesky-Gold et al. 1995). Mutations in this locus appeared not to affect any other sensory modalities.

Clues to the nature of light perception by the larva also comes from various opsin genes that are expressed in BO. Out of 4 opsin genes expressed in the adult visual system 3 were reported to be expressed in the larva (Pollack and Benzer 1988). Together with colleagues in the Desplan lab (NYU) we have shown recently that Rh5 and Rh6 are expressed in BO whereas the predominant adult opsin Rh1 is not expressed in this visual system (**Appendix I**). This suggests that the larva can perceive the blue-green part of the visual spectrum. Further, the blue wavelength sensitive Rh5 opsin appears to mediate the photonegative response (Hassan et al. Unpublished results). Ablation or silencing of photoreceptor neurons using an Rh5 promoter and not the Rh6 promoter abolishes the photonegative behaviour (Hassan et al., unpublished results).

In summary, gene products that participate larval response to light can be considered to operate through a variety means. These may include genes that affect development of BO or genes that affect phototransduction or mutations that affect the development of CNS or the neuromuscular apparatus.

In this chapter, we described our first comprehensive foray into the development and standardization of larval photobehavioural paradigms. Previous attempts at using larval photobehaviour paradigms to observe the consequence of mutations in genes

affecting adult visual system were not sensitive (Sawin-Mccormack et al. 1995). These experiments were conducted using larval culture media that were found to be deficient in vitamin A. For example, mutation in the *norpA* gene was not reported to affect larval photobehaviou

r under these conditions. The experiments described in this chapter were primarily directed towards establishing assays that will be optimized for maximum response to expeditiously screen new mutations that affect larval response to light. Additionally, to that end we have developed a semi-automated assay system, and we demonstrate it by conducting a pilot screen. As a direct consequence of the following experiments and the two behaviour paradigms that were developed in this study we have been able to describe the behaviour phenotypes of mutants more accurately. A larger and more comprehensive screen that uses this paradigm is currently under way (Nadia Scantlebury unpublished results).

## Results

### I. Plate assay and optimization of response

#### A. Vitamin A is necessary for optimal photoresponse in *Drosophila* larva

Vitamin A deficiency in adult *Drosophila* has been shown to result in loss of mature opsin pigments (Harris and Stark 1977). The lack of opsin also greatly reduces visual sensitivity in ERG experiments (Chen and Stark 1992). Such reduction in sensitivity can be attributed to lack of functional opsin or even loss of transcription of opsin itself (Picking et al. 1996).

Before adopting a photobehavioural assay for screening mutations that affect visual response it was necessary to verify whether vitamin A was available in the culture medium of the larvae. We considered the plate assay for studying photobehaviour in the *Drosophila* third instar larvae (Lilly and Carlson 1990, **Figure 3**). Preliminary experiments using the wild type strains namely, Canton-S and $ry5^{+}$ yielded a response index of 0.4-0.6. This response is too minimal to allow us to detect partial lack of function (hypomorphic response) to light. Upon studying the ingredients of the larval culture medium I noticed that the medium was deficient in a source for Vitamin A. Supplementation of β-carotene at a dosage of 1.25 g/lit. medium (Ashburner M 1989) resulted in a significant improvement of response to light in the plate assay (**Figure 4**).

The improvement in response was further demonstrated by testing larvae that were grown in a synthetic Sang's minimal medium (kindly provided by Bill Stark) (Sang 1956) (**Figure 5**). Larvae cultured in Sang's medium without supplementation of β-carotene displayed significantly reduced response to light as compared with larvae cultured in Sang's medium supplemented with β-carotene.

**B. Sensitivity and response kinetics of larval response to light in the plate assay.**

For this experiment we used various neutral density filters (Lee Filters) to obtain a series of light throughput from the light-box (Hall Productions, Model BL-1824 with 2 General Electric's fluorescent lamps at 15W each, "Cool White" type) and on to the test plate. The filters were placed between the light box and the plate and the intensity was measured on the surface of the agar on the plate. The light intensity was measured using a visual range photometer ( Photodyne Inc. Opticon 88XLA, Kindly provided by Dr. Alexander Ball). The light throughput on the plate without any filters was 340 μW per $cm^2$. The photometer that was used did not measure luminance in terms of SI units (eg. lux or candelas/$m^2$).

The plate assay is conducted in an arena (the plate) that is placed over a light box. The light stimulation for the assay is provided by 2 fluorescent lamps inside the light box. Towards establishing conditions for an optimal response to light, first, effect

of lower light intensities on response was tested in the plate assay. This was conducted by using a combination of neutral density filters (Lee Filters) and measuring light intensity transmitted through plate. Plate assays were conducted from 5-90 microwatts/$cm^2$ of light intensity. From this experiment it is evident that an optimal response to light can be achieved even at sub-normal intensities (**Figure 6**). The response in the plate assay appears to plateau at 90 microwatt/$cm^2$.

The plate assay is conducted for a duration of five minutes after the larvae have been placed in the middle of the arena. A response index is calculated by counting the larvae that have chosen the light quadrants and the dark quadrants. I evaluated whether this interval of time is sufficient to allow distribution of all larvae. The kinetics of distribution of larvae in the plate during the light was counted every 30 seconds during the experiment by recording the assay using a CCD camera (Elmo, model -TSE272S) and a VCR. The data from this experiment clearly shows that the response of wild type larvae in the plate assay reaches a plateau well before the 5 minute period allocated for the experiment (**Figure 7**).

**II. Single larval assays**

**Checker assay**: The Checker assay was conceived and developed to facilitate testing photoresponse at the single larval level while subjecting a larva to respond to

stationary stimulus boundaries arranged spatially. The design of this experiment drew parallels from experiments that have been described by Bolwig (Bolwig 1946). In his own words –" Quite amusing is a little experiment I carried out: the larvae were allowed to crawl on a sheet of black paper in which was a number of round holes. The paper was illuminated from below. The route taken by larvae was marked with chalk and later reconstructed on a sheet of millimeter paper. The experiment showed that larvae avoided the holes in the paper. This proves that the anterior end of a full grown larva is highly sensitive to light from the ventral side." (Bolwig 1946). Our modification of this makes use of the same petri-plate arena that was used in the plate assay. A checkered template made on a clear glass plate (3 mm thickness) is however placed between the light arena and the plate (see **Appendix G**). This allows light to be transmitted onto the petri-plate in a checkered manner.

Experiments using a single wild type larva in this arena showed that the larval residence time in dark squares is noticeably longer than the light squares. The behaviour at the dark/light boundary and the track pattern of an individual wild type larval movement in the presence and absence of light is shown in **Figure 8 A, B** and **C**, respectively. When the lights are off in the assay a wild type larva typically exhibits a relatively linear locomotory path on the plate. However, when the lightbox is switched on the locomotory behaviour of the larva is already qualitatively distinct as it maneuvers

to remain predominantly in the dark squares. The dark squares appear to induce a higher frequency of turns also known as klinokinetic behaviour. This assay is conducted over a period of 3 min. A response index is calculated by scoring the residence time in the dark with respect to the light squares during the assay. This assay elicits a response index of ~ 0.5 for an Oregon-R wild type strain (**Figure 9**). We also ascertained that the response index in a transgenic stock (*gl-hid*) where the Bolwigs Organ is ablated shows a response index close to zero. Response index reflects the residence time of larva in individual squares. This assay was used in collaboration with Jana Hassan to conduct an action spectra, abolishment of response by complete ablation by targeting a cell death gene to the BO, and also demonstrated that mutations in the Rh1 opsin gene does not affect larval response to light (Hassan et al. 2000, see **Appendix B**).

**On/Off assay**

Initial explorations into designing another individual larval assay was based on qualitative differences in larval path shape with respect to a 5 minute pulse of light and darkness. Larvae exhibited distinct linear locomotory behaviour in response to 5 min of dark pulse and an erratic head swinging and frequent change in direction during 5 min of light pulse (**Figure 10**). This demonstrated that a mostly linear larval locomotion is inhibited in the presence of light. We aimed however to design this assay for faster

analysis of photobehaviour and hence modified the assay to consist of alternating dark and light pulses of 10 sec each. A measurement method was adopted where one compares the total distance traveled in the light pulse against the distance traveled in the dark pulse. The response index for wild type photoresponse clearly showed that the larva responds to light by exhibiting a repulsive behaviour that involves inhibition of locomotion (**Figure 11**). Mutant *norpA* larvae show very low response index corroborating earlier experiments using the plate assay. The larvae were also observed to exhibit brief cessation of locomotion, head swinging and change in direction of movement at the stimulus boundaries (dark/light and light/dark) that is distributed temporally at 10 sec intervals (**Figure 12**). This assay was used in collaboration with Macarena Busto for quantifying subsets of behaviour at the stimulus boundaries. The subsets of behaviours like head swinging and change in direction of movement was used to genetically define the response in known adult visual system mutants (Busto et al. 1999, see **Appendix A**).

The procedure to quantitate response in the On/Off assay is laborious one. Briefly, this methodology for generating movement data consisted of capturing the experiment using a CCD camera to video tape the experiment, followed by replaying from the video tape and producing a hand drawn path tracing by placing a transparency sheet over a TV monitor. The digitized image (flatbed scanner) was then imported into

NIH-Image public domain image analysis software where the path lengths were measured in pixel units. The pixel unit was converted to centimeter units by using an appropriate calibration standard that was also video taped prior to the actual experiment.

We modified the On/Off set up so that the experiment can be conducted with minimal human input and produce response data in an automated and expedited manner.

**III. Automation of the On/Off assay**

We used the Macintosh platform (PowerMac 9500/200), a macro program written in public domain image analysis software called NIH-Image and a tablet peripheral device to generate real-time movement data. The analog video signals from a CCD camera were processed at video rate of ~28 frames per second using the Scion AG-5 frame grabber (Scion Corporation, Maryland USA) (**Figure 13**). A macro program that runs in NIH-Image was written to track the larval movement defined by x, y coordinates of the tracking cursor, time, and distance traveled parameters (see **Appendix J**). To track a moving larva we used the Intuos tablet (Wacom technology co. WA) and stylus connected to the ADB port. This enabled a better control of the cursor which was used to track the tail end of the larva. The most unique aspect of this setup is the interfacing

of a serial device called MacIO microcontroller (MacBrick, Netherlands) to control a relay unit that in turn gates the lights on and lights off 10 sec pulses.

When the macro is executed during live capture, distance data and pulse number is written every 10s in real time in a separate window (Dist/10s) (**Figure 14**). The macro also sends a command to the serial port to control the lights on and off pulse through the MacIO microcontroller. The termination of the programme by a simple click using the stylus button triggers a response index calculation in the same window (**Figrue 14**). Tracking data that includes x, y co-ordinates of the tracking cursor, time and distance traveled is stored in the memory buffer and is invoked in a results window when the macro is stopped. The data in the results window can now be saved as a tab delimited text file and is used to recreate a graphical path tracing with time annotation (**Figure 15**). This semi-automatic tracking design simplifies and expedites the assay procedure considerably, while preserving the accuracy of the tracking procedure. This tracking system performs reliably. **Figure 16** shows the response index and locomotory data for wild type Canton-S, *yw*, and *norpA* larvae. A comparison Canton-S response index using the original labor intensive tracking protocol against the automated procedure shows that the new tracking process reliably reproduces the wild type response index.

We also analyzed larval aversion response which involves inhibition of locomotion and change in direction of movement, in the foraging and wandering stages

of larval development (**Figure 17 A**). Larval response to light begins to decay in the wandering stage. The locomotory behaviour is not noticeably different in these two stages (**Figure 17 B**). These experiments corroborate previous observations that showed that wandering wild type larva are indifferent to light stimulation (Sawin-Mcormack et al. 1995). We have begun to use this system to screen for mutations that affect larval photobehaviour. This setup was also used in collaboration with Boullianne and colleagues to characterize motor behaviour defects of larvae that are mutant for the *amphiphysin* gene. *amphiphysin* gene product is involved in synaptic vesicle endocytosis in *Drosophila* (Leventis et al. 2001, see **Appendix D**).

**IV. Pilot screen for isolating photobehaviour mutants**

Using the semi-automated setup we screened a subset of P-element induced 2nd chromosome lethal stocks that show late larval or pupal lethality. **Figure 18** shows two rounds of screening using homozygous mutant larvae. In round 1 the response indices were plotted against the respective locomotory rates. In order to compare the motor activity while the larvae performed in the On/Off assay we also measured distance traveled in the first 40s of the On/Off assay. In round 2, we screened all larvae that scored response index below 0.15 against their locomotory behaviour during the assay. This enabled us to determine two mutant lines namely 13510 and 16504 that show lower

response index while their locomotion appears to be only partially affected. It is also apparent that strains that display large variations in response to light exhibit poor locomotion. Thus a threshold locomotion is necessary in mutant larvae in order to elicit a true response to light.

## Discussion

Our motivation to use larval photobehaviour as a paradigm is directed towards isolation of mutant animals that are defective in a response pathway. A response pathway can be considered to involve sensory organs that receive light stimulation, the central nervous system that processes this information to trigger the motor apparatus so that the animal can maneuver away from the light source. Foraging *Drosophila* larvae spend most of this developmental stage burrowing inside a food substrate and exhibit an aversion behaviour to light stimulation during this stage. We adopted the plate assay to conduct a screen to identify mutations that affect larval response to light (Lilly and Carlson 1990). In the plate assay larvae distribute with respect to the light and dark quadrants of the plate. The light passing through the two quadrants of the plate affect the locomotion of the larvae such that larvae preferentially distribute mainly in the dark quadrant.

Initial experiments with wild type larvae using the plate assay showed a response index of 0.4 (± 0.08 SEM, $ry5^+$ strain) (70 larvae in the light and 30 in the dark). For a mutant screen we predicted that this response would not allow us to identify hypomorphic responses. The 70/30 distribution is in close proximity to a 50/50 distribution that will only be elicited in blind larvae. Hypothetically, a distribution of 90 in the dark and 10 in the light quadrant (R.I=0.8) will allow us to identify partial loss of function mutations that may result in a response index of 0.4. In other words operating a screen at a wild type 0.4 response index is does not allow a sufficient margin to isolate hypomorphic responses.

In order to elicit an optimal response we investigated whether the larval growth medium contained a vitamin A source. None of the ingredients that were used in the laboratory to make the larval culture medium contained any source of vitamin A. Supplementation of vitamin A by using a commercially available β-carotene tablets resulted in a significantly higher response by the wild type larvae in the plate assay. The effect of vitamin A supplementation on response to light was demonstrated again by culturing larvae in the presence of antibiotics in a synthetic medium. Vitamin A supplementation thus elicited an optimal response of 0.84 (±0.02 SEM) to 0.7 (± 0.04 SEM) in two wild type strains that were tested.

Next we asked whether the 5 minutes testing period in the plate assay is sufficient to reach an optimal response in this assay. Calculation of response indices every 30 seconds showed that the maximum response index of 0.70 is achieved by wildtype larva well before the 5 minute period.

In order to test larval sensitivity to light in the plate assay we used a series of neutral density filters that were placed between the plate and the lightbox. In this experiment the larvae responded in a graded manner. Both wild type strains that were tested showed that a response of 0.7 can be achieved at $1/3^{rd}$ of the light intensity that is projected under normal conditions.

These experiments comprised the initial optimization of the plate assay in order to screen mutations that affect larval behaviour towards light. While we proceeded to conduct a screen using this population assay we also embarked on developing individual larval photo-behavioural assays. The larval distribution in the plate assay can be hypothetically due to modulation of locomotory behaviour such that they move faster in the light quadrant as compared to the dark quadrant (orthokinesis) or the larvae may exhibit an increased rate of change in direction of locomotion in when they encounter light/dark transition (klinokinesis). Observation of individual larval behaviour in the plate assay clearly showed that the larval distribution in the plate assay was mostly due to larval encounter with the dark/light boundary of the quadrants

which appeared to initiate a head swinging and change in direction of locomotion response. In order to exploit this observation at an individual larva level we designed two new assays namely Checker assay and the On/Off assay.

**Single larval assays open *Drosophila* larva for genetic analysis of motor control**

Larval response to light in both the individual larval assays clearly show that light induces a stereotypic pattern of motor response. Upon light stimulation the larva is often seen to cease its locomotion and to contract its head/thoracic segments which is followed often by a head swing that can result in change in direction of locomotion (**Figure 12**).

Both assays that were developed in this study induce motor behaviours that are quantified in different ways. The parameters that are measured in these two assays reflect the most amenable aspect of the response. While the Checker assay subjects the larva to a spatially defined stimulus boundary, the On/Off assay is based on stimuli that are temporally ordered. The response index in the Checker assay is based on the preference of the larva when given a choice between light and dark zones. In this assay the residence time in the preferred dark zone is directly reflected in the response index. The response index in the On/Off assay induces a reflexive behaviour that inhibits locomotion upon light stimulation, and this inhibition is reflected in the calculation of

the response index. This inhibition of linear locomotion followed by higher incidence of turning behaviour in an ecological setting perhaps enables the larva to quickly burrow into a food substrate. Thus in the On/Off assay other aspects of motor behaviour like head swinging and change in direction represent a robust behaviour pattern that enables us to describe various mutants more elaborately (Busto et. al. 1999).

Comparatively speaking the Checker assay design demands more locomotory coordination than the On/Off assay. In other words response index in the Checker assay can be considered to be more sensitive to locomotory deficits. Locomotory mutants will result in an artificially high response index, although this problem can be overcome by conducting the assays in the absence of light. Such a control experiment will enable us to evaluate the effect of basal locomotory deficit on response to light in this assay. This assay has also been used elsewhere to characterize larval behaviour using mutations in gene that affect adult visual function (Hassan et al. 2000, Busto 2000).

It is clear that the larval visual system uses many of the same molecular components that are used by the adult visual system. For example, *norpA* gene product (Phospholipase C) is fundamental is to phototransduction in the adult visual system. Although mutation in this gene causes larval blindness it is to be noted that this transcript is qualitatively different in the larval stages. The larval transcript includes another exon (named 4A) that is absent in adult visual system (Kim et al. 1995).

Correspondingly, the expression of this subtype in R1-R6 photoreceptors in the adult visual system alters the ERG profile of a transgenic line (Shortridge pers. comm.).

Next, a semi-automation of the On/Off assay was successfully accomplished. This setup was tested using a Canton-S wild types strain. The response index of this strain in both these assays are in distinguishable. Consistent with the manual mode of tracking the semi-automated assay also showed that *norpA* mutant larvae are blind to light stimulation. The semi automated assay was also successfully used to demonstrate that a mutant screen for locomotion or visual system function can now be carried out in an expedited manner. This pilot screen for mutant larvae also clearly shows that when motor behaviour is abnormal it affects the measurement of response to light in the On/Off assay. This is evident from the variation in response when larvae suffer from poor locomotion. This experiment allows us to identify a locomotory threshold at ~50 pixles/30s. Larvae that travel less than 50 pixels in 30s cannot be reliably tested for their visual response.

Similar to the absence of an avoidance response to light of *norpA* mutant in the On/Off assay, a genetic ablation of Bolwig's Organ by targeted expression of a cell death gene (*hid*) also results in a blind larva as observed using the Checker assay. Locomotory deficits can also affect response measurement in the Checker assay. For example, larvae that do not move from the first dark square during the entire 3 min interval during the

assay will appear to be extremely aversive to light as their response index will be very high. Wild type larvae do not exhibit such a behaviour. In order to overcome problem, we evaluate visual response only in the context of a control experiment where the larvae are tested in the absence of light. This control experiment allows us to study their basal locomotory behaviour and its impact on visually influenced behaviour. Similar to On/Off assay larvae that are severely impaired in locomotion cannot be tested in the Checker assay.

In conclusion, these two assays are sensitive with respect to the visual system function in the larva, albeit severe locomotory mutants cannot be reliably tested for visual response using these assays. These individual larval assays further allow us to proceed towards high resolution analysis of motor control where shape changes, larval locomotory rhythm, head swinging behaviour and change in direction of locomotion upon light stimulation can be further analyzed. The study of these behaviours at a higher resolution in the context of single gene mutations or reverse genetic approaches will allow us to elucidate the genetic basis of neural control in simple motor behaviours.

## References

Akam, M. 1987. The molecular basis for metameric pattern in the *Drosophila* embryo. *Development* 101:1-22.

Ayyub, C., Paranjape, J., Rodrigues, V., Siddiqi, O. 1990. Genetics of olfactory behaviour in *Drosophila melanogaster*. *J Neurogenet* 6:243-62.

Balakireva, M., Stocker, R. F., Gendre, N., Ferveur, J. F. 1998. Voila, a new *Drosophila* courtship variant that affects the nervous system: behavioural, neural, and genetic characterization. *J Neurosci* 18:4335-43.

Bate, M., Landgraf, M., Ruiz Gomez Bate, M. 1999. Development of larval body wall muscles. *Int Rev Neurobiol* 43:25-44

Bodily, K. D., Morrison, C. M., Renden, R. B., Broadie, K. 2001. A novel member of the Ig superfamily, turtle, is a CNS-specific protein required for coordinated motor control. *J Neurosci* 21:3113-25.

Bolwig, N. Senses and sense organs of the anterior end of the House Fly larvae. 1946 *Vidensk. Medd. Dansk naturhist. For.* 109:81--217

Campos, A. R., Lee, K. J., Steller, H. 1995. Establishment of neuronal connectivity during development of the *Drosophila* larval visual system. *J Neurobiol* 28:313-29.

Casey 1991 Energetics of caterpillar locomotion: Biomechanical constraints of a hydraulic skeleton. *Science*, Vol. 252: 112-114.

Carlson, J. R. 1996. Olfaction in *Drosophila*: from odor to behaviour. *Trends Genet* 12:175-80.

Cattaert, D., Birman, S. 2001. Blockade of the central generator of locomotor rhythm by noncompetitive NMDA receptor antagonists in *Drosophila* larvae. *J Neurobiol* 48:58-73

Chang, T., Mazotta, J., Dumstrei, K., Dumitrescu, A., Hartenstein, V. 2001. Dpp and Hh signaling in the *Drosophila* embryonic eye field. *Development* 128:4691-704.

Chen, D. M., Stark, W. S. 1992. Electrophysiological sensitivity of carotenoid deficient and replaced *Drosophila*. *Vis Neurosci* 9:461-9.

Cheyette, B. N., Green, P. J., Martin, K., Garren, H., Hartenstein, V., Zipursky, S. L. 1994. The *Drosophila* sine oculis locus encodes a homeodomain-containing protein required for the development of the entire visual system. *Neuron* 12:977-96.

Chouinard, S. W., Wilson, G. F., Schlimgen, A. K., Ganetzky, B. 1995. A potassium channel beta subunit related to the aldo-keto reductase superfamily is encoded by the *Drosophila* hyperkinetic locus. *Proc Natl Acad Sci U S A* 92:6763-7.

Chung, Y. D., Zhu, J., Han, Y., Kernan, M. J. 2001. nompA encodes a PNS-specific, ZP domain protein required to connect mechanosensory dendrites to sensory structures. *Neuron* 29:415-28.

Daniel, A., Dumstrei, K., Lengyel, J. A., Hartenstein, V. 1999. The control of cell fate in the embryonic visual system by atonal, tailless and EGFR signaling. *Development* 126:2945-54.

Fleury, F., Allemand, R., Fouillet, P., Bouletreau, M. 1995. Genetic variation in locomotor activity rhythm among populations of Leptopilina heterotoma (Hymenoptera: Eucoilidae), a larval parasitoid of *Drosophila* species. *Behav Genet* 25:81-9.

Foe, V. E. 1989. Mitotic domains reveal early commitment of cells in *Drosophila* embryos. *Development* 107:1-22.

Godoy-Herrera, R. 1978. Selection for digging behaviour in *Drosophila melanogaster* larvae. *Behav Genet* 8:475-9.

Gorczyca, M. G., Budnik, V., White, K., Wu, C. F. 1991. Dual muscarinic and nicotinic action on a motor program in *Drosophila*. *J Neurobiol* 22:391-404.

Green, P., Hartenstein, A. Y., Hartenstein, V. 1993. The embryonic development of the *Drosophila* visual system. *Cell Tissue Res* 273:583-98.

Harris, W. A., Stark, W. S. 1977. Hereditary retinal degeneration in *Drosophila melanogaster*. A mutant defect associated with the phototransduction process. *J Gen Physiol* 69:261-91.

Heimbeck, G., Bugnon, V., Gendre, N., Haberlin, C., Stocker, R. F. 1999. Smell and taste perception in *Drosophila melanogaster* larva: toxin expression studies in chemosensory neurons. *J Neurosci* 19:6599-609.

Holmes, A. L., Raper, R. N., Heilig, J. S. 1998. Genetic analysis of *Drosophila* larval optic nerve development. *Genetics* 148:1189-201.

Jacobs, J. R. 2000. The midline glia of *Drosophila*: a molecular genetic model for the developmental functions of glia. *Prog Neurobiol* 62:475-508.

Jones, B., McGinnis, W. 1993. A new *Drosophila* homeobox gene, *bsh*, is expressed in a subset of brain cells during embryogenesis. *Development* 117:793-806.

Keshishian, H., Chang, T. N., Jarecki, J. 1994. Precision and plasticity during *Drosophila* neuromuscular development. *Faseb J* 8:731-7.

Kim, S., McKay, R. R., Miller, K., Shortridge, R. D. 1995. Multiple subtypes of phospholipase C are encoded by the norpA gene of *Drosophila melanogaster*. *J Biol Chem* 270:14376-82.

Landgraf, M., Bossing, T., Technau, G. M., Bate, M. 1997. The origin, location, and projections of the embryonic abdominal motorneurons of *Drosophila*. *J Neurosci* 17:9642-55.

Lanoue, B. R., Jacobs, J. R. 1999. Rhomboid function in the midline of the *Drosophila* CNS. *Dev Genet* 25:321-30

Lilly, M., Carlson, J. 1990. *smellblind:* a gene required for *Drosophila* olfaction. *Genetics* 124:293-302.

Loughney, K., Kreber, R., Ganetzky, B. 1989. Molecular analysis of the para locus, a sodium channel gene in *Drosophila*. *Cell* 58:1143-54.

Maitland, D. P. 1992. Locomotion by jumping in the mediterranean fruit-fly larva *Ceratitis capitata*. Nature Vol. 355. 159-161.

Mast, S. O. 1911 Light and the behaviour of organisms. New York: John Wiley & Sons, 1911.

Namba, R., Minden, J. S. 1999. Fate mapping of *Drosophila* embryonic mitotic domain 20 reveals that the larval visual system is derived from a subdomain of a few cells. *Dev Biol* 212:465-76.

Nelson, H. B., Heiman, R. G., Bolduc, C., Kovalick, G. E., Whitley, P., et al. 1997. Calmodulin point mutations affect *Drosophila* development and behaviour. *Genetics* 147:1783-98.

Park, Y., Caldwell, M. C., Datta, S. 1997. Mutation of the central nervous system neuroblast proliferation repressor *ana* leads to defects in larval olfactory behaviour. *J Neurobiol* 33:199-211.

Picking, W. L., Chen, D. M., Lee, R. D., Vogt, M. E., Polizzi, J. L., et al. 1996. Control of *Drosophila* opsin gene expression by carotenoids and retinoic acid: northern and western analyses. *Exp Eye Res* 63:493-500.

Pouchet, G. De l'influence de la lumière sur les larves de diptères privées d'organes extèrieures de la vision. 1872. Rev. Mag. Zool. 23, (sèr. 2).

Rodrigues, V., Sathe, S., Pinto, L., Balakrishnan, R., Siddiqi, O. 1991. Closely linked lesions in a region of the X chromosome affect central and peripheral steps in gustatory processing in *Drosophila*. *Mol Gen Genet* 226:265-76.

Rudolph, K. M., Liaw, G. J., Daniel, A., Green, P., Courey, A. J., et al. 1997. Complex regulatory region mediating tailless expression in early embryonic patterning and brain development. *Development* 124:4297-308.

Schmucker, D., Jackle, H., Gaul, U. 1997. Genetic analysis of the larval optic nerve projection in *Drosophila*. *Development* 124:937-48.

Sewell, D., Burnet, B., Connolly, K. 1974. Genetic analysis of larval feeding behaviour in *Drosophila melanogaster*. *Genet Res* 24:163-73.

Sokolowski, M. B. 1980. Foraging strategies of *Drosophila melanogaster*: a chromosomal analysis. *Behav Genet* 10:291-302.

Sokolowski, M. B., Hansell, K. P. 1992. The foraging locus: behavioural tests for normal muscle movement in rover and sitter *Drosophila melanogaster* larvae. *Genetica* 85:205-9

Steller, H., Fischbach, K. F., Rubin, G. M. 1987. Disconnected: a locus required for neuronal pathway formation in the visual system of *Drosophila*. *Cell* 50:1139-53.

Suzuki, T., Saigo, K. 2000. Transcriptional regulation of atonal required for *Drosophila* larval eye development by concerted action of eyes absent, sine oculis and hedgehog signaling independent of fused kinase and cubitus interruptus. *Development* 127:1531-40.

Thompson, J. N., Jr., Schnee, F. B., Seale, T. W. 1983. Polygenic analysis of larval locomotor activity in *Drosophila melanogaster*. *Behav Genet* 13:579-89.

Tix, S., Minden, J. S., Technau, G. M. 1989. Pre-existing neuronal pathways in the developing optic lobes of *Drosophila*. *Development* 105:739-46.

Wang, J. W., Sylwester, A. W., Reed, D., Wu, D. A., Soll, D. R., Wu, C. F. 1997. Morphometric description of the wandering behaviour in *Drosophila* larvae: aberrant locomotion in Na+ and K+ channel mutants revealed by computer-assisted motion analysis. *J Neurogenet* 11:231-54.

Wang, J. W., Wu, C. F. 1996. In vivo functional role of the *Drosophila* hyperkinetic beta subunit in gating and inactivation of Shaker K+ channels. *Biophys J* 71:3167-76.

Wozniak, R. H. 1993. Jacques Loeb, Comparative physiology of the brain, and comparative psychology. In J. Loeb, *Comparative physiology of the brain and comparative psychology* (pp- vii-xxiii). London: Routledge/Thoemmes Press; Toyko: Kinokuniya. (http://www.brynmawr.edu/Acads/Pssych/rwozniak/loeb.html).

Wu, C. F., Ganetzky, B. 1992. Neurogenetic studies of ion channels in *Drosophila*. *Ion Channels* 3:261-314

Yang, P., Shaver, S. A., Hilliker, A. J., Sokolowski, M. B. 2000. Abnormal turning behaviour in *Drosophila* larvae. Identification and molecular analysis of scribbler (sbb). *Genetics* 155:1161-74.

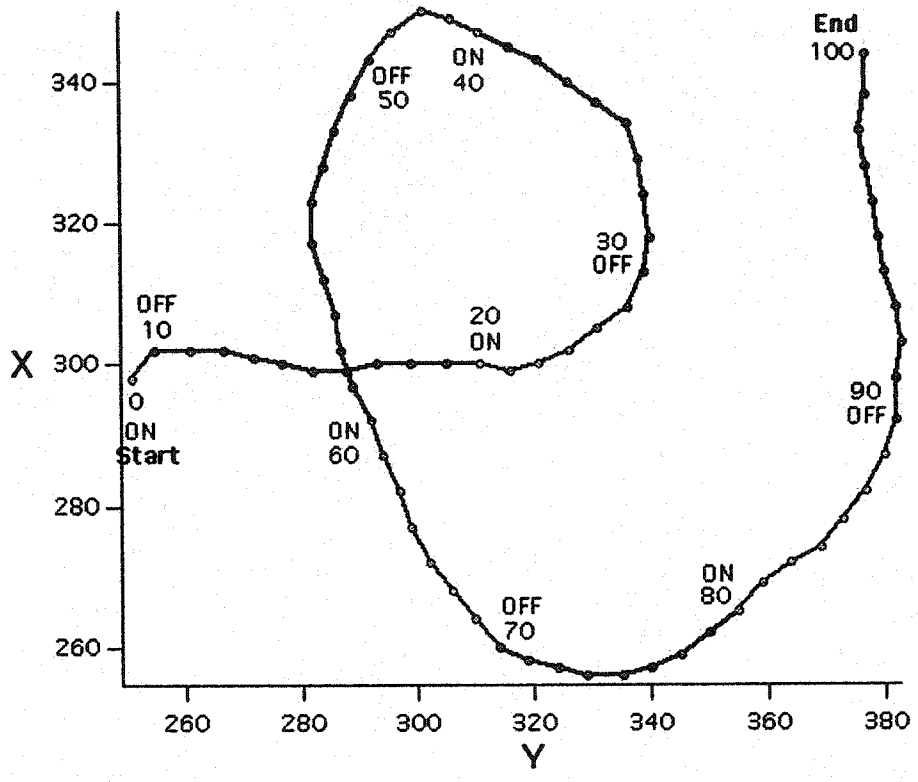
End
100
ON
40
OFF
50
340
320
30
OFF
OFF
10
20
ON
X
300
0
ON
Start
ON
60
90
OFF
280
ON
80
OFF
70
260
260
280
300
320
340
360
380
Y

**Figure 15.**

**Reconstruction and annotation of the On/Off experiment**

X-Y coordinates from the results window (previous figure) were used to reconstruct and annotate the path travelled by the larva during the session. The graphical output was generated through the IGOR-PRO software.

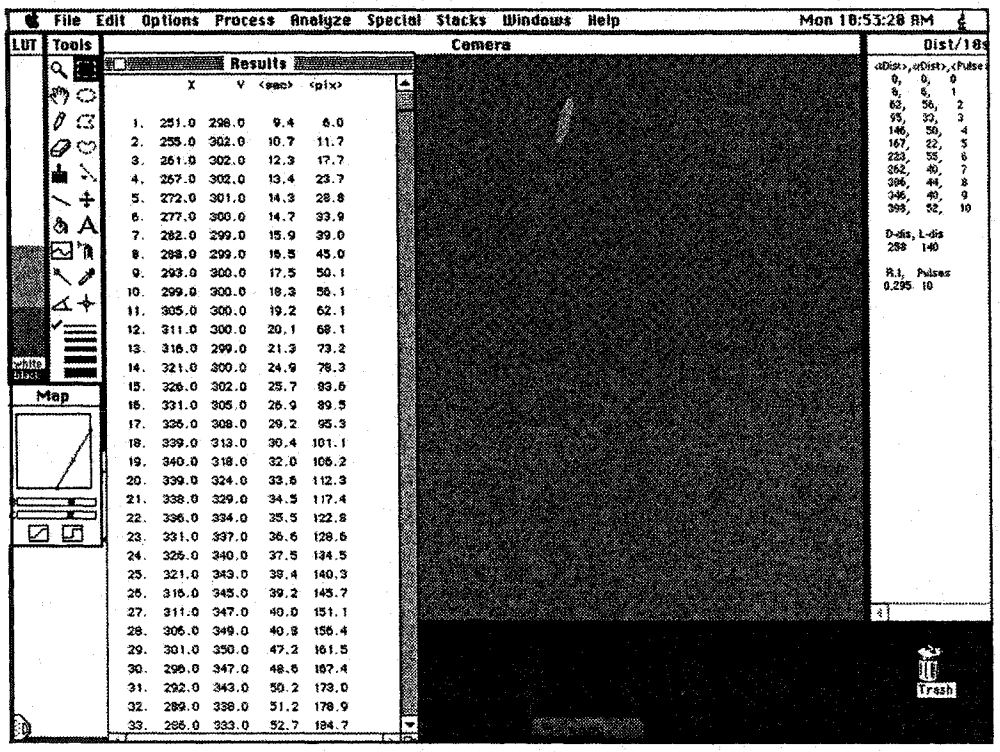
File Edit Options Process Analyze Special Stacks Windows Help
Mon 10:53:28 AM
LUT
Tools
Camera
Dist/10s
Results
X Y <sec> <pix>
1. 251.0 298.0 9.4 6.0
2. 255.0 302.0 10.7 11.7
3. 261.0 302.0 12.3 17.7
4. 267.0 302.0 13.4 23.7
5. 272.0 301.0 14.3 28.8
6. 277.0 300.0 14.7 33.9
7. 282.0 299.0 15.9 39.0
8. 288.0 299.0 16.5 45.0
9. 293.0 300.0 17.5 50.1
10. 299.0 300.0 18.3 56.1
11. 305.0 300.0 19.2 62.1
12. 311.0 300.0 20.1 68.1
13. 316.0 299.0 21.3 73.2
14. 321.0 300.0 24.9 78.3
15. 326.0 302.0 25.7 83.6
16. 331.0 305.0 26.9 89.5
17. 335.0 308.0 29.2 95.3
18. 339.0 313.0 30.4 101.1
19. 340.0 318.0 32.0 106.2
20. 339.0 324.0 33.6 112.3
21. 338.0 329.0 34.5 117.4
22. 336.0 334.0 35.5 122.8
23. 331.0 337.0 36.6 128.6
24. 326.0 340.0 37.5 134.5
25. 321.0 343.0 38.4 140.3
26. 316.0 345.0 39.2 145.7
27. 311.0 347.0 40.0 151.1
28. 306.0 349.0 40.8 156.4
29. 301.0 350.0 47.2 161.5
30. 296.0 347.0 48.6 167.4
31. 292.0 343.0 50.2 173.0
32. 289.0 338.0 51.2 178.9
33. 285.0 333.0 52.7 184.7
Map
Trash

**Figure 14.**

**Screenshot of the semi-automated tracking macro at the end of a tracking session**

The figure shows the camera window, the results window and the dist/10s window. The camera window shows a larva that was being tracked in this particular instance. Cessation of the macro by using the top stylus button produces the results window, that contains all the x-y coordinates of the tracking session. The dist/10s window is triggered to appear at the onset of tracking by pressing the bottom stylus button. This window updates movement data every 10 s coinciding with the lights-on/lights-off pulse. The window also shows total distance traveled (tDist), real distance travelled in 10s (rdist) and the pulse number. Termination of tracking also outputs the calculated response index. The program also converts odd number of pulses to even number of total pulses by eliminating the last pulse value for a sensible calculation of response index. In this instance since 10 pulses were used no corrections are reported.

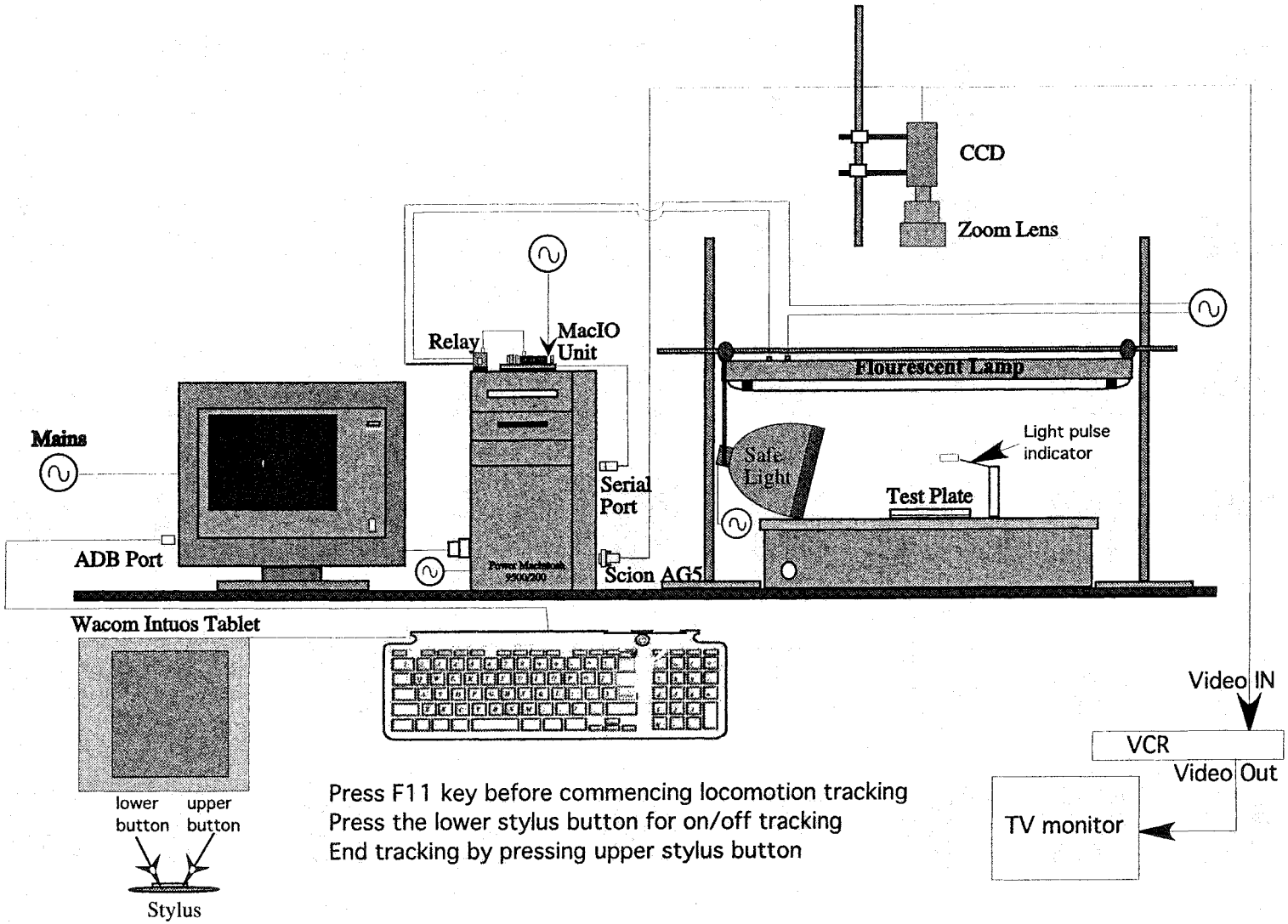
CCD
Zoom Lens
Relay
MacIO Unit
Flourescent Lamp
Mains
Light pulse indicator
Safe Light
Test Plate
Serial Port
ADB Port
Scion AG5
Wacom Intuos Tablet
Video IN
VCR
Video Out
TV monitor
lower button
upper button
Stylus
Press F11 key before commencing locomotion tracking
Press the lower stylus button for on/off tracking
End tracking by pressing upper stylus button

**Figure 13.**

**Schematic presentation of the semi-automated tracking setup**

Please see description in the results section (page 96).

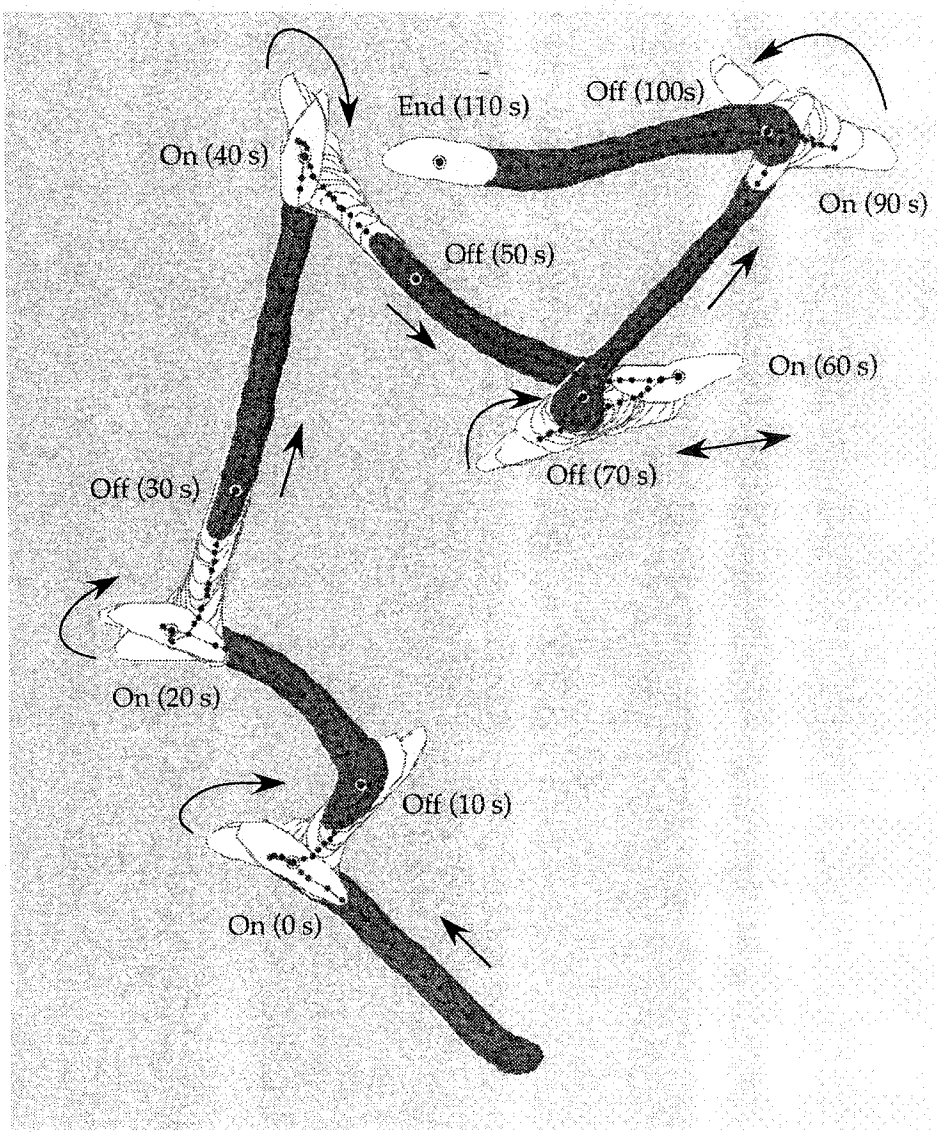
End (110 s)
Off (100s)
On (40 s)
On (90 s)
Off (50 s)
On (60 s)
Off (70 s)
Off (30 s)
On (20 s)
Off (10 s)
On (0 s)

**Figure 12.**

**A wild type larval response to light in the On/Off assay**

The figure shows elements of motor behaviours exhibited by a Canton-s larva response to intermitted light stimulation during the On/Off assay. The movie clip in this experiment was captured at video rate and modified to include approximately 2 frames per second. The outlined difference image with an area based centroid of the larva was calculated and rendered using DIAS software (Solltech Inc.). The larva was allowed to adapt to the substrate in the dark for approximately 10 s. Following which automated light stimulation began at the 0 s point and the light stimulation cycle continued for the course of the assay. Light stimulation causes cessation of locomotion and change in direction of locomotion as indicated using curved arrows. Distance traveled during the lights-on pulse is also clearly reduced. Light also causes the larval anterior end region to retract into the body, this is seen clearly at the 60s mark. Change in direction is less frequent during the light-on/lights-off transition.

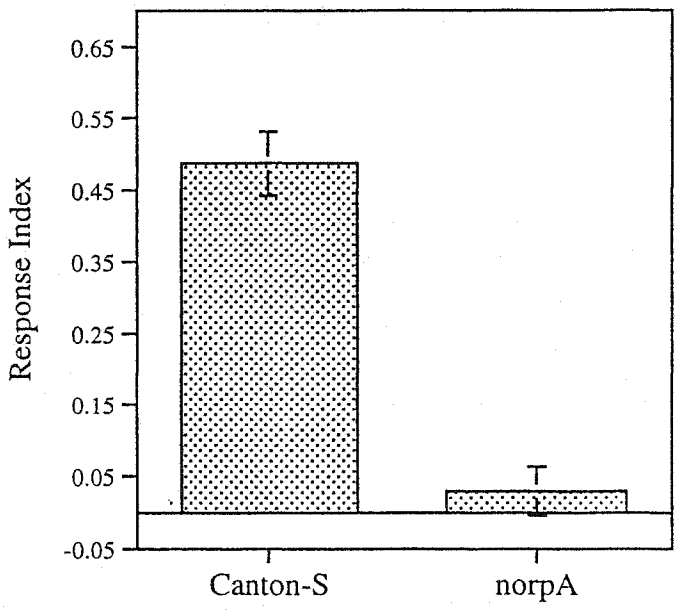
Response Index
0.65
0.55
0.45
0.35
0.25
0.15
0.05
-0.05
Canton-S
norpA

**Figure 11.**

**Response index of wild type and a visual system mutant larva in the On/Off assay**

The response index in the On/Off assay is reflects the distance traveled by a larva in the dark period that is 10 s in duration (Lights off pulse) compared to distance traveled in the lights-off pulse of equal duration, response index = [(distance traveled in Dark pulses – distance traveled in Light pulses)/total time]. Response index value is directly proportional to the light sensitivity displayed by the larva. All On/Off tests contain at least 2 dark pulse and 2 lights-on pulse. The figure shows a wild type Canton-S larval response index of ~ 0.45. Compared to a wild type response a previously characterized adult visual system mutant called *norpA*$^{p24}$ (no receptor potential) null mutant, shows no sensitivity to light stimulation. Canton-S, $n$=10; *norpA*$^{p24}$, $n$=12.

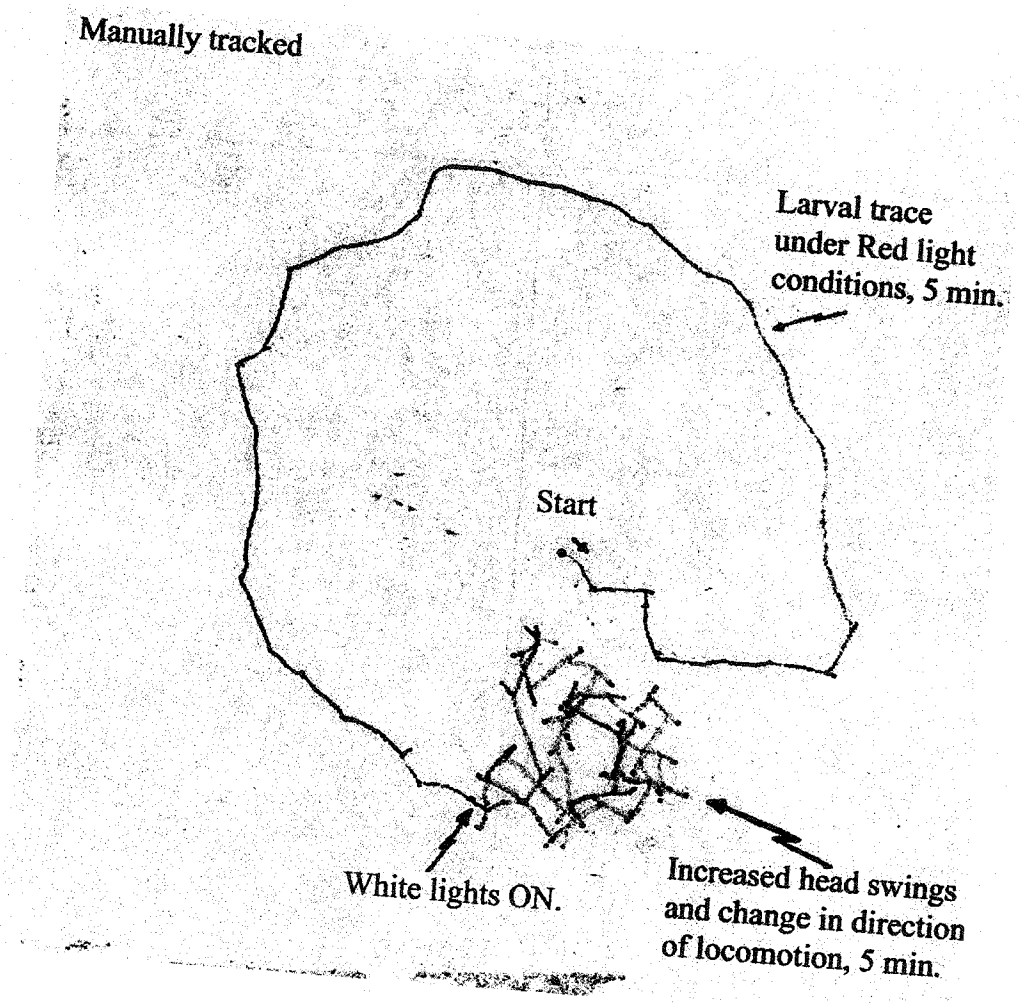
Manually tracked
Larval trace under Red light conditions, 5 min.
Start
White lights ON.
Increased head swings and change in direction of locomotion, 5 min.

**Figure 10.**

**Klinokinetic response of a wild type larva to a non directional light source**

A Canton-S larva was allowed to crawl in complete absence of light for 5 min. During this period the larva showed mostly linear pattern of locomotion. At the end of 5 minutes the white fluorescent lights were switched on from above for another 5 min. During the lights-on phase of the experiment the larval locomotory behaviour was altered. Light stimulation causes an aversive response that is reflected in increased rate of change in direction of movement. Increased rate of change of direction in response to a sensory stimuli is also called klinokinesis.

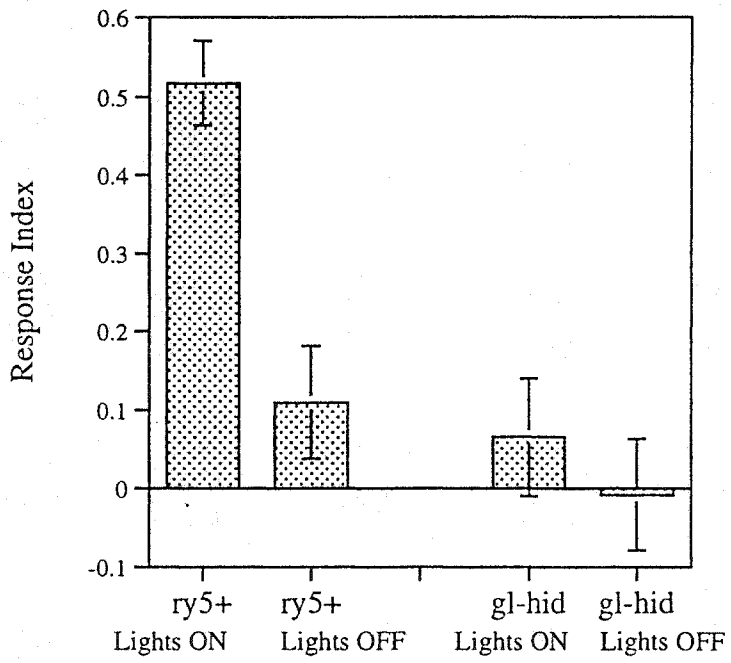
Response Index
0.6
0.5
0.4
0.3
0.2
0.1
0
-0.1
ry5+
Lights ON
ry5+
Lights OFF
gl-hid
Lights ON
gl-hid
Lights OFF

**Figure 9.**

**Wild type and genetically ablated mutant response in the Checker assay**

The figure shows a wild type (ry5+) response index [(total residence time in the Dark squared – total residence time in the Light Squares)/total time] in the presence of light and in the absence of light in the Checker assay. A wild type response index of ~ 0.5 is elicited when the light is switched on in the Checker assay. In the absence of light the response is close to zero. Similar experiments using a transgenic strain where expression of a cell death gene is targeted to the larval visual system results in indistinguishable response in the presence or absence of light in the assay. ry5+, (Lights On), $n$=17, ry5+(Lights Off), $n$=19; *gl-hid*, (Lights On), $n$=15; *gl-hid*, (Lights Off), $n$=14.

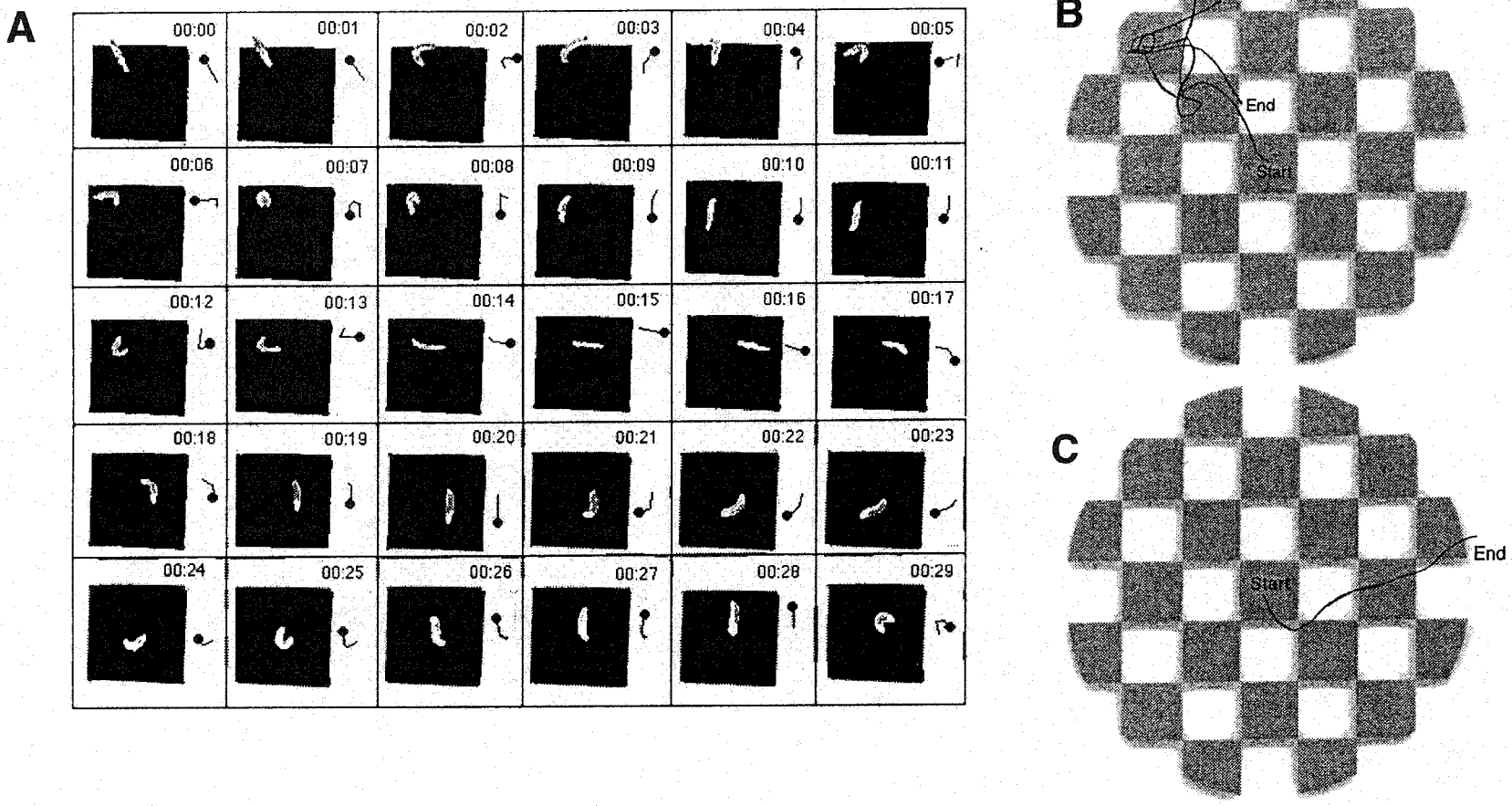
A
00:00
00:01
00:02
00:03
00:04
00:05
00:06
00:07
00:08
00:09
00:10
00:11
00:12
00:13
00:14
00:15
00:16
00:17
00:18
00:19
00:20
00:21
00:22
00:23
00:24
00:25
00:26
00:27
00:28
00:29
B
End
Start
C
End
Start

**Figure 8.**

**Larval behaviour in the Checker assay**

Panels A, B and C show the behaviour of an individual larva in the Checker assay. A. The repulsion behaviour of a larva is displayed as a 30 s montage from a video taped session. The sequence shows the behaviour of larva inside a favorable dark square of the Checker assay. A wild type larva encounters the dark/light stimulus boundary which appears to trigger head swinging behaviour followed by a complete reversal in the direction of movement. This enables it to orient itself so as to remain inside the dark square. B. This panel shows the track pattern of the larval movement on the checker template while the light box projected light from below. The larval track was hand traced by following the tail of a wild type larva and shows that the majority of turns in this experiment takes place inside the dark square. The turning behaviour allows the larva to remain in the dark square. C. When the light box is switched off, the larva is impervious to the checker template and does not show any preference for light/dark areas of the template.

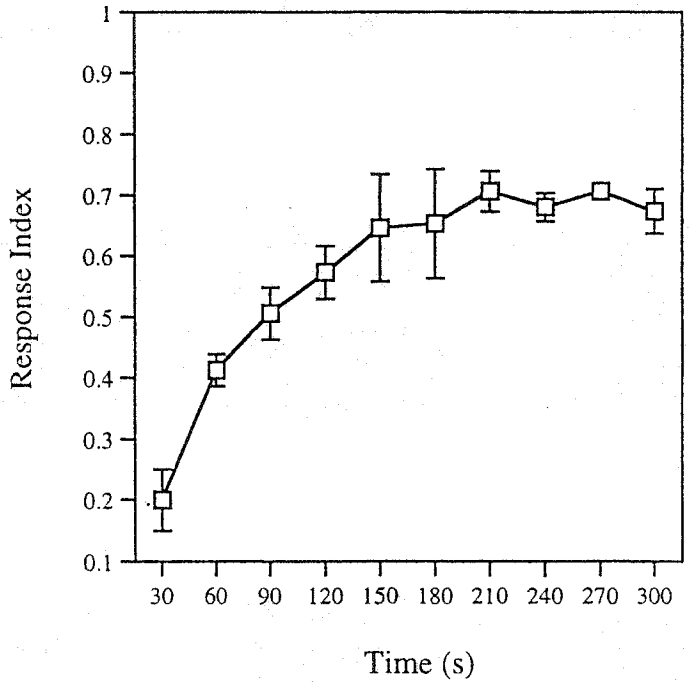
Response Index
1
0.9
0.8
0.7
0.6
0.5
0.4
0.3
0.2
0.1
30
60
90
120
150
180
210
240
270
300
Time (s)

**Figure 7.**

**Larval response kinetics in the plate assay**

The figure shows mean response index of wild type larvae that was calculated every 30 s during 5 minute runs of multiple plate assays. Maximal larval response is attained during mid-course of the assay (180 s). $n$=3.

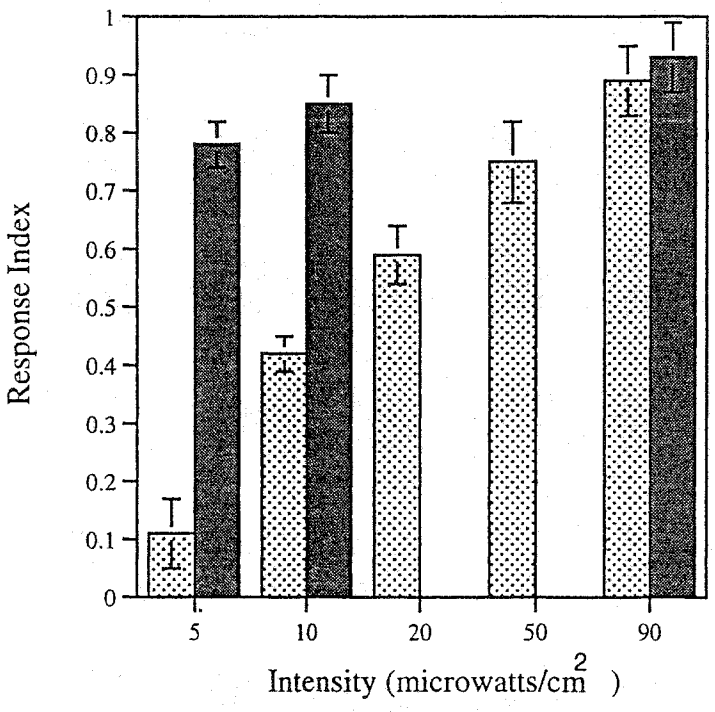


R.I With Neutral Density Filters

R.I Without Neutral Density Filters at 320 microwatts/cm$^2$

**Figure 6.**

**Response of wild type larva to varying light intensities**

Wild type ry5+ larvae were subjected to a series of light intensities in the plate assay. Larvae that showed reduced response in 5 and 10 microwatts/$cm^2$ light intensities were retested again after removal of the neutral density filters. The figure shows that in lower light intensities larval response is reduced and upon restoration of the original light intensity a wild type response level is attained. The experiment also shows that maximal larval response was attained at below normal light intensities (90 microwatts/$cm^2$), working intensity is that of 320 microwatts/$cm^2$. $n$=3, for each light intensity level.

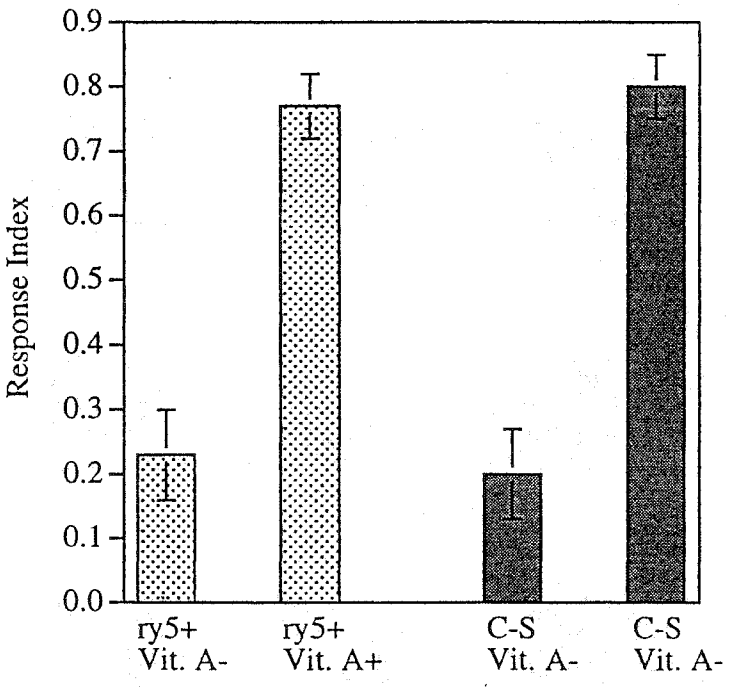
Response Index
0.9
0.8
0.7
0.6
0.5
0.4
0.3
0.2
0.1
0.0
ry5+
Vit. A-
ry5+
Vit. A+
C-S
Vit. A-
C-S
Vit. A-

**Figure 5.**

**Demonstration of reduced response to light by larvae grown in synthetic medium**

Canton-S and ry5+ wild type larvae were grown in a synthetic medium (Sang's minimal medium) with or without vitamin A supplementation. Absence of vitamin A in Sang's medium results in a consistent reduction in response to light in the plate assay by both the wild types. Supplementation of vitamin A results in normal wild type response. $n$=2, for each condition. Larval growth at 80-90 h was significantly reduced when grown in Sang's medium.

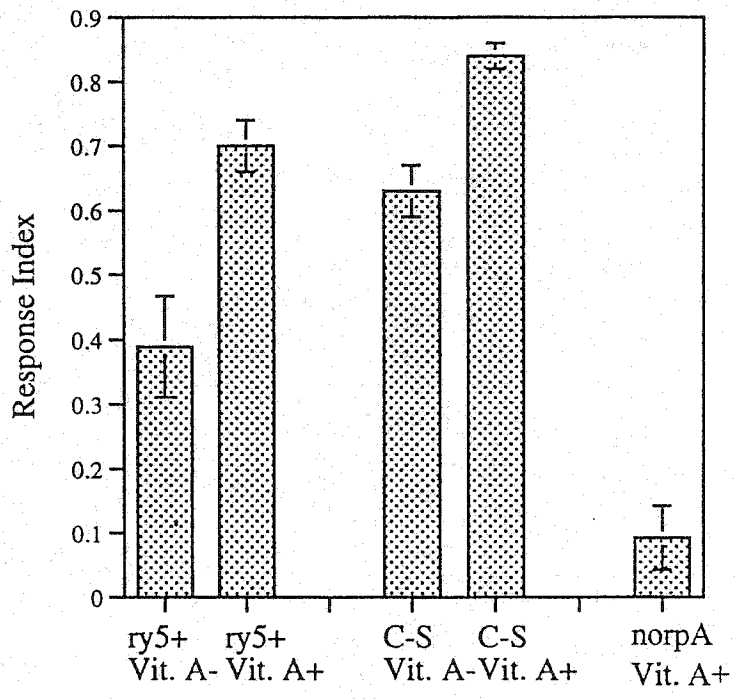
Response Index
0.9
0.8
0.7
0.6
0.5
0.4
0.3
0.2
0.1
0
ry5+ Vit. A-
ry5+ Vit. A+
C-S Vit. A-
C-S Vit. A+
norpA Vit. A+

**Figure 4.**

**Response to light by wild type larvae grown in regular fly medium**

A population of larvae were tested in the plate assay after growing larvae in the presence or absence of vitamin A. The figure shows increase in response in both Canton-S and ry5+upon growing each in a vitamin A supplemented medium. The assay was also used to demonstrate lack of response in the presence of vitamin A of the *norpA* mutant larvae. These mutant larvae have been previously reported to lack response to light. Canton-s (Vit. A+), $n$=5; Canton-S (Vit.A-), $n$=5; ry5+ (Vit.A-), $n$=10; ry5+, (Vit. A+), $n$=10.

**The Plate assay:**

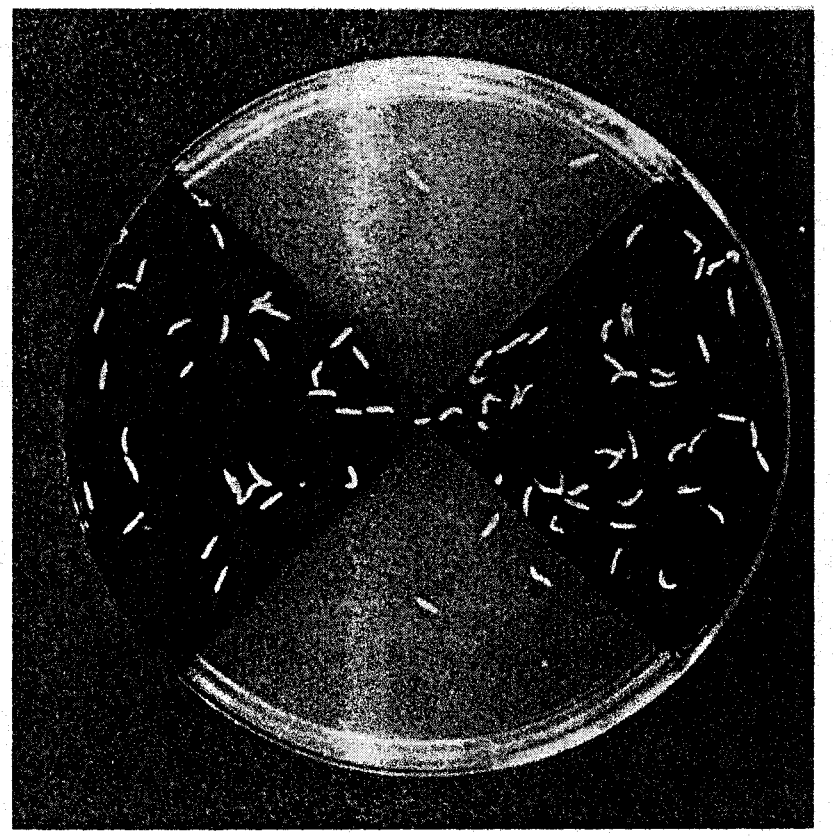

| R.I | L | D |
|---|---|---|
| 1 | 0 | 100 |
| 0.8 | 10 | 90 |
| 0.7 | 15 | 85 |
| 0.6 | 20 | 80 |
| 0.4 | 30 | 70 |

$$\text{Response Index} = \frac{\text{No. of Larvae in Dark - No. of Larvae in Light}}{\text{Total No. of Larvae}}$$

**Figure 3.**

**The plate assay**

The plate assay consists of a petri plate casts two dark quadrants and two light quadrants. Approximately, 100 larvae are heaped in the center of the plate and are allowed to distribute themselves over 5 minutes. Wild type foraging stage larvae are aversive to light and hence predominantly distribute in the dark quadrants. A response index is calculated based on relative distribution of larvae between dark and light quadrants.

# Figure 2

## A: The Development of the Bolwig's organ



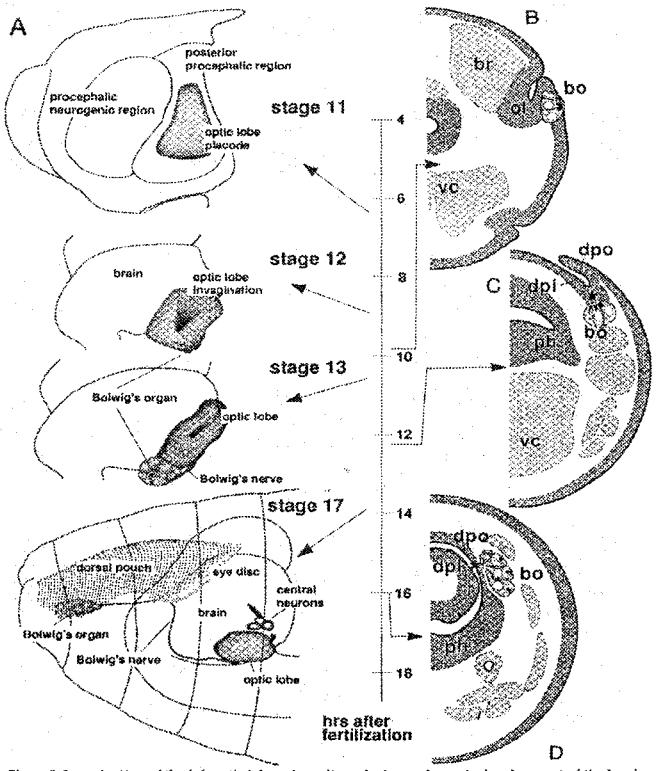


*Figure 9* Invagination of the left optic lobe primordium during embryonic development of the head region in *Drosophila*. (*A*) Lateral views of the embryonic head region. (*Right panel*) Sections through Bolwig's organ at the following stages. (*B*) stage 13; (*C*) stage 15; (*D*) stage 17. The positions of the basal bodies (black profiles in Bolwig's organ photoreceptors) rearrange from apical, in *C*, to basal, in *D* (asterisks). (bo) Bolwig's organ; (br) brain; (dpi) dorsal pouch, inner layer; (dpo) dorsal pouch, outer layer; (ol) optic lobe primordium; (ph) pharynx; (vc) ventral ganglion. (Modified, with permission of Springer-Verlag, from Green et al. 1993.)

From: Meinertzhagen and Hanson, The Development of *Drosophila*, CSHL press, Vol II.

## B: Final morphology of Bolwig's Organ

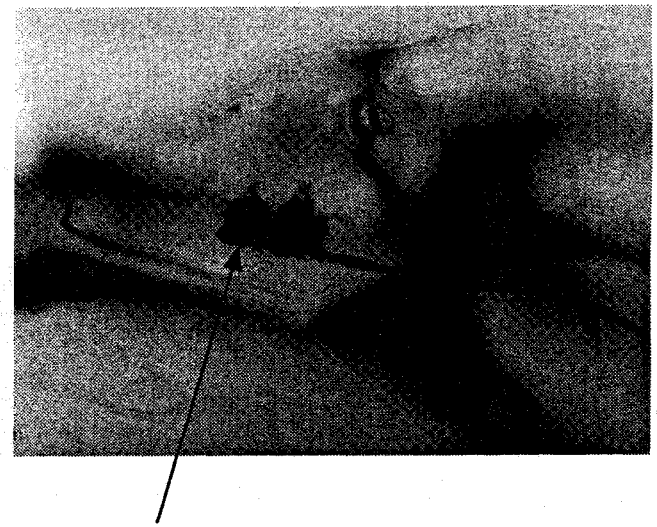

Bolwig's Organ

**Figure 2.**

**2A.** Early embryonic development of Bolwig's Organ in the head segment of the embryo. Please see chapter 3. **2B.** The final morphology of Bolwig's Organ. The photoreceptor clusters and the Bolwig's nerve can be easily visualized in a third instar larva using an antibody against the cell surface antigen "chaoptin". *Chaoptin* gene is expressed in a photoreceptor specific manner. The photoreceptor cluster is placed with the cephalophayrngeal skeleton that also contains the mouth hook of the larva.

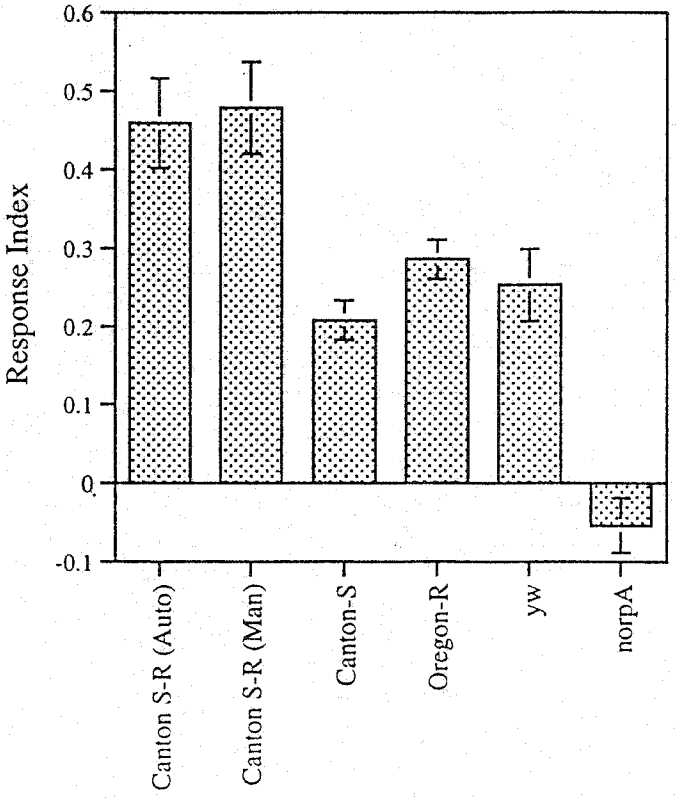
Response Index
0.6
0.5
0.4
0.3
0.2
0.1
0
-0.1
Canton S-R (Auto)
Canton S-R (Man)
Canton-S
Oregon-R
yw
norpA

**Figure 16.**

**Demonstration of response using semi-automated On/Off setup**

The figure shows On/Off experiments that were conducted using three wildtype strains and two mutant lines. Canton-SR strain is a wild type stock that was used from yet another flylab (Roger Jacobs). Simultaneous recording of On/Off experiment on a video tape for manual response measurement and semi-automated tracking and measurement was performed. The response indices in both cases are similar and hence proving semi-automated tracking to be reliable. The Canton-S (Campos lab strain) and the Oregon-R wild types and yw mutant strain show comparable wild typed like responses obtained by others. The semi-automated assay also shows that *norpA* strain is blind to light stimulation. Canton-SR (Auto), $n$=12; Canton-SR (Manual), $n$=12; Canton S (Auto), $n$=20; Oregon-R (Auto), $n$=18; *yw* (Auto), $n$=10.

A.

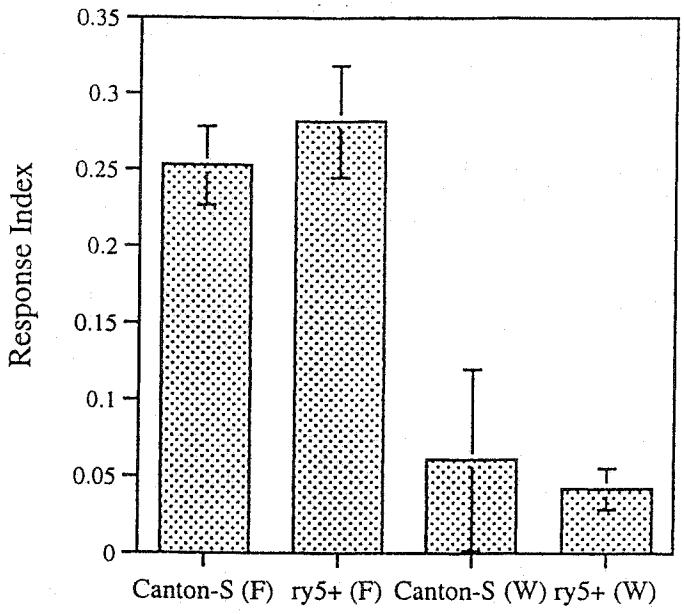
Response Index
0.35
0.3
0.25
0.2
0.15
0.1
0.05
0
Canton-S (F)
ry5+ (F)
Canton-S (W)
ry5+ (W)

B.

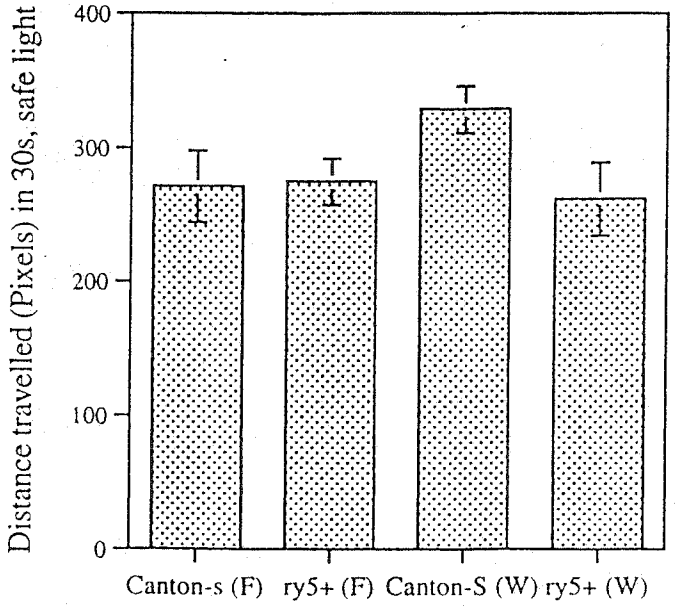
Distance travelled (Pixels) in 30s, safe light
400
300
200
100
0
Canton-s (F)
ry5+ (F)
Canton-S (W)
ry5+ (W)

**Figure 17.**

**Larval response to light is diminished in wandering phase**

**A.** The figure shows response indices of two wild type strains Canton-S and ry5+ at foraging stage (80-90 hrs AEL) and wandering stage (110-120 hrs AEL). Both wild type strains tested show similar decay of response to light in the On/Off assay. **B.** The figure shows distance travelled in 30s by the wild type larva in foraging and wandering stages. Locomotory rate does not appear to be significantly altered in these two stages during development. Canton-S (F), $n$=10; ry5+ (F), $n$=10; Canton-S (W), $n$=10; ry5+(W), $n$=10.

**Figure 18.**

**Pilot screen using the semi-automated tracking setup**

The figures show two rounds of screening. **Round 1.** Response indices are plotted against the respective locomotory rates for 50 strains tested. Larvae that exhibited response index less than 0.15 were selected for the second round for further qualification as putative photobehaviour mutants. **Round 2.** Selected larvae from round 1 were tested again for reduced response to light. Several locomotory mutants and two putative visual system defective strains 13510 and 16504 can be identified.

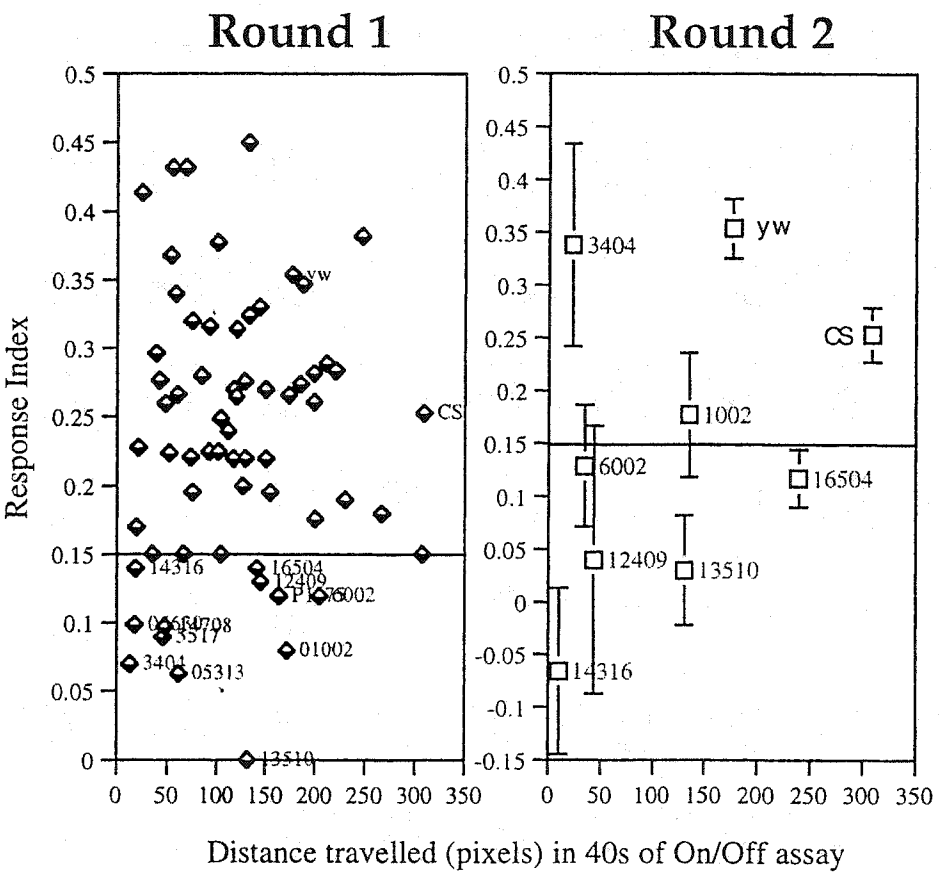
Round 1
Round 2
Response Index
Distance travelled (pixels) in 40s of On/Off assay
yw
CS
3404
1002
6002
16504
12409
13510
14316
01002
05313
0 50 100 150 200 250 300 350
0.5 0.45 0.4 0.35 0.3 0.25 0.2 0.15 0.1 0.05 0 -0.05 -0.1 -0.15

## Chapter 5 A:

## Isolation and phenotypic characterization of mutations in *tamas* locus - a gene encoding the mitochondrial DNA polymerase catalytic subunit.

## Introduction

Human mitochondrial DNA is a circular double stranded molecule that codes for a set of 37 gene products among which 13 are involved in oxidative phosphorylation (oxphos) and the remaining are required for protein synthesis (Anderson et al. 1981). Numerous point mutations and deletions in mitochondrial genome that lead to mitochondrial pathogenesis have been identified. These mutations lead to a wide variety of degenerative diseases that affect the CNS, PNS, muscle, eye, blood, endocrine system, heart, gastrointestinal system, sensori-neuronal hearing loss and kidney (reviewed in DiMauro and Schon 2001). Mutations in nuclear genes that indirectly affect the expression levels of oxphos components, or nuclear genes that are major components of the "respirasome" like complex I and complex II have also been identified to cause mitochondrial pathologies (reviewed in Triepels et al 2001, Rustin and Rotig 2002). For example, mutations in mitochondrial rRNA and tRNA genes lead to deafness in humans (reviewed in Jacobs 1997) and mutations in nuclear encoded complex I subunit like NDUFS7 (NADH-ubiquinone oxidoreductase) can cause Leigh's syndrome that is characterized by lesions in the brain (Triepels et al. 1999). It is estimated that over 90% of the genes that are required for mitochondrial function is encoded by the nuclear genome and their gene products are exported into the mitochondria (reviewed in Neupert 1997, Schleiff 2000).

The initial clue that nuclear DNA plays a critical role in the maintenance of mitochondria came from autosomally inherited disorders that result in mitochondrial DNA (mtDNA) deletions. The loss of mtDNA integrity results in dominant progressive ophthalmoplegia in humans (Zeviani et al. 1989). Recently, mutations in a mitochondria targeted helicase was identified to result in progressive ophthalmoplegia in humans (Spelbrink et. al 2001). Also multiple mtDNA deletions have been identified in humans suffering from ophthalmoplegia due to mutations in a gene encoding the adenine nucleotide translocator 1 (ANT1) (Napoli et al. 2001). Maintenance of mitochondrial DNA hence appears to be crucially dependent on the proteins that are encoded by nuclear DNA. It will be useful to develop animal models were nuclear control of mitochondrial biogenesis and function can be dissected using a genetic approach.

The pattern of lesions due to mitochondrial dysfunction often appears to affect the brain and neuromuscular system. It is likely that genetic screens using *Drosophila* behavioural assays will be useful in identifying mutations in many components that function in the mitochondria.

Behaviour screens have played a very important role in the isolation of mutations that affect function of the nervous system (reviewed in Pflugfelder 1998). For example, simple behaviour assays that involve subjecting flies to mechanical shock

through banging/agitation or raising the ambient temperature has been used to isolate mutations that affect the nervous system (Benzer 1971, Wu and Ganetzsky 1980, Gatenzky and Wu 1982). In wild type flies, neither a stressful mechanical agitation, nor a raise in ambient temperature to 29 °C causes paralysis. Many mutations have been identified where flies undergo paralysis upon mechanical disturbance. These observations have been used extensively to identify gene products that participate in nerve excitability and neurotransmitter release (Wu and Ganetsky 1982, Pavlidis and Tanouye 1995). For example, one such mutant called *easily shocked* codes for the choline/ethanolamine kinase (Pavlidis et al. 1994). This gene product has been proposed to play a role in preserving membrane integrity and in proper neurotransmitter secretion.

Mutations that affect mitochondrial function also appear to induce similar bang sensitiveness. Mutations in the *technical knockout* (*tko*) gene was recently shown to disrupt development, courtship behaviour and also cause paralysis upon subjecting to a banging stimulus (Royden et al. 1987, Toivonen et al 2001). *tko* gene codes for a mitochondria targeted bacterial homologue of ribosomal protein S12. In *tko* mutants mitochondrial protein synthesis was shown to be greatly reduced. Interestingly, in humans, an autosomally inherited deafness trait maps to a region in chromosome 19

DFNA4 locus that contains the gene coding for S12 ribosome and a mitochondrial serylt-RNA synthetase (Chen et al. 1995, Johnson et al. 1998).

Mutations in *stress sensitive B* (*sesB*) gene was also isolated due to bang sensitive phenotype and has been reported to code for ADP/ATP translocase, a component that participates in ATP production in the mitochondria (Zhang et al. 1997). Both *tko* and *sesB* also suffer from developmental delay (Toivonen et al 2001).

Genetic screens using the third instar larva proved that this developmental stage is also a good model for the identification of novel behavioural genes (Kernan *et al.* 1994, Yang et al. 2000, Bodily et al. 2001). We used this stage to identify mutations that affect the larval photobehaviour. Specifically, we used a collection of homozygous lethal lines which have their lethal phase in late larval/pupal stage. Many studies have identified that a significant portion of the genome that codes for gene products mutate to lethality (Thaker and Kankel 1992, Nusselein-Volhard 1994, Miklos and Rubin 1996). The last estimate stands at ~3,600 lethally mutable loci among 12,000 genes (Miklos and Rubin 1996). Thus many such genes that mutate to inviability would be precluded from adult behavioural screens. Hence we decided to screen a collection of pupal lethal strains to identify genes that affect larval behaviour.

The following screen was carried out after standardization of a behavioural paradigm using the plate assay. We identified one mutant strain (*P183*), which showed

reduction in the response to light of the foraging third instar larva in the population assay, and no response in a single larva assay developed in our laboratory. Deficiency and meiotic recombination mapping demonstrated that this mutation is allelic to mutations in a previously identified lethal complementation group, *l(2)34Dc* (Woodruff and Ashburner 1979). The *P183* strain displays disruption in the pattern of compound eye development and failure to undergo the behavioural changes characteristic of the wandering third instar larva. Further characterization of the behavioural phenotype demonstrated that the failure to respond to light was likely due to a locomotory deficit. Sequencing of this gene from 4 available mutant alleles revealed changes consistent with the notion that this gene encodes for the catalytic subunit of the mitochondrial DNA polymerase. Similar mutations in humans mtDNA polymerase catalytic subunit causes degeneration of muscles that control eye movements (Van Goethem 2001).

## Results

### I. Screening methodology

**The crosses for DTS balancer.** We received 65 recessive lethal lines mapped to the second chromosome from Art Hiliker and Marla Sokolowski for the purpose of testing these lethal lines for photobehavioural defects. These lines were balanced over a Curly of Oster balancer chromosome. In order to select genotypes that will possess a homozygous lethal mutation bearing chromosome for behaviour tests we chose to introduce a $CyO^{DTS}$ balancer. This balancer that contains a dominant temperature sensitive marker on the CyO chromosome. The crossing and testing scheme is presented in **figure 19.** Screen results are presented in **figure 20.** In the first round of tests all lines that exhibited a response index of over 0.6 were discarded. Lines that showed a response index below 0.6 were tested again in a second round. I isolated two lines that continued to show a response index below 0.5. The use of $CyO^{DTS}$ balancer for isolating homozygous larvae is not an efficient method as this balancer is considered to be leaky at the restrictive temperature. We then crossed these two putative photobehaviour mutants into a *yw;CyO(y+)* background. In this background the line E22 exhibited a lethal phase in the second instar stage, hence this was not pursued further. Homozygous larvae of line P183 showed lethality in late 3$^{rd}$ instar stage. All further characterization of the P183 line was undertaken in this background.

**II. Genetics analysis of the P183 line**

**A. Recombination mapping and deficiency mapping.** First, the lethality of this line was mapped by meiotic recombination using the multiply marked chromosome *black* (*b*), *purple* (*pr*), *curved* (*c*), *plexus* (*px*), *speck* (*sp*). Females of the genotype *P183/b pr c px sp* were crossed to $y^1$ $w^1$; *S/CyO-*$y^+$ and putative recombinant chromosomes were recovered over *CyO-*$y^+$ (**Appendix K**, crossing scheme). Out of 367 lines tested 103 retained the lethality associated with *P183*, out of which only one of recombinants carried *b*, suggesting that the *P183* lethality mapped close to *b*. Suggesting that this lethal loci was 1 cM unit away from the *black* locus. This recombinant was later determined to have been the result of a crossover between *b* and the lethal mutation located in 35B.

Deficiency mapping was conducted using a set of deficiencies spanning the *black* region (see **Figure 21, Table 2**). All deficiency chromosomes were kept over a *Cy* balancer. We tested for complementation by crossing the *P183/CyO-*$y^+$ flies to deficiency stocks. The presence of straight wing flies among the progeny of the cross was indicative of complementation of the *P183* chromosome by the deficiency. A minimum of 100 flies were counted for each cross. The deficiency mapping experiment resulted in identification of two non-overlapping deficiencies spanning the 34D and 35B regions did not complement *P183*. This suggested that the *P183* strain carried two lethal mutations in the second chromosome. Next, the two lethal mutations were mapped more precisely

by crossing to other deletions and to alleles of known lethal complementation groups in these regions. This finer map enabled us to identify one of the mutational event to be located in the gene coding for *Suppressor of Hairless, Su(H)*, a well characterized neurogenic gene involved in the Notch signal transduction pathway (reviewed in Bray and Furriols 2001). The identity of the other lethal mutation in 34D region was determined to be in a lethal complementation group called *l(2)34Dc*. All the pre-existing alleles of this uncharacterized complementation group showed non-complementation of lethality when heterozygous with the P183 chromosome. We named this locus - *tamas* (org. Sanskrit – Dark Inertia, the name was inspired more by a movie based on communal riots in India during partition in 1947.).

**B. Recombination of *tamas* from the P183 (double mutation) chromosome.** In order to characterize the phenotypic consequence of mutations in the *tamas* locus of the P183 strain, a meiotic recombination experiment was carried out to separate this mutant locus from the P183 chromosome. The crossing scheme describing this is presented in **Appendix K**. A screen of 323 lines resulted in the isolation of one lethal recombinant that was further confirmed by demonstrating that this recombinant line results in complementation of lethality with lethal allele of *Su(H)* and non-complementation with

the pre-exiting alleles of this locus and a deficiency chromosome that is deleted for the 34D region (**Table 3**).

**III. The *Su(H)* mutation in the P183 strain shows a neurogenic phenotype of the developing optic lobe.**

The $Su(H)^{P183}$ allele from the P183 strain was separated from the 34Dc mutation during the meiotic recombination experiments to map the lethal phenotype of the P183 strain. Phenotypic characterization of the $b^{-}$, $Su(H)^{P183}$ strain showed that the optic lobe development in late 3$^{rd}$ instar larvae is severely affected. Loss of function in this gene leads neuroectodermal cells to adopt a neural fate (Lecourtois and Schweisguth 1995). Similarly, in the case of the *Su(H)* allele in P183 strain the cells in the optic lobe primordium appear to differentiate into neurons as visualized using an antibody against the Elav protein, a post mitotic neuronal marker (**Figure 22**). The proliferation centers in the optic lobe are also severely affected in these mutants as visualized by the BrdU incorporation. This is presumably due to change of cell fate that diminishes proliferative activity in the developing optic lobe.

**IV. Phenotypic characterization of strains mutant for the *tamas* locus.**

**A. Mutations in the *tamas* locus results in prolonged larval foraging stage.** Under laboratory conditions late 3rd instar *Drosophila* larvae undergo a transition from a mainly burrowing/foraging behaviour on food substrate to cessation in feeding and wandering behaviour. This transition takes place at approximately ~ 110 hours AEL (After Egg Laying). This behavioural transition is correlated with increased levels of ecdysone secretion, that also acts as a stimulus for pupariation (reviewed by Truman et al. 1994). In the wandering phase the larva empties the food in the digestive tract, in preparation for 4 days for pupation. The process of gut-emptying can be visualized by feeding the larva food that is colored with bromophenol blue prior to wandering phase followed by observing the disappearance of the blue color in the larval gut through the transparent larval body wall (Maroni and Stamey 1983). Homozygous *P183* larvae failed to wander out of the food substrate at ~110 hours as compared to a heterozygote wild type and correspondingly, the mutant larvae do not exhibit this process. Furthermore, homozygous P183 larvae displayed a prolonged foraging phase that could last up to 20 days (AEL) after which they died presumably due to deteriorating condition of the food substrate (**Figure 23 A-D**). Larvae heterozygous for other alleles of *tam* and a deficiency of the 34D region (**Figure 23 E** and **F**) also show similar prolonged foraging period. Larvae homozygous for mutations of *Su(H)* wander at the appropriate time and die

during mid-pupal period. Thus mutations in the *tam* gene affect larval behaviour transition from foraging to wandering stage during larval development.

**B. Imaginal disc development is affected due to mutations in the *tamas* gene.** Imaginal discs are clusters of undifferentiated epidermal cells that give rise to adult appendages during metamorphosis in holometabolous insects. In *Drosophila* these structures can be identified based on their shape and position along the antero-posterior axis. Imaginal discs in homozygous P183 3$^{rd}$ instar larvae are severely reduced in size as compared to wild type controls at the same stage (**Figure 24 B**). This phenotype is mainly due to mutation in the *tamas* locus. Larvae heterozygous for P183 and a *Su(H)* allele do not show such severely retarded growth of imaginal discs.

**C. Eye imaginal disc differentiation defects in *tamas* mutants.** In order to investigate the role of the *tam* gene in the larval response to light we analyzed the morphology of the visual system with the 24B10 monoclonal antibody (Zipursky *et al.* 1984). This antibody labels a photoreceptor-specific antigen present in both the developing larval and adult visual systems in the third instar larva (**Figure 25 A, B**; Zipursky *et al.* 1984). The visual system of the original double mutant strain *P183* was characterized by overall reduction in the size of the eye-antennal imaginal disc (**Figure 25 B**). While labeling

with the 24B10 monoclonal was found in the posterior portion of the disc it was not seen in the usual clustering pattern representing the developing ommatidia. Rather, the expression of the epitope recognized by this monoclonal antibody seemed to be continuous throughout the developing retina. These observations may indicate that all cells in the disc were adopting a disorganized photoreceptor fate. Subsequent analysis using the *P183* chromosome heterozygous with chromosomal deficiencies that remove either the 35B (*Su(H)*) or the 34D (*tam*) regions and with mutant alleles of each gene demonstrated that this particular phenotype was due to disruption of the *Su(H)* gene.

Disruption of *tam* gene function lead to less severe disruption in the pattern of the developing ommatidia by comparison with the original double mutant strain (**Figure 25 C** and **D**). The eye disc, while still reduced compared to a wild-type control, showed the usual pattern of clustering albeit somewhat disorganized. The projection of the photoreceptor axons into the optic lobes was also disrupted probably due to the abnormal differentiation of the retinal cells and abnormal proliferation of target cells in the optic lobe primordium (**Figure 25 C**). Closer inspection of the homozygous $tam^{9}$ mutant eye disc under higher magnification suggested that older retinal cells were degenerating or losing the antigen as recognized by the 24B10 monoclonal antibody (**Figure 25 F**). The larval visual system was present, however the projection defects observed in the developing adult visual system masked the terminus of the larval visual

system, at that time in development. An interesting aspect of the phenotype of the visual system of *tam* mutant larvae was the delayed onset of retinal differentiation. 24B10 labeling could only be seen in *tamas* mutant larvae several days after it was seen in wild-type larvae (**Figure 25 E, F**). The phenotype observed in the developing eye disc was reflected in the compound eye of adult escaper flies heterozygous for all lethal alleles of *tam* and a hypomorphic allele $tam^{10}$ in the *In(2L)b79h1A* chromosome (**Table 3**). These escapers have disorganized compound eyes which are significantly smaller than the control flies and fused ommatidia and bristle defects in the head (**Figure 26**).

We investigated whether the mutant larvae also exhibit abnormal patterns of cell death in the developing imaginal discs. While the eye-antennal imaginal disc is reduced in size the pattern of cell death in both the eye and the antennal areas of the disc was abnormal in *tam* mutants (**Figure 27 C** and **D**). At later stages (120 h, AEL) whereas the wild type controls had begun pupariation, the mutant antennal disc continued to show excessive cell death (**Figure 27 F**). The general morphology of the CNS as seen by labeling with the anti-Elav monoclonal antibody appeared to be normal.

**D. Abnormal response to light in *tamas* mutant larvae is due to a locomotory deficit.**

Single larval assays that were being simultaneously developed during the characterization of *P183* line were now ready to be used. The Checker assay was

considered to be very much akin to the plate assay as the larva encounters light stimulation very similar to the plate assay. This assay measures the response to light in individual larvae as the relationship between residence time in light and dark squares with light stimulus and compared to residence time in safe light conditions (Chapter 4). Larvae homozygous for the original double mutant chromosome *P183* or for the recombinant strain carrying only the $tam^9$ mutation showed no response to light in the Checker assay (**Figure 28**). Larvae heterozygous for $tam^9$ and other mutant alleles of the *tam* gene responded to light ($tam^3$ and $tam^2$) suggesting partial complementation of this phenotype. Visual inspection of the larvae during the course of the Checker assay suggested that these organisms moved considerably less than the wild-type background strain. Hence measurement of basal locomotion in the absence of any light stimulation was undertaken. This assay clearly showed that *tamas* mutants exhibited reduced locomotion (**Figure 29**). Larvae heterozygous for the $tam^9$ allele and a *tam* deficiency (*Df(2L)b80c1*) could not be tested in the Checker assay because of a severe deficit in locomotion, this is borne out by the observation in the locomotory assay where this combination shows very severe locomotory defect (**Figure 28** and **29**). This deficit in locomotion was not seen in $tam^9/+$ or *Df(2L)b80c1*/+ larvae (**Figure 28**) and these larvae responded to light in the Checker assay (Figure 28). Further, changing the genetic background of mutants (+; $tam^9/tam^9$) clearly showed that poor response to light can be

overcome but locomotory defect continued to prevail (**Figure 24, 25**). Thus, lack of response to light seen in the *tam*$^{9}$ mutant larvae was concluded to be mainly due to poor locomotion.

**V. The genetics of the 34D region**

The genetic order of complementation groups in the 34D-35F region has been determined from numerous lethal screens and extensive deletion mapping was carried out in the laboratory of Michael Ashburner (**Figure 21** and **Table 1**). The lethal complementation groups in the immediate vicinity of *black* are *l(2)34Db*, *Son of sevenless* (*Sos*), *tam* , and *Sop2*. *l(2)34Db* has been shown to map distal to *black* by the criterion that many $b^{-}$ deletions, (e.g. *Df(2L)b84a9)*, remove *Sos*, *tam*, and *Sop2* but not *l(2)34Db*. Both *Sos* and *tam* are adjacent to black by the criterion that many aberrations are either $Sos^{-}$ $b^{-}$ $l(2)34Dc^{+}$ or $Sos^{+}$, $b^{-}$, $l(2)34Dc^{-}$, (e.g. *In(2L)b82c44* and *In(2L)b83b22* respectively). That *Sos* is distal and *tam* is proximal to *black* is confirmed by the aberration *In(2L)b81l7* which is deleted for *l(2)34Db*, *Sos* and *black*, but not *tam* or *Sop2* therefore the genetic order is *l(2)34Db*, *Sos*, *black*, *tam*, *Sop2* (John Roote pers. comm.).

## VI. Sequencing *tamas* alleles and identification of *tamas* neighbours using the genome project physical map.

### A. *tamas* codes for the mtDNA polymerase catalytic subunit.

While the genetic mapping experiments where under way, the Berkeley *Drosophila* Genome Project announced the complete sequence of a P1 clone that consisted of 80 KB DNA sequence in the *black* region. The superimposition of the genetic map onto the physical map showed that *tam* gene could be located on the P1 DS00941 in a region tightly packed with open reading frames coding for known gene products (Ashburner et al. 1999, **Figure 30**). The region of interest was delimited distally by *Sos* (*BG:DS00941.4*) which codes for guanine nucleotide exchange factor (Rogge *et al.* 1991; Bonfini *et al.* 1992) and proximally by the profilin associated protein gene, *Sop2* (*BG:DS00941.7*) transformants of which have been shown to rescue the lethality of the *l(2)34Dd* complementation group (Hudson and Cooley 1998; **Figure 21**). Since the glutamate decarboxylase (*BG:DS00941.5*) and mitochondrial DNA polymerase (*BG:DS00941.6*) genes were the only open reading frames between *Sos* and *sop2*, we hypothesized that *tam* was the more proximal of these, *DNApol-γ125*. In order to test this hypothesis we sequenced this gene from the genomic DNA of all mutant alleles available. In the $tam^{9}$ allele a single nucleotide change (A to C) in the spacer region between the exonuclease and polymerase domains changes a codon coding for glutamic

acid to alanine (G595A) (**Figure 30 B**). The functional consequence of the change found in *tam*$^{9}$ for enzymatic activity has been tested using the DNA polymerase enzyme assays, and it showed that this mutation results in loss of activity (pers. comm. Laurie Kaguni). The mutation found in the *tam*$^{2}$ allele was a point mutation that changes amino acid glutamic acid to valine in the highly conserved polymerase domain (E813V) (**Figure 30 C, C'**). The deletion found in the *tam*$^{3}$ and *tam*$^{4}$ alleles demonstrate that the catalytic subunit of the mitochondrial DNA polymerase was disrupted in *tam* mutants (**Figure 30 D** and **E**).

Next, we investigated the profile of mitochondria in *tam*$^{9}$ mutant using the mitochondria selective dye, MitoTracker (Molecular Probes Inc.). Visualization of larval brain hemispheres using this dye in larvae that failed to pupariate showed several abnormalities that included disruption of reticular mitochondrial staining pattern and many punctate/circular staining profiles that were never observed in wandering stage wild type controls. Hence, together with these results we concluded that the *tamas* gene codes for the catalytic subunit of mitochondrial DNA polymerase γ.

## Discussion

We used a previously described assay to conduct a screen to isolate mutations that affect *Drosophila* larval response to light. A collection of pupal lethal lines were used under the rationale that mutations that cause lethality at this stage are a sample that may not have been available for screening in adult behaviour paradigms. Also, most genes required for the development and function of the nervous system have been shown to be pleiotropic and thus affecting the viability of the organism during its development (Thaker and Kankel 1992, Miklos and Rubin 1996, Nusselein Volhard 1994, Pflugfelder, 1998 ). The P183 line that was isolated in this screen distributed abnormally in the dark quadrant and light quadrant of the plate assay, thus displaying a low response index compared to the wild type control. Since P183 continued to show a mean response index of 0.45 in another genetic background, this prompted us to consider this line to be a hypomorphic mutation that affected the larval response to light.

**Mutations in the *tamas* locus and in the *Su(H)* locus cause developmental defects.** The two lethal mutations were shown to map to the *black/Adh* region. The lethal hit in the 35B region was identified to be allelic to the *Su(H)* gene. *Su(H)* gene product is a transcription factor that has homology to mammalian C-Promoter Binding Factor 1 and

participates in Notch signalling (Fortini and Artavanis-Tsakonas1994). Notch receptor mediated signaling is central to neuronal cell fate determination and it involves lateral inhibition among groups of ectodermal precursor cells (reviwed in Artavanis-Tsakonas, 1995, Greenwald, 1998). The outcome of lateral inhibition process is determination of a single progenitor cell that will adopt a neuroblast fate. Neuroblasts give rise to daughter cells that will eventually differentiate into neurons. The mechanism of Notch signaling involves a proteolytic cleavage of Notch to produce an intracellular fragment that physically interacts with Su(H) protein to induce its transcriptional activity (Kidd, 1998 et al. Furriols and Bray 2000). Su(H) mediated transcription allows the expression of neurogenic genes like *E(Spl)* complex. Expression of genes in this complex function to repress neuronal fate. *Su(H)* null mutation gives rise to a neurogenic phenotype similar to Notch mutant phenotype (Lecourtois and Schweissguth 1995). Homozygous *Su(H)* zygotic mutant animals die during pupation. Lethality at pupal stage is thought to occur due to perdurance of maternal contribution of Su(H), this allows the larval development in *Su(H)* mutant animals. *Su(H)* expression shows two peaks during development, one at the embryonic stage when it is expressed in cells of the PNS and later in most 3rd instar imaginal discs (Schweisguth and Posakony 1992).

Since the lethal phase of a $Su(H)^{P183}$ (recombinant of the *Su(H)* mutation from the P183 line) mutation is in the pupal stage, we examined the optic lobe development in

these mutants using BRDU, that labels all mitotically active cells and using anti-Elav antibody that labels all post-mitotic neurons. The optic lobe is formed from a group of ectodermal cells that are located dorso-laterally in a region posterior to the procephalic neurogenic region (Green et al. 1993). In $Su(H)^{P183}$ homozygous mutant animals, optic lobe defect is seen as an abnormally large anti-Elav staining area. The other alleles of *Su(H)* (hypomorphic or amorphic alleles) have not been reported to have any abnormalities during larval stages. Although, in some trans-heterozygous combinations of null alleles some "sick larvae" do result as a low penetrance phenotype (Schweisguth. pers. comm.). Assuming that the maternal gene product is usually sufficient for optic lobe development in zygotic mutant embryos (amorphic or hypomorphic alleles), the *Su(H)* mutation in the P183 strain may affect the developmental transition from the larval to pupal stage with respect to optic lobe development.

We named the other lethal hit in the 34D region of the P183 strain as $tam^9$. The lethal phase of $tam^9$ was observed to be at late larval stage. A characteristic phenotype due to this mutation was an extended larval foraging phase in the culture medium lasting up to 2-3 weeks after egg laying and dying thereafter, rarely exhibiting the wandering behaviour nor entering pupariation.

The flybase curation listed 8 other pre-existing alleles originally isolated in this gene. Although only 3 alleles were available from the stock centers. We renamed these

alleles as follows: *l(2)34Dc*$^{2}$ as *tam*$^{2}$, *l(2)34Dc*$^{3}$ as *tam*$^{3}$, and *l(2)34Dc*$^{4}$ as *tam*$^{4}$. We observed early embryonic/first instar lethality in homozygous animals of all these alleles. Although heterozygous combination of the alleles with a deficiency, namely *Df(2L)b80c1* produces lethal phases similar the recombinant *tam*$^{9}$. This suggested that the pre-existing alleles of the *tam* lethal complementation group may have background recessive lethal hits.

The *tamas* mutations belong to a class of mutations that is characterized by prolonged 3rd instar stage while affecting imaginal disc growth. For example, in a 3rd chromosome screen conducted on 3167 chromosomes, 134 lethals were found to be late larval lethals out of which nearly 50% of the lines showed imaginal disc abnormalities concomitant with prolongation of the third instar stage (Shearn et. al., 1971). *tam*$^{9}$ mutation fits in this class, as it clearly affects the growth of the eye and leg imaginal discs, which appear reduced in size when compared to a wild type control larvae. This observation entertains the hypothesis that a feedback loop that communicates the state of the imaginal disc with a developmental clock to trigger pupariation at the right time (Simpson et al. 1980, Simpson and Morata 1980). Irradiating imaginal discs precursors in the first instar larva with various doses of radiation results in a delay in pupariation (Poodry and Woods, 1990). However, in the *discless* mutant larvae where imaginal discs are completely absent, a pupariation delay is not observed supporting the hypothesis

that a negative feedback loop from the imaginal discs controls the transition to pupariation (Szabad and Bryant, 1982). In *tam* mutant larvae, the extended foraging stage may be due to the maturation state of the imaginal disc. It is likely that slow growth of the eye-imaginal discs may result in photoreceptors to differentiate later than normal in *tam* mutants.

It has been reported previously that in mutations that abolish photoreceptors, the lamina neurogenesis is arrested followed by their elimination through cell death (Selleck et al. 1992). It has been hypothesized that retinal innervation at the right time window is necessary for recruitment of synaptic partners in the lamina target field and deeper visual centers. This may be one of the reasons for the defects observed in the adult visual system in allelic combination of *tamas* mutants and when heterozygous with a deficiency chromosome. We also identified a strain with a chromosomal inversion, *In(2L)b79h1A*, that appeared to be a hypomorphic allele to the *tam* mutations and thus allowing a small percentage of heterozygotes to survive pupation and result in adults. The surviving adults showed severe defects in compound eyes and bristle pattern in the head and thorax.

We used the recombined $tam^{9}$ mutation from the P183 strain for a more detailed analysis of behaviour phenotype. We also selected a single larval photobehaviour assay, the Checker assay, that demands very similar behaviour from the larva as in the plate

assay for further analysis of behaviour in *tam* mutants. In this assay, the homozygous *tam* mutant once again failed to respond to light. Similarly, larvae that were heterozygous for $tam^9$ and a deficiency chromosome showed very poor locomotory behaviour and were untestable in this assay. Clearly suggesting that the lack of response to light was due to very poor motor behaviour in the animals. Heterozygous combination of $tam^9$ with $tam^3$ resulted in positive response to light. These larvae showed better locomotory capacity, although continuing to shown significantly lower locomotion compared to a control strain. Thus we concluded that the primary behavioural deficit due to mutations in this locus is that of locomotory defect.

Using the genetic map and the first available draft of the physical map for the *Adh* region (**Figure 30**) we hypothesized that the *tam* mutations represented disruptions in the transcriptional unit that codes for catalytic subunit of mitochondrial DNA polymerase. This was confirmed by conducting direct sequencing of this gene from all the four mutant alleles. Sequence of $tam^2$ allele clearly showed that this mutant allele is a point mutation within a highly conserved polymerase domain of the enzyme, thus this can be considered to be a null mutant of the gene. Both $tam^4$ and $tam^3$ alleles may result in a partial loss of function for this gene product as they cause deletions after the C-terminal polymerase domain of the molecule. The $tam^9$ mutation is located in the spacer region that separates the exonuclease (proof-reading) domains and the polymerase

domains. This suggests that this mutation may not drastically affect protein function. Although a recent report of a similar mutation in this spacer region of Human PolG subunit results in a disease known as progressive external ophthalmoplegia (PEO) in a Belgian pedigree (Goethem et al. 2001). PEO is a degenerative disease that affects the motor movements of the human eye. Taken together these experiments clearly show that the *tam* gene codes for catalytic subunit of mitochondrial DNA polymerase.

Point mutations in mitchondrial DNA that affect tRNA genes have been reported to also affect mitochondrial morphology (Hayashi J-I et al. 1994, van den Ouweland 1999). Reduction in mitochondrial DNA levels as a consequence of mitochondrial transcription factor A (*mtTFA*) knockout also cause abnormal mitochondrial profiles (Larsson et al. 1998). These reports lead to the analysis of mitochondrial morphology in *tam* mutants. The wild type control larval brain hemispheres show a distinctly reticular nature of mitochondrial profile surrounding the nucleus. Visualization of mitochondrial profile in the *tam* mutants show morphologically abnormal mitochondria in the larval brain hemispheres. The size of the brain hemispheres was also reduced in mutant animals. We observed varying levels of defects in the mutant brain samples, they include punctate vesicular profiles in the reticulum, many nuclei lacking a uniform distribution of mitochondrial network and large empty regions in the brain that lacked any uptake. These observations that appear to compromise the mitochondrial reticulum

are similar to observations of mitochondria in human cell lines where the mitochondrial DNA has been chemically depleted (Gilkerson et. a l. 2000).

The results reported in this chapter were the first description of the consequence of mutations in mitchondrial DNA polymerase (Pol γ-α/*tamas*) (Iyengar et. al 1999). *In vivo* overexpression of Pol γ-α has also been recently reported to cause mtDNA depletion in *Drosophila,* as well as cuticular defects and pupal lethality (Lefai et. al. 2000). The machinery responsible for mtDNA replication appears to involve at least 3 other components, namely, mitochondrial single stranded DNA binding protein (mtSSB/*lopo*) (Maier et al. 2001), a helicase (Spelbrink 2001, see **Appendix L** for a putative *Drosophila* homologue) and mitochondrial transcription factor A (mtTFA) (Takata et al.2001, Larsson et al. 1998). Mutations in genes that code for all these components have been reported to result in mtDNA depletion and organismal lethality. Mutations in *Drosophila lopo* (low power, *mtSSB*) gene causes lethality in late third instar stage suggesting once again as in *tam,* the presence of a strong maternal contribution that takes larval development until third instar stage. Similar to mutations in the *tam* locus, *lopo* mutations cause reduced proliferation in the developing optic lobe. The resulting visual system phenotype has been compared to that of *tamas* mutants (Maier et al. 2001). Other phenotypes due to mutations in *lopo* include severe depletion of mitochondrial

DNA and reduced respiration in larval tissues. At an ultrastructural level variable defects in mitochondrial morphology were observed (Maier et al. 2001).

Another component whose mutational analysis has not been conducted in *Drosophila* is the nuclear gene that codes for mitochondrial transcription factor A (*mtTFA*). *mtTFA* gene product is thought to be required to initiate replication of mtDNA by making an RNA transcript that is used as a primer by the polymerase holoenzyme, after cleavage by an RNAseH like activity (Smitt et al. 1993). Knockout of *mtTFA* gene in mouse model using the cre/loxp system results in embryonic lethality after implantation stage and delayed development of the nervous system and absence of optic discs (Larsson et al. 1998). Homozygous mutant embryos also show severe reduction in mtDNA levels. Interestingly, heterozygote knockout mice display a generally lower mtDNA levels, and in the heart tissue, lower transcript and protein levels of the respiratory chain was reported. In this study an examination of mitochondrial ultrastructure from mutant embryos also showed abnormal mitochondrial morphology (Larsson et al. 1998).

Recently, a mitochondria specific helicase has been implicated in maintenance of mtDNA. Screening patients who suffered from an autosomally inherited dominant progressive ophthalmoplegia (adPEO) with multiple mtDNA deletions lead to the identification of a gene called *twinkle* (Spelbrink et. al 2001). The gene product was

shown to be localized to mitochondrial nucleoids (a large mtDNA protein complex). A total of 11 mutations in this gene were isolated from 12 different families. Most of the mutations were shown to be localized to phylogenetically conserved regions of the molecule although none appeared to affect the catalytic region of the enzyme. This entertained the suggestion that most mutations may affect the multimerization of subunits or other components of the mtDNA replication machinery in a dominant manner.

According to the current working hypothesis of mtDNA replication each of these components play a critical role. Central to the replication machinery is *tamas*/Pol γ-α or POLG. This is the only dedicated polymerase that conducts mitochondrial DNA replication (Clayton 1982). Previously, Pol γ-α in *Drosophila* was isolated, cloned and characterized through biochemical reconstitution experiments (Lewis et. al 1996). Through *in vitro* experiments, Pol γ-α in *Drosophila* and vertebrates has been shown to be highly accurate in its catalytic function due to its mispair specific 3'-5' exonuclease activity (Kaguni et. al 1989, Insdorf and Bogenhagen 1989, Lewis et. al 1996, Pinz et al. 1995, Spelbrink et. al. 2000). The human poly γ-α function is estimated to produce a conservatively estimated error rate of approximately 1 in 1-20 million base pairs and is considered to be much less efficient than nuclear DNA polymerase (Johnson and

Johnson 2001). Thus the catalytic subunit takes the center stage with respect to mtDNA replication and maintenance.

Mutational analysis of the components that orchestrate mtDNA replication *in vivo* will lead us to a better understanding of the mtDNA replication in homeostasis and in disease. The *Drosophila* model system is favourable for studying this process mainly due to its genetic tractability. The work that is presented here can now be used to isolate other interacting proteins that participate in the replication process by screening for enhancers and suppressors of phenotypes due to *tamas* mutation.

# Chapter 5 B:

# Identification of mutations in the gene encoding the accessory subunit of mitochondrial DNA polymerase and its phenotypic consequences

## Introduction

The Pol γ-α as been shown to possess both the polymerase and proof-reading activity (Spelbrink et al. 2000, Wernette and Kaguni 1986, Lewis et al. 1996). Initial biochemical experiments that isolated the mitochondrial DNA polymerase holoenzyme also showed the existence of a ~35kDa accessory subunit associated with the catalytic subunit (Wernette and Kaguni 1986). Both subunits have been cloned and characterized in a variety of systems, including *Drosophila* (Lewis et al. 1996, Wang et al. 1997) . While the catalytic subunit contains both 5′→3′ DNA polymerase and 3′→5′ exonuclease activities biochemical studies have demonstrated that the accessory subunit is essential for the catalytic efficiency and the high processitivity of the holoenzyme (Carrodeguas et al. 1999, Wang and Kaguni 1999, Lim et al. 1999, Carrodeguas et al. 2000, Johnson et al. 2000). Structural and functional studies support the hypothesis that the accessory subunit has an additional role as a primer recognition factor (Fan et al. 1999, Carrodeguas et al. 2001, Fan and Kaguni 2001). A cellular requirement for the accessory subunit has not yet been demonstrated, because mutations in the gene encoding it have not been described in any organism. In this chapter, we describe the candidate *Drosophila* gene that codes for the accessory subunit of mtDNA polymerase, identification of mutants for this locus and followed by description of organismal consequences of lesions in this gene.

## Results

### I. Identification and molecular characterization of mutations in the accessory-subunit gene of DNA polymerase γ.

The 10 Kb micro-region containing the gene for the accessory subunit of DNA polymerase γ, *pol γ–β*, is depicted in **Figure 30 A**. We identified as candidate mutations in *pol γ–β*, two mutant alleles isolated previously within the complementation group l(2)34De. Sequence analysis demonstrated that these mutant strains indeed carried disruptions in the *pol γ–β* gene (**Figure 31 B**). The mutant allele *pol γ–β*$^{1}$ is an EMS-induced mutation resulting in a glutamic acid substitution of a highly conserved glycine residue in the N-terminal domain of the accessory subunit (**Figure 31 C** and **D**). The *pol γ–β*$^{2}$ allele is a spontaneous mutation caused by an in-frame 74 bp insertion in the N-terminal domain, that creates a premature stop (**Figure 31E**). The lethal complementation group l(2)34De is thus demonstrated as encoding the accessory subunit of DNA polymerase γ (*pol γ–β*). This conclusion was further substantiated by the finding that one copy of the *pol γ–β* gene under the control of the heat shock promoter Hsp70 partially complements the lethality caused by the *pol γ–β*$^{1}$ mutation (See **Appendix M**).

**II. Loss of mtDNA due to mutations in the accessory subunit gene disrupts mitochondrial morphology.**

Biochemical studies have demonstrated that the accessory subunit of *Drosophila* Pol γ is essential to maintain the catalytic efficiency of the holoenzyme (Fan and Kaguni 2001, Carrodeguas et al. 2001). The accessory subunit is likely involved in maintaining the holoenzyme structural integrity through contacts between the M and C regions and multiple sites in the exonuclease (exo) region, and part of the spacer between the exo and DNA polymerase (pol) regions, in the catalytic subunit (Fan and Kaguni 2001). Furthermore, structural modeling predicted roles for the accessory subunit in both primer recognition and in holoenzyme processivity (Fan et al. 1999). It was thus important to evaluate mtDNA content and integrity in the *pol γ–β* mutants. The evaluation of mtDNA levels in mutants was conducted by Laurie Kaguni and her colleagues. **Figure 32** shows a quantitative Southern blot of wild-type and *pol γ–β* mutant DNA hybridized with a mtDNA probe, and with a multiple copy genomic probe as a control. These experiments reproducibly fail to detect any mtDNA, demonstrating severe mtDNA depletion in the *pol γ–β* mutants. Estimation of Pol γ–β protein in mutant larvae by immunoblot analysis also did not result in any detectable level of protein, presumably limited by the sensitivity of the enhanced chemiluminiscent detection system (pers. comm. Laurie Kaguni).

To analyze the consequences of mtDNA depletion on mitochondrial physiology and morphology we labeled brains dissected from *pol γ–β* mutant larvae with the selective dye Mitotracker Red, concomitantly with the nuclear stain DAPI. The uptake and fluorescence of Mitotracker Red is dependent upon the presence of a membrane potential and oxidative conditions within the mitochondria, and can thus be used to assess mitochondrial integrity as well as morphology and abundance.

The organization of mitochondria in wild-type *Drosophila* neuron is similar to that described for live mammalian cells using the fluorescent dye JC-1 (Gilkerson et al. 2000). Typically, mitochondria are found in a reticulum surrounding the nucleus (**Figure 33 A**). Reduction in *pol γ–β* gene function results in an overall disorganization of this reticular pattern. There is an expansion of areas showing no mitochondrial staining, together with the appearance of nuclei lacking a surrounding mitochondrial reticulum (**Figure 33 B** and **C**). Also similar to that observed in mtDNA-depleted mammalian cells, the mitochondrial reticulum appears fragmented, as evidenced by the increased presence of vesicular profiles. These results also suggest, at least at this level of resolution, that mitochondrial number is not reduced drastically. Likewise, mutations that disrupt the function of the catalytic subunit of Pol γ (Pol γ-α) show a similar phenotype (**Figure 33 D**, **E** and **F**).

**III. Mutations in the accessory subunit gene are lethal to the organism and impair cell proliferation in the central nervous system and exhibit melanotic "tumor" profiles.**

Mutations in the *pol γ–β* gene are strict organismal lethals in transheterozygous with a deficiency of the region, and fail to complement each other (**Table 4**). In all cases, lethality occurs during the early pupal period. The *pol γ–β* mutants begin pupariation, on average, 2-3 days later than wild-type controls, and die soon after. These results indicate that the two mutant alleles of the *pol γ–β* gene represent complete lack of gene function with regard to organismal lethality, and suggest the presence of a maternal contribution sufficient for embryonic and larval development.

The two *pol γ–β* mutations complement completely null alleles of the *tamas* gene encoding the catalytic subunit (*pol γ-α*, **Table I**). Thus, a single copy of each of the genes encoding the two subunits of the pol γ holoenzyme provides sufficient gene product for organismal viability. The external appearance of larvae lacking the accessory subunit of Pol γ–α is indistinguishable from wild type, while larvae mutant for the catalytic subunit gene are noticeably smaller (Iyengar et al. 1999). **Figure 34** depicts a lateral view of brain hemispheres of these mutants seen under Normarski optics. The CNS of larvae carrying mutations in the accessory subunit gene are smaller than that of wild-type controls, but not as much as that of larvae in catalytic-subunit gene mutants (**Figure 34 D, E** and **F**). In order to assess cell proliferation, we labeled third instar larvae with

bromodeoxyuridine, BrdU. An overall reduction in BrdU incorporation in the CNS was observed in both mutants. This is well illustrated by the aberrant BrdU labeling observed in the proliferation center of the optic lobes.

Late third instar larva that fail to wander and pupariate on schedule show many melanotic tumours (**Figure 35**). All mutant genotype combinations display such profiles. These melanotic aggregations appear in the fat body area and the lymph gland region of the animal. This may suggest that these tissue are sensitive to loss of Pol γ-β in late third instar stage.

**IV. Larval behaviour is affected moderately by reduction in accessory subunit function**

To evaluate the consequences of lack of accessory-subunit gene function for overall nervous system and muscle function, we measured larval locomotion in the absence of any light stimulus. The heteroallelic combination of the two alleles, and the *pol* $\gamma$–$\beta^1$ allele heterozygous over a deficiency of the region, did not impair significantly larval locomotion, and locomotion was affected only when the larvae carried the *pol* $\gamma$–$\beta^2$ allele over a deficiency of the region (**Figure 36 A**). In contrast, null mutations in the catalytic-subunit gene reduced locomotion more severely, and prevented the larval response to light (Iyengar et al. 1999). Larval locomotory deficit in *pol* $\gamma$-$\beta^2$/*Df(2L)b80c1*

did not exhibit abnormal response to light however they continued to show abnormal locomotion during the On/Off assay (**Figure 36 B**).

## Discussion

According to *in vitro* biochemical reconstitution experiments, the accessory subunit of mitochondrial DNA polymerase has been reported to play a crucial role in mtDNA synthesis. It functions to enhance the catalytic efficiency of the holoenzyme by imparting higher processivity or stability during synthesis of a new mtDNA strand. *In vitro* expression of a recombinant catalytic subunit of *Drosophila* Pol γ-α (*tamas*) monomer has been shown to possess at least 20-50 times lower catalytic activity as compared to the heterodimer (Wang and Kaguni 1999). The importance of Pol γ-β has also been highlighted in mtDNA replication models where this subunit has been hypothesized to play a role in RNA primer recognition. According to this model based on in vitro experiments, mtDNA replication originates in a lead strand where initiation of replication is coupled to transcription through generation of RNA primers (Lee and Clayton 1998). This model proposes that the nascent transcript primers resemble tRNA like structures that may be recognized by the Pol γ-β subunit, thus this subunit may act as primer recognition factor/processivity clamp loader and thereby allowing the recruitment of the catalytic subunit. In *Drosophila,* this hypothesized role of Pol γ-β is supported by structural models which indicate that portions of its C-terminal region resembles anticodon binding domain of class IIa amino acyl-tRNA synthetases (Fan et al 1999).

In the previous study on *tam* gene we observed that the *pol* $\gamma$-$\beta$ resided only ~3.8 kb downstream of *tam*. We asked whether mutations in this gene also affected nervous system development and function similar to mutations in *tamas*. The genetic map strongly suggested two previously identified lethal complementation groups in the neighbourhood of the *tamas* gene to be putative candidates for *pol* $\gamma$-$\beta$. By direct sequencing, we showed that the two available alleles of *l(2)34De* were indeed mutated in the gene coding for *pol* $\gamma$-$\beta$. Individual homozygous mutants are not viable beyond the embryonic stage, although we did observe a very small fraction of *pol* $\gamma$-$\beta^1$ individuals to survive until larval stage. Since heterozygous combination of individual alleles with a deficiency chromosome that is deleted for this gene allows larval development, we believe that background lethals may contribute to the earlier stage of lethality. Using these mutant alleles we showed that these mutations cause mtDNA depletion and disruption in mitochondrial morphology and cell proliferation in the CNS.

The results of these experiments did not determine whether all tissues are equally affected by these mutations. For example, the DNA samples used in southern analysis were obtained from total larval homogenate. The level of mtDNA in the CNS or any other specific tissue that may represent a fraction of the total sample may not be detected in such experiment as it may fall below the level of resolution. Hence the sensitivity of various tissues to loss of mtDNA remains to be investigated. The two

available *pol* $\gamma$-$\beta$ mutations, namely an insertion in the amino terminus, which creates a premature stop, and an amino acid substitution in a very conserved glycine residue within the conserved motif GPLGVEL, with respect to glycyl-tRNA synthase, similarly disrupt *Drosophila* development (**Figure 31**). Both alleles in combination with a chromosomal deficiency as well as the heteroallelic combination cause organismal lethality at the same stage during metamorphosis. This is also the case for nearly all other mutant phenotypes. It is reasonable to conclude that an insertion of a premature stop so near the amino terminus will generate a truncated protein, which is largely devoid of function and must thus represent a null mutation. Taken together these observations suggest that the *pol* $\gamma$-$\beta^1$ allele also represent a near complete lack-of-function mutation in this gene. Therefore the presence of Glycine in position 31 is essential for the function of the accessory subunit in mtDNA synthesis.

The GPLGVEL stretch is highly conserved when one compares the atypical motif 1 (M1) of glycyl-tRNA synthetase from *Thermus thermophilus* to homologs of Pol $\gamma$-$\beta$ in *Drosophila*, humans and mouse. Although, M1 as defined by sequence similarity outside the GPLGVEL motif is partly missing in the *Drosophila* gene. This motif has been described as a functionally important region for the *T.thermophilus* glycy-tRNA synthetase dimerization and its activity due to interaction of this motif with the active site of the other monomer (Eriani et al. 1993, Logan et al. 1995). Within the helical part

of this motif the Glycine residue has been identified as a consensus residue. This conclusion is based on a comprehensive comparison made among prokaryotic and eukaryotic dimeric gly-tRNA synthetase protein alignments (Mazauric et al. 1998). Phylogenetic tree analysis shows that the *pol* $\gamma$-$\beta$ may have evolved as a result of horizontally transferred gene from a prokaryotic *Thermus-Deinococcus* group Interestingly, this process is proposed to have occurred not as a part of endosymbiosis of mitochondria by eukaryotes but was acquired only before the arthropod chordate lineages separated, since one cannot identify a similar gene in *C. elegans* genome (Wolf and Koonin 2001). As a rare example, this gene product appears to have been recruited for a vital function after its acquisition by arthropods and chordates lineages.

The consequence of substitution of Glycine 31 for the biochemical function of the accessory subunit has not yet been determined. It can however be inferred from previously reported in vitro studies using various deletion mutants of the mouse *pol* $\gamma$-$\beta$ gene. Deletions including the very well conserved motif GPLGVEL, completely lack activity and do not bind, with the catalytic subunit and to a primer template oligonucleotide (Carrodeguas et al. 1999), suggesting that interaction with the catalytic subunit is mediated through this domain and that it is necessary for the function of the holoenzyme.

Recent crystalographic studies suggest that the mouse Pol γ-β exists as a homodimer and that the M1, as defined by sequence similarity and encompassing the conserved GPLGVEL motif is part of the interface that participates in dimerization (Carrodeguas et al 2001). Our finding that an amino acid change within this conserved motif represents a null mutation in this gene supports the hypothesis that the function of this motif is conserved and its integrity essential for the activity of the holoenzyme.

The current hypothesis of Pol γ-β function is based on *in vitro* biochemical assays and structural-functional analysis. It proposes that the accessory subunit function as a processitivity clamp and primer recognition factor and is therefore essential for mtDNA replication (Fan et al. 1999). Thus, it was our expectation that lack of function mutations in the genes coding for either one of the subunits would disrupt development and organismal homeostasis similarly. Surprisingly this is not entirely the case. Mutations in the catalytic subunit gene appear to have more drastic consequences for the organism than mutations in the accessory subunit. *tamas* mutant larvae are considerably smaller, displaying smaller CNS and small malformed imaginal discs, than similarly aged larvae carrying mutations in the accessory subunit gene. This is also true for the extent of the locomotory deficit.

The difference in the stage of lethality may reflect a difference in the requirement of these genes during development. *tam* mutant larvae exhibit a significantly longer

larval stage and die as third instar foraging larvae while on the food substrate (Iyengar et al. 1999). These mutants never enter pupariation or exhibit the behavioural and developmental changes that signal the end of larval stage and the beginning of metamorphosis. By contrast, accessory subunit mutants are able to wander and enter pupariation and die soon after. This difference in the developmental stage of lethality of these two mutants may be attributable to differences in cell growth and cell proliferation.

In *Drosophila*, cells that will form the adult fly or imago, the so called imaginal discs, are diploid and actively divide during the larval stages, while cells that form the larva never divide and are polytene (Madhavan and Scheiderman 1977, Smith and Orr-Weaver 1991). Starvation or adverse nutritional conditions can delay larval development and the onset of pupariation, a phenocopy of mutations in the catalytic subunit gene (Mensua and Moya 1983). These starved larvae are, like the *tamas* mutant, noticeably reduced in size. Similarly, partial but not complete ablation of imaginal discs either by gamma-irradiation or using cell lethal mutations delay the onset of pupariation (Simpson et al. 1980, Poodry and Woods 1990). These observations suggest that the developmental delay observed in larvae mutant for the catalytic subunit gene may be largely due to disruption of both cell growth and proliferation. The cell proliferation defects can occur due to mitochondrial dysfunction. Recently, hypoxic conditions have

been shown to induce cell cycle arrest in *Drosophila* embryos, implicating the role of oxidative phosphorylation in driving cell proliferation (Digregorio et al. 2001). Taken together, these observations suggest that mutations in the accessory subunit gene still allow for overall mitochondrial function sufficient for the larval transition into pupariation. By contrast, mutations in the catalytic subunit gene disrupt mitochondrial function such that transition into metamorphosis is completely prevented presumably by the inability of the larva to reach the appropriate size and developmental stage. Alternatively, the observed differences between the phenotypes of the accessory and catalytic mutants may reflect a difference in the amount or in the perdurance of the maternal contribution of these two genes in tissues that are critical for the viability of the organism. This point is supported by the observation of melanotic tumors in mutant larvae that fail to pupariate on time. Such profiles are not observed in *tam* mutants.

Melanotic tumor formation in larva has been understood to be a consequence of larval immune system response (Sparrow 1978). The circulating hemocytes have been described to attack damaged tissues so as to engulf and isolate the damage (Rizki 1960). Cells that fail to undergo apoptosis have been hypothesized to be targets for such an immune response (Song et al. 1997). For example, *dcp-1* (caspase-1) mutants show similar localizations of melanotic profiles as *pol* $\gamma$-$\beta$ mutants (Song et al. 1997). The

melanotic tumor formation in the fat body area and the lymph gland remains to be investigated further.

The difference in the effect of mutations in the two subunits can also be discussed in the light of their expression profiles during development. The mRNA steady state level and rate of transcription of the accessory subunit gene is maximal during 6-10 h AEL while the expression of the catalytic subunit gene remains low from 3 h AEL onwards (Lefai et al. 2000). While this study did not address the relative maternal contribution of catalytic and accessory subunit proteins it supports the hypothesis that the phenotypic consequence may be due to differential regulation.

The work presented in this chapter is the first attempt at addressing the in vivo role of *pol γ-β*. *Drosophila* is an ideal model to carry out *in vivo* structure-function analysis because it is amenable to mutational and genetic approaches. Further mutational analysis of *pol γ-β* can be carried out through chemically-induced mutations in this gene. Following such an experiment one can easily identify mutant alleles by lack of complementation with the null mutations described in this chapter.

## References

Anderson, S., Bankier, A. T., Barrell, B. G., de Bruijn, M. H., Coulson, A. R., et al. 1981. Sequence and organization of the human mitochondrial genome. *Nature* 290:457-65.

Artavanis-Tsakonas, S., Matsuno, K., Fortini, M. E. 1995. Notch signaling. *Science* 268:225-32.

Ashburner, M., Misra, S., Roote, J., Lewis, S. E., Blazej, R., et al. 1999. An exploration of the sequence of a 2.9-Mb region of the genome of *Drosophila melanogaster*: the Adh region. *Genetics* 153:179-219.

Bodily, K. D., Morrison, C. M., Renden, R. B., Broadie, K. 2001. A novel member of the Ig superfamily, turtle, is a CNS-specific protein required for coordinated motor control. *J Neurosci* 21:3113-25.

Bonfini, L., Karlovich, C. A., Dasgupta, C., Banerjee, U. 1992. The Son of sevenless gene product: a putative activator of Ras. *Science* 255:603-6.

Campos, A. R., Fischbach, K. F., Steller, H. 1992. Survival of photoreceptor neurons in the compound eye of *Drosophila* depends on connections with the optic ganglia. *Development* 114:355-66.

Chen, A. H., Ni, L., Fukushima, K., Marietta, J., O'Neill, M., et al. 1995. Linkage of a gene for dominant non-syndromic deafness to chromosome 19. *Hum Mol Genet* 4:1073-6.

Clayton, D. A. 1982. Replication of animal mitochondrial DNA. *Cell* 28:693-705.

DiGregorio, P. J., Ubersax, J. A., O'Farrell, P. H. 2001. Hypoxia and nitric oxide induce a rapid, reversible cell cycle arrest of the *Drosophila* syncytial divisions. *J Biol Chem* 276:1930-7.

DiMauro, S., Schon, E. A. 2001. Mitochondrial DNA mutations in human disease. *Am J Med Genet* 106:18-26.

Eriani, G., Cavarelli, J., Martin, F., Dirheimer, G., Moras, D., Gangloff, J. 1993. Role of dimerization in yeast aspartyl-tRNA synthetase and importance of the class II invariant proline. *Proc Natl Acad Sci U S A* 90:10816-20.

Fadic, R., Johns, D. R. 1996. Clinical spectrum of mitochondrial diseases. *Semin Neurol* 16:11-20.

Fortini, M. E., Artavanis-Tsakonas, S. 1994. The suppressor of hairless protein participates in notch receptor signaling. *Cell* 79:273-82.

Furriols, M., Bray, S. 2000. Dissecting the mechanisms of suppressor of hairless function. *Dev Biol* 227:520-32.

Ganetzky, B., Wu, C. F. 1982. *Drosophila* mutants with opposing effects on nerve excitability: genetic and spatial interactions in repetitive firing. *J Neurophysiol* 47:501-14.

Gilkerson, R. W., Margineantu, D. H., Capaldi, R. A., Selker, J. M. 2000. Mitochondrial DNA depletion causes morphological changes in the mitochondrial reticulum of cultured human cells. *FEBS Lett* 474:1-4.

Green, P., Hartenstein, A. Y., Hartenstein, V. 1993. The embryonic development of the *Drosophila* visual system. *Cell Tissue Res* 273:583-98.

Greenwald, I. 1998. LIN-12/Notch signaling: lessons from worms and flies. *Genes Dev* 12:1751-62.

Hayashi, J., Ohta, S., Kagawa, Y., Takai, D., Miyabayashi, S., et al. 1994. Functional and morphological abnormalities of mitochondria in human cells containing mitochondrial DNA with pathogenic point mutations in tRNA genes. *J Biol Chem* 269:19060-6.

Insdorf, N. F., Bogenhagen, D. F. 1989. DNA polymerase gamma from Xenopus laevis. II. A 3'----5' exonuclease is tightly associated with the DNA polymerase activity. *J Biol Chem* 264:21498-503.

Johnson, A. A., Johnson, K. A. 2001. Exonuclease proofreading by human mitochondrial DNA polymerase. *J Biol Chem* 276:38097-107.

Johnson, D. F., Hamon, M., Fischel-Ghodsian, N. 1998. Characterization of the human mitochondrial ribosomal S12 gene. *Genomics* 52:363-8.

Kaguni, L. S., Olson, M. W. 1989. Mismatch-specific 3'----5' exonuclease associated with the mitochondrial DNA polymerase from *Drosophila* embryos. *Proc Natl Acad Sci U S A* 86:6469-73.

Kernan, M., Cowan, D., Zuker, C. 1994. Genetic dissection of mechanosensory transduction: mechanoreception- defective mutations of *Drosophila*. *Neuron* 12:1195-206.

Kidd, S., Lieber, T., Young, M. W. 1998. Ligand-induced cleavage and regulation of nuclear entry of Notch in *Drosophila melanogaster* embryos. *Genes Dev* 12:3728-40.

Larsson, N. G., Wang, J., Wilhelmsson, H., Oldfors, A., Rustin, P., et al. 1998. Mitochondrial transcription factor A is necessary for mtDNA maintenance and embryogenesis in mice. *Nat Genet* 18:231-6.

Lecourtois, M., Schweisguth, F. 1995. The neurogenic suppressor of hairless DNA-binding protein mediates the transcriptional activation of the enhancer of split complex genes triggered by Notch signaling. *Genes Dev* 9:2598-608.

Lee, D. Y., Clayton, D. A. 1996. Properties of a primer RNA-DNA hybrid at the mouse mitochondrial DNA leading-strand origin of replication. *J Biol Chem* 271:24262-9.

Lefai, E., Fernandez-Moreno, M. A., Alahari, A., Kaguni, L. S., Garesse, R. 2000. Differential regulation of the catalytic and accessory subunit genes of *Drosophila* mitochondrial DNA polymerase. *J Biol Chem* 275:33123-33.

Lewis, D. L., Farr, C. L., Wang, Y., Lagina, A. T., 3rd, Kaguni, L. S. 1996. Catalytic subunit of mitochondrial DNA polymerase from *Drosophila* embryos. Cloning, bacterial overexpression, and biochemical characterization. *J Biol Chem* 271:23389-94.

Logan, D. T., Mazauric, M. H., Kern, D., Moras, D. 1995. Crystal structure of glycyl-tRNA synthetase from Thermus thermophilus. *Embo J* 14:4156-67.

Maier, D., Farr, C. L., Poeck, B., Alahari, A., Vogel, M., et al. 2001. Mitochondrial single-stranded DNA-binding protein is required for mitochondrial DNA replication and development in *Drosophila melanogaster*. *Mol Biol Cell* 12:821-30.

Mazat, J. P., Rossignol, R., Malgat, M., Rocher, C., Faustin, B., Letellier, T. 2001. What do mitochondrial diseases teach us about normal mitochondrial functions...that we already knew: threshold expression of mitochondrial defects. *Biochim Biophys Acta* 1504:20-30.

Mazauric, M. H., Keith, G., Logan, D., Kreutzer, R., Giege, R., Kern, D. 1998. Glycyl-tRNA synthetase from Thermus thermophilus--wide structural divergence with other prokaryotic glycyl-tRNA synthetases and functional inter-relation with prokaryotic and eukaryotic glycylation systems. *Eur J Biochem* 251:744-57.

Miklos, G. L., Rubin, G. M. 1996. The role of the genome project in determining gene function: insights from model organisms. *Cell* 86:521-9.

Napoli, L., Bordoni, A., Zeviani, M., Hadjigeorgiou, G. M., Sciacco, M., et al. 2001. A novel missense adenine nucleotide translocator-1 gene mutation in a Greek adPEO family. *Neurology* 57:2295-8.

Neupert, W. 1997. Protein import into mitochondria. *Annu Rev Biochem* 66:863-917
Nusslein-Volhard, C. 1994. Of flies and fishes. *Science* 266:572-4.

Pavlidis, P., Ramaswami, M., Tanouye, M. A. 1994. The *Drosophila easily shocked* gene: a mutation in a phospholipid synthetic pathway causes seizure, neuronal failure, and paralysis. *Cell* 79:23-33.

Pavlidis, P., Tanouye, M. A. 1995. Seizures and failures in the giant fiber pathway of *Drosophila bang- sensitive* paralytic mutants. *J Neurosci* 15:5810-9.
Pflugfelder, G. O. 1998. Genetic lesions in Drosophila behavioural mutants. *Behav Brain Res* 95:3-15.

Rogge, R. D., Karlovich, C. A., Banerjee, U. 1991. Genetic dissection of a neurodevelopmental pathway: Son of sevenless functions downstream of the sevenless and EGF receptor tyrosine kinases. *Cell* 64:39-48.

Rustin, P., Rotig, A. 2002. Inborn errors of complex II - Unusual human mitochondrial diseases. *Biochim Biophys Acta* 1553:117-22.

Schleiff, E. 2000. Signals and receptors--the translocation machinery on the mitochondrial surface. *J Bioenerg Biomembr* 32:55-66.

Schmitt, M. E., Bennett, J. L., Dairaghi, D. J., Clayton, D. A. 1993. Secondary structure of RNase MRP RNA as predicted by phylogenetic comparison. *Faseb J* 7:208-13.

Schweisguth, F., Posakony, J. W. 1992. Suppressor of Hairless, the *Drosophila* homolog of the mouse recombination signal-binding protein gene, controls sensory organ cell fates. *Cell* 69:1199-212.

Simpson, P., Berreur, P., Berreur-Bonnenfant, J. 1980. The initiation of pupariation in *Drosophila*: dependence on growth of the imaginal discs. *J Embryol Exp Morphol* 57:155-65.

Simpson, P., Morata, G. 1980. The control of growth in the imaginal discs of *Drosophila. Basic Life Sci* 16:129-39

Song, Z., McCall, K., Steller, H. 1997. DCP-1, a *Drosophila* cell death protease essential for development. *Science* 275:536-40.

Spelbrink, J. N., Li, F. Y., Tiranti, V., Nikali, K., Yuan, Q. P., et al. 2001. Human mitochondrial DNA deletions associated with mutations in the gene encoding Twinkle, a phage T7 gene 4-like protein localized in mitochondria. *Nat Genet* 28:223-31.

Spelbrink, J. N., Toivonen, J. M., Hakkaart, G. A., Kurkela, J. M., Cooper, H. M., et al. 2000. In vivo functional analysis of the human mitochondrial DNA polymerase POLG expressed in cultured human cells. *J Biol Chem* 275:24818-28.

Szabad, J., Bryant, P. J. 1982. The mode of action of "discless" mutations in *Drosophila* melanogaster. *Dev Biol* 93:240-56.

Takata, K., Yoshida, H., Hirose, F., Yamaguchi, M., Kai, M., et al. 2001. *Drosophila* mitochondrial transcription factor A: characterization of its cDNA and expression pattern during development. *Biochem Biophys Res Commun* 287:474-83.

Toivonen, J. M., O'Dell, K. M., Petit, N., Irvine, S. C., Knight, G. K., et al. 2001. Technical knockout, a *Drosophila* model of mitochondrial deafness. *Genetics* 159:241-54.

Triepels, R. H., van den Heuvel, L. P., Loeffen, J. L., Buskens, C. A., Smeets, R. J., et al. 1999. Leigh syndrome associated with a mutation in the NDUFS7 (PSST) nuclear encoded subunit of complex I. *Ann Neurol* 45:787-90.

Triepels, R. H., Van Den Heuvel, L. P., Trijbels, J. M., Smeitink, J. A. 2001. Respiratory chain complex I deficiency. *Am J Med Genet* 106:37-45.

van den Ouweland, J. M., Maechler, P., Wollheim, C. B., Attardi, G., Maassen, J. A. 1999. Functional and morphological abnormalities of mitochondria harbouring the tRNA(Leu)(UUR) mutation in mitochondrial DNA derived from patients with maternally inherited diabetes and deafness (MIDD) and progressive kidney disease. *Diabetologia* 42:485-92.

Van Goethem, G., Dermaut, B., Lofgren, A., Martin, J. J., Van Broeckhoven, C. 2001. Mutation of POLG is associated with progressive external ophthalmoplegia characterized by mtDNA deletions. *Nat Genet* 28:211-2.

Wallace, D. C. 1999. Mitochondrial diseases in man and mouse. *Science* 283:1482-8.

Wang, Y., Farr, C. L., Kaguni, L. S. 1997. Accessory subunit of mitochondrial DNA polymerase from *Drosophila* embryos. Cloning, molecular analysis, and association in the native enzyme. *J Biol Chem* 272:13640-6.

Wernette, C. M., Kaguni, L. S. 1986. A mitochondrial DNA polymerase from embryos of *Drosophila melanogaster*. Purification, subunit structure, and partial characterization. *J Biol Chem* 261:14764-70.

Woodruff, R. C., Ashburner, M. 1979a. The genetics of a small autosomal region of *Drosophila melanogaster* containing the structural gene for alcohol dehydrogenase. I. Characterization of deficiencies and mapping of ADH and visible mutations. *Genetics* 92:117-32.

Woodruff, R. C., Ashburner, M. 1979b. The genetics of a small autosomal region of *Drosophila melanogaster* containing the structural gene for alcohol dehydrogenase. II. Lethal mutations in the region. *Genetics* 92:133-49.

Wu, C. F., Ganetzky, B. 1992. Neurogenetic studies of ion channels in *Drosophila*. *Ion Channels* 3:261-314

Yang, P., Shaver, S. A., Hilliker, A. J., Sokolowski, M. B. 2000. Abnormal turning behaviour in *Drosophila* larvae. Identification and molecular analysis of scribbler (*sbb*). *Genetics* 155:1161-74.

Zeviani, M., Servidei, S., Gellera, C., Bertini, E., DiMauro, S., DiDonato, S. 1989. An autosomal dominant disorder with multiple deletions of mitochondrial DNA starting at the D-loop region. *Nature* 339:309-11.

Zhang, Y. Q., Roote, J., Brogna, S., Davis, A. W., Barbash, D. A., et al. 1999. *stress sensitive B* encodes an adenine nucleotide translocase in *Drosophila melanogaster*. *Genetics* 153:891-903.

Zipursky, S. L., Venkatesh, T. R., Teplow, D. B., Benzer, S. 1984. Neuronal development in the *Drosophila* retina: monoclonal antibodies as molecular probes. *Cell* 36:15-26.

**Figure 19.**

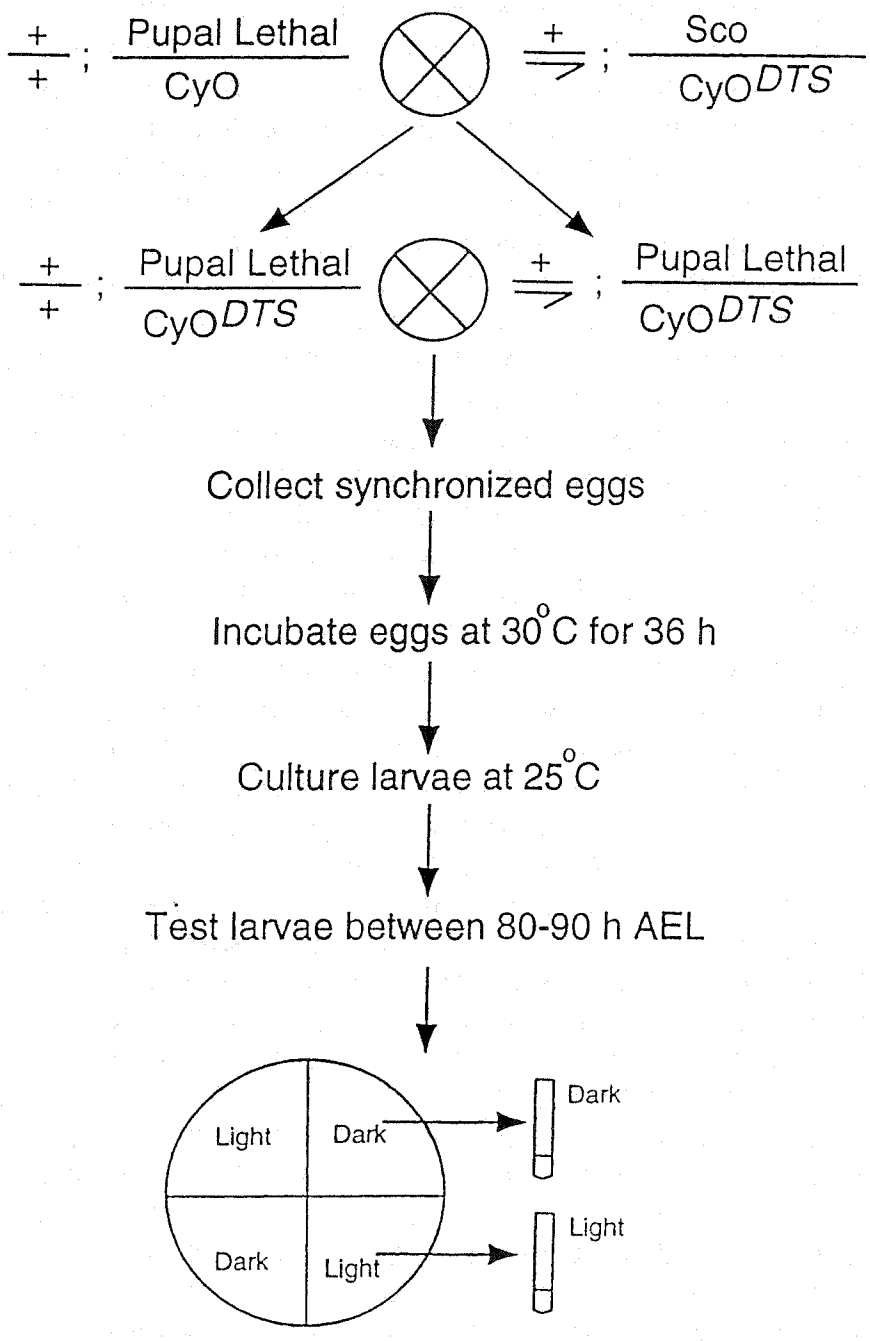


Final Response Index

$$= \frac{\text{(Dark-Dark escapers) - (Light -Light escapers)}}{\text{(Dark-Dark escapers) + (Light -Light escapers)}}$$

**Figure 19.**

**The flowchart used for the plate assay screen.** The figure first shows the crossing scheme that was used to obtain second chromosome lethal mutations in a conditional $CyO^{DTS}$ genetic background. This allows isolation of homozygous lethal mutation carrying larvae after subjecting all larvae to a 30° C temperature regimen during embryonic development. Following which the surviving larvae were tested for the response to light in the plate assay. Larvae from the assays were separated with respect to their distribution on the plate. The separated larvae were allowed to pupate and were scored for escapers. The escaper data was used to correct the original response index to obtain a true response index.

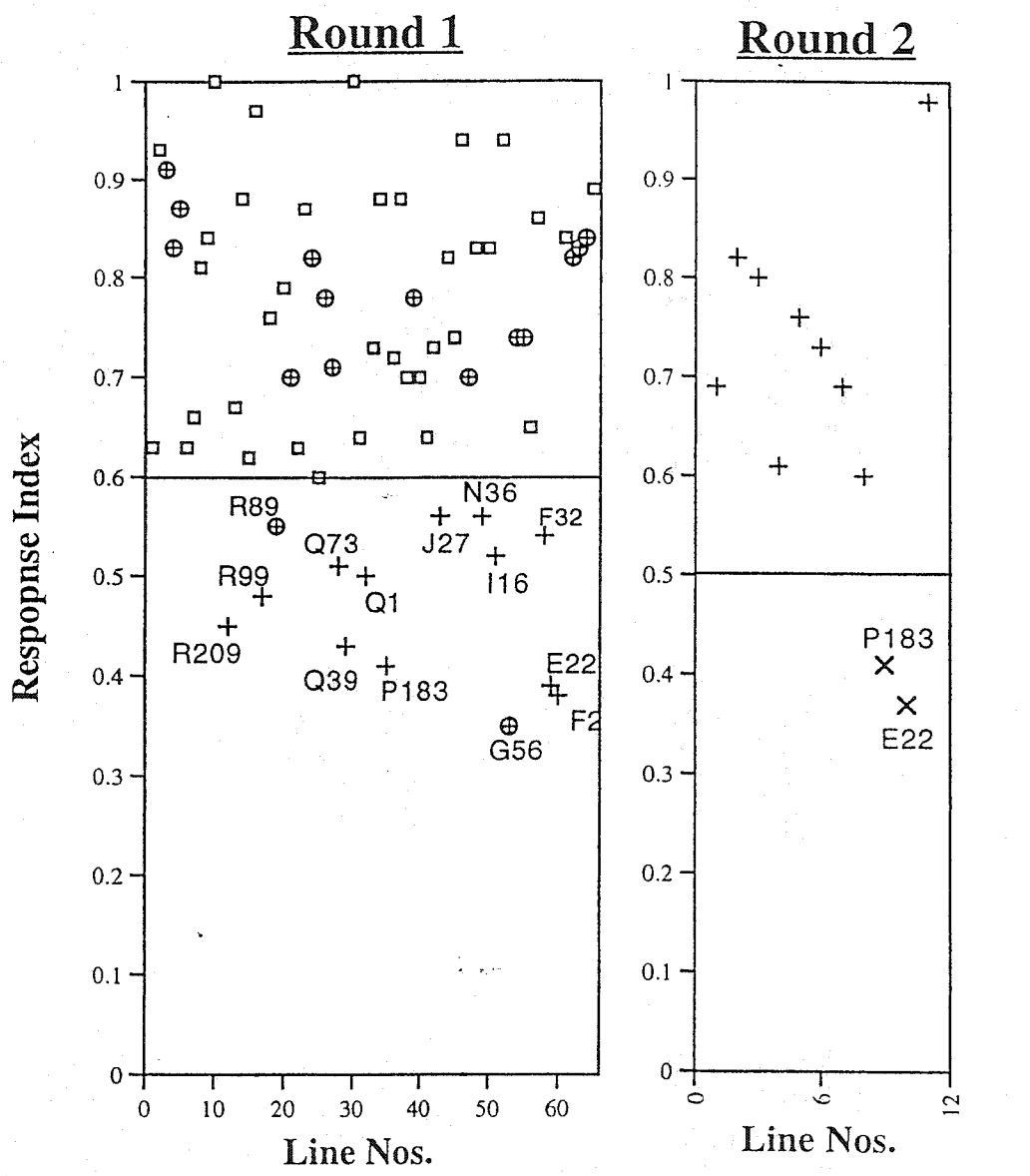


□ Normal Response Index

\+ Abnormal Response Index Selected for Round 2

⊕ Putative Foraging Mutants Isolated by another group

\+ Normal Response Index

× Abnormal Response Index

**Figure 20.**

**Behavioural screen using plate assay:** This is a scatterplot of the final response indices after the first round and the second round of screening. In the first round the lines which showed response index above 0.6 were discarded. Strains with response indices indicated by (+) were screened again. The second screen resulted in two lines (*E22* and *P183*) that were tentatively considered to be behaviour mutants.

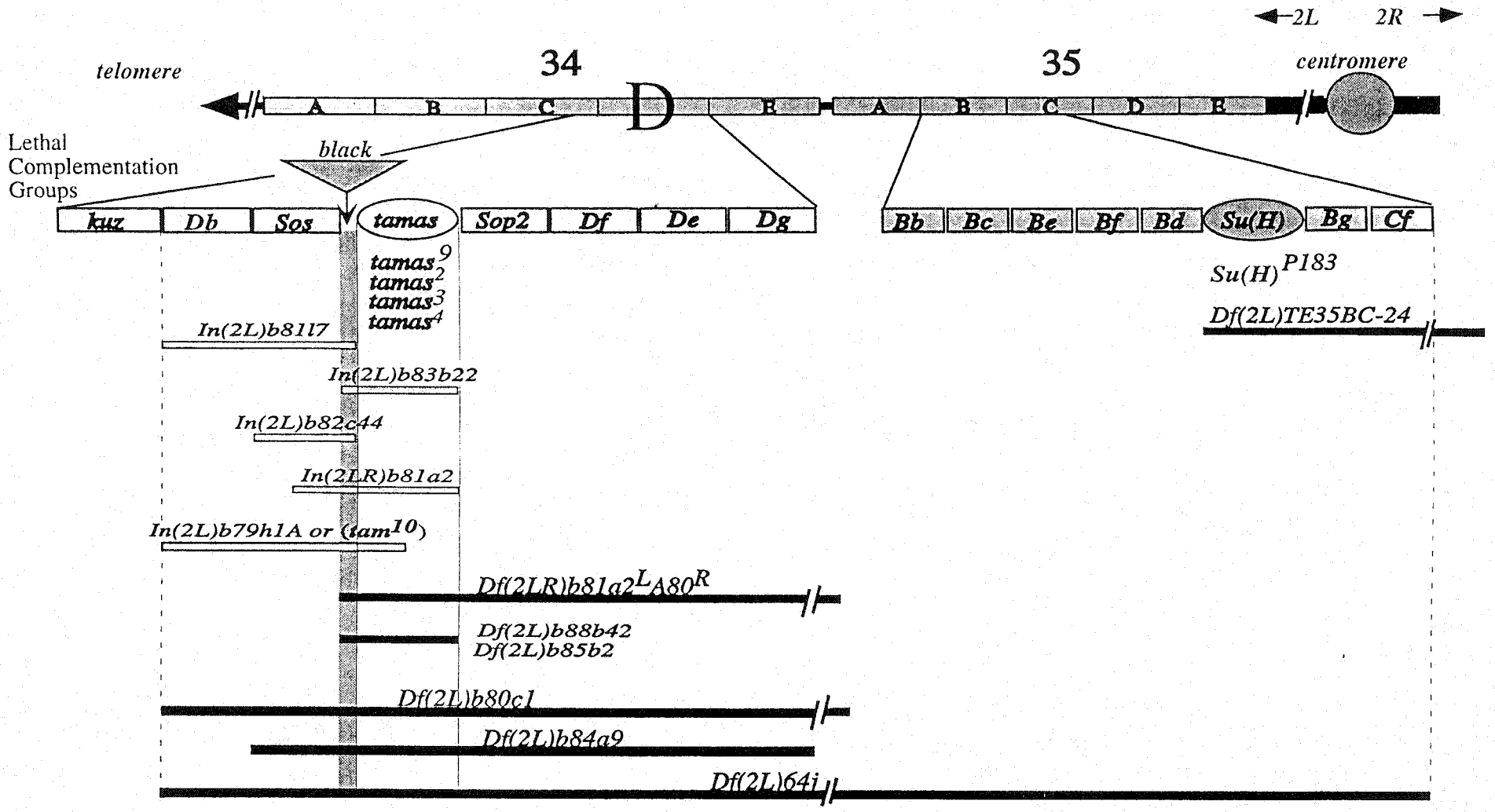
2L
2R
telomere
34
35
centromere
A
B
C
D
E
A
B
C
D
E
Lethal
Complementation
Groups
black
kuz
Db
Sos
tamas
Sop2
Df
De
Dg
Bb
Bc
Be
Bf
Bd
Su(H)
Bg
Cf
tamas9
tamas2
tamas3
tamas4
Su(H)P183
Df(2L)TE35BC-24
In(2L)b81l7
In(2L)b83b22
In(2L)b82c44
In(2LR)b81a2
In(2L)b79h1A or (tam10)
Df(2LR)b81a2LA80R
Df(2L)b88b42
Df(2L)b85b2
Df(2L)b80c1
Df(2L)b84a9
Df(2L)64i

**Figure 21.**

**Genetic analysis of *P183***

A diagram of the left arm of the second chromosome cytological regions, 34 and 35. The 34D and 35B regions are expanded to show the lethal complementation groups included in these sub-divisions (Woodruff and Ashburner 1979). The rectangular boxes represent the lethal complementation groups, the oval shaped boxes represent the lethal hits present in the *P183* line. The triangular insert in the 34D region is the non-vital gene *black*. Below the lethal complementation groups the chromosomal aberrations that were used in this study are shown. Solid bars depict the chromosomal segments that are deleted in the deficiency strains. In strains carrying chromosomal inversions the inverted segment is shown here as a gray bar.

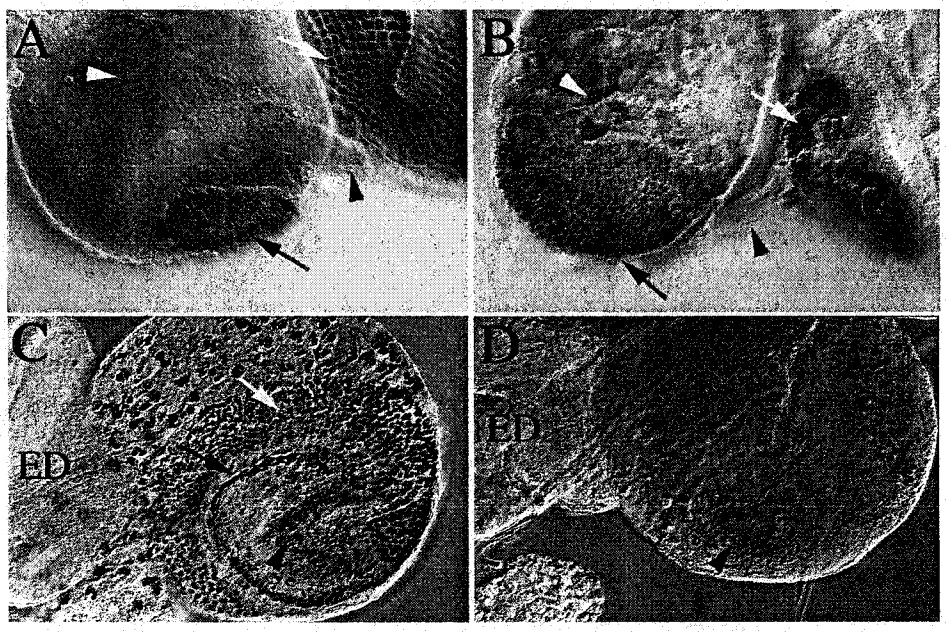
A
B
C
ED
D
ED

**Figure 22.**

**Optic lobe development is abnormal in homozygous *b, Su(H)*[P183] larvae**

A- Shows the developing adult visual system (obliquely lateral view) in a wild type larva visualized using an antibody against the post-mitotic neuron specific antigen, elav. The anti- elav staining pattern in the wild type suggest that the some cells have been committed to neuronal fate in the lamina region (black arrow). and a patch of cells (white arrowhead) have also differentiated to neurons, that are perhaps the neurons that will form the deeper visual center like lobula. The black arrowhead is indicates the photoreceptor projection route. Panel B- Shows the optic lobe area and the photoreceptor projection in *b, Su(H)*[P183] homozygous mutant larvae visualized with anti-elav. The black arrow in optic lobe area shows immunoreactivity for Elav antigen. The distribution of elav-positive cells is abnormal, and in relation the brain the staining area appears to be larger. White arrow indicates the photoreceptors in the eye imaginal disc and the black arrowhead indicates the optic stalk. Panel C and D- Shows BrdU staining pattern to visualize mitotically active cells in the wild type optic lobe. The outer proliferation center (OPC) (white arrow), lamina precursor cells (arrowhead) and the inner proliferation center are seen to be arranged in a stereotypically concentric manner. This arrangement of the proliferation centers is almost absent in *b, Su(H)*$^{[P183]}$ homozygous mutant larvae. The inner proliferation center (arrowhead) and a very marginalized and reduced OPC and scattered S-phase cells are seen.

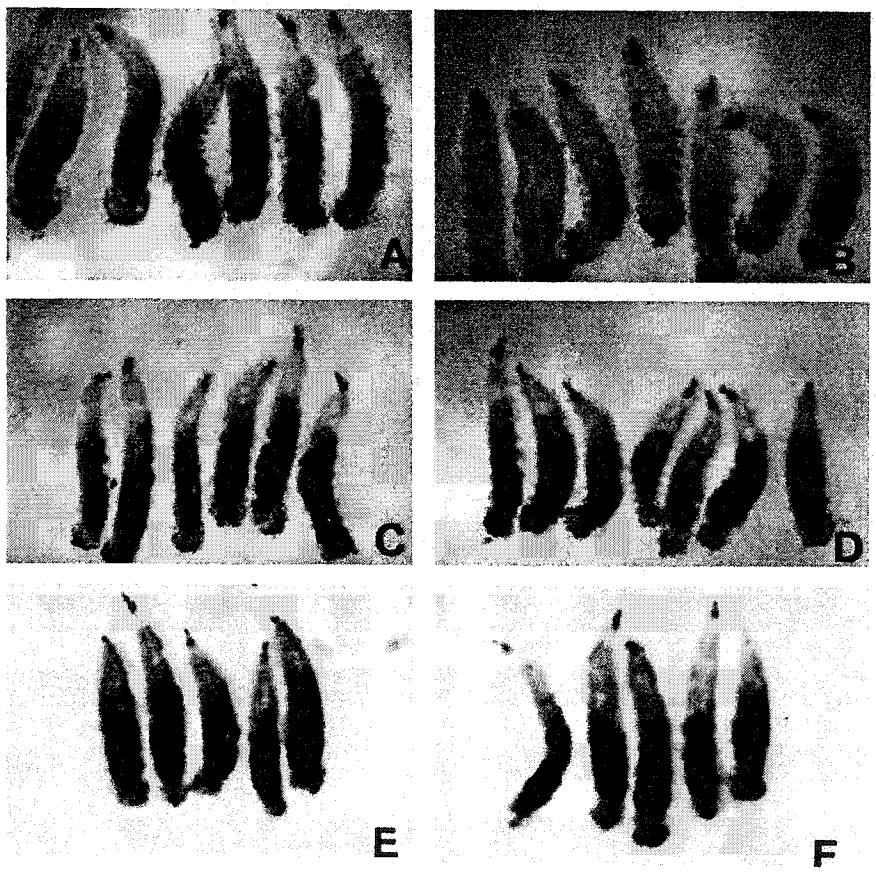
A
B
C
D
E
F

**Figure 23.**

**Mutations in the *tam* gene resulted in prolonged foraging in third instar larvae**

The larvae were grown in medium supplemented with bromophenol blue. Emptying of the guts as seen by the disappearance of blue coloration is a landmark of the transition from foraging to wandering stage (A) Wild type (*P183/CyO-y*$^{+}$), 108 hours AEL (after egg lay). At this time larvae are at the wandering/foraging boundary. At this point in development wild-type larvae show blue coloration of the gut. (B) Wild-type (*P183/CyO-y*$^{+}$), 117 hours AEL. Larvae at the wandering phase show reduced blue coloration in the gut. (C) *P183/P183* larvae at 108 hours AEL. (D) *P183/tam*$^{3}$ larvae at 108 hours AEL. (E) *P183 /P183* larvae at 117 hours AEL. (F) *P183/tam*$^{3}$ larvae at 119 hours AEL. The retention of blue coloration at time points where the wild-type larvae show reduced coloration indicated that the mutant larvae did not wander on time.

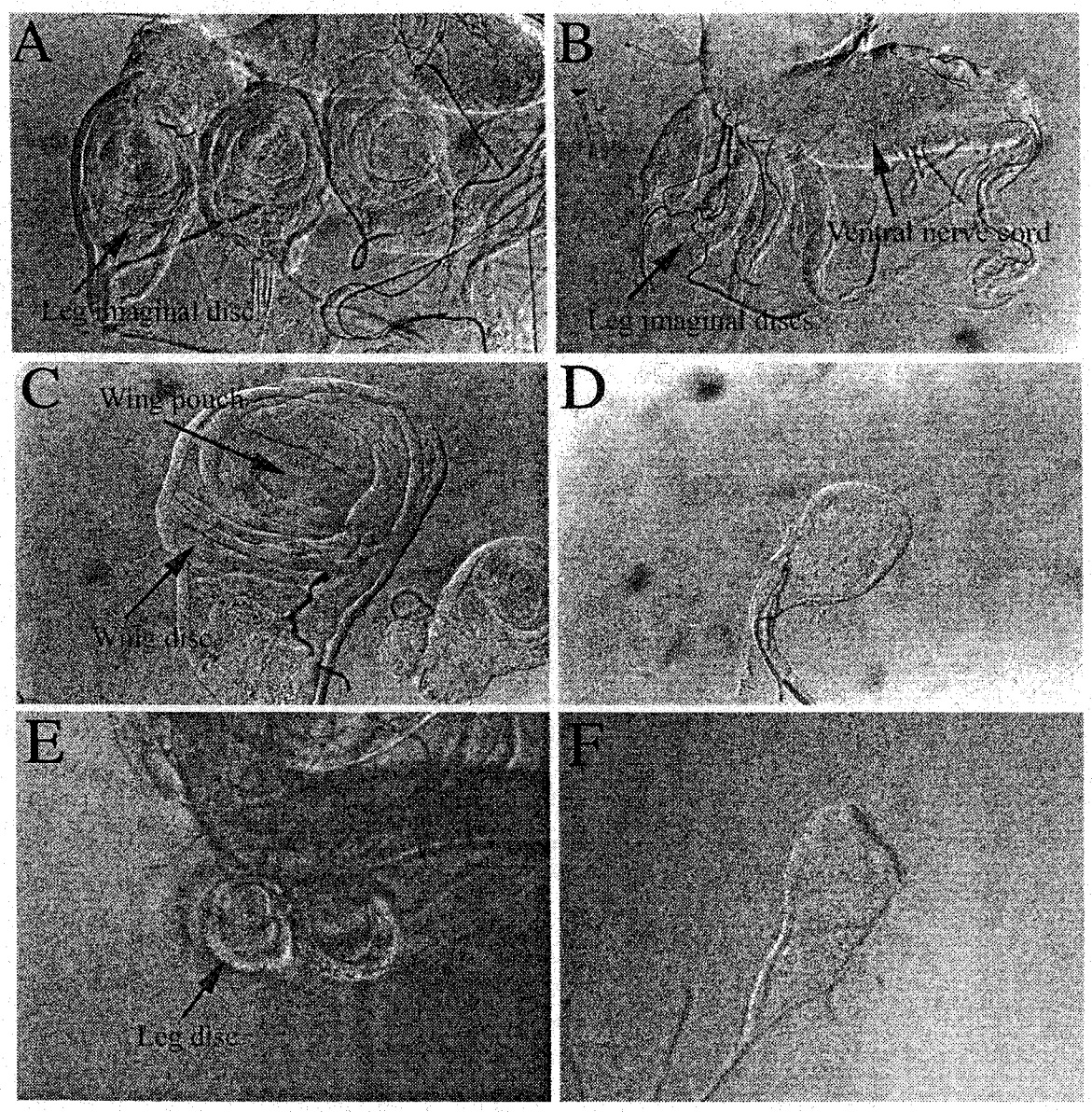
A
Leg imaginal disc
B
Ventral nerve cord
Leg imaginal discs
C
Wing pouch
Wing disc
D
E
Leg disc
F

**Figure 24.**

***P183* and the *tamas*$^{9}$ mutants show abnormal imaginal disc growth**

Panels A and B show leg discs and wing discs of a wild type (*P183/CyO(y+)*) and a P183 homozygous, ~110 h AEL larvae, respectively. Panels C and D show wing discs of (*P183/CyO(y+)*) and P183 homozygous mutant larva at the same age. The double mutant strain shows severe reduction in growth of both discs. Similarly the *tam*$^{9}$ mutant larvae also shows reduced leg disc and wing disc growth (E and F) at the same ~110 h age. All panels were captured at equal magnification. Wild type wing disc pouch measure approximately 150 μ in width at late third instar stage.

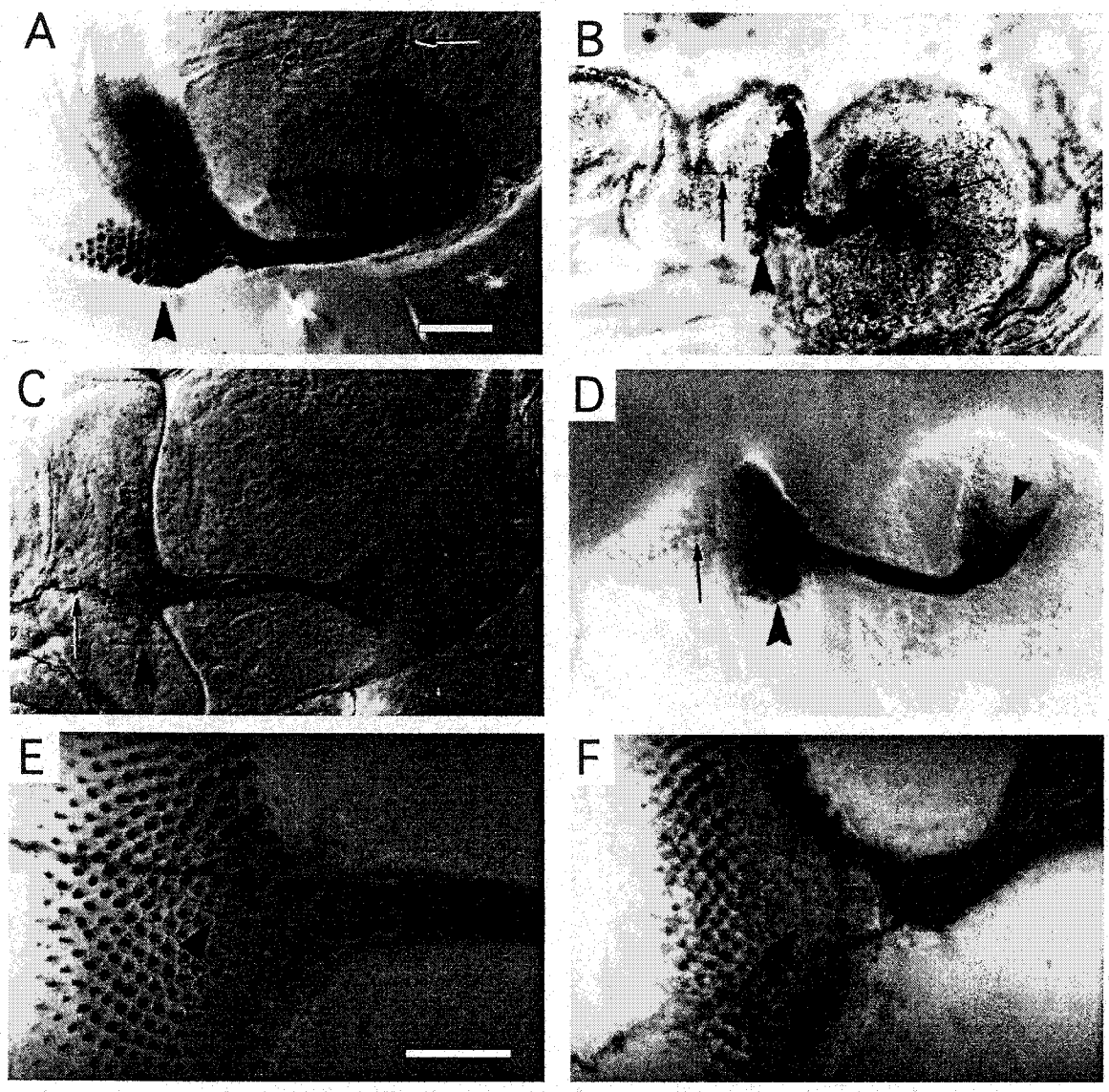
A
B
C
D
E
F

the mutant larvae. In mutant eye discs a similar clustered staining pattern at the posterior regions of the eye disc appears not to be maintained. Scale bar = 50 μm.

**Figure 25.**

**Morphology of the developing adult visual system in *tam* mutants**

The micrograph shows the developing adult visual system as seen by labeling with 24B10 primary antibody and HRP- conjugated secondary antibody. (A) Wild-type (Oregon-R) projection pattern viewed horizontally. In eye imaginal disc differentiating arrays of photoreceptors (large arrowhead) and the photoreceptor axonal projections of R1-R6 and R7-R8 into the optic lobe (smaller arrowheads) are seen. The larval optic nerve terminates deeper in the brain (arrow). (B) *P183/P183* . The photoreceptor differentiation is abnormal (arrowhead). Likewise photoreceptor axonal projection is disorganized (arrow). The larval optic nerve is present (thinner arrow). (C ) *P183/Df(2L)b80c1*. The defects in photoreceptor differentiation are apparent (arrowhead). Abnormal projection pattern of photoreceptors in the optic lobe can also be seen (smaller arrowhead). The larval optic nerve in present (arrow). (D) $P183/tam^{3}$. As well as showing delayed photoreceptor differentiation, the eye disc is smaller and the area of differentiated photoreceptors is abnormal (big arrowhead). The projection pattern is also abnormal (smaller arrowhead). (E) Wild type. The older photoreceptor clusters located more posteriorly retain the clustered staining pattern as the differentiation proceeds more anteriorly. (F) $tam^{9}/tam^{9}$. The differentiating eye disc of

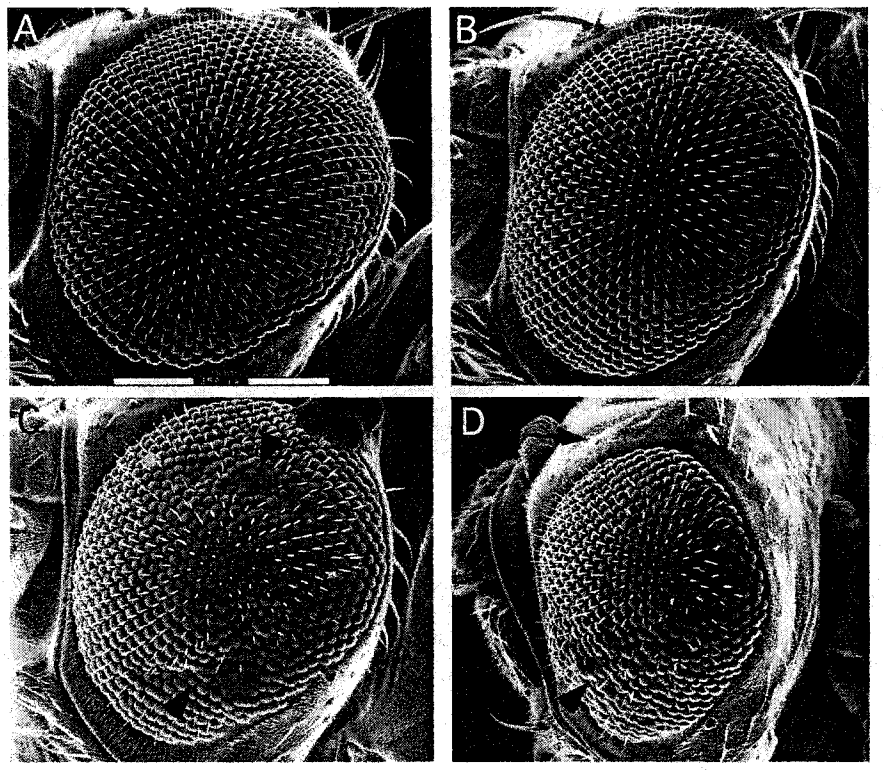
A
B
C
D

**Figure 26.**

**ESEM scan of compound eye defects in *tam* escapers**

(A) Wild-type control *In(2L)b79h1A/CyO-y*$^{+}$. (B) *In(2L)b79h1A/kuz*$^{1}$. *kuzbanian* (*kuz*) is the first known lethal complementation group to the left of *In(2L)b79h1A ;* it is not disrupted by this inversion as seen by the wild-type pattern of the compound eye. (C) *In(2L)b79h1A/tam*$^{9}$. The compound eye is characterized by disorganized surface, fused ommatidia and missing bristles (arrowhead). (D) *In(2L)b79h1A/tam*$^{3}$. The arrowhead shows the rough surface, missing bristles and fused ommatidia. These flies show a more severe disorganization of the eye than *In(2L)b79h1A/tam*$^{9}$. The scale bar in A represents 250μm, and is valid for all panels.

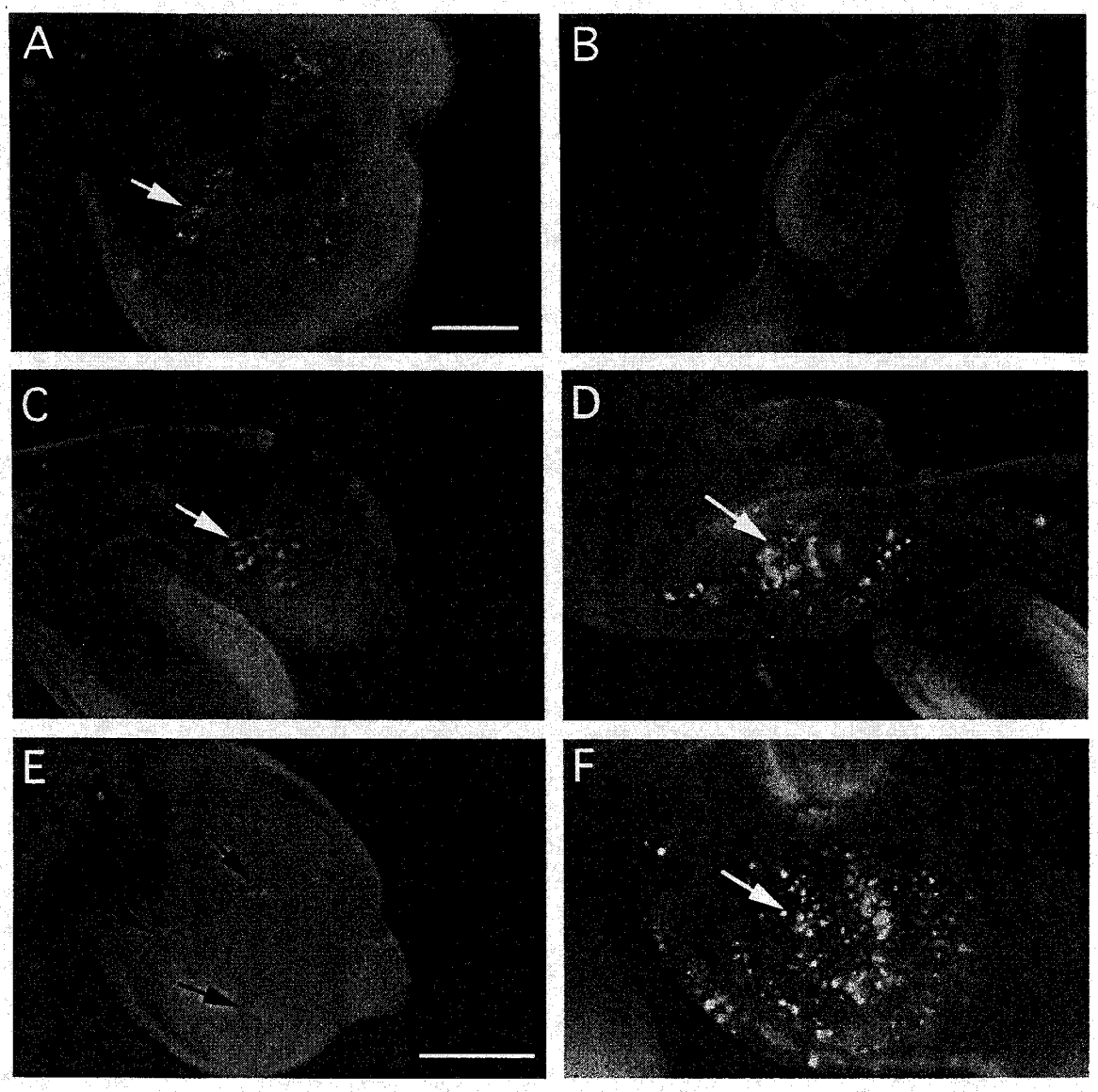
A
B
C
D
E
F

**Figure 27.**

**Cell death profile of *tam* mutants**

The micrographs show acridine orange staining of the developing eye disc where anterior is to the left (Panels A, C and E) and of the antennal disc (Panels B, D, and F). (A) Wild-type (*tam*$^{9}$/*CyO-y+*), eye disc portion of the eye antennal imaginal disc at 96 hours AEL. (B) Wild-type (*tam*$^{9}$/*CyO-y+*), antennal disc at 96 hours AEL. (C) *tam*$^{9}$/*tam*$^{9}$, mutant eye disc, at 96 hours AEL. (D) *tam*$^{9}$/*tam*$^{9}$, mutant antennal disc, at 96 hours AEL. (E) *tam*$^{9}$/*tam*$^{9}$, mutant eye disc, at 120 hours AEL. (F) *tam*$^{9}$/*tam*$^{9}$, mutant antennal disc at 120 hours AEL. The developing eye disc did not show the wild-type pattern of cell death. In younger mutant larvae cell death pattern is unlike the wild type, while in later samples cell death was not detected indicating delay in development. Scale bar in A represents 50μm and is valid for B, C and D. Scale bar in E represents 50μm and is valid for F.

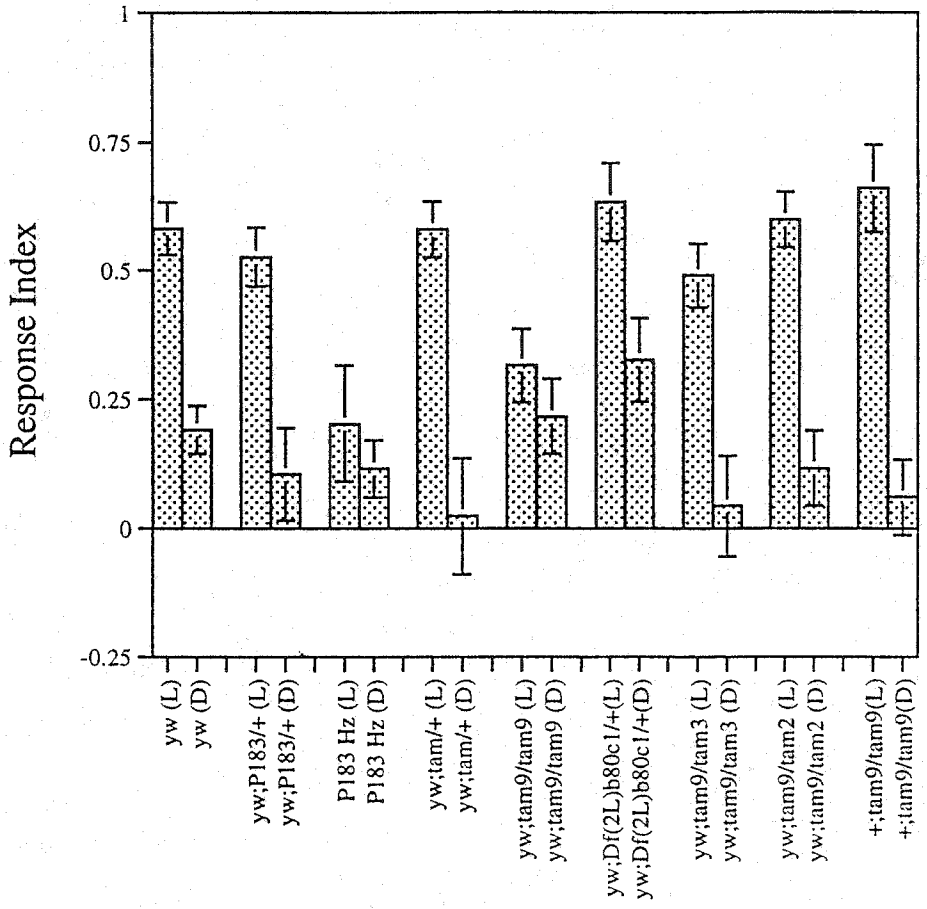
Response Index
1
0.75
0.5
0.25
0
-0.25
yw (L)
yw (D)
yw;P183/+ (L)
yw;P183/+ (D)
P183 Hz (L)
P183 Hz (D)
yw;tam/+ (L)
yw;tam/+ (D)
yw;tam9/tam9 (L)
yw;tam9/tam9 (D)
yw;Df(2L)b80c1/+(L)
yw;Df(2L)b80c1/+(D)
yw;tam9/tam3 (L)
yw;tam9/tam3 (D)
yw;tam9/tam2 (L)
yw;tam9/tam2 (D)
+;tam9/tam9(L)
+;tam9/tam9(D)

**Figure 28.**

**Genetic analysis of photobehaviour defect in *tam* mutants**

In the Checker assay each genotype was assayed with lights on (test assay) and lights off (control assay). A response to light is present when the response index obtained with lights on is significantly different from the response index obtained with lights off. The response index with lights on is not significantly different from that obtained with lights off in the homozygous *P183* and $tam^9$ strains at any level of comparison, indicating a lack of response to light. In all other strains tested the response index obtained with lights on is significantly higher than that obtained with the lights off (**$P$ <0.001, *P<0.01 by Student's $t$-test.). Wild-type control, lights on $n$=17, lights off $n$=19; *P183/+*, lights on $n$=22, lights off $n$=19; *P183/P183*, lights on $n$=14, lights off $n$=17; $tam^9$/+, lights on $n$=17, lights off $n$=16; $tam^9/tam^9$, lights on $n$=17, lights off $n$=15; *Df(2L)b80c1/+* , lights on $n$=12, lights off $n$=13; $tam^9/tam^3$, lights on $n$=22, lights off $n$=16.

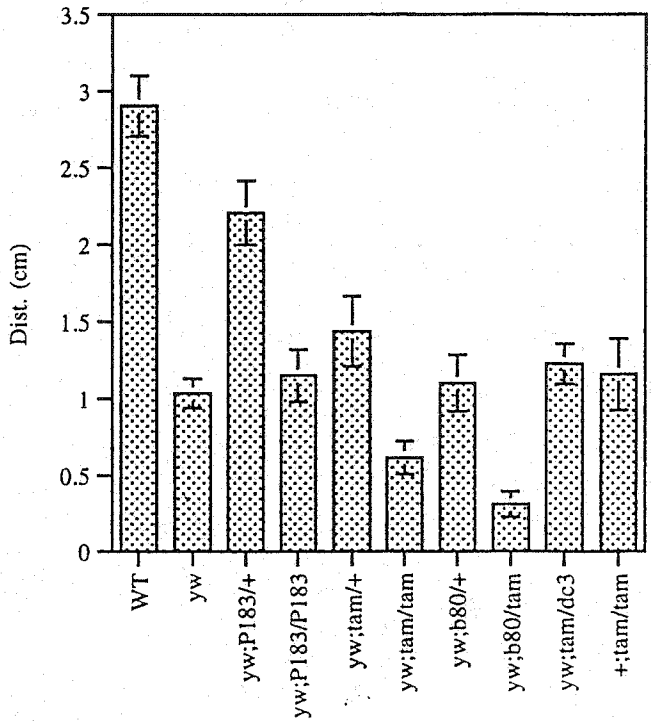
Dist. (cm)
3.5
3
2.5
2
1.5
1
0.5
0
WT
yw
yw;P183/+
yw;P183/P183
yw;tam/+
yw;tam/tam
yw;b80/+
yw;b80/tam
yw;tam/dc3
+;tam/tam

**Figure 29.**

**Genetic analysis of locomotory defect in *tam* mutants**

The graph depicts the mean distance traveled (SEM) in 30 seconds on a non-nutritive substrate in the absence of light. The following comparisons were made by Student's *t*-test: $tam^9/tam^9$ vs *P183/P183*, T=2.66, *P*=0.013; $tam^9/tam^9$ vs $tam^9$/*Df(2L)b80c1*, T=2.23 *P*=0.033; $tam^9$/+ vs *Df(2L)b80c1*/+, T= 1.71, *Df(2L)b80c1*/$tam^9$ vs. *Df(2L)b80c1*/+, T=3.89, *P*=0.0006; *P*=0.095; $tam^9/tam^9$ vs $tam^9/tam^3$, T=-3.16,*P*=0.001; $tam^3$/+ *vs* $tam^9/tam^3$, T=1.91, *P*=0.070. Wild-type control, *n*=19; *P183*/+, *n*=21; *P183/P183*, *n*=18; $tam^9$/+, *n*=22; $tam^9/tam^9$, *n*=17; *Df(2L)b80c1*/+, *n*=20; *Df(2L)b80c1*/$tam^9$, *n*=18; $tam^9$/+, *n*=12; $tam^3/tam^9$, *n*=18.

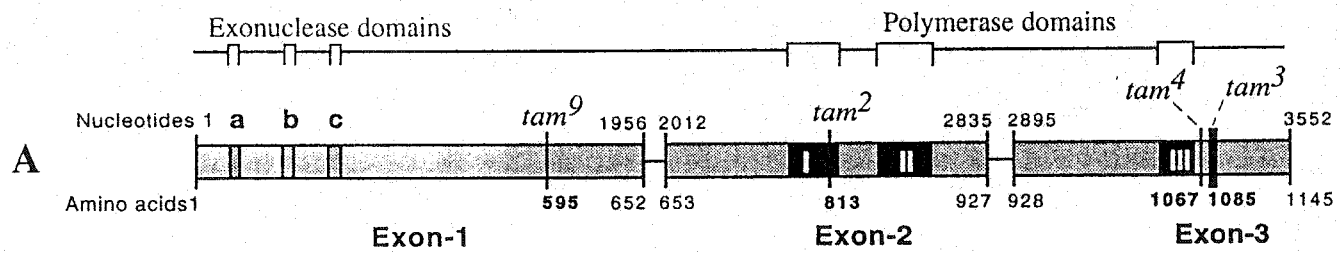


**B**

| | | |
|---|---|---|
| Wild type | 1770 | CGACTGCCCATGGAGCAACTTCTGGCG |
| | 591 | R L P M E Q L L A |
| *tam*$^{9}$ | | CGACTGCCCATGGCGCAACTTCTGGCG |
| | | R L P M A Q L L A |

**C**

| | | |
|---|---|---|
| Wild type | 2415 | GTTGGTGCCGATGTCGATTCGCAGGAGCT |
| | 805 | GV G A D V D S Q E L |
| *tam*$^{2}$ | | GTTGGTGCCGATGTCGATTCGCAGGTGCTG |
| | | V G A D V D S Q V |
| | | L |

**C'**

Pol 1

| | | | |
|---|---|---|---|
| DmPolγ | APPGYRL | VGADVDSQEL | WAIS |
| ScPolγ | APPGYCF | VGADVDSEEL | WAIS |
| XlPolγ | VPPGYHL | IGADVDSQEL | WIAA |

* *

**D**

| | | |
|---|---|---|
| Wild type | 3354 | TCGGTGGCCTTCTTCTCGTCCGTGGAGGTAGACACT |
| | 1080 | S V A F F S S V E V D T |
| *tam*$^{3}$ | | TCGGTGGCCTTCTTCTC-----TGGAGGTAGACGCT |
| | | S V A F F |

**E**

| | | |
|---|---|---|
| Wild type | 3186 | ATGACGCGCTCCTTTTGTGTGTCCCGCATC |
| | 1062 | M T R S F C V S R I |
| | | ATGACGCGCTCCTTT-GTGTGTCCCGCATC |
| *tam*$^{4}$ | | M T R S F V C P A |

**Figure 30.**

**Molecular lesions in *tam* mutant alleles**

The sequence data was aligned to the wild-type mitochondrial DNA polymerase catalytic subunit (DNA*pol-γ125*) gene sequenced by the BDGP. (A) Schematic depiction of the structure of DNA*pol-γ125* gene (Lewis *et al.* 1996). Boxes 1, 2 and 3 represent the conserved 3′-5′ exonuclease domains, and X, Y and Z represent the conserved DNA polymerase domains. Numbers above the exon boxes indicate the nucleotides from 1 to 3552 and numbers below the exon boxes indicate the amino acids from 1 to 1145. (B) Sequence alignment of $tam^{9}$ allele against Oregon-R wild type sequence. The shaded box shows mutation at nucleotide 1783 in $tam^{9}$ (A to C); this causes an amino acid change (glutamic acid to alanine). Panel (C) Sequence alignment of $tam^{2}$ allele against the corresponding parental sequence. The alignment shows an amino acid change from glutamic acid to valine at amino acid position 813 in a highly conserved polymerase domain. Panel (D) Sequence alignment of $tam^{3}$ against corresponding parental strain showing a 5-bp deletion beginning at nucleotide position 3371. (E) Shows the alignment of $tam^{4}$ against the corresponding parental sequence. The alignment resulted in identification of a single base pair at position 3201; this causes a frameshift of the remaining coding region.

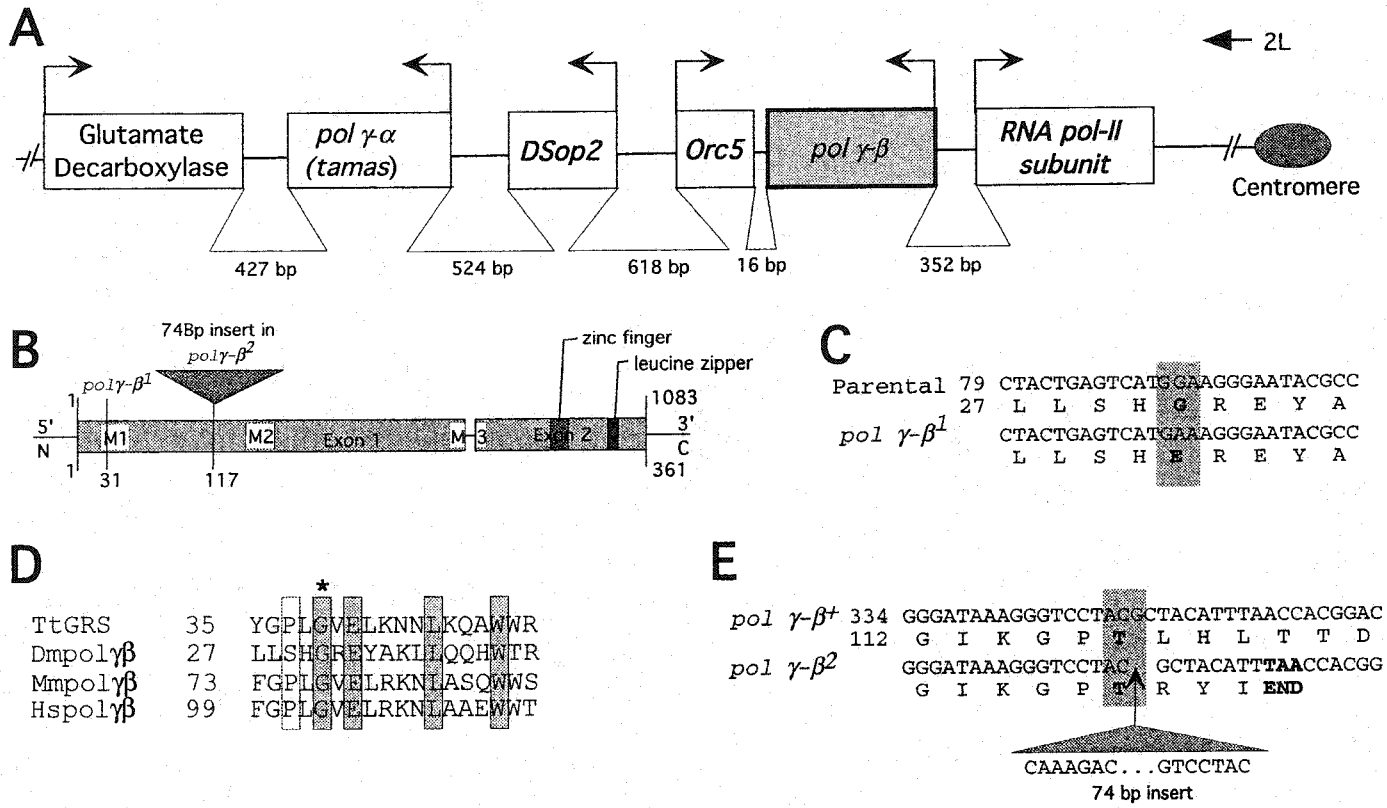
A
2L
Glutamate Decarboxylase
pol γ-α (tamas)
DSop2
Orc5
pol γ-β
RNA pol-II subunit
Centromere
427 bp
524 bp
618 bp
16 bp
352 bp
B
74Bp insert in pol γ-β2
pol γ-β1
zinc finger
leucine zipper
5'
N
M1
M2
Exon 1
M3
Exon 2
3'
C
1083
361
31
117
C
Parental 79 CTACTGAGTCATGGAAGGGAATACGCC
27 L L S H G R E Y A
pol γ-β1 CTACTGAGTCATGAAAGGGAATACGCC
L L S H E R E Y A
D
TtGRS 35 YGPLGVELKNNLKQAWWR
Dmpolγβ 27 LLSHGREYAKLLQQHWTR
Mmpolγβ 73 FGPLGVELRKNLASQWWS
Hspolγβ 99 FGPLGVELRKNLAAEWWT
E
pol γ-β+ 334 GGGATAAAGGGTCCTACGCTACATTTAACCACGGAC
112 G I K G P T L H L T T D
pol γ-β2 GGGATAAAGGGTCCTAC GCTACATTTAACCACGG
G I K G P T R Y I END
CAAAGAC...GTCCTAC
74 bp insert

**Figure 31.**

**Molecular characterization of mutations in the accessory subunit gene of *Drosophila* Pol γ**

(A) Schematic representation of the ~12 Kb micro region that contains the tightly-packed open reading frames (ORFs) of 6 genes, including the mitochondrial DNA polymerase catalytic subunit (*pol* $\gamma$-$\alpha$) and its accessory subunit (*pol* $\gamma$-$\beta$). Arrows indicate the direction of transcription; distances between the ORFs are indicated below the schematic. (B) Key features in the *pol* $\gamma$-$\beta$ ORF. The gene contains two exons. The positions of the sequenced mutations are indicated. (C) Nucleotide and amino acid sequence alignments of the parental strain with the *pol* $\gamma$-$\beta^1$ mutant allele. The base substitution at nucleotide 92 results in a codon change to glutamic acid for a highly conserved glycine (amino acid 31) (D) Amino acid sequence alignment within motif 1 of *T. thermophilus* Glycyl-tRNA synthetase with *D. melanogaster*, mouse and human Pol γ-β. The asterisk denotes the residue that is mutated in the *pol* $\gamma$-$\beta^1$ allele. The unshaded box represents a similar amino acid and the shaded boxes indicate conserved amino acids among all four proteins. (E) Nucleotide and amino acid sequence alignments of wild type strain with the *pol* $\gamma$-$\beta^2$ mutant allele. The *pol* $\gamma$-$\beta^2$ allele contains a 74 base pair insertion after nucleotide position 350, within the codon for threonine 117 within exon 1. This will result in premature termination of the translational product.

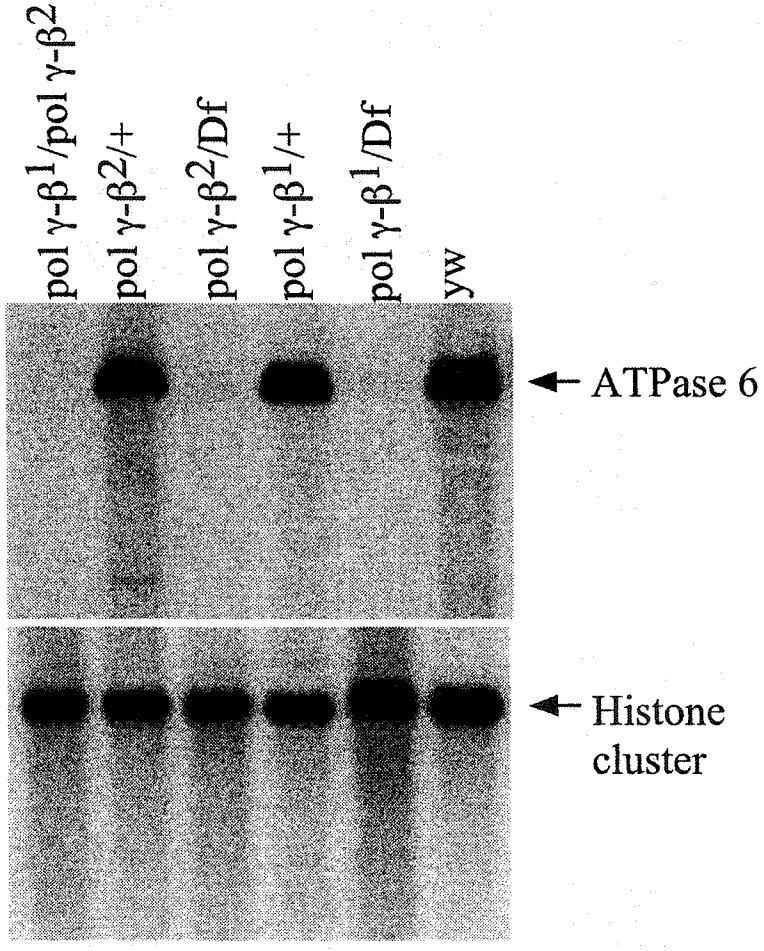
pol γ-β1/pol γ-β2
pol γ-β2/+
pol γ-β2/Df
pol γ-β1/+
pol γ-β1/Df
yw
ATPase 6
Histone cluster

**Figure 32.**

**Mitochondrial DNA is absent in mutants of the accessory subunit of *Drosophila* Pol γ.**

3 μg of total DNA that was isolated from third instar larvae was digested with *XhoI*, which cleaves mtDNA once, and duplicate samples of the DNAs (1 μg) were electophoresed in a 0.8% agarose gel, transferred to a nylon membrane and hybridized with [$^{32}$P]-labelled DNA probes from the ATPase 6 gene of mtDNA, and a repeated histone gene cluster as a nuclear DNA control. (This experiment was done by Laurie Kaguni and her colleagues in Michigan State Univ. Michigan, USA).

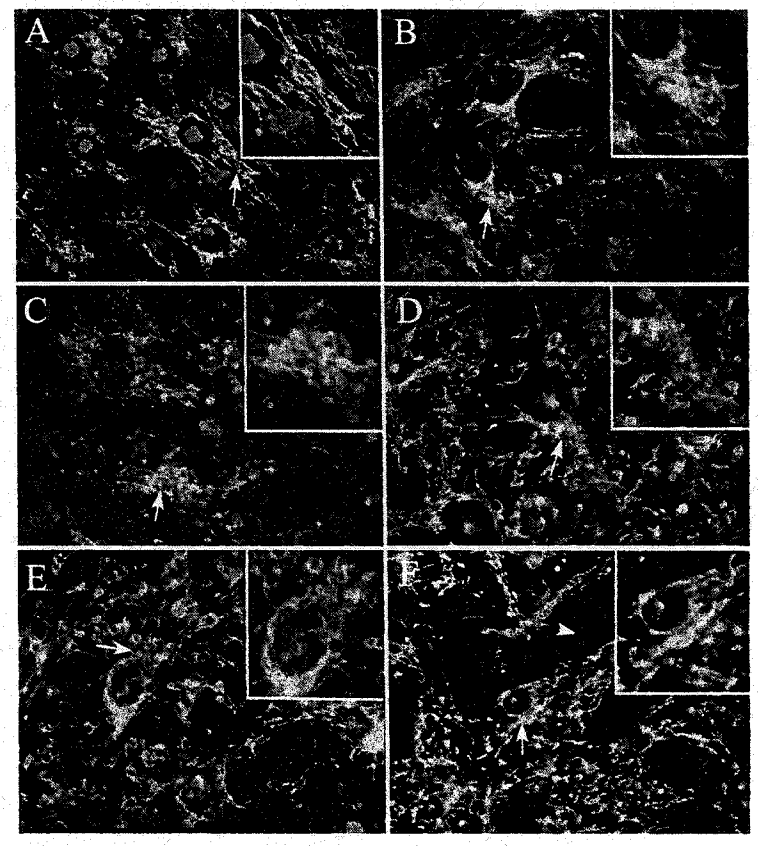
A
B
C
D
E
F

**Figure 33.**

**Mitochondrial morphology and localization are altered in mutants of Pol γ**

All panels depict photomicrographs of third instar larval brain hemispheres labeled with mitochondrial probe Mitotracker (red) and the nuclear stain DAPI (blue), photographed at the same magnification. The arrows point to the mitochondrial reticulum in all panels that is magnified in the inset. In wild type cells mitochondria are found in a reticulum tightly arranged in the periphery of the nucleus (arrow in A). Disruption of Pol γ function either by mutations in genes encoding the accessory subunit (B, C and D) or the catalytic subunit (E and F) disrupt this reticulum similarly. Abnormal mitochondrial morphology is characterized by vesicular staining pattern. (A) Wild type CNS (*pol γ-β$^1$/+*); (B) *pol γ-β$^1$* mutant CNS (*pol γ-β$^1$/Df(2L)b80c1*); (C) Heteroallelic combination of two accessory subunit mutant alleles (*pol γ-β$^2$/pol γ-β$^1$*); (D) *pol γ-β$^2$* mutant CNS (*pol γ-β$^2$/Df(2L)b80c1*). Catalytic subunit mutant CNS; (E) *tam$^2$/Df(2L)b80c1* (F) *tam$^9$/Df(2L)b80c1*. The arrowhead indicates empty regions devoid of any staining.

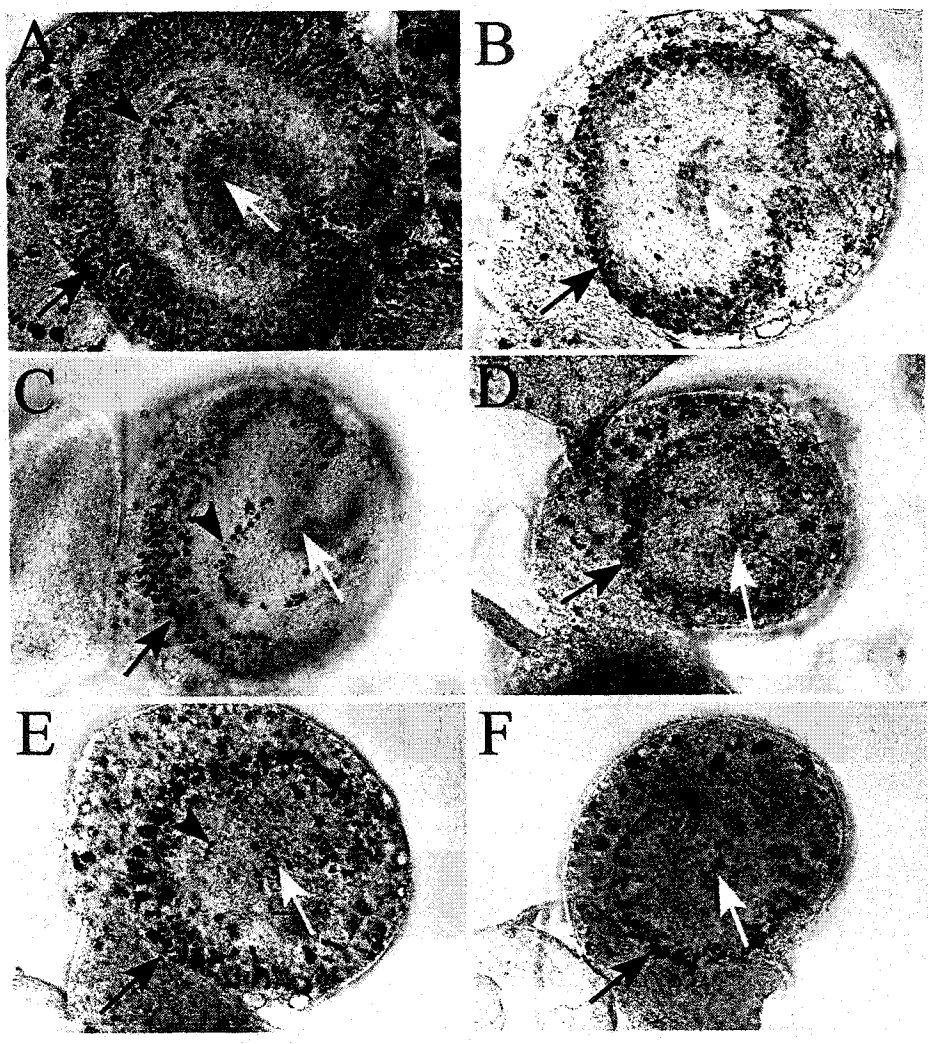
A
B
C
D
E
F

**Figure 34.**

**DNA replication and cell proliferation are impaired in mutants of Pol γ**

All panels depict photomicrographs of a lateral view of third instar larval brain hemispheres dissected from larvae that had incorporated BrdU in order to visualize mitotically active cells S-phase cells found in the developing adult optic lobes. All specimens were photographed at the same magnification. In all panels the black arrow indicates outer proliferation center (OPC), the arrowhead indicates the lamina precursor cells (LPC) and the white arrow indicates the inner proliferation center (IPC). Disruption of Pol γ function either by mutations in genes encoding the accessory subunit (B, C and D) or the catalytic subunit (E and F) disrupt these proliferation centers to the same extent. (A) Wild type CNS (*pol γ-β$^{1}$/+*). (B) *pol γ-β$^{1}$* mutant CNS (*pol γ-β$^{1}$/Df(2L)b80c1*). (C) Heteroallelic combination of two accessory subunit mutant alleles (*pol γ-β$^{2}$/pol γ-β$^{1}$*). (D) *pol γ-β$^{2}$* mutant CNS (*pol γ-β$^{2}$/Df(2L)b80c1*). Catalytic subunit mutant CNS. (E) *tam$^{2}$/Df(2L)b80c1*. (F) *tam$^{9}$/Df(2L)b80c1*.

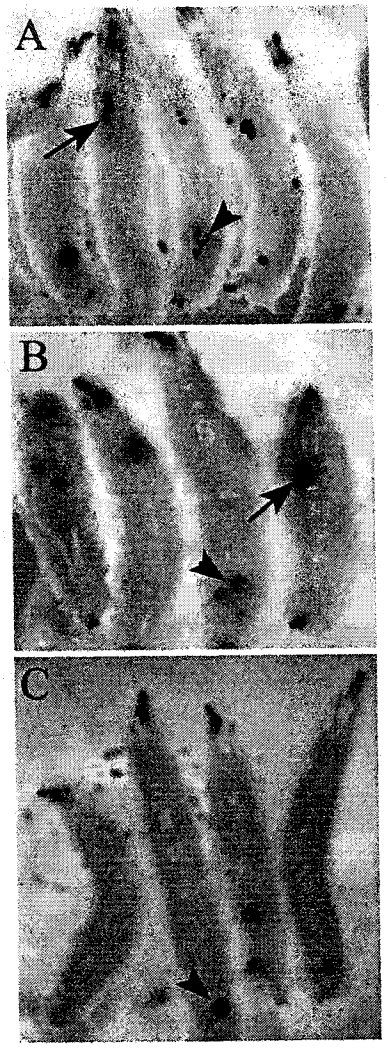
A
B
C

**Figure 35.**

**Mutations in *pol γ-β* result in melanotic "tumors" prior to pupariation**

Panels A, B and C show mutant larvae of the following genotype: A- *yw; pol γ-β¹/Df(2L)b80c1*, B- *yw; pol γ-β²/Df(2L)b80c1*, C- yw; *pol γ-β¹/ pol γ-β²*. All larvae are oriented with their anterior end pointing the top and their posterior facing the bottom. Arrows point to the lymph gland and the arrowheads point to the fat body location in the larvae.

**Figure 36.**

**Genetic analysis of larval locomotion and response to light**

(A) Mean distance traveled in 30 sec on an agar surface under safelight conditions. The following statistical comparisons were made using Mann and Whitney tests at a 95% confidence interval: *pol g-b*$^{1}$ *Df(2L)b80c1* (*n*=14) vs. *pol g-b*$^{2}$*Df(2L)b80c1* (*n*=19), test statistic (W)= 315.0, p=0.0053; *pol g-b*$^{2}$/+ (n=26) vs. *pol g-b*$^{2}$/ *Df(2L)b80c1* (*n*=19), test statistic (W)= 254.0, p<0.001; *pol g-b*$^{2}$*/Df(2L)b80c1* (*n*=19) vs. *pol g-b*$^{1}$*/pol g-b*$^{2}$ (*n*=14), test statistic (W)= 261.5, p=0.0263. (B) The figure shows mean response index in the On/Off assay. Larvae of mutant genotypes do not appear to differ in their response to light in this assay as compared to the wild type control larvae. *34De*$^{1}$ */ Df(2L)b80c1*, *n*=15 *34De*$^{2}$ */ Df(2L)b80c1*, *n*=19; *pol* $\gamma$-$\beta^{1}$/+, *n*=19; *pol* $\gamma$-$\beta^{2}$/+, *n*= 26; *pol* $\gamma$-$\beta^{2}$*/pol* $\gamma$-$\beta^{1}$, *n*= 13; Df(2L) b80c1/+, *n*= 18.

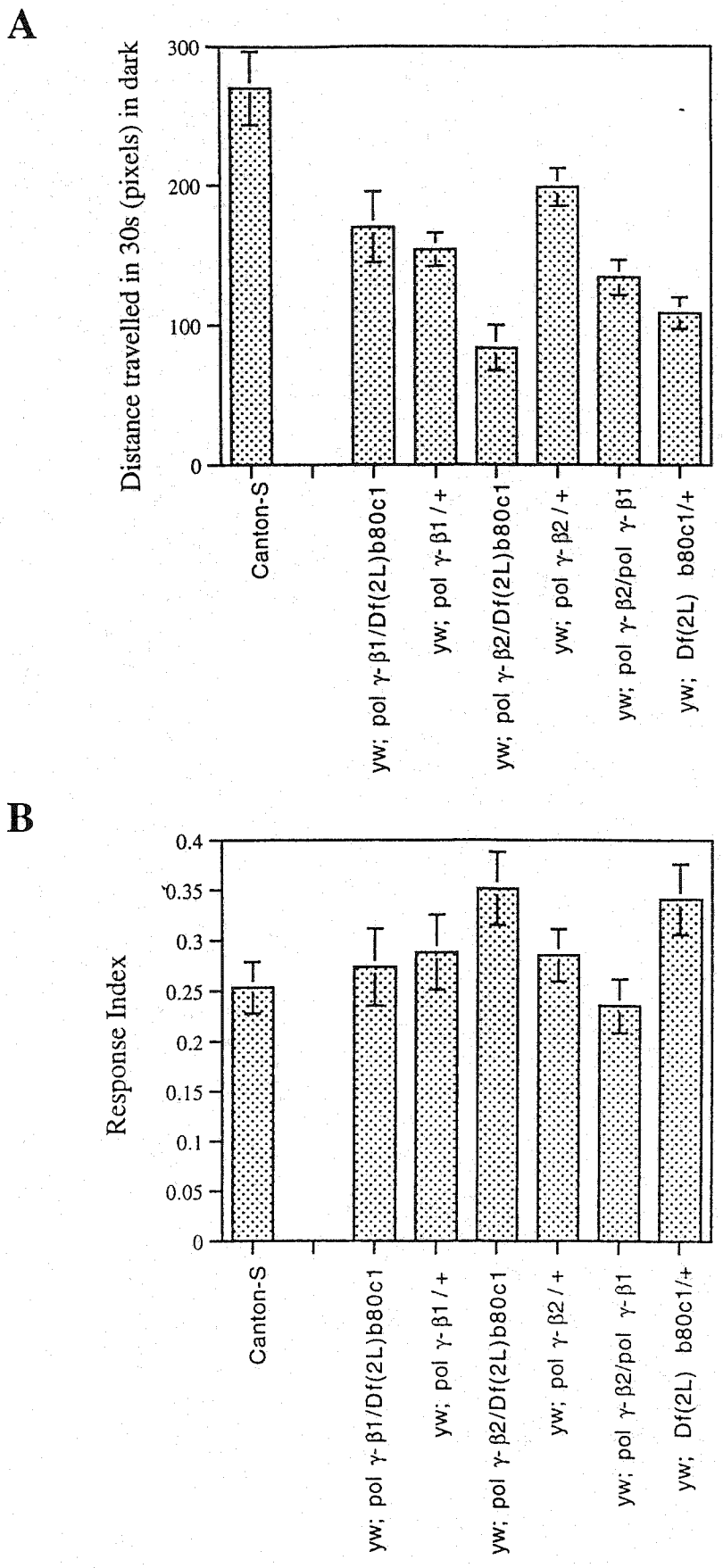
A
Distance travelled in 30s (pixels) in dark
300
200
100
0
Canton-S
yw; pol γ-β1/Df(2L)b80c1
yw; pol γ-β1 / +
yw; pol γ-β2/Df(2L)b80c1
yw; pol γ-β2 / +
yw; pol γ-β2/pol γ-β1
yw; Df(2L) b80c1/+
B
Response Index
0.4
0.35
0.3
0.25
0.2
0.15
0.1
0.05
0
Canton-S
yw; pol γ-β1/Df(2L)b80c1
yw; pol γ-β1 / +
yw; pol γ-β2/Df(2L)b80c1
yw; pol γ-β2 / +
yw; pol γ-β2/pol γ-β1
yw; Df(2L) b80c1/+

## TABLE 2

### Mapping lethality in the *P183* line

A

| | *Df(2L)TE35BC-24* | *Df(2L)b80c1* | *Df(2L)64j* |
|---|---|---|---|
| *P183* | - (0/180) | - (0/129) | - (0/182) |

B

| | $kuz^3$ | $l(2)34Db^3$ | $Sos^6$ | $tam^3$ | $Sop2^1$ | $l(2)34De^2$ | $l(2)34Df^2$ | $l(2)34Dg^1$ |
|---|---|---|---|---|---|---|---|---|
| *P183* | +(48/149) | +(34/105) | + (38/120) | - (0/176) | +(47/132) | +(44/110) | +(32/123) | +(49/145) |

C

| | $l(2)35Bb^5$ | $l(2)35Bc^2$ | $l(2)35Be^1$ | $l(2)35Bf^5$ | $l(2)35Bd^4$ | $Su(H)^8$ | $l(2)35Bg^2$ |
|---|---|---|---|---|---|---|---|
| *P183* | + (40/126) | +(65/209) | +(41/147) | +(38/117) | +(50/135) | - (0/262) | +(39/118) |

The heterozygote combinations when indicated by (-) stands for lethality and (+) for viability. Numerator indicates the number of viable adult flies that were heterozygous either for the chromosomal aberration or the alleles of lethal complementation groups, with the *P183* chromosome. The denominator indicates the number of flies with a marked balancer chromosome. (A) Indicates mapping lethality using deficiencies in the *black* region. (B and C) Results of complementation tests using representative alleles of lethal complementation groups in the 34D region and 35B region, respectively.

## Table 3

### Complementation analysis of *tamas* locus

| | Df(2L)b80c1 | $tam^{10}$ | $tam^{2}$ | $tam^{3}$ | $tam^{4}$ | $tam^{9}$ | In(2L)b82c44 | Df(2L)b85b2 | Df(2L)b88b42 | In(2L)b83b22 | In(2L)b81a2 | In(2L)b81l7 | $In(2L)b81a2^{L}$ $A80^{R}$ |
|---|---|---|---|---|---|---|---|---|---|---|---|---|---|
| $tam^{2}$ | - (0/120) | + (22/562) | - | -(0/302) | - (0/111) | - (0/154) | | | | | | | |
| $tam^{3}$ | - (0/353) | + (69/427) | - | - | - (0/295) | - (0/396) | + (40/101) | - (0/134) | - (0/133) | - (0/142) | - (0/164) | +(13/100) | - (0/119) |
| $tam^{4}$ | - (0/193) | + (6/67) | - (0/167) | | | - (0/171) | | | | | | | |
| $tam^{9}$ | - (0/289) | + (121/412) | | | - | | + (35/102) | - (0/131) | - (0/154) | - (0/105) | - (0/111) | +(45/146) | - (0/131) |
| $l(2)\ 34Da^{1}$ | | + (34/53) | | | | | | | | | | | |
| $l(2)\ 34Bh^{1}$ | | | | | | + (39/174) | | | | | | | |
| l(2) 34Ea | | | | | | | | +(13/33) | +(48/125) | +(31/57) | | | |
| $l(2)\ 34Dd^{1}$ | | | | | | | | +(4/4) | +(50/100) | +(12/42) | | | |

(+ ) indicates heterozygotes that result in complementation. (-) indicates non-complementation. Numerator indicates the number of adult flies that were heterozygous either for the allele or chromosomal aberration with respective combinations.

**Table 4. Complementation analysis of *pol γ-β* alleles**

| | *tam*$^{9}$ | *tam*$^{2}$ | *Df(2l)b80c1* | *pol* γ-β$^{1}$ |
|---|---|---|---|---|
| *pol* γ-β$^{1}$ | + (23/79) | + (36/76) | - (0/147) | - (0/200) |
| *pol* γ-β$^{2}$ | + (91/167) | + (43/77) | - (0/100) | - (0/183) |

Minus sign indicates non-complementation of lethality and plus sign indicates complementation of lethality. Numerator indicated the number of adult viable flies the denominator indicates the number of heterozygous flies that were marked with a balancer chromosome.

# Chapter 6

# Conclusions and Future Directions

## Conclusions

We began this study with the aim of using larval behaviour to isolate new genes that affect the nervous system. Few studies had previously used the larval photobehaviour as model after the seminal work by Bolwig in 1946 (Bolwig 1946, Hotta and Keng 1989, Lily and Carlsson 1991, Sawin-McCormack 1994). The previous attempts that used a behaviour-genetic approach for studying larval visual system were neither entirely successful nor comprehensive. This may be due to lack of new assay designs and sub-normal response elicited in these attempts.

Further utilization of this fixed action pattern into a reliable paradigm was possible due to the realization that vitamin A is necessary for eliciting optimal response. The enhancement of this aversion response as demonstrated using the population plate assay encouraged us to develop new assays that aimed to exploit the micro-behaviours seen in the population plate assay.

Using the Checker assay and the On/Off assay designs we first chose to measure the response in the simplest form in each case. The response index thus measured was sufficient to identify a wild type larval response from blind mutant response. Further analysis of micro-behaviours like head swinging and change in direction of locomotion was also carried out by other colleagues (Busto 2000, MSc. thesis, Hassan et al. 2001 MSc. thesis). These efforts resulted in the first comprehensive genetic analysis of larval

response to light with the On/Off assay using mutations that were isolated for adult visual system defects (Busto et al. 2000, **Appendix A**). We also analyzed the larval behaviours in the Checker assay using adult visual system mutants while also demonstrating the behavioural consequence of targetted ablation of the Bolwig's Organ (Hassan et al. 2001, **Appendix B**). More recently, these assays have enabled us to identify the critical role of larval photoreceptors expressing the Rh5 opsin in mediating the aversion behaviour to white light (unpublished results Hassan et al. 2001)

As a next step in assay development we undertook the automation of the originally laborious On/Off assay for facilitating its use in screening for mutants. This setup is unlike any that have been used to study *Drosophila* behaviour and assumes very little skill to operate. This assay system was used to characterize the locomotory deficits of strains that were mutant for the *amphiphysin* gene (Leventis et al. 2001, **Appendix D**). We also demonstrated a pilot screen using this setup. The screen resulted in identification of several locomotory and 2 putative visual behaviour mutants.

Following establishment of an optimized population plate assay we used it for a behaviour screen. We isolated one mutant that showed abnormal behaviour in this assay. The *tam* mutant also showed mutant photoreponse in the Checker assay. We studied this mutant response together with locomotory assay and concluded that the abnormal response to light was due to locomotory deficits. Genetic characterization and

direct sequencing of mutant alleles showed that this mutation disrupts a gene that codes for the catalytic subunit of mitochondrial DNA polymerase. This is a dedicated enzyme that had been previously described to play a central role for mitochondrial DNA replication and maintenance using in vitro experiments (Lewis et al. 1996). Identification of *tamas* mutations allowed us to describe the phenotypic consequence of for the first time in any metazoan (Iyengar et al. 1999, **Appendix C**).

The 34D region of the second chromosome where the *tamas* gene is located was also noted to contain the accessory subunit of the mitochondrial DNA polymerase. We embarked on identifying mutations in this locus to understand the role of this subunit in development and nervous system function. Two alleles that map to this locus were found through direct sequencing of both the alleles. A point mutation in the N-terminus portion of the gene product was identified in one of the alleles. This enabled us to identify a core motif that is highly conserved in a homologous molecule of evolutionary significance in *Thermus thermophilus* and in the accessory subunit of vertebrate models. Mutations in this gene are lethal to the organism, show developmental and mitochondrial defects although not as severe as in the catalytic sub-unit mutations (Iyengar et al. 2002, see **Appendix E**).

**Larval screens and their scope to isolate genes that affect behaviour**

Larval behaviours in *Drosophila* are increasingly being used to identify genes that affect specific biological processes. This is mainly due to the realization that during this stage the larva displays many simple fixed action patterns. For example, a larval behavioural response to hypoxia was used to understand the role of nitric oxide signaling in mediating this response (Wingrove and O'Farrell 1999). The response involves cessation of burrowing activity due to detection of hypoxic conditions and initiation of exploratory behaviour. Using yet another larval paradigm the development of the peristaltic motor apparatus was studied to understand the role of sensory inputs in patterning this output (Suster and Bate 2002). In this elegant study, it was demonstrated that the central pattern generator is assembled to function without the requirement of sensory feedback.

Only a few behavioural screens using mutant lines have been used to isolate interesting genes the affect behaviour at the larval stage (discussed in Chapter 1). It is now a well accepted observation that most mutations that affect specific behaviours may also participate in other developmental contexts, demonstrating pleiotropy on numerous occasions. Only specific mutant alleles of the respective genes isolated in such screens suggests a behavioural role, and on most occasions other alleles mapping to the same

locus have shown the functioning of such genes in other developmental processes. Hence the bona fide behavioural genes are a minority class.

Within this minority class, many of the genes participate in the respective sensory modalities, due to evolutionary specialization towards accurate perception, for example Rhodopsins, which confer sensory perception at specific wavelengths of light. It is important to recognize that if only a minority of genes exist that may affect specific behaviours it then becomes imperative to screen a very large number of mutant lines to isolate such highly specialized genes. This also implies that the frequency of isolation of genes that affect motor behaviours in general will be higher due to multiple to multiple modalities that are involved in generation this output Such a motor apparatus will include the neurons, muscles and the skeletal apparatus. Thus, it is also expected that the diversity of genes participating in the development and function of motor apparatus to be larger in numbers. Hence it is not surprising that screens that are limited in scale such as the screens conducted in the course of this study yielded mutants that for example affect cellular respiration. It is also interesting to note that as we have continued to screen more mutagenised lines we have isolated two more mutant lines whose gene products appear to participate in mitochondrial function (Nadia Scantlebury et al., unpublished data).

## The future

The larval behaviour paradigms that have been developed here are promising as a platform to isolate new genes through mutagenesis and also to dissect neural circuits *in vivo*. First, it is important to note that this developmental stage allows characterization of a substantial part of the genome that otherwise mutate to lethality. The additional advantage of using this stage is due to a transparent larval cuticle. It is now possible to use transgenic fluorescent markers to visualize the entire nervous system in intact living animals (**Figure 1**). This will complement behaviour screening by allowing us to detect the morphological defects in the nervous system.

Transgenic approaches can also allow us to label various regions of the nervous system through the use of P[Gal4] expression that uses specific enhancers. Thus marking neurons in such a manner can allow the expression of genes that interfere with neuronal function. For example, such a technique was used to demonstrate the effect of expression of *Shibire*$^{ts1}$ (*shi*$^{ts1}$) gene in the Bolwig's Organ (Kitamoto 2001). *Shi*$^{ts1}$ codes for a dominant temperature sensitive allele of Dynamin, which is required for synaptic vesicle endocytosis. Thus at restrictive temperature *Shibire*$^{ts1}$ can abrogate synaptic function. Yet another technique that allows the dissection of neural circuits uses our ability to create genetic mosaics. The "mosaic analysis with a repressible cell marker" or MARCM system allows one to create clones of cells in an organism where transgenes of

interest are expressed (Lee and Luo 2001). For example, the MARCM technique was used recently to study the formation of circuits in the fly olfactory system (Jefferis et al. 2001) . The authors demonstrated that in the formation of olfactory circuits the olfactory receptor neurons and the projection neurons that carry information beyond the glomeruli into the brain are independently specified. Another inference from this study is that single neuronal clones can be labelled by well controlled expression of FLPase. The FLPase enzyme carries out mitotic recombination by targeting chromosomes that contain FRT sequences (Golic et al. 1997).

**Mitochondrial dysfunction and the nervous system**

The work presented in this thesis resulted in the identification of mutations in nuclear genes that affect mitochondrial biogenesis. Mutations in the genes coding for a key holoenzyme responsible for mitochondrial DNA replication and maintenance now sets the stage for further analysis with respect to nuclear control of mitochondrial DNA replication. For example, we do not know whether tissue specific requirements of mtDNA levels are regulated by the nucleus. We also do not know whether each of the mutants characterized in this study affects the organism in a tissue specific manner to cause lethality. This can now be addressed using inhibitory RNA (RNAi) constructs that can be directed to CNS or muscles to deplete mtDNA in a tissue specific manner

(Kennerdell and Carthew 2000). The identification mutations and other chromosomal deletions in the 34D region also will allow us to carry out a mutagenesis experiment to produce more alleles of *tam* and *pol* $\gamma$-$\beta$ genes to study structure function analysis. The phenotypes described in the study due to mutations in these genes can also motivate us to identify other players that may participate in the mtDNA replication machinery. For example, we identified a *Drosophila* homologue of the human mitochondrial helicase gene, *twinkle* (Spelbrink et al. 2001, see **Appendix L**). The gene that is designated as CG5924 maps to the 30E region of the second chromosome. It will be interesting in the near future to isolate mutant alleles of this gene to study its role in development and nervous system function.

## References

Lilly, M., Carlson, J. 1990. smellblind: a gene required for *Drosophila* olfaction. *Genetics* 124:293-302.

Sawin-McCormack, E. P., Sokolowski, M. B., Campos, A. R. 1995. Characterization and genetic analysis of *Drosophila melanogaster* photobehaviour during larval development. *J Neurogenet* 10:119-35.

Lewis, D. L., Farr, C. L., Wang, Y., Lagina, A. T., Kaguni, L. S. 1996. Catalytic subunit of mitochondrial DNA polymerase from *Drosophila* embryos. Cloning, bacterial overexpression, and biochemical characterization. *J Biol Chem* 271:23389-94.

Kitamoto, T. 2001. Conditional modification of behaviour in *Drosophila* by targeted expression of a temperature-sensitive shibire allele in defined neurons. *J Neurobiol* 47:81-92.

Spelbrink, J. N., Li, F. Y., Tiranti, V., Nikali, K., Yuan, Q. P., et al. 2001. Human mitochondrial DNA deletions associated with mutations in the gene encoding Twinkle, a phage T7 gene 4-like protein localized in mitochondria. *Nat Genet* 28:223-31.

Golic, M. M., Rong, Y. S., Petersen, R. B., Lindquist, S. L., Golic, K. G. 1997. FLP-mediated DNA mobilization to specific target sites in *Drosophila* chromosomes. *Nucleic Acids Res* 25:3665-71.

Jefferis, G. S., Marin, E. C., Stocker, R. F., Luo, L. 2001. Target neuron prespecification in the olfactory map of *Drosophila*. *Nature* 414:204-8.

Kennerdell, J. R., Carthew, R. W. 2000. Heritable gene silencing in *Drosophila* using double-stranded RNA. *Nat Biotechnol* 18:896-8.

Lee, T., Luo, L. 2001. Mosaic analysis with a repressible cell marker (MARCM) for *Drosophila* neural development. *Trends Neurosci* 24:251-4.

Wingrove JA, O'Farrell PH. 1999. Nitric oxide contributes to behavioural, cellular, and developmental responses to low oxygen in *Drosophila*. *Cell*. 1999 Jul 9;98(1):105-14.

Suster ML, Bate M. 2002. Embryonic assembly of a central pattern generator without sensory input. Nature. Mar 14;416(6877):174-8.

# Appendix

**A: Manuscript -** Genetic dissection of behaviour: modulation of locomotion by light in the *Drosophila melanogaster* larva requires genetically distinct visual system functions

The Journal of Neuroscience, May 1, 1999, 19(9):3337–3344

# Genetic Dissection of Behavior: Modulation of Locomotion by Light in the *Drosophila melanogaster* Larva Requires Genetically Distinct Visual System Functions

**Macarena Busto, Balaji Iyengar, and Ana Regina Campos**

*Department of Biology, McMaster University, Hamilton, Ontario, Canada L8S 4K1*

The *Drosophila* larva modulates its pattern of locomotion when exposed to light. Modulation of locomotion can be measured as a reduction in the distance traveled and by a sharp change of direction when the light is turned on. When the light is turned off this change of direction, albeit significantly smaller than when the light is turned on, is still significantly larger than in the absence of light transition. Mutations that disrupt adult phototransduction disrupt a subset of these responses. In larvae carrying these mutations the magnitude of change of direction when the light is turned on is reduced to levels indistinguishable from that recorded when the light is turned off, but it is still significantly higher than in the absence of any light transition. Similar results were obtained when these responses were measured in strains where the larval photoreceptor neurons were ablated by mutations in the *glass* (*gl*) gene or by the targeted expression of the cell death gene *head involution defective* (*hid*). A mutation in the homeobox gene *sine oculis* (*so*) that ablates the larval visual system, or the targeted expression of the *reaper* (*rpr*) cell death gene, abolishes all responses to light detected as a change of direction. We propose the existence of an extraocular light perception that does not use the same phototransduction cascade as the adult photoreceptors. Our results indicate that this novel visual function depends on the blue-absorbing rhodopsin Rh1 and is specified by the *so* gene.

*Key words: insect; larval photobehavior; locomotion;* Drosophila*; photoreceptor; Bolwig's organ*

The *Drosophila melanogaster* larva spends most of its life foraging, burrowed in the food substrate. Consistent with this general behavior pattern, the *D. melanogaster* larva is repelled by light (Lilly and Carlson, 1990; Gordesky-Gold et al., 1995; Sawin-McCormack et al., 1995). In the middle of the third instar the larva ceases foraging and leaves the food substrate in search of an adequate site in which to undergo metamorphosis. This behavior is referred to as wandering (Sokolowski et al., 1984). Modulation of larval photobehavior has been reported to occur during this transition from foraging to wandering (Sawin-McCormack et al., 1995). Interestingly, it coincides with the contact of the larval optic nerve by a serotonergic arborization (Mukhopadhyay and Campos, 1995), suggesting extrinsic modulation of this sensory pathway by 5-HT as demonstrated in other systems (Katz, 1995).

The larval visual system was first described in the house fly *Musca domestica* by Bolwig (1946) and henceforth was named the Bolwig's organ. Similarly, in *D. melanogaster*, the larval visual system is composed of two bilateral groups of 12 photoreceptor cells located anteriorly and juxtaposed to the mouth hooks (Steller et al., 1987). The axons of the photoreceptor cells form the larval optic nerve that innervates the optic lobe primordium area of the brain lobes. The early development and the establishment of connectivity in this system has been described previously (Green et al., 1993; Campos et al., 1995).

We report that in the *Drosophila* larva a light stimulus modulates the direction of movement as well as quantitative aspects of locomotion such as path length and frequency of turning. Mutations that disrupt phototransduction in the adult eye disrupt aspects of the larval response to light measured in our assay. These results suggest that the larval and adult visual systems are similar from the functional point of view. These mutations, however, fail to abolish all perception of light, suggesting the existence of a light detection mechanism that does not require these gene products. The analysis of developmental mutants and of strains where the cell death genes *reaper* (*rpr*) and *head involution defective* (*hid*) are ectopically expressed suggests that this novel light detection mechanism is not located in the Bolwig's organ.

## MATERIALS AND METHODS

### *Fly stocks*

Fly strains were grown at 25°C in 12 hr light/dark cycles on standard medium containing inactivated yeast, sucrose, and agar supplemented with fresh active yeast. Tegosept in ethanol and propionic acid were used to prevent mold growth. Strains used in addition to wild types *Canton-S* (*CS*) and *Oregon-R* (*OR*) are listed below:

*glass.* The *glass* (*gl*) gene encodes a zinc finger transcription factor required for the development of photoreceptor cells (Moses et al., 1989): $gl^{60j}$ is a severe allele that contains a 30 kb insertion (Moses et al., 1989); $gl^{1}$ is a moderate allele; and $gl^{+}$ contains a wild-type *gl* gene in a $gl^{60j}$ background.

*glass* multimer reporter-*head involution defective.* This strain contains a fusion vector in which the cell death gene *hid* is expressed under the control of the *gl* promoter (Grether et al., 1995).

*glass* multimer reporter-*reaper.* This strain contains a fusion vector in which the cell death gene *rpr* is expressed under the control of the *gl* promoter (White et al., 1996).

*neither inactivation nor afterpotential C.* The *neither inactivation nor afterpotential C* (*ninaC*) gene encodes two isoforms (3.6 and 4.8 kb RNA)

Received Dec. 1, 1998; revised Jan. 25, 1999; accepted Feb. 12, 1999.

This work was supported by an operating grant to A.R.C by the Medical Research Council (MRC) of Canada. We are indebted to W. J. Bell, M. B. Sokolowski, and T. Tully for discussions on behavior, and to Roger Jacobs, Colin Nurse, and Andre Bedard for comments on this manuscript. We thank the generosity of the following fly workers: Joe O'Tousa, Randall Shortridge, and Kathy Matthews for the prompt donation of stocks.

M.B. and B.I. contributed equally to this work.

Correspondence should be addressed to Ana Regina Campos, Department of Biology, McMaster University, 1280 Main Street West, Hamilton, Ontario, Canada L8S 4K1.

of adult photoreceptor specific cytoskeleton proteins consisting of a protein kinase and a myosin head domain (Montell and Rubin, 1988). *ninaC*$^{5}$ is a null mutant that has reduced levels of both the 3.6 and 4.8 kb RNA and leads to abnormal ERG, light and age-dependent retina degeneration (Porter and Montell, 1993; Hofstee et al., 1996) as well as a defect in response termination (Porter et al., 1992). *ninaC*$^{2}$ is a mutant that has reduced levels of the 4.8 Kb RNA (Montell and Rubin, 1988).

*neither inactivation nor afterpotential E.* The *neither inactivation nor afterpotential E* (*ninaE*) gene encodes the opsin moiety of the Rh1 rhodopsin and is expressed in the adult photoreceptors R1–R6 (O'Tousa et al., 1985) as well as the larval visual system (Zuker et al., 1985; Pollock and Benzer, 1988). *ninaE*$^{17}$ contains a 1.6 kb deletion. Flies have very low rhodopsin levels and respond poorly to light stimulus (O'Tousa et al., 1989). *ninaE*$^{8}$ contains three missense mutations within the sixth transmembrane domain, T283 M, W289R, C297S (Washburn and O'Tousa, 1989). Flies have <1% normal rhodopsin levels (O'Tousa et al., 1989).

*no-receptor potential A.* The *no-receptor potential A* (*norpA*) gene encodes a phospholipase C, which in null mutants, leads to a complete block of the phosphoinositide cascade mediating phototransduction (Hardie and Minke, 1995). Adult flies lack light elicited receptor potentials in the compound eyes and ocelli (Pak et al., 1970). *norpA*$^{P24}$ contains a 28 base pair deletion in the *norpA* gene which produces a premature termination codon (Pearn et al., 1996). *norpA*$^{P12}$ contains a nucleotide substitution in the *norpA* gene which produces a premature termination codon (Pearn et al., 1996).

*sine oculis.* The *sine oculis* (*so*) gene encodes a homeobox containing protein required for visual system determination (Fischbach and Technau, 1984). *so*$^{mda}$ exhibits absence of larval photoreceptors and target area (Serikaku and O'Tousa, 1994).

### *Harvest of synchronized larvae*

Adult flies aged from 1–7 d were allowed to lay eggs in a fresh food plate (100 mm × 15 mm; Fisher Scientific, Houston, TX) supplemented with vitamin A (Jamisons β carotene, 1.25 gm/l) and coated with yeast paste. After a minimum of two 2-hr precollections, a 1 hr egg collection was incubated at 25°C. At 20–22 hr after egg lay (AEL) all newly hatched first instar larvae were removed under a dissection microscope. After a 1 hr incubation period, ~70 newly hatched first instar larvae were collected and transferred to a fresh food plate coated with yeast paste. Third instar larvae were tested for photobehavior between 84 and 90 hr AEL.

### *Photobehavior assays*

Measurements of larval photobehavior were made in the ON/OFF assay. This consists of a plastic Petri dish (100 mm × 15 mm; Fisher Scientific) containing 15 ml of 1% agarose cooled to room temperature. *Drosophila* larvae prefer to remain in crevices. For this reason test plates need to be free of depressions (agar bubbles), and the test cannot be performed near the edge of the plate where the agar touches the side of the plate. Thus a circular 1 cm boundary from the plate edge was established beyond which the the collected data were discarded.

Manipulation of the larvae before the test was conducted using a darkroom light (20 W lamp with Kodak GBX-2 filter), and testing was conducted using a cool white bulb with a spectrum of 400–650 nm with peaks at 440 and 560 nm (20 W Cool White, Philips) and with a throughput of ~320 microwatts/cm$^2$. The darkroom light (20 W lamp with Kodak GBX-2 filter) used in this assay is the same used to record circadian-regulated locomotory behavior of *Drosophila* in free-running conditions ("constant darkness") (Sehgal et al., 1992). Larval photobehavior assays (Lilly and Carlson, 1990; M. Busto, J. Hassan, B. Iyengar, and A. R. Campos, unpublished observations) conducted using the darkroom light as the sole light source yielded response indices close to zero, confirming previous reports that *Drosophila* does not respond to light stimulus above the 650 nm range (Ashburner, 1989).

With use of a moist paintbrush, individual larva were removed from the culture dish. Each larva was carefully rinsed with distilled water to remove any excess food particles. They were removed from the distilled water, using a flathead paintbrush, and placed on a pre-test plate for a period of 1 min to allow them to acclimatize to the agar surface. Each larva was then positioned in the center of the test plate and allowed to move.

Individual plates were placed on a dark background and illuminated from above [20 W cool white bulb (Phillips) in a Rapid Start mechanism (Thomas Lighting)] in intermittent 10 sec pulses of light and dark. Throughout the duration of the assay the darkroom light (20 W lamp with Kodak GBX-2 filter) was on to allow recording of larval behavior. To estimate the influence of different light sources, controls using different kinds of light bulbs (incandescent, daylight, and cool white) were performed. Current oscillation causes the light sources to flicker at 60 Hz frequency. The amplitude of this oscillation varies according to the light source (i.e., fluorescent or incandescent). Response indices (RIs) obtained using various light sources were not significantly different ($F_{(5,40)} = 1.47, p > 0.05$). In addition, RIs derived for wild-type larvae over the course of the 100 sec did not vary ($F_{(4,87)} = 1.77, p > 0.05$).

### *Temperature*

Surface temperature recordings were taken in 25 sec intervals for 200 sec during the course of the ON/OFF using a 21× Micrologger (Campbell Scientific). Temperature readings in the ON/OFF assay or under safelight conditions were 21.5 ± 0.5°C.

### *Data collection and analysis*

Larval movement was visualized through a Fujinon TV·Z zoom lens (Fuji Optical) attached to a CCD TV camera (Elmo) and recorded on videotape (Fuji HQ-120, RCA VCR). Larvae were recorded either until they reached the 1 cm boundary or total test time (100 sec) had elapsed. Data derived for each of the strains were obtained from two to three sets of samples in which 10 larvae were tested.

Paths in the ON/OFF assay were first traced from a video monitor (8 inch × 10 inch Hitachi 1-chrome) onto acetate sheets and digitized using an Apple One Scanner at 72 dpi. Path length and the angle between path direction before and after the light switch were analyzed using public domain NIH Image software (developed at National Institutes of Health and available at http://rsb.info.nih.gov/nih-image/) on a Macintosh Performa 5200CD computer. Response indices [(path length in dark-path length in light)/total path length per cycle] were calculated on a per larva basis, and a mean average of these individual indices was taken.

The data are depicted as means ± SEM. Transformation of the data were not necessary because variances did not differ significantly ($F_{max}$ test). ANOVAs and Tukey-Kramer multiple comparison tests ($\alpha = 0.05$) were performed on the raw data using SAS-Jmp and Minitab software for MacIntosh (Sokal and Rohlf, 1995).

## RESULTS

### Light modulates the larval pattern of locomotion

The larval response to light has been measured in assays where opposing light conditions are presented to the animal at the same time (Lilly and Carlson, 1990; Gordesky-Gold et al., 1995; Sawin-McCormack et al., 1995; Busto, Hassan, Iyengar, and Campos, unpublished observations). In these assays locomotion is apparently a reflection of the larva's attempt to remain in the dark environment (i.e., light avoidance when confronted with a dark/light boundary) combined with a direct effect of light on locomotion. Thus the behavior measured in these assays is in fact the composite of various responses.

We hypothesized that single gene mutations can be used to dissect the network of cell types and molecules required for specific aspects of the *Drosophila* larva response to light. To test this hypothesis it was necessary to design a new assay that measures discrete aspects of the individual larva's response to light. To that end an assay was designed (ON/OFF) in which the larva is subjected to intermittent pulses of light (10 sec each), and its locomotion is recorded. Visual inspection of the recorded larval behavior under the conditions of this assay suggest that the distance traveled in the presence of light is considerably shorter than in the absence of light. Likewise, head swinging and change of direction of the larval path are apparently triggered by light (Fig. 1*A*,*B*).

These phenomena were quantified by analyzing the path tracings derived from the recordings using an image analysis software (NIH image). The effect of light on the distance traveled is represented by an RI derived from the resulting path length difference between light and dark (distance traveled in dark-distance traveled in light/total distance traveled in light and

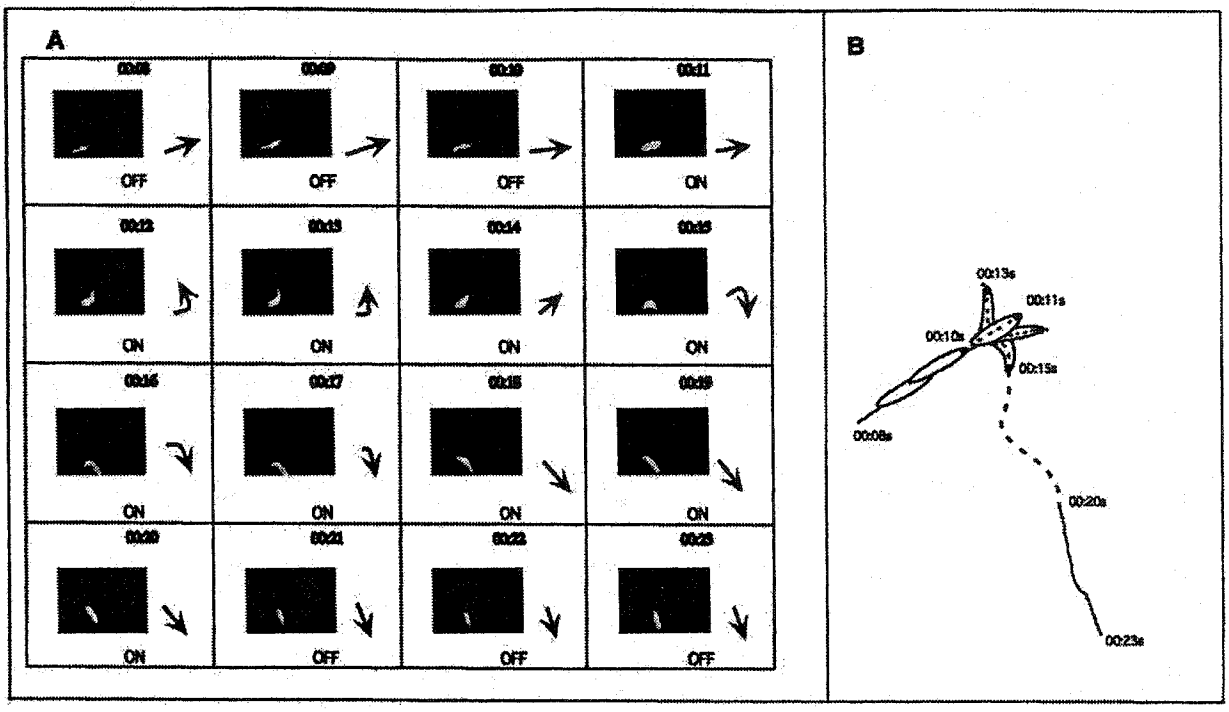


*Figure 1.* Larval behavior during the ON/OFF assay. *A*, Videotape of a single *CS* larva tested in the ON/OFF assay was used to generate frame-by-frame photographs depicting 16 consecutive seconds. To the *right* of each panel is a schematic diagram of the larva representing the relative position of the head (*arrowhead*) and body (*line*). The *first three frames* (seconds *00.08–00.10*) show a larva immediately before a lights *OFF* to *ON* transition. Lights are turned ON in the eleventh second, and head swinging is observed (*00.12–00.14*) followed by a change in direction (*00.15–00.18*). The *final three frames* show a larva during lights OFF immediately after the lights ON to OFF transition (*00.20–00.21*). *B*, Line drawing of larval path shown in *A*. The *solid lines* represent the larval path during a portion of the dark pulse (*00.08–00.10* and *00.21–00.23*). The *broken line* represents larval path during the light pulse (*00.11–00.20*). The *larval outline* depicts the larval head swinging that occurs soon after the lights are turned on. During this time (*00.12–00.15*) the larva is stationary. This behavior is followed by a sharp change in the direction of the larval path.

dark). An RI of ~0.3 reflects a 50% reduction in path length when the light is turned on. To quantify head swinging behavior under the two light conditions, path tracings were drawn following the position of the mouth hooks such that head movements as well as the direction of the path were recorded (Fig. 1*B*).

The wild-type strains tested reduce their path lengths when exposed to light as determined by the RI (Fig. 2). This response was abolished by mutations in genes that disrupt the phototransduction cascade (*norpA* and *ninaC*) but not by mutations in the blue-absorbing rhodopsin gene *ninaE* (Rh1) (Fig. 2). The two *ninaC* mutants tested ($ninaC^5$ and $ninaC^2$) yielded opposite results. The $ninaC^5$ mutants exhibited a severely reduced RI, whereas $ninaC^2$ mutants behaved as wild type. Larvae homozygous for two mutant alleles of the *ninaE* ($ninaE^{17}$ and $ninaE^8$) gene displayed RIs in this assay that were indistinguishable from wild type (Fig. 2).

The *ninaC* gene encodes two retina-specific chimeric proteins consisting of a protein kinase and a myosin head domain (Montell and Rubin, 1988). One of these, a 132 kDa protein (p132), is expressed primarily in the cytoplasm. The other, a 174 kDa protein (p174), is localized predominantly in the rhabdomere (Hicks and Williams, 1992; Porter et al., 1992). Although $ninaC^5$ has reduced levels of both p132 and p174, $ninaC^2$ has reduced levels of only p174. Therefore, the wild-type response seen in $ninaC^2$ mutant larvae but not $ninaC^5$ larvae indicates that p132, not p174, is required for the larval response to light as measured by RI.

The *norpA* gene encodes a phospholipase C, an essential component of the phototransduction signaling cascade in the adult

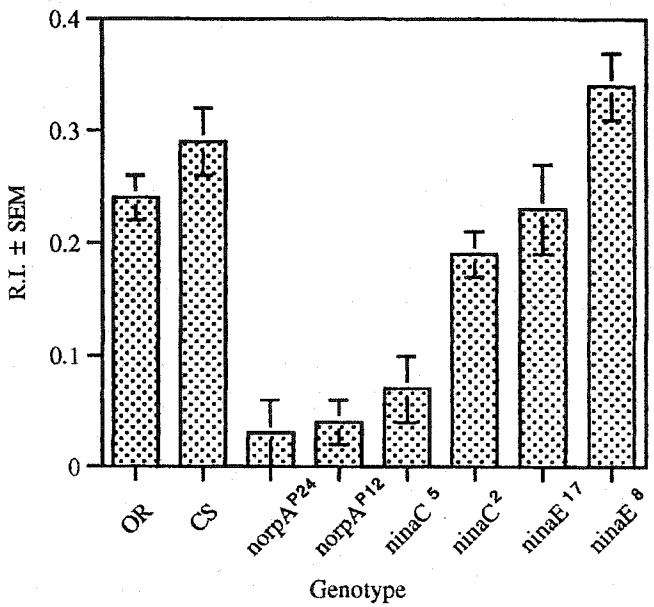


*Figure 2.* Response in the ON/OFF assay of wild type and larvae with mutations in genes involved in phototransduction. A response index (*R.I.*) was derived per larva, and a genotype average was calculated. The RIs for the strains are significantly different (ANOVA $F_{(1,181)} = 16.90, p < 0.001$). *Post hoc* analysis of paired mean comparisons reveals no differences between the wild-type strains (*OR*, $n = 30$; *CS*, $n = 30$) and *ninaE* [$ninaE^{17}$ ($n = 20$); $ninaE^8$ ($n = 20$)], but a significant reduction in the larval response to light of the *norpA* [$norpA^{P24}$ ($n = 30$); $norpA^{P12}$ ($n = 20$)] and *ninaC* [$ninaC^5$ ($n = 20$); $ninaC^2$ ($n = 19$)] mutants.

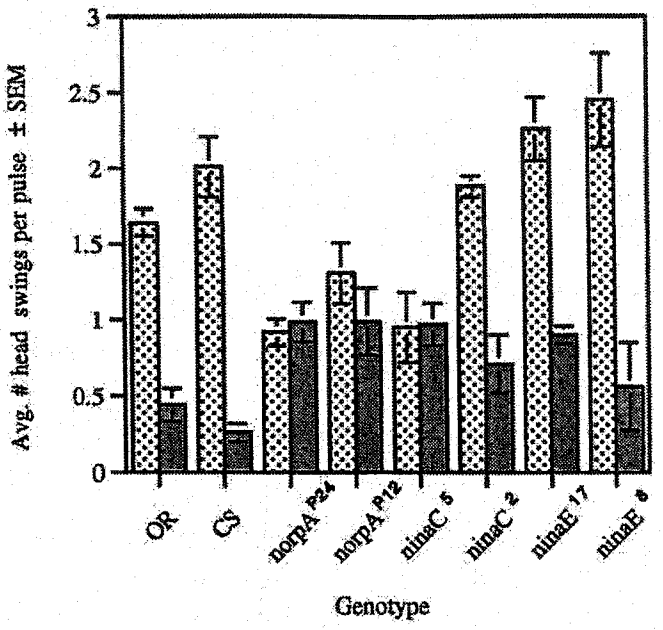


*Figure 3.* Head swinging behavior of wild-type strains and larvae with mutations in genes involved in phototransduction during the ON/OFF assay. Head swings, defined as an abrupt movement of the anterior portion of the larva away from original path choice, were counted in light (*stippled bar*) and dark (*gray bar*) pulses on a per larva basis, and an average for each genotype was derived. There is a significant increase in head swinging by wild-type larvae (*CS*, $n = 30$; *OR*, $n = 30$) during light pulses, relative to that during dark (ANOVA: *CS*, $F_{(1,58)} = 15.69$, $p < 0.001$; *OR*, $F_{(1,58)} = 20.51$, $p < 0.001$). This difference is abolished in the phototransduction mutants $norpA^{P24}$ ($n = 30$), $norpA^{P12}$ ($n = 20$), and $ninaC^{5}$ ($n = 20$) but not in the $ninaC^{2}$ ($n = 18$), $ninaE^{17}$ ($n = 20$), and $ninaE^{8}$ ($n = 20$) mutants (ANOVA: $norpA^{P24}$, $F_{(1,58)} = 0.09$, NS; $norpA^{P12}$, $F_{(1,38)} = 2.58$, NS; $ninaC^{5}$, $F_{(1,38)} = 0.05$, NS; $ninaC^{2}$, $F_{(1,34)} = 11.53$, $p < 0.001$; $ninaE^{17}$, $F_{(1,38)} = 30.82$, $p < 0.001$; $ninaE^{8}$, $F_{(1,38)} = 29.81$, $p < 0.001$).

eye (Bloomquist et al., 1988; Ranganathan et al., 1995). The *norpA* gene is expressed as two developmentally regulated transcripts (subtypes I and II) generated by alternative splicing (Kim et al., 1995). Subtype I is specific to the adult eye, whereas subtype II is found in the CNS of adults and larvae (Kim et al., 1995). Therefore, disruption in the response to light in larvae carrying a null allele of the *norpA* gene may be caused by lack of this gene's function in the CNS and/or larval visual system.

In addition to reduction in path length during the light pulse measured as an RI, wild-type larvae also exhibited a significant increase in head swinging when the light was turned on (Fig. 3). This response was also abolished in the $norpA^{P24}$, $norpA^{P12}$, and $ninaC^{5}$ mutants but not in the $ninaC^{2}$ mutants (Fig. 3). These results suggest that p132 is required for this behavior also. Wild-type responses were also seen in larvae with severely reduced levels of Rh1 ($ninaE^{17}$ and $ninaE^{8}$ mutants) (Fig. 3).

Taken together these results suggest that reduction in path length is attributable, at least in part, to immobilization of the larva while it swings its head in an apparent search for a dark environment. These responses are performed by a similar phototransduction cascade described for the adult visual system. Additionally, these results demonstrate that light-induced path length reduction and head swinging can be mediated by photoreceptors expressing rhodopsins other than Rh1.

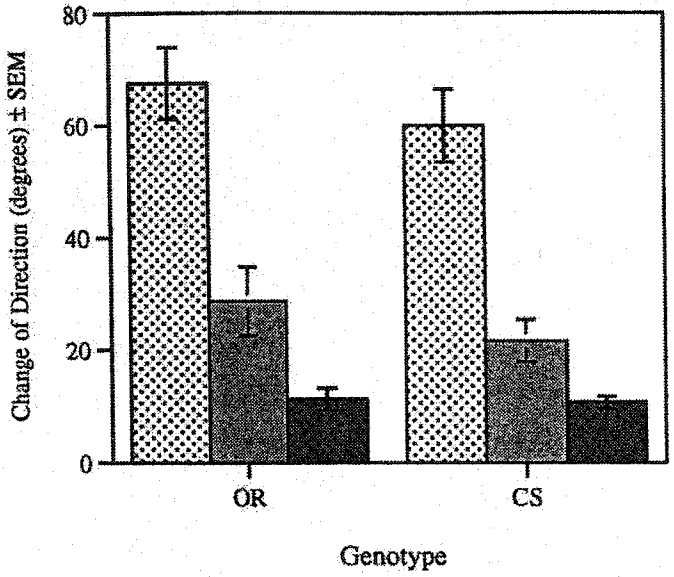


*Figure 4.* Change of direction in wild-type strains during the ON/OFF assay. Change of direction (in degrees) was measured at the dark to light (*stippled bar*), light to dark (*gray bar*), and in the absence of light transitions (*solid bar*). *OR* larvae display a significant difference between each of the light conditions ($n = 30$, $F_{(1,87)} = 33.89$, $p < 0.001$). *CS* larvae display a significant difference between the dark to light and light to dark transitions only ($n = 30$, $F_{(1,87)} = 42.49$, $p < 0.001$).

## Change of direction in larval path in different light conditions reveals a genetically distinct visual system function

Change of direction in the larval path was quantified by measuring the angle formed by the path tracing at the dark-to-light and light-to-dark boundaries. The magnitude of the angle formed by the two paths reflects the magnitude of the change in the direction of the larval path at the time of transition. Controls are represented by similar calculations performed at 10 sec intervals in path tracings derived from recordings performed in the absence of a light stimulus (Figs. 1*B*, 4).

In wild-type strains (*CS* and *OR*), direction changes significantly more when the light is turned on [dark to light (D to L)] than when it is turned off (Fig. 4). Furthermore, comparison of paired means within genotypes demonstrates that in *OR*, change of direction when the lights are turned off [light to dark (L to D)] is significantly above that recorded in the absence of light transition (D to D). That is, D to L > L to D > D to D. In the wild-type strain *CS*, the change of direction when the lights are turned off (L to D) is considerably higher than that recorded in control conditions (absence of light transitions). Statistical analysis (comparison of paired means) indicates that this difference is not significant.

Similar to what is found for the other larval responses to light, two mutations in the *norpA* gene ($norpA^{P24}$ and $norpA^{P12}$) and the $ninaC^{5}$ mutation abolish the light-induced difference in the amplitude of change of direction at the transitions D to L and L to D. Interestingly, these *norpA* and *ninaC* mutations did not affect the difference between the change of direction found at L to D and that recorded during the absence of light pulses (D to D) (Fig. 5). In contrast to the previous measured responses (RI and head swings), the $ninaC^{2}$ mutants did not respond like wild type (Fig. 5). Although light had a significant effect on direction change, the correlation seen in wild type was not exhibited by

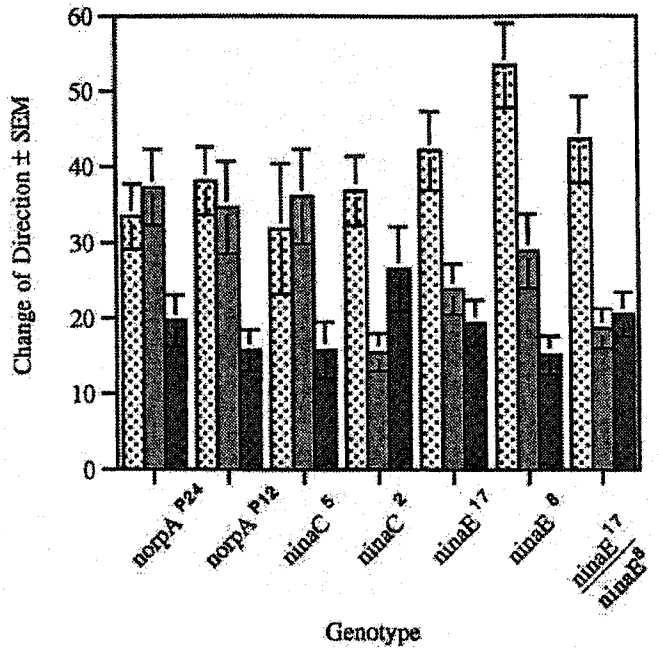


*Figure 5.* Change of direction in strains with mutations in genes involved in adult phototransduction during the ON/OFF assay. Change of direction (in degrees) was measured at the dark to light (*stippled bar*), light to dark (*gray bar*), and in the absence of light transitions (*solid bar*). $norpA^{P24}$ ($n = 30$, $F_{(2,87)} = 10.12$, $p < 0.001$), $norpA^{P12}$ ($n = 20$, $F_{(2,57)} = 6.21$, $p < 0.005$), and $ninaC^{5}$ ($n = 20$, $F_{(2,57)} = 5.17$, $p < 0.006$) mutant larvae exhibit changes of direction at the dark to light and light to dark transitions that are not different from each other but are different from change of direction in the absence of light. $ninaC^{2}$ mutant larvae ($n = 20$, $F_{(2,57)} = 5.64$, $p < 0.008$) exhibit a significant difference at the dark to light and light to dark transition changes that in turn is not significantly different from that measured in the absence of light transition. $ninaE^{17}$ mutant larvae also exhibit a significant difference between dark to light and light to dark, but the difference between the light to dark and absence of light transitions has been abolished ($n = 20$, $F_{(2,57)} = 8.93$, $p < 0.001$). The same is true of larvae that are heterozygous [$ninaE^{17}/ninaE^{8}$ ($n = 20$, $F_{(2,57)} = 12.2$, $p < 0.001$)]. $ninaE^{8}$ ($n = 20$, $F_{(2,57)} = 12.21$, $p < 0.001$) larvae display a significant difference between each of the transitions.

these larvae. Instead, the only statistically significant difference was that the change of direction at D to L was greater than that at the L to D transition.

In contrast, the $ninaE^{17}$ mutation reduces the change of direction at the L to D transition to levels indistinguishable from that recorded in the absence of light transition (D to D). These mutant larvae do exhibit a D to L change of direction that is greater than both the L to D change of direction and direction change in the absence of light transition. Although the $ninaE^{8}$ homozygous larvae behave as wild type at all transitions, in the heterozygous flies ($ninaE^{8}/ninaE^{17}$) the difference in change of direction at L to D and D to D transitions is abolished. Our interpretation of these results is that Rh1 expression in the $ninaE^{8}$ strain is lower than wild type but still above the threshold for the performance of this particular behavior. This level of Rh1 expression, however, is not sufficient to overcome the deficit caused by the $ninaE^{17}$ mutation.

These results suggest the existence of a visual system function(s) that distinguishes between lights being turned on (D to L), lights being turned off (L to D), and no light transition (D to D). The distinction between lights being turned on and off requires the same phototransduction cascade as that described for RI and head swings; that is, it is abolished by mutations in the *norpA* and *ninaC* genes. The results described above indicate that this light perception is not mediated by Rh1. However, Rh1-mediated phototransduction is required to distinguish presence from absence of light transitions.

## Ablation of the Bolwig's organ disrupts only a subset of the larval responses to light

In *D. melanogaster*, the larval visual system (Bolwig's organ) is composed of two bilateral groups of 12 photoreceptor cells located anteriorly and juxtaposed to the mouth hooks, similar to what is found in larger flies (Steller et al., 1987). These photoreceptors project posteriorly and ventrally around the brain hemispheres and terminate in the optic lobe primordium (Schmucker et al., 1992, 1997; Green et al., 1993; Campos et al., 1995). To further dissect larval visual system requirements, *so* and *gl*, two genes directly involved in visual system specification and development, were studied.

The *so* gene encodes a homeodomain protein expressed in a number of places during embryogenesis (Cheyette et al., 1994; Serikaku and O'Tousa, 1994). In the visual system, *so* functions during embryogenesis in the regulation of genes necessary for proper optic lobe invagination and Bolwig's organ formation (Serikaku and O'Tousa, 1994). Here, we used the $so^{mda}$ allele, the only allele that specifically disrupts the development of the larval visual system.

The *gl* gene, which encodes a transcription factor essential for photoreceptor development, is expressed in a more spatially restricted manner and acts downstream of *so* (Moses et al., 1989; Serikaku and O'Tousa, 1994). *gl* is expressed in the larval and adult photoreceptor neurons as well as in two groups of ~21 neurons in each brain hemisphere (Moses et al., 1989). The effect of *gl* mutations in the development of the *gl*-expressing central neurons is not known. This is attributable to the absence of markers, besides *gl* gene expression itself, that allow the visualization of these neurons.

To determine whether the photoreceptors in Bolwig's organ mediate the various responses to light measured in the ON/OFF assay, larvae carrying mutations in the *so* and *gl* gene were assayed. In addition, a *gl* mutant strain displaying wild-type adult phenotype, attributable to the expression of a wild-type *gl* gene present in a P element transposon, was tested (Moses et al., 1989). Two strains in which a cell death gene (*hid* or *rpr*) is under the control of the *gl* promoter were similarly analyzed (Grether et al., 1995; White et al., 1996).

No significant difference between the RIs obtained for the wild-type strains and $gl^{+}$ or *glass* multimer reporter-*reaper* (pGMR-*rpr*) was detected (Fig. 6). A significant reduction in the RI was observed in the $so^{mda}$, $gl^{60j}$, $gl^{1}$, and *glass* multimer reporter-*head involution defective-hid* (pGMR-*hid*) mutant strains. Similar results were found when the frequency of head swinging was calculated during light and dark pulses (Fig. 7). The significant increase in head swinging frequency during the light pulse displayed by wild-type larvae is abolished by mutations in both the *so* and *gl* genes. This differential head swinging was restored by the $gl^{+}$-containing transposon. Again, although the increase in head swinging during the light pulse was abolished in larvae carrying the pGMR-*hid* fusion, larvae containing the pGMR-*rpr* fusion were not affected in this manner.

Disruption in the development of the larval visual system, caused by *gl* mutations or expression of the *hid* gene, abolished the difference in the magnitude in the change of direction at the D to L and L to D transitions (Fig. 8). However, change of

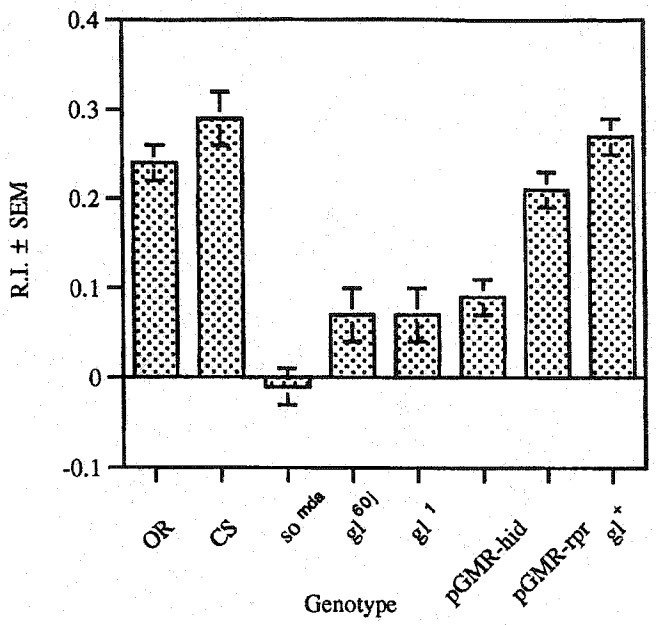


*Figure 6.* RI in the ON/OFF assay of larvae with mutations in the *so* and *gl* genes. The RIs for the strains are significantly different ($F_{(7,178)} = 15.55$, $p < 0.001$). *Post hoc* analysis of paired means reveals no difference between the wild-type strains (*OR*, $n = 30$; *CS*, $n = 30$) and the *pGMR-rpr* ($n = 20$) and $gl^+$ ($n = 16$). A significant reduction is observed in the larval response to light of the $so^{mda}$ ($n = 20$), $gl^{60j}$ ($n = 20$), $gl^1$ ($n = 20$), and *pGMR-hid* ($n = 30$) mutants.

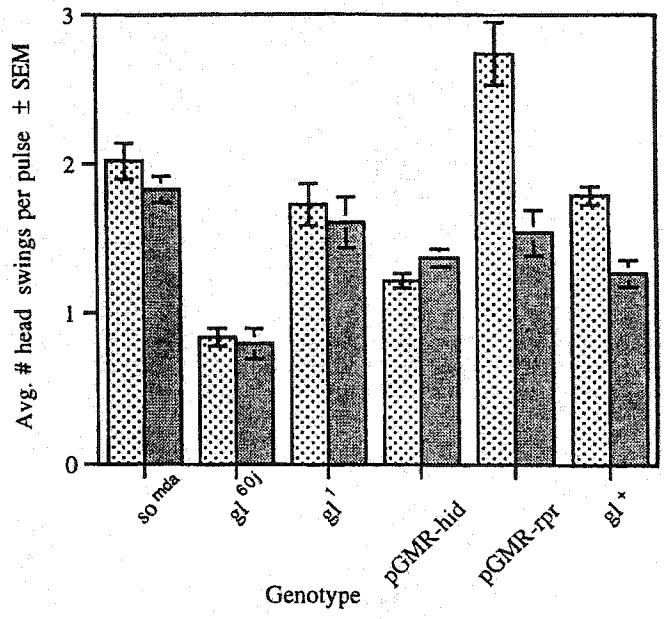


*Figure 7.* Head swinging behavior in the ON/OFF assay of larvae with mutations in the *so* and *gl* genes. The increase in head swinging behavior seen during the light pulses (*stippled bar*) over that seen during the dark pulses (*gray bar*) is abolished in the $so^{mda}$ mutant ($n = 20$, $F_{(1,38)} = 0.76$, $p > 0.05$) as well as in the *gl* mutants $gl^{60j}$ ($n = 20$, $F_{(1,38)} = 0.03$, $p > 0.05$) and $gl^1$ ($n = 20$, $F_{(1,38)} = 0.03$, $p > 0.05$) and in the *pGMR-hid* strain ($n = 30$, $F_{(1,58)} = 0.03$, $p > 0.05$), which lacks larval photoreceptor cells. A light pulse elicits differential head swinging behavior in *pGMR-rpr* ($n = 20$, $F_{(1,38)} = 15.33$, $p < 0.001$), which exhibits a less severe adult phenotype than *pGMR-hid*, and in $gl^+$ ($n = 16$, $F_{(1,30)} = 9.44$, $p < 0.005$), which is the *gl* rescue line.

direction in the absence of a light transition is still significantly lower than either of the test conditions (Fig. 8). In contrast, the $so^{mda}$ mutation or the expression of the cell death gene *rpr* under the *gl* promoter (pGMR-*rpr*) abolished the difference in the magnitude of change of direction at all transitions (Fig. 8).

The apparent contradiction in the results obtained with pGMR-*hid* and pGMR-*rpr* strains can be attributed to different sensitivity of diverse cell types to the ectopic expression of these cell death genes. In fact, developing adult photoreceptors are more sensitive to the ectopic expression of *hid* than *rpr* (H. Steller, personal communication). These observations lend further support to the proposal that these various responses to light are mediated by genetically distinct cell types.

These results demonstrate that the larval visual function, which is dependent on a phototransduction cascade similar to that described for the adult stage, requires at least the proper development of the larval photoreceptors. Although a mutation in the *so* gene abolishes all responses to light, as measured in this assay, mutations in the *gl* gene appear to disrupt only a subset of these responses. These larvae, at the L to D transition, exhibit changes of direction greater than at the D to D transition. Thus, these results demonstrate that a larval visual function exists that is not dependent on an adult-like phototransduction cascade. The cells that mediate this proposed visual function are not housed in *gl*-dependent neurons but in neurons dependent on the function of the homeobox-containing transcription factor *so*. Our results indicate that these neurons, although not dependent on *gl* gene function, do express this transcription factor.

## DISCUSSION

The *Drosophila* larval response to light represents a quantifiable behavior likely to include components of more complex behaviors executed by higher organisms. As a model system, *Drosophila* provides high-resolution genetic and molecular biology tools to dissect the components, molecular and cellular, required for the larval response to light (Miklos and Rubin, 1996).

### The *Drosophila* larva response to light can be defined as klinokinesis and orthokinesis

The locomotory reaction of organisms to biotic or abiotic factors has been traditionally defined relative to the source of stimulus (Fraenkel and Gunn, 1961). In a directed reaction (taxis), the movement is modulated to position the long axis of the organism toward or away from the source of stimulation. In undirected locomotory reactions (kinesis), quantitative aspects of locomotion such as speed and frequency of turning are modulated by the stimulus. These definitions can be further refined when the stimulus is varied temporally and quantitatively. In klinotaxis, orientation is achieved by comparison of the stimulus intensity over time, whereas in tropotaxis the differential stimulation of paired receptors in space orients the animal relative to the stimulus source.

Kineses are similarly distinguished as klinokinesis, where the path shape (frequency of turning) is modulated by the differential intensity of stimulation over time, or orthokinesis, where quantitative aspects of locomotion (speed or frequency of locomotion) are affected by the intensity of the stimulation (Fraenkel and Gunn, 1961). Our results demonstrate that the *Drosophila* larva displays kinesis. In our assay, frequency of turning (change of direction) and frequency of locomotion (path length) are affected by alternating pulses of light and dark over time, suggesting that the *Drosophila* larva is able to compare light intensity over time. These observations suggest that the ON/OFF assay is assessing

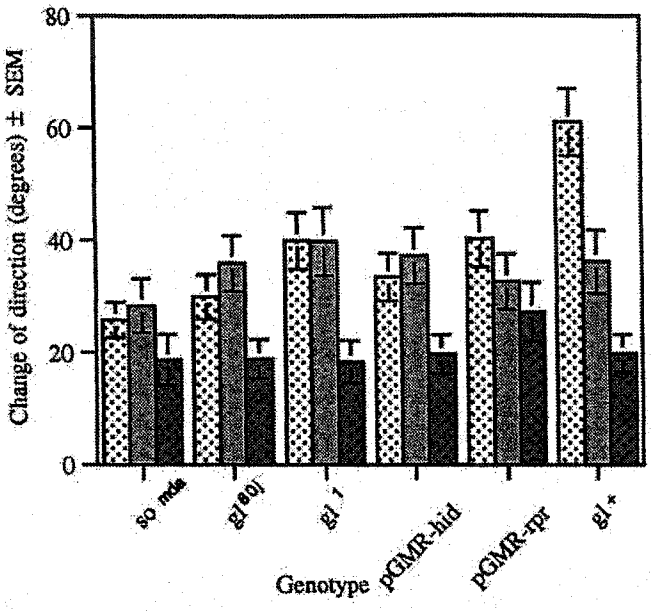


*Figure 8.* Change of direction in the ON/OFF assay of larvae with mutations in the *so* and *gl* genes. Change of direction (in degrees) was measured at the dark to light (*stippled bar*), light to dark (*gray bar*), and in the absence of light transitions (*solid bar*). Light has a significant effect on path direction in each of the strains tested, with the exception of *pGMR-rpr* ($n = 20$, $F_{(1,57)} = 0.98$, $p > 0.05$) and $so^{mda}$ ($n = 20$, $F_{(1,57)} = 1.79$, $p > 0.05$), in which the presence or absence of light had no effect. The *gl* mutant strains $gl^{60j}$ ($n = 20$, $F_{(1,57)} = 4.42$, $p < 0.02$) and $gl^{1}$ ($n = 20$, $F_{(1,57)} = 6.23$, $p < 0.005$) and *pGMR-hid* ($n = 30$, $F_{(1,87)} = 4.57$, $p < 0.01$) show no difference between degree of direction change at the light transitions. However, change of direction in the absence of light transitions is significantly lower than either of the test conditions. The $gl^{+}$ strain displays a degree of direction change in the dark to light transition that is significantly higher than the other test conditions ($n = 16$, $F_{(2,45)} = 16.23$, $p < 0.001$).

behaviors previously described as klinokinesis and orthokinesis (Fraenkel and Gunn, 1961).

The reduction in path length seen when the light turns on can be caused by different factors. The larva may stop more often as it searches for a preferred dark environment (head swinging). Alternatively, or additionally, the presence of light may change fundamental aspects of locomotion such as frequency of the peristaltic contractions that constitutes the larval stride or the amplitude of these contractions. The current assay does not have the level of resolution that distinguishes between these two alternatives.

### Klinokinesis and orthokinesis in the ON/OFF assay are dependent on an adult-like phototransductions cascade

We demonstrate that in the wild-type strains tested, the change of direction of the larval path is significantly greater when the light is turned on than when it is turned off. This directionality in the temporal perception of the light stimulus is abolished by null mutations in the *norpA* and *ninaC* genes but not by mutations in the *ninaE* gene, suggesting that this light perception is performed by a phototransduction cascade similar to that described for the adult visual system but is not mediated by the blue-absorbing rhodopsin Rh1. Moreover, the absence of this response in strains that lack the Bolwig's organ (*gl* and $so^{mda}$ mutants) further confirms this structure as the *Drosophila* larva's main photosensory organ. Locomotion in the absence of a light stimulus was not significantly affected by these mutations (data not shown), demonstrating that intact phototransduction is not required for basic aspects of larval locomotion. These observations also demonstrate that these mutations do not have a pleiotropic effect on larval behavior.

### The ON/OFF assay defines a novel extraocular light perception function

In the wild-type strains tested, change of direction when the light is turned off is greater than in the absence of light transitions, suggesting that turning off the light is a transition perceived by the animal. This observation supports the notion that a simple mechanism for the perception of light exists in the *D. melanogaster* larva that distinguishes changes in light conditions from absence of light transitions but is unable to distinguish whether the light is being turned on or off. This light response is mediated by the blue-absorbing rhodopsin (Rh1) because it is abolished in part by mutations in the *ninaE* gene. Interestingly, it does not rely on the same phototransduction pathway as that of the adult visual system as seen by the wild-type response of *norpA* and *ninaC* mutant larvae.

Our results indicate that these hypothetical photoreceptors are not housed within the Bolwig's organ, defined as the larval photoreceptors that depend on the *gl* gene function for differentiation. However, the observation that the function of this visual system is impaired in larvae where the cell death gene *rpr* is expressed under the control of the *gl* promoter demonstrates that these are cells in which the *gl* transcription factor is functional. Thus it is possible that this novel function is performed by a small number of cells that express Rh1 and the *gl* gene product but whose differentiation and Rh1 expression are not under the control of the *gl* gene.

Two different groups of cells are likely to be involved in this novel light perception. The observation that it is dependent on the *so* gene function but not *gl* suggests that these cells are included in the optic lobe primordium. The ablation of this proposed function by expression of the cell death gene *rpr* under the *gl* promoter suggests that the central brain neurons that express the *gl* gene are also involved in this behavior.

A precedent for a light detector that does not rely on known elements of the phototransduction machinery in adults is the photic input pathway required for the entrainment of the circadian rhythm (Wheeler et al., 1993). The novel visual system function proposed in this paper presents other parallels with cells involved in the control and generation of circadian rhythms. Mutations in the *gl* gene do not abolish circadian rhythms. However, the expression of the *period* (*per*) gene under the control of the *gl* promoter is sufficient to restore circadian rhythmicity in *per* mutant flies (Vosshall and Young, 1995). These results strongly suggest that the *gl*-expressing cells that are not the photoreceptors house the circadian pacemaker. It is possible that this novel visual function that distinguishes changes in light condition from absence of light transitions but is unable to distinguish whether light is being turned on or off is also involved in the control of pacemaker oscillation.

## REFERENCES

Ashburner M (1989) Developmental biology. In: Drosophila: A laboratory handbook, pp 139–298. Cold Spring Harbor, NY: Cold Spring Harbor Laboratory.

Bloomquist BT, Shortridge RD, Schneuwly S, Perdew M, Montell C, Steller H, Rubin G, Pak WL (1988) Isolation of a putative phospho-

lipase C gene of *Drosophila*, *norpA*, and its role in phototransduction. Cell 54:723–733.
Bolwig N (1946) Sense and sense organs of the anterior end of the house fly larvae. Vidensk Medd Dan Naturhist Foren 109:81–217.
Campos AR, Lee KJ, Steller H (1995) Establishment of neuronal connectivity during development of the *Drosophila* visual system. J Neurobiol 28:313–329.
Cheyette BNR, Green PJ, Martin K, Garren H, Hartenstein V, Zipursky SL (1994) The *Drosophila sine oculis* locus encodes a homeodomain-containing protein required for the development of the entire visual system. Neuron 12:977–996.
Fischbach KF, Technau G (1984) Cell degeneration in the developing optic lobes of the *sine oculis* and *small-optic-lobes* mutants of *Drosophila melanogaster*. Dev Biol 104:219–239.
Fraenkel GS, Gunn DL (1961) The orientation of animals. New York: Dover.
Gordesky-Gold B, Warrick JM, Bixler A, Beasley JE, Tompkins, L (1995) Hypomorphic mutations in the *larval photokinesis A* (*lphA*) gene have stage-specific effects on visual system function in *Drosophila melanogaster*. Genetics 139:1623–1629.
Green P, Hartenstein AY, Hartenstein V (1993) The embryonic development of the *Drosophila* visual system. Cell Tissue Res 273:583–598.
Grether ME, Abrams JM, Agapite J, White K, Steller H (1995) The *head involution defective* gene of *Drosophila melanogaster* functions in programmed cell death. Genes Dev 9:1694–1708.
Hardie RC, Minke B (1995) Phosphoinositide-mediated phototransduction in *Drosophila* photoreceptors: the role of $Ca^{2+}$ and *trp*. Cell Calcium 18:256–274.
Hicks JL, Williams DS (1992) Distribution of the myosin I-like *ninaC* proteins in the *Drosophila* retina and ultrastructural analysis of mutant phenotypes. J Cell Sci 101:247–254.
Hofstee CA, Henderson S, Hardie RC, Stavenga DG (1996) Differential effects of *ninaC* proteins (p132 and p174) on light-activated currents and pupil mechanisms in *Drosophila* photoreceptors. Vis Neurosci 13:897–906.
Katz PS (1995) Intrinsic and extrinsic neuromodulation of motor circuits. Curr Opin Neurobiol 5:799–808.
Kim S, McKay RR, Millern K, Shortridge RD (1995) Multiple subtypes of phospholipase C are encoded by the *norpA* gene of *Drosophila melanogaster*. J Biol Chem 270:14376–14382.
Lilly M, Carlson JR (1990) *smellblind*: a gene required for *Drosophila* olfaction. Genetics 124:293–302.
Miklos GLG, Rubin GM (1996) The role of the genome project in determining gene function: insights from model organisms. Cell 86:521–529.
Montell C, Rubin GM (1988) The *Drosophila ninaC* locus encodes two photoreceptor cell specific proteins with domains homologous to protein kinases and the myosin heavy chain head. Cell 52:757–772.
Moses K, Ellis MC, Rubin GM (1989) The *glass* gene encodes a zinc-finger protein required by *Drosophila* photoreceptor cells. Nature 340:531–536.
Mukhopadhyay M, Campos AR (1995) The larval optic nerve is required for the development of an identified serotonergic arborization in *Drosophila melanogaster*. Dev Biol 169:629–643.
O'Tousa JE, Baehr W, Martin RL, Hirsh J, Pak WL, Applebury ML (1985) The *Drosophila ninaE* gene encodes an opsin. Cell 40:839–850.
O'Tousa JE, Leonard DS, Pak WL (1989) Morphological defects in *ora*$^{JK84}$ photoreceptors caused by mutation in R1–6 opsin gene of *Drosophila*. J Neurogenet 6:41–52.
Pak WL, Grossfield J, Arnold KS (1970) Mutants of the visual pathway of *Drosophila melanogaster*. Nature 227:518–520.
Pearn MT, Randall LL, Shortridge RD, Burg MG, Pak WL (1996) Molecular, biochemical, and electrophysiological characterization of *Drosophila norpA* mutants. J Biol Chem 271:4937–4945.
Pollock JA, Benzer S (1988) Transcript localization of four opsin genes in the three visual organs of *Drosophila*; RH2 is ocellus specific. Nature 333:779–782.
Porter JA, Montell C (1993) Distinct roles of the *Drosophila ninaC* kinase and myosin domains revealed by systematic mutagenesis. J Cell Biol 122:601–612.
Porter JA, Hicks JL, Williams DS, Montell C (1992) Differential localizations of and requirements for the two *Drosophila ninaC* kinase/myosins in photoreceptor cells. J Cell Biol 116:683–693.
Ranganathan R, Malicki DM, Zuker CS (1995) Signal transduction in *Drosophila* photoreceptors. Annu Rev Neurosci 18:283–317.
Sawin-McCormack E, Sokolowski MB, Campos AR (1995) Characterization and genetic analysis of Drosophila melanogaster photobehaviour during larval development. J Neurogenet 10:119–135.
Schmucker D, Taubert H, Jaeckle H (1992) Formation of the *Drosophila* larval photoreceptor organ and its neuronal differentiation require continuous *Kruppel* gene activity. Neuron 9:1025–1039.
Schmucker D, Jaeckle H, Gaul U (1997) Genetic analysis of the larval optic nerve projection in *Drosophila*. Development 124:937–948.
Serikaku MA, O'Tousa JE (1994) *Sine oculis* is a homeobox gene required for *Drosophila* visual system development. Genetics 138:1137–1150.
Sehgal A, Price J, Young MW (1992) Ontogeny of a biological clock in *Drosophila melanogaster*. Proc Natl Acad Sci USA 89:1423–1427.
Sokal RR, Rohlf FJ (1995) Biometry, Ed 3. New York: W.H. Freeman and Company.
Sokolowski MB, Kent C, Wong J (1984) *Drosophila* larval foraging behaviour: developmental stages. Anim Behav 32:645–651.
Steller H, Fischbach KF, Rubin G (1987) *disconnected*: a locus required for neuronal pathway function in the visual system of *Drosophila*. Cell 50:1139–1153.
Vosshall LB, Young MW (1995) Circadian rhythms in *Drosophila* can be driven by *period* expression in a restricted group of central brain cells. Neuron 15:345–360.
Washburn T, O'Tousa JE (1989) Molecular defects in *Drosophila* rhodopsin mutants. J Biol Chem 264:15464–15466.
Wheeler DA, Hamblen-Coyle MJ, Dushay MS, Hall JC (1993) Behavior in light:dark cycles of *Drosophila* mutants that are arrhythmic, blind or both. J Biol Rhythms 8:67–94.
White K, Tahaoglu E, Steller H (1996) Cell killing by the *Drosophila* gene *reaper*. Science 271:805–807.
Zuker CS, Cowman AF, Rubin GM (1985) Isolation and structure of a rhodopsin gene from *Drosophila melanogaster*. Cell 40:851–858.

**B: Manuscript -** Behavioural characterization and genetic analysis of the *Drosophila melanogaster* larval response to light as revealed by a novel individual assay

*Behavior Genetics, Vol. 30, No. 1, 2000*

# Behavioral Characterization and Genetic Analysis of the *Drosophila melanogaster* Larval Response to Light as Revealed by a Novel Individual Assay

**Jana Hassan,[1] Macarena Busto,[1] Balaji Iyengar,[1] and Ana Regina Campos[1,2]**

*Received 17 May 1999—Final 1 Oct. 1999*

A new assay was designed, named checker, that measures the individual response to light in the fruitfly *Drosophila melanogaster* larva. In this assay the *Drosophila* larva apparently modulates its pattern of locomotion when faced with a choice between a dark and lit environment by orienting its movement towards the dark environment. We show that, in this assay, a response to light can be measured as an increase in residence time in the dark versus the lit quadrant. Mutations that disrupt phototransduction in the adult *Drosophila* abolish the larval response to light, demonstrating that this larval visual function is similar to that of the adult fly. Similarly, no response to light was detected in strains where the larval visual system (photoreceptors and target area) was disrupted by a mutation in the homeobox containing gene *sine oculis (so)* gene. Ablation of photoreceptors by the targeted expression of the cell death gene *hid* under the control of the photoreceptor-specific transcription factor *glass (gl)* abolishes this response entirely. Finally, we demonstrate that this response to light can be mediated by rhodopsins other than the blue absorbing Rh1.

**KEY WORDS:** Insect; larval photobehavior; locomotion; *Drosophila;* behavioral mutants.

## INTRODUCTION

The larval stages of the holometabolous insect *Drosophila melanogaster* has recently emerged as a model system for the genetic analysis of behavior (Monte *et al.,* 1989; Busto *et al.,* 1999; Kernan *et al.,* 1994; Osborne *et al.,* 1997; Park *et al.,* 1997; Tully *et al.,* 1994). Most of the larval development of *Drosophila melanogaster* is spent burrowed in the food substrate; a behavior described as foraging. During the last instar the larva ceases foraging and leaves the food substrate in search of an adequate site to undergo metamorphosis. Among the various behavioral changes that occur at this transition is the decrease in the larva's response to light in a population assay that assesses larval preference for a dark environment (Lilly and Carlson, 1990; Gordesky-Gold *et al.,* 1995; Sawin-McCormack *et al.,* 1995). Larval response to light has been detected in this population assay as early as the first instar (Sawin-McCormack *et al.,* 1995).

Little is known about the *Drosophila* larva visual system function and how larval locomotion is modulated by the light stimulus. Recently, using a novel individual assay we have demonstrated that a larval response to light can be measured as a reduction in the distance traveled, as a sharp change of direction and as an increase in head swinging (Busto *et al.,* 1999). Mutations that disrupt adult vision disrupt a subset of these responses suggesting the existence of a light perception function that does not utilize the same phototransduction cascade as the adult photoreceptors. Our results indicated that this novel visual function depends in part on the blue absorbing rhodopsin Rh1 and is specified by the *sine oculis (so)* gene (Busto *et al.,* 1999). However it may not reside in the larval photoreceptor organs, the so called Bolwig's

[1] Department of Biology, McMaster University, 1280 Main Street West, Hamilton, Ontario L8S 4K1, Canada.
[2] To whom correspondence should be addressed. Fax: (905) 522-6066. e-mail: camposa@mcmail.cis.mcmaster.ca



0001-8244/00/0100-0059$18.00/0 

organ (Bolwig, 1946; Steller *et al.,* 1987; Busto *et al.,* 1999).

From the morphological point of view the larval visual system of the *Drosophila* larva is very simple. It is comprised of two bilateral groups of twelve photoreceptor cells located anteriorly and juxtaposed to the mouth hooks similar to what is found in larger flies organ (Bolwig, 1946; Steller *et al.,* 1987). The axons of the photoreceptor cells form the larval optic nerve which innervates the optic lobe primordium area of the brain lobes. The early development and the establishment of connectivity in this system has been described in some detail (Green *et al.,* 1993; Campos *et al.,* 1995). The reported simplicity of the larval visual system is in contrast to the morphological complexity observed in the adult visual system. The main visual organ of the adult fly, the compound eyes, consist of circa 800 ommatidial units containing of 8 photoreceptor cells each. These photoreceptors project in a complex sterotypical pattern to the target area, the optic lobes in the brain (Meinertzhagen and Hanson, 1993).

In order to begin understanding the neural mechanisms underlying the regulation of larval locomotion by light we decided to take a genetic approach. Such an approach requires the isolation of single gene mutations to be used as tools in the identification of cell types and ultimately gene products required for the performance of the behavior under study. To that end appropriate assays need to be designed and the analysis of this behavior using previously isolated mutations need to be carried out in some detail. We reasoned that individual assays would be better suited for this purpose for the following reasons. First, it precludes the need of large numbers of synchronized larvae which is cumbersome in a mutant screen. Second, it allows the detection of other phenotypes (such as deficits in locomotion) that may interfere with the final response measured. Third, the progression of the assay can be recorded on video tape such that additional analysis of the larval behavior can be performed. Finally, the ability to test a behavioral phenotype in a single larva provides us with the tool to undertake a mosaic analysis where each individual is distinct regarding the distribution of mutant and wild type patches.

Two assays were designed that use single animals and where a per larva response index can be obtained. These assays, checker (this report) and the on/off (Busto *et al.,* 1999) are relatively quick. Each larva can be tested in less than 5 minutes making these assays suitable for large scale mutant screens.

Here, using the checker assay, we report that in the *Drosophila* third instar foraging larva the light stimulus modulates the direction of movement and that this response can be reliably measured in individual organisms. Mutations that disrupt phototransduction in the adult eye also disrupt this larval response. These results suggest that the larval and adult visual systems are similar from the functional point of view. The analysis of developmental mutants in which all or part of the larval visual system is missing, demonstrates that larval light detection measured by the checker assay is located in the larva's main visual organ the so called Bolwig's organ.

## MATERIALS AND METHODS

### Fly Stocks

Fly strains were grown at 25°C in 12 hr light/dark cycles on standard medium containing inactivated yeast, sucrose and agar supplemented with fresh active yeast and β carotene (1.25 g/l). Tegosept in ethanol and propionic acid were used to prevent mold growth. Strains used in addition to wild types *Canton-S* (*CS*) and *Oregon-R* (*OR*) are listed below:

*Glass Multimer Reporter-Head Involution Defective* (*pGMR-hid*). This strain contains a fusion vector in which the cell death gene *hid* is expressed under the control of the *gl* promoter (Grether *et al.,* 1995).

*Neither Inactivation nor Afterpotential C* (*ninaC*). The *ninaC* gene encodes two isoforms (3.6 and 4.8 kb RNA) of adult photoreceptor specific cytoskeleton proteins consisting of a protein kinase and a myosin head domain (Montell and Rubin, 1988). The $ninaC^5$ mutant allele used is a null that causes the reduction of the 3.6 and 4.8 kb RNA. $ninaC^5$ mutants show abnormal ERG, light and age-dependent retinal degeneration (Porter and Montell, 1993; Hofstee *et al.,* 1996) as well as a defect in response termination (Porter *et al.,* 1992).

*Neither Inactivation nor Afterpotential E* (*ninaE*). The *ninaE* germ encodes the opsin moiety of the Rh1 rhodopsin and is expressed in the adult photoreceptors R1–R6 (Serikaku and O'Tousa, 1994) as well as the larval visual system (Zuker *et al.,* 1985; Pollock and Benzer, 1988). The $ninaE^{17}$ mutation contains a 1.6 kb deletion. Mutant flies have very low rhodopsin levels and respond poorly to light stimulus (O'Tousa *et al.,* 1989).

*No-Receptor Potential A* (*norpA*). The *norpA* gene encodes a phospholipase C, which when absent, leads to a complete block of the phosphoinositide cascade

mediating phototransduction (Hardie and Minke, 1995). Adult flies lack light-elicited receptor potentials in the compound eyes and ocelli (Pak *et al.*, 1970). The *norpA*$^{P24}$ contains a 28 base pair deletion in the coding region which produces a premature termination codon (Pearn *et al.*, 1996).

*Sine Oculis* (*so*). The *so* gene encodes a homeobox containing protein required for adult and larval visual system development (Fischbach and Technau, 1984; Serikaku and O'Tousa, 1994). The *so*$^{mda}$ mutation prevents the development of the larval visual system (photoreceptors and target area) (Serikaku and O'Tousa, 1994).

### Harvest of Synchronized Larvae

Adult flies aged from one to seven days were allowed to lay eggs in a fresh food plate (100 mm × 15 mm; Fisher Scientific) supplemented with vitamin A precursor (βcarotene, 1.25 g/L) and coated with yeast paste. After a minimum of two 2 hr precollections, a 1 hour egg collection was incubated at 25°C. At 20–22 hours after egg lay (AEL) all newly-hatched first instar larvae were removed under a dissection microscope. After a one-hour incubation period approximately 70 newly hatched first instar larvae were collected and transferred to a fresh food plate coated with yeast paste. Third instar larvae were tested for photobehavior at between 84–90 hours AEL.

### Photobehavior Assay

Measurements of larval photobehavior were made on the checker assay. It consists of a plastic petri dish (100 mm × 15 mm; Fisher Scientific) containing 15 ml of 1% agarose cooled to room temperature. Irregularities on the agar surface affect larval behavior. *Drosophila* larvae like to remain in crevices. Therefore test plates need to be free of depressions (agar bubbles) and the test can not be performed near the edge of the plate where the agar touches the side of the plate. Thus a circular 1 cm boundary from the plate edge was established beyond which the data collected was discarded.

Manipulation of the larvae prior to the test was conducted using a dark room light (20 W lamp with Kodak GBX-2 filter). Testing was conducted using a cool white bulb with a spectrum of 400–650 nm with peaks at 440 and 560 nm (20W Cool White, Philips) and with a throughput of 1050 microwatts/cm$^2$. Light intensity was measured with a Newport Digital Power meter (Model 818-SL). The dark room light (20 W lamp with Kodak GBX-2 filter) used in this assay is the same employed to record circadian regulated locomotory behavior of *Drosophila* in free running conditions ("constant darkness") (Sehgal *et al.*, 1992). Larval photobehavior assays (Lilly and Carlson, 1990; Busto M.Sc. thesis, 1999) conducted using the dark room light as the sole light source yielded response indices close to zero confirming previous reports that *Drosophila* does not respond to light stimulus above the 650 nm range (Ashburner, 1989).

Individual larvae were removed, using a moist paintbrush, from the culture dish. Each larva was carefully rinsed with distilled water to remove any excess food particles, removed from the distilled water using a flathead paintbrush, and placed on a pre-test plate for a period of 1 minute to allow for acclimatization to the agar surface. Each larva was then positioned in the center of the test plate. Each plate was positioned on a template consisting of 1 cm squares constructed in a checker board manner using black adhesive tape on the upper surface of the glass plate. The dark squares block out light while the light squares permit light transmission. Template and dish were positioned on a light box that was modified to emit light only in an 11 cm diameter. Template and dish were lit from below by a light box.

### Temperature

Surface temperature recordings were taken in 25 sec intervals for 200 sec during the course of the checker assay using a 21X Micrologger (Campbell Scientific Ltd.). Temperature readings in either the checker assay (light or dark checks), or under safe light conditions were 21.5 ± 0.5°C (data not shown).

### Data Collection and Analysis

Larval movement was visualized through a Fujinon TV · Z zoom lens (Fuji Optical Co.) attached to a CCD TV camera (Elmo TSE 272S) and recorded on videotape (Fuji HQ-120, RCA VCR). Larval behavior was recorded either until they reached the 1 cm boundary or total test time (180 seconds) had elapsed. Data derived for each of the strains was obtained from two to three sets of samples in which approximately ten larvae were tested each time.

Residence time in the dark and light quadrants were obtained using the VCR timer and started 5 seconds after the larva was placed in the center of dark

checker. Response indices (R.I.) [(time in dark – time in light)/total time of test or path length per cycle], with lights on ($R.I.^{on}$) and without lights ($R.I.^{off}$) were calculated on a per larva basis and an average of these individual indices was taken. A response to light is present when the R.I. with the light on is significantly higher ($p < 0.05$) than that obtained in the absence of light. In most experiments the same larva was tested with and without light (see below). Two standard wild type strains (CS and OR) showed a response to light whether the same or a different set of larvae were assayed with or without light. The data are depicted as means plus or minus standard error ($X \pm SEM$). The data, shown in Figs. 2, 3, and 5, were analyzed with paired T tests (two-tailed) at a level of significance of $\alpha = 0.05$. Part of the data shown in Fig. 4 was analyzed with paired T tests (*ninaE*$^{17}$), the rest of the data shown in this figure and Fig. 6 were analyzed with two-sampled T-tests at the same level of significance.

### Immunohistochemistry

Larval brains with the eye-antenna imaginal discs were dissected from third instar larvae in PBS (Phosphate Buffer Saline), and fixed in 4% paraformaldehyde (pH 7.4) for 45 min at room temperature. This was followed by 3–4 PBS washes. Brains were incubated in a blocking solution, which contained PBS with 0.3% Triton X-100 and 5% goat serum at room temperature for 1 hr, followed by addition of a fresh 100 µl of blocking solution containing 2 µl of 24B10 primary. After 8–12 hrs of incubation at 4°C the samples were washed with PBT (phosphate Buffer Triton) for 4 hrs, with changes every 10–20 min, followed by incubation in blocking solution as described above and finally incubated with a secondary antibody conjugated to horseradish peroxidase for another 8–12 hrs. Specimens were washed thoroughly for 4 hrs and stained with 0.5 ml of 3, 3′-diaminobenzidine (0.5 mg/ml, Sigma 72H3614) in the presence of hydrogen peroxide. The reaction was stopped by washing several times with PBS. Samples were mounted in 70% glycerol in PBS, and observed with a Zeiss axiophot microscope.

## RESULTS

### Larval Response to Light Can be Measured as Increased Residence Time in Dark

The checker assay follows the general design of the original plate assay (Lilly and Carlson, 1990) except that smaller quadrants and individual larvae are tested. Observations of larval behavior during the course of this assay suggest that the wild type larva remain preferentially in the dark environment. As the larva encounters a light quadrant it retracts its head and returns to the original dark environment. It is seen often with more than half of its body length positioned over the dark/light boundary. Even in this situation the larva is often able to return to the original position of the dark checker (Fig. 1A, frame 00:03).

While the larva is in the lit quadrant the path shape is typically straight (Fig. 1B). While in the dark quadrant the path shape is often convoluted, likely reflecting an attempt to remain in the dark quadrant and/or a repulsion to light (Fig. 1B). Therefore, in this assay, path shape or the modulation of locomotion in the two environments is apparently a reflection of the larva's attempt to remain in the dark environment (i.e. light avoidance when confronted with a dark/light boundary).

In an attempt to quantify these observations two response indices (R.I.), with the light on ($R.I.^{on}$) and with the light off ($R.I.^{off}$), were calculated for each larva. The response index is based on residence time in dark and light quadrants (R.I. = (total time in dark quadrants – total time in light quadrants)/total (test time)). Thus a response to light in this test is represented by a significant effect of light on the R.I. The R.I.'s obtained with the light on and off were significantly different in the two wild type strains tested indicating an effect of light on larval behavior (Fig. 2).

In a mutant screen, lack of response may be due to reduction in sensitivity that may represent a specific phenotype. Alternatively, variability in the sensitivity of larvae due to variables in food and rearing conditions may reduce its ability respond to a light stimulus in this assay. In order to determine how sensitive the larval visual system is in this assay we used neutral density filters to reduce the light throughput in the lit quadrants in a stepwise fashion thereby reducing the difference between the lit and dark quadrants. The two wild type strains used (OR and CS) were able to respond in this assay even when the light throughput of the lit quadrant was only 14.3% of the original test condition (Fig. 2 and 3). However, upon further reduction of light, the CS strain was unable to respond in this assay while the OR strain responded normally. These results demonstrate that the conditions of this assay allow us the detection of a larval response to light above the threshold of variations in light sensitivity of two standard wild type strains.

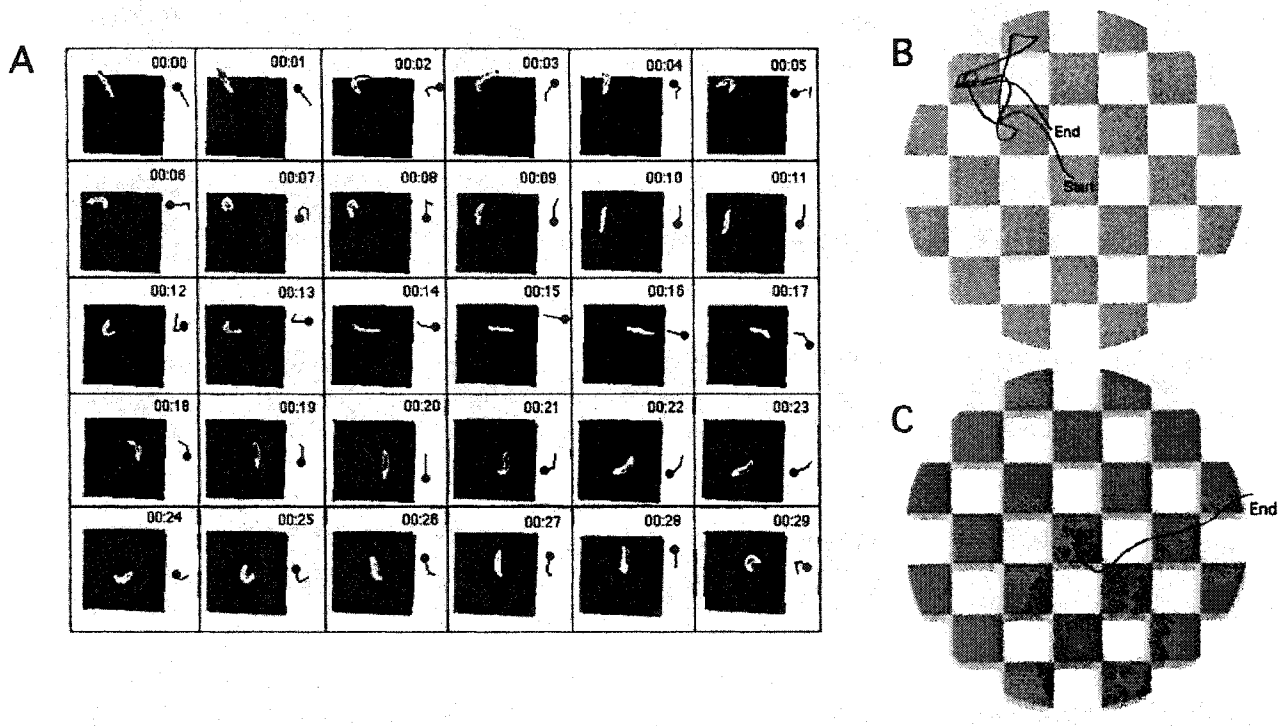


**Fig. 1.** Larval behavior in the checker assay. A-Video of a single *CS* larva tested in the checker assay was used to generate frame by frame photographs. On the right of each panel a schematic drawing depicts the relative position of the head (filled circle) and body (line). Frames 0 to 7 show a larva that, as it approaches the dark/light boundary, reacts by retracting its head (frames 2 to 4) and then returns to the dark square by making a 180° turn towards the opposite direction (frames 5 to 9). Frames 10 to 29 show the larva circling within the dark check without approaching the light/dark boundary. B-Diagramatic representations of path taken by a wild type *CS* larva in both test (Light) and control (Dark) conditions.

## The Light Response Measured in the Checker Assay Is Mediated by a Phototransduction Pathway Similar to Adult Visual System Function

In order to determine whether this assay was detecting larval visual function similar to the one previously described for adult flies, larvae carrying null mutations in *norpA, ninaC* and *ninaE* genes were tested as described above. These genes are required in the adult fly for visual system function and for phototransduction in the compound eye (reviewed by Ranganathan *et al.,* 1995).

The *ninaC* gene encodes two retina-specific chimeric proteins consisting of a protein kinase and a myosin head domains (Montell and Rubin, 1988). One of these a 132 kD protein (p132), is expressed primarily in the cytoplasm. The other, a 174 kD protein (p174) is localized predominantly in the rhabdomere (Porter *et al.,* 1992; Porter and Montell, 1993). The $ninaC^5$ mutant allele has reduced levels of both p132 and p174.

The *norpA* gene encodes a phospholipase C, an essential component of the phototransduction signaling cascade in the adult eye (Bloomquist *et al.,* 1988; Ranganathan *et al.,* 1995). The *norpA* gene is expressed as two developmentally-regulated transcripts (subtypes I and II) generated by alternative splicing (Kim *et al.,* 1995). Subtype I is specific to the adult eye while subtype II is found in the CNS of adults and larvae (Kim *et al.,* 1995). Therefore, disruption in the response to light in larvae carrying a null allele of the *norpA* gene may be due to lack of this gene's function in the larval CNS and/or larval visual system.

The values obtained for $R.I.^{on}$ and $R.I.^{off}$ were not significantly different in larvae homozygous mutant for the *norpA* and *ninaC* genes indicating that mutations in these genes abolish the larval response to light as measured in this assay (Fig. 4). In contrast, lack of the blue absorbing rhodopsin Rh1 had no effect on the larval response to light suggesting that in this assay, larval response can be mediated by photoreceptors expressing other rhodopsins (Fig. 4).

Mutations that severely disrupt locomotion cannot be tested in the checker assay (Iyengar *et al* 1999).

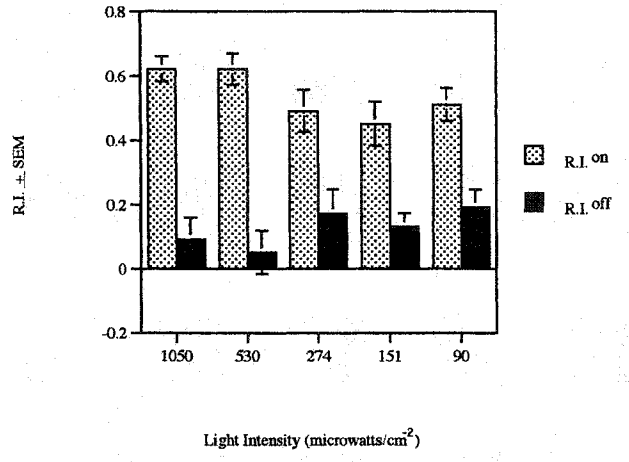


**Fig. 2.** Response of the wild type strain OR in the checker assay at various light intensities. OR foraging third instar larvae were tested in five different light intensities spanning the range from 1050 microwatts/cm$^2$ to 90 microwatts/cm$^2$. Two R.I. were calculated per larva: in the presence (R.I.$^{on}$) and in the absence (R.I.$^{off}$) of light. A significant difference between R.I$^{on}$ and R.I.$^{off}$ represents a response to light. Paired t-tests were used to determine significancy ($p < 0.05$). Significant differences were calculated for all light intensities: 1050 microwatts/ cm$^2$ ($n = 20$, $p < 0.001$), 530 microwatts/ cm$^2$ ($n = 20$, $p = 0.001$), 274 microwatts/ cm$^2$ ($n = 20$, $p < 0.0024$), 151 microwatts/ cm$^2$ ($n = 20$, $p = 0.001$), 90 microwatts/ cm$^2$ ($n = 20$, $p < 0.001$).

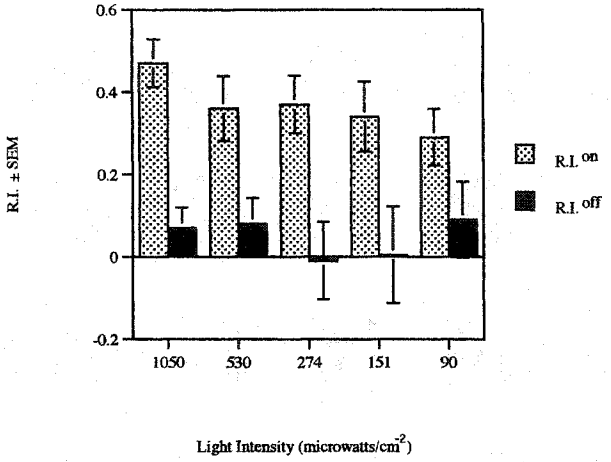


**Fig. 3.** Response of the wild type strain CS in the checker assay at various light intensities. CS foraging third instar larvae were tested in five different light intensities spanning the range from 1050 microwatts/ cm$^2$ to 90 microwatts/ cm$^2$. Two R.I. were calculated per larva: in the presence (R.I.$^{on}$) and in the absence (R.I.$^{off}$) of light. A significant difference between R.I$^{on}$ and R.I.$^{off}$ represents a response to light. Paired t-tests were used to determine significancy ($p < 0.05$). Significant differences were found for four light intensities: 1050 microwatts/ cm$^2$ ($n = 25$, $p < 0.001$), 530 microwatts/ cm$^2$ ($n = 20$, $p = 0.0069$), 274 microwatts/ cm$^2$ ($n = 20$, $p < 0.001$), 151 microwatts/ cm$^2$ ($n = 15$, $p = 0.014$). No significant difference between R.I.$^{on}$ and R.I.$^{off}$ was found when CS larvae were tested at 90 microwatts/ cm$^2$ ($n = 20$, $p = 0.14$).

In order to determine whether locomotion was affected by any of the mutations used in this paper we measured the distance traveled in 30 sec in the absence of light. These were compared to the two wild type strains used as baseline for the response to light measured in the checker assay (CS and OR). Locomotion in these wild type strains is significantly different, with OR displaying less locomotion than CS (Fig. 6). Their response to light is however indistinguishable, i.e., R.I.$^{on}$ is significantly different from R.I.$^{off}$ in both strains. These observations suggest that locomotion which is within the range exhibited by CS and OR strains does not affect the response to light evaluated in the checker assay. All the mutant strains used here except for one (*pGMR-hid*) display locomotion within the range established for OR and CS wild type strains. (Fig. 6). The locomotion measured for *pGMR-hid* mutant larvae is significantly lower that that shown for OR and this strain does not respond to light (below and Fig. 6). This result could be interpreted as an inability of *pGMR-hid* mutant larvae to respond to light due to reduced locomotion. However, several other strains with locomotion measurements indistinguishable from that calculated for *pGMR-hid* mutant larvae have been shown to respond to light in this assay (Iyengar *et al* 1999). We concluded that the lack of response seen in *pGMR-hid* mutant larvae is due to a defect in the visual system and not a significant effect on locomotion.

## Ablation of the Bolwig's Organ and the Optic Lobe Primordium Disrupts the Larval Response to Light

In *D. melanogaster,* the larval visual system is comprised of two bilateral groups of twelve photoreceptor cells located anteriorly and juxtaposed to the mouth hooks similar to what is found in larger flies (Steller *et al.,* 1987). These photoreceptors project posteriorly and ventrally around the brain hemispheres terminating in the optic lobe primordium (Campos *et al.,* 1995; Green *et al.,* 1993; Schmucker *et al.,* 1997). The *so* gene encodes a homeodomain protein expressed in the optic lobe primordium and in the developing larval photoreceptors during embryogenesis and in the developing adult visual system (photoreceptor cells and optic lobes) in larvae (Cheyette *et al.,* 1994; Serikaku and O'Tousa, 1994). *so* functions include,

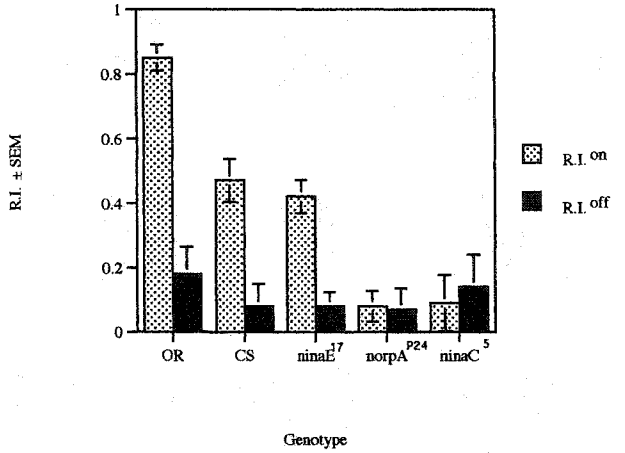


**Fig. 4.** Response in the checker assay of wild type larvae and larvae with mutations in genes required for adult phototransduction. Two R.I. were calculated: in the presence ($R.I.^{on}$) and in the absence ($R.I.^{off}$) of light. A significant different between $R.I^{on}$ and $R.I.^{off}$ represents a response to light ($p < 0.05$). The genotypes tested in this assay are: wild type strains CS (light on, n = 30; light off, n = 20) and OR (light on, n = 18; light off, n = 20) as well as the phototransduction mutants $norpA^{P24}$ (light on, n = 29; light off, n = 30), $ninaC^{5}$, (n = 20) and $ninaE^{17}$, (n = 19). $R.I^{on}$ and $R.I.^{off}$ for wild type strains CS and OR and $ninaE^{17}$, mutant larvae are significantly different (CS, $p < 0.001$; OR, $p < 0.001$, $ninaE^{17}$ $p < 0.001$). In contrast, the $R.I^{on}$ and $R.I.^{off}$ for the phototransduction mutants $norpA^{P24}$ and $ninaC^{5}$ are not significantly different ($norpA^{P24}$, $p = 0.87$, $ninaC^{5}$, $p = 0.69$).

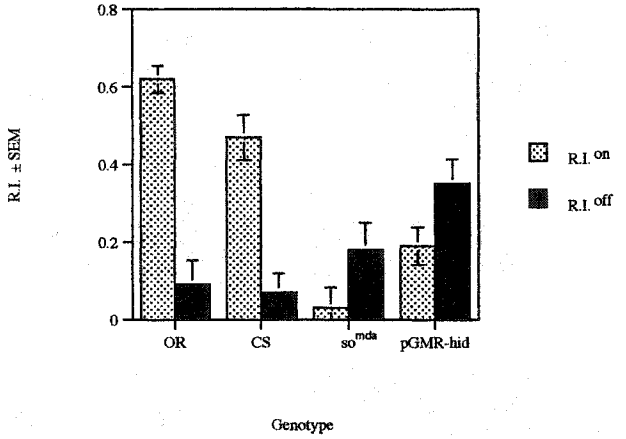


**Fig. 5.** Response in the checker assay of wild type strains CS and OR and the visual system mutants, *pGMR-hid* and $so^{mda}$. Two R.I. were calculated: in the presence ($R.I.^{on}$) and in the absence ($R.I.^{off}$) of light. A significant difference between $R.I^{on}$ and $R.I.^{off}$ represents a response to light ($p < 0.05$). The $R.I^{on}$ and $R.I.^{off}$ for both wild type strains OR (n = 20, $p < 0.001$) and CS (n = 25, $p < 0.001$) are significantly different. The $R.I^{on}$ and $R.I.^{off}$ for the visual system mutants $so^{mda}$ (n = 20, $p = 0.13$) and *pGMR-hid* (n = 30, $p = 0.064$) are not significantly different.

regulating genes necessary for proper optic lobe invagination and Bolwig's organ formation during embryogenesis (Serikaku and O'Tousa, 1994). In order to determine whether the larval visual system, as defined by the so gene function, mediate the response to light measured here, larvae carrying a mutation in the so gene were assayed.

The $so^{mda}$ mutant allele prevents the formation of the optic lobe placode that gives rise to photoreceptors and optic lobe primordium of the larval and adult visual system (Serikaku and O'Tousa, 1994). Therefore these strains lack not only the photoreceptor cells but also the target area which in the embryo is called the optic lobe primordium. No significant response to light was detected in $so^{mda}$ mutant larvae demonstrating that the visual function that mediates the response to light measured in the checker assay resides in cells that require the so gene function (Fig. 5).

Next we sought to determine whether the photoreceptor cells, defined as the retinular cells that require the zinc finger transcription factor *gl* for differentiation, are the main photosensory organ required for this light response. To that end a strain in which a cell death gene (*hid*) is under the control of the *gl* promoter (*pGMR-hid*), was analyzed (Grether *et al.*, 1995). In adult flies ectopic expression of the *hid* gene in the developing adult photoreceptors is sufficient to ablate these cells (Grether *et al.*, 1995). Larvae carrying two copies of the *pGMR-hid* construct did not respond to light when tested in the checker assay (Fig. 5).

*gl* is expressed in the larval and adult photoreceptor neurons and in two groups of approximately 21 neurons in each brain hemisphere (Moses *et al.*, 1989). Not all cell types are equally sensitive to ectopic expression of cell death genes (H. Steller, personal communication). Therefore lack of response of the *pGMR-hid* larvae in the checker assay could be due to ablation of all *gl*-expressing cells or of a subset of these cells. For example, the larval retinular cells may not have been entirely killed by the ectopic expression of the cell death gene *hid,* suggesting that the complete set of retinular cells are required for the light response being measured in the checker assay.

In order to address these questions the integrity of *gl*- expressing cells in *pGMR-hid* larvae was estimated by labeling larval brains with the monoclonal antibody 24B10 that detects a photoreceptor—specific protein (Zipursky *et al.*, 1984). A monoclonal antibody that recognizes the *gl* gene product (Moses *et al.*, 1989) and

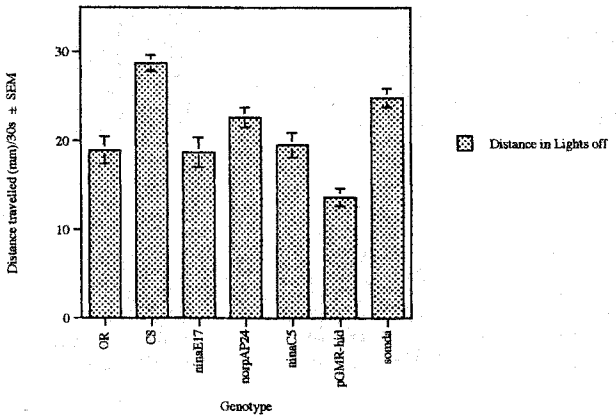


**Fig. 6.** Locomotion of OR, CS and of the mutant strains used. The graph depicts the mean distance traveled (SEM) in 30 seconds on a non-nutritive substrate in the absence of light. The locomotion measured for the OR wild type strain (n = 22) is significantly lower than that of $norpA^{P24}$ (n = 30; p = 0.048) and of $so^{mda}$ (n = 20, p = 0.0033) and significantly higher that that of *pGMR-hid* (n = 31, p = 0.0038). It is indistinguishable from $ninaC^{5}$ (n = 16, p = 0.78) and $ninaE^{17}$ (n = 20, p = 0.91). The locomotion of the CS wild type strain is significantly higher than all mutant strains tested ($norpA^{P24}$ $p < 0.001$; $so^{mda}$ $p = 0.0033$; *pGMR-hid* $p < 0.001$; $ninaC^{5}$ $p < 0.001$; $ninaE^{17}$ $p < 0.001$).

thus also other *gl*-expressing cells besides the retinular cells was also used in *pGMR-hid* strains. Additionally, larval brains from p*GMR-hid* larvae also carrying the *pGMR-lacZ* reporter construct were dissected and labeled with X-Gal histochemistry. The advantage of using the expression the *lacZ* gene under the control of the *gl* promoter is that the reporter (*lacZ*) can be found in the axons as well as cell bodies while the *gl* gene product is found only in the nuclei.

No labeling with the 24B10 monoclonal antibody was detected in *pGMR-hid* brains indicating that all larval photoreceptors were either absent or severely damaged by the ectopic expression of the cell death gene *hid* (Fig. 7B). Similar conclusions were reached when the expression of the *pGMR-lacZ* reporter construct was used to identify the larval photoreceptor cells (data not shown). Surprisingly, the *gl*-expressing central brain neurons were apparently not affected by the expression of the cell death gene *hid* as seen by the normal appearance of the *lacZ* expression (cell bodies and projection pattern) and of the expression of *gl* gene product (Fig. 7C to E). We concluded that the cell death gene *hid* is unable to affect other *gl*-expressing cells besides the larval retinular cells demonstrating that the absence of a light response in the *pGMR-hid* strain is due to absence of Bolwig's organ.

## DISCUSSION

The *Drosophila* larval response to light represents a simple and easily quantifiable behavior likely to include components of more complex behaviors executed by higher organisms. *Drosophila* as, a model system, provides high resolution genetic and molecular biology tools to dissect the components, molecular and cellular, required for larval response to light (Miklos and Rubin, 1996).

In order to initiate a genetic dissection of larval response to light an assay was designed that tests a single larva. This assay is fundamentally different from the previously reported on/off assay as it makes different demands upon the larva (Busto *et al.*, 1999), see below. Therefore, it can be used to identify disruptions in different aspects of larval behavior.

In the checker assay the larva responds to light by performing complex maneuvers in order to remain in the preferred dark environment. Consequently, the pattern of larval locomotion in the dark is consequence of its avoidance of the light quadrant. A response to light in this assay is measured as an increase in residence time in the dark quadrant over that of the lit quadrant. Our results demonstrate that the larval response to light being measured in the checker assay is mediated by the Bolwig's organ and its first order neurons located in the optic lobe primordium. Ablation of Bolwig's organ only by the targeted expression of the cell death gene *hid* is sufficient to completely abolish the response to light measured in this assay. This is in contrast with previous findings using the on/off assay (Busto *et al.*, 1999). During the course of this assay the individual larva is subjected to intermittent pulses of light and dark (10 sec) and its behavior is recorded. The path tracing derived from individuals is used to measure various locomotory parameters such as change of direction at the transition between light and dark as well as path length, and head swinging frequency during the light and dark pulses. Analysis of these behaviors in wild type strains demonstrated that light modulates locomotion as seen by the reduction in the distance traveled that occurs during the light pulse. Additionally, turning on the light triggers a change in the direction of the larval path greater than when the light is turned off which in turn is greater than that measured in the absence of any light transition. Ablation of Bolwig's organ abolishes only the increased change of direction triggered by the dark to light transition (Busto *et al.*, 1999). These observations support the notion that an extra ocular light detection function exists that per-

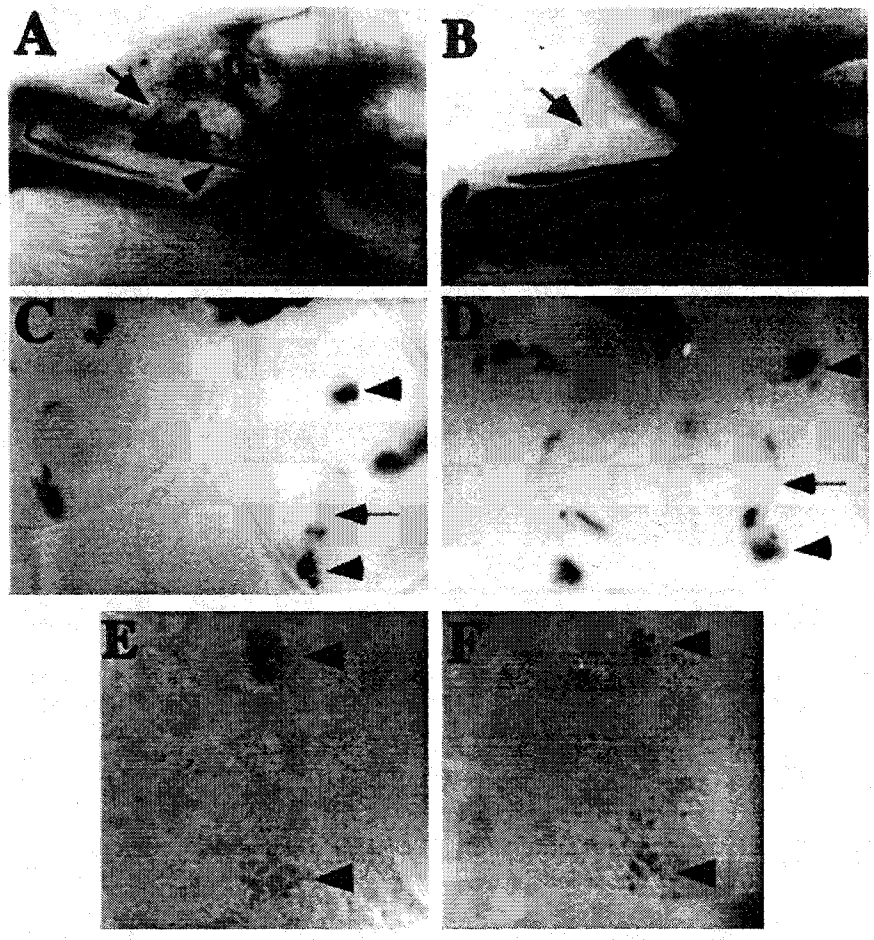


**Fig. 7.** Visualization of *gl-* expressing cells in *pGMR-hid* larvae. Whole mount immuno histochemistry of mouth hooks (A, B) where the Bolwig's organ is located and central nervous systems (C-F) dissected from third instar larvae. A minimum of 8 brain hemispheres were analyzed from each mutant strain. The monoclonal antibody 24B10 which labels the membrane of all retinular cells was used to visualize Bolwig's organ: (A) Wild type specimen showing the cell bodies (arrow) and the larval optic nerve (arrowhead), (B) *pGMR-hid* specimens do not show any 24B10 labeling (arrow). The expression of the *pGMR-lacZ* reporter construct as seen by βgalactosidase activity was used to identify gl-expressing cells in the central nervous system of third instar larvae. The pattern of βgalactosidase activity, which labels both the cell bodies (arrowheads in one brain hemisphere in C and D) and the axonal projections (arrows in one brain hemisphere in C and D), is the same in wild type (C) and *pGMR-hid* larvae (D). The anti-Glass antibody was also used to visualize the central nervous system *gl*-expressing neurons in wild type (arrowheads in E) and *pGMR-hid* larvae (arrowheads in F). No difference was observed between specimens of these two strains.

ceives the presence of light transitions but which cannot distinguish between the light being turned on from off (Busto *et al.*, 1999).

The light response measured by the checker assay can be mediated by rhodopsins other than the blue absorbing Rh1 encoded by the *ninaE* gene. This observation is similar to that found in the on/off assay (Busto *et al.*, 1999). These results do not exclude the potential role of this rhodopsin in mediating the light response detected in the checker assay. This question can only be addressed by the spectral sensitivity analysis of this behavior.

No statistically significant difference was found between the R.I.$^{on}$ and the R.I.$^{off}$ for the $so^{mda}$ and *pGMR-hid* mutant strains indicating that these mutant strains do not respond to the light stimulus in this assay. However, in these two strains the R.I.$^{off}$ was slightly higher than the R.I.$^{on}$. A possible explanation for this observation is that a residual light perception exists that cannot discriminate between the dark (preferred) and the lit (repulsive) environments but which nevertheless propels the larva forward. In the absence of light (test run in complete darkness) the larva remains in the dark quadrant, the location where it was placed at the

beginning of the test, which leads to a slightly higher, but non significant, R.I..

The locomotory reaction of organisms to biotic or abiotic factors has been traditionally defined relative to the source of stimulus (Fraenkel and Gunn, 1961). In a directed reaction (taxis), movement is modulated in order to position the long axis of the organism towards or away from the source of stimulation. In undirected locomotory reactions (kinesis), quantitative aspects of locomotion such as speed and frequency of turning are modulated by the stimulus.

These definitions can be further refined when the stimulus is varied temporally and quantitatively. In klinotaxis orientation is achieved by comparison of the stimulus intensity over time while in tropotaxis the differential stimulation of paired receptors in space orients the animal relative to the stimulus source. Thus in taxis the movement of the organism during orientation reflects the different way in which the stimulus is perceived. So for example, in klinotaxis orientation is indirect resulting from the alternating movements of the body necessary for the temporal measurement of the stimulus intensity. The resulting path is wavy with its overall direction towards or away from the stimulus source. In tropotaxis no deviations of the path are observed because the relative intensity of the stimulus is perceived in space due to the unequal stimulation of bilateral receptors. Thus, in this case the resulting path is straight towards or away from the source (Fraenkel and Gunn, 1961).

Using the checker assay, we show that the *Drosophila* larva is able to orient its body axis away from the light source, a behavior defined as taxis. This behavior, during the course of the assay, results in an increase in the residence time in the dark quadrant over that recorded for the lit quadrant. Whether the comparison of relative light intensity is being performed by the larval visual system temporally (klinotaxis) or spatially (tropotaxis) was not directly addressed by the experiments described in this paper. The observation that the larva upon entering a lit quadrant will, most of the time, return to its previous position in the dark suggests that a measurement of light was performed over time, a characteristic of the behavior described as klinotaxis (Fraenkel and Gunn, 1961). However, the presence of paired photoreceptors (the Bolwig's organ) and the fact that the larval path through the lit quadrant is straight, strongly suggest that the behavior being observed in this assay fits instead the classical definition of tropotaxis (Fraenkel and Gunn, 1961). Therefore, the checker assay described here measures an aspect of the *Drosophila* larval response to light fundamentally different from the one measured by the on/off assay (Busto *et al.*, 1999). The latter measures the modulation by light of quantitative aspects of locomotion such as speed and frequency of turning; a behavior defined as kinesis (Fraenkel and Gunn, 1961).

## ACKNOWLEDGMENTS

The authors are indebted to Drs. W. J. Bell, M. B. Sokolowski, and T. Tully for discussions on larval behavior. We thank the generosity of the following fly workers: Joe O'Tousa, Randall Shortridge and Kathy Mathews for the prompt donation of stocks. This work was supported by an operating grant to A. R. C. by the Medical Research Council (MRC) of Canada.

## REFERENCES

Ashburner, M. (1989). Drosophila: *A Laboratory Handbook,* Cold Spring Habor Laboratory Press, Cold Spring Harbor.

Bloomquist, B. T., Shortridge, R. D., Schneuwly, S., Perdew, M., Montell, C., Steller, H., Rubin., G., and Pak., W. L. (1988). Isolation of a putative phospholipase C gene of *Drosophila, norpA,* and its role in phototransduction. *Cell* **54**:723–733.

Bolwig, N. (1946). Sense and sense organs of the anterior end of the house fly larvae. *Vidensk. Medd. Dan. Naturhist. Foren.* **109**: 81–217.

Busto, M., Iyengar, B., and Campos, A. R. (1999). Genetic dissection of behavior: Modulation of locomotion by light in the *Drosophila melanogaster* larva requires genetically distinct visual system functions. *J. Neurosci.* **19**:3337–3344.

Campos, A. R., Lee, K. J., and Steller, H. (1995). Establishment of neuronal connectivity during development of the *Drosophila* visual system. *J. Neurobiol.* **28**:313–329.

Cheyette, B. N. R., Green, P. J., Martin, K., Garren, H., Hartenstein, V., and Zipursky, S. L. (1994). The *Drosophila sine oculis* locus encodes a homeodomain-containing protein required for the development of the entire visual system. *Neuron* **12**: 997–996.

Fischbach, K. F., and Technau, G. (1984). Cell degeneration in the developing optic lobes of the *sine oculis* and small-optic-lobes mutants of *Drosophila melanogaster. Dev. Biol.* **104**:219–239.

Fraenkel, G. S., and Gunn, D. L. (1961). *The Orientation of Animals,* Dover, New York.

Gordesky-Gold, B., Warrick, J. M., Bixler, A., Beasley, J. E., and Tompkins, L. (1995). Hypomorphic mutations in the larval photokinesis A (lphA) gene have stage-specific effects on visual system function in *Drosophila melanogaster. Genetics* **139**: 1623–1629.

Green, P., Hartenstein, A. Y., and Hartenstein, V. (1993). The embryonic development of the *Drosophila* visual system. *Cell Tissue Res.* **273**:583–598.

Grether, M. E., Abrams, J. M., Agapite, J., White, K., and Steller, H. (1995). The *head involution defective* gene of *Drosophila melanogaster* functions. *Genes Dev.* **9**:1694–1708.

Hardie, R. C., and Minke, B. (1995). Phosphoinositide-mediated phototransduiction in Dorosophila photoreceptorsd: The role of Ca2+ and trp. *Cell Calcium* **18**:256–274.

Hofstee, C. A., Henderson, S., Hardie, R. C., and Stavenga, D. G. (1996). Differential effects of *ninaC* proteins (p132 and p174)

on light-activated currents and pupil mechanisms in *Drosophila* photoreceptors. *Visual Neurosci.* **13**:897–906.

Kernan, M., Cowan, D., and Zuker, C. (1994). Genetic dissection of mechanosensory transduction mechanoreception- defective mutations of *Drosophila. Neuron* **12**:1195–1206.

Kim, S., McKay, R. R., Miller, K., and Shortridge, R. D. (1995). Multiple subtypes of phospholipase C are encoded by the *norpA* gene of. *J. Biol. Chem.* **270**:14376–14382.

Lilly, M., and Carlson, J. R. (1990). *Smellblind:* A gene required for *Drosophila* olfaction. *Genetics* **124**:293–302.

Meinertzhagen, I. A., and Hanson, T. E. (1993). The development of the optic lobe. In Bate, M., and Arias, A. M., (eds.), The Development of *Drosophila melanogaster,* Cold Spring Harbor Laboratory Press, Cold Spring Harbor, pp. 1363–1482.

Miklos, G. L. G., and Rubin, G. M. (1996). The role of the genome project in determining gene function: Insights from model organisms. *Cell* **86**:521–529.

Monte, P., Woodard, C., Ayer, R., Lilly, M., Sun, H., and Carlson, J. R. (1989). Characterization of the larval olfactory response in *Drosophila* and its genetic basis. *Behav. Genet.* **19**: 267– 283.

Montell, C., and Rubin, G. M. (1988). The *Drosophila ninaC* locus encodes two photoreceptor cell specific proteins with domains homologous to protein kinases and the myosin heavy chain head. *Cell* **52**:757–772.

Moses, K., Ellis, M. C., and Rubin, G. M. (1989). The *glass* gene encodes a zinc-finger protein required by *Drosophila* photoreceptor cells. *Nature* **340**:531–536.

Osborne, K. A., Robichon, A., Burgess, E., Butland, S., Shaw, R. A., Coulthard, A., Pereira, H. S., Greenspan, R. J., and Sokolowski, M. B. (1997). Natural behavior polymorphism due to a cGMP protein kinase of *Drosophila. Science* **277**:834–836.

O'Tousa, J. E., Leonard, D. S., and Pak, W. L. (1989). Morphological defects in Orajk84 photoreceptors caused by mutation in R1-6 opsin gene of *Drosophila. J. Neurogenet.* **6**:41–52.

Pak, W. L., Grossfield, J., and Arnold, K. S. (1970). Mutants of the visual pathway of *Drosophila melanogaster. Nature* **227**:518–520.

Park, Y., Caldwell, M. C., and Datta, S. (1997). Mutation of the central nervous system neuroblast proliferation repressor ana leads to defects in larval olfactory behavior. *J. Neurobiol.* **33**:199–211.

Pearn, M. T., Randall, L. L., Shortridge, R. D., Burg, M. G., and Pak, W. L. (1996). Molecular, biochemical, and electrophysiological characterization of. *J. Biol. Chem.* **271**:4937–4945.

Pollock, J. A., and Benzer, S. (1988). Transcript localization of four opsin genes in the three visual organs of *Drosophila;* RH2 is ocellus specific. *Nature* **333**:779–782.

Porter, J. A., Hicks, J. L., Williams, D. S., and Montell, C. (1992). Differential localizations of and requirements for the two *Drosophila ninaC* kinase/myosins in photoreceptor cells. *J. Cell. Biol.* **116**:683–693.

Porter, J. A., and Montell, C. (1993). Distinct roles of the *Drosophila ninaC* kinase and myosin domains revealed by systematic mutagenesis. *J. Cell. Biol.* **122**:601–612.

Ranganathan, R., Malicki, D. M., and Zuker, C. S. (1995). Signal transduction in *Drosophila* photoreceptors. *Annu. Rev. Neurosci.* **18**:283–317.

Sawin-McCormack, E., Sokolowski, M. B., and Campos, A. R. (1995). Characterization and genetic analysis of *Drosophila melanogaster* photobehavior during larval development. *J. Neurogenetics* **10**:119–135.

Schmucker, D., Jackle, H., and Gaul, U. (1997). Genetic analysis of the larval optic nerve projection in *Drosophila. Development* **124**:937–948.

Sehgal, A., Price, J., and Young, W. (1992). Ontogeny of a biological clock in *Drosophila melanogaster. PNAS* **89**:1423–1427.

Serikaku, M. A., and O'Tousa, J. E. (1994). Sine oculis is a homeobox gene required for *Drosophila* visual system development. *Genetics* **138**:1137–1150.

Steller, H., Fischbach, K. F., and Rubin, G. (1987). *Disconnected:* A locus required for neuronal pathway function in the visual system of *Drosophila. Cell* **50**:1139–1153.

Tully, T., Cambiazo, V., and Kruse, L. (1994). Memory through metamorphosis in normal and mutant *Drosophila.* J. Neurosci. **14**:68–74.

Zipursky, S. L., Venkatesh, T. R., Teplow, D. B., and Benzer, S. (1984). Neuronal development in the *Drosophila* retina: monoclonal antibodies as molecular probes. *Cell* **36**:15–26.

Zuker, C. S., Cowman, A. F., and Rubin, G. M. (1985). Isolation and structure of a rhodopsin gene from D. *melanogaster. Cell* **40**:851–858.

**C: Manuscript -** The *tamas* gene, identified as a mutation that disrupts larval behaviour in *Drosophila melanogaster*, codes for the mitochondrial DNA polymerase catalytic subunit (DNApol-γ125)

# The *tamas* Gene, Identified as a Mutation That Disrupts Larval Behavior in *Drosophila melanogaster*, Codes for the Mitochondrial DNA Polymerase Catalytic Subunit (*DNApol-γ125*)

**Balaji Iyengar,* John Roote† and Ana Regina Campos***

**Department of Biology, McMaster University, Hamilton, Ontario L8S 4K1, Canada and*
†*Department of Genetics, University of Cambridge, Cambridge CB2 3EH, United Kingdom*

Manuscript received December 23, 1998
Accepted for publication August 31, 1999

ABSTRACT

From a screen of pupal lethal lines of *Drosophila melanogaster* we identified a mutant strain that displayed a reproducible reduction in the larval response to light. Moreover, this mutant strain showed defects in the development of the adult visual system and failure to undergo behavioral changes characteristic of the wandering stage. The foraging third instar larvae remained in the food substrate for a prolonged period and died at or just before pupariation. Using a new assay for individual larval photobehavior we determined that the lack of response to light in these mutants was due to a primary deficit in locomotion. The mutation responsible for these phenotypes was mapped to the lethal complementation group *l(2)34Dc*, which we renamed *tamas* (translated from Sanskrit as "dark inertia"). Sequencing of mutant alleles demonstrated that *tamas* codes for the mitochondrial DNA polymerase catalytic subunit (*DNApol-γ125*).

INVERTEBRATE behavioral paradigms have been extensively and successfully used in the fruit fly *Drosophila melanogaster* (HEISENBERG 1997) and the nematode *Caenorhabditis elegans* (CHALFIE and SULSTON 1981) in the search for genes involved in behavior. Vertebrate model systems have also benefited from a genetic approach to the study of behavior. Recently, a novel gene required for the generation of circadian rhythms was isolated in the mouse in a screen for semidominant mutations that disrupt circadian modulated locomotion (VITATERNA *et al.* 1994).

In Drosophila a genetic approach was fundamental to the identification of components of the phototransduction pathway underlying adult photobehavior (HEISENBERG and BUCHNER 1977; HEISENBERG and WOLF 1984; KOENIG and MERRIAM 1977; PAK 1979; ZUKER *et al.* 1985). In this case mutations were useful not only for the identification of gene products but also as instruments in the identification of specific cell types required for the performance of particular light-induced behaviors. For example, Drosophila mutant strains lacking different subsets of adult photoreceptors were used to address the role of these photoreceptor cell types in the performance of different types of photobehaviors. Photoreceptor cells R1 through R6, the outer photoreceptor cells, mediate optomotor responses while photoreceptor R7 is involved in fast phototaxis and some types of slow phototaxis (reviewed by HEISENBERG and WOLF 1984).

*Corresponding author*: A. R. Campos, Department of Biology, McMaster University, 1280 Main St. West, Hamilton, Ontario L85 4K1, Canada. E-mail: camposa@mcmail.cis.mcmaster.ca

Traditionally, Drosophila genetic screens using behavioral paradigms have been conducted using adult flies. A few recent examples include the isolation of mutations that disrupt associative learning (BOYNTON and TULLY 1992), circadian rhythms (SEHGAL *et al.* 1992), and hygro- and/or thermosensation (SAYEED and BENZER 1996). Genetic screens using the third instar larva proved that this developmental stage is also a good model for the identification of novel behavioral genes (KERNAN *et al.* 1994).

The Drosophila larvae are repelled by light during the foraging stage, which spans the beginning of the first instar until the onset of wandering behavior during the third instar stage. Once larvae leave the food substrate in search of an adequate site for metamorphosis, repulsion to light steadily decreases until soon before pupariation when the larva behaves indifferently toward a light stimulus (SAWIN-MCCORMACK *et al.* 1995).

Although the larval photoreceptor cell cluster has an organization somewhat similar to the adult compound eye ommatidium (GREEN *et al.* 1993), little is known about the functional organization of these cells. It has been reported that the larval photoreceptor cell clusters express the same rhodopsin genes as found in the adult compound eye (POLLOCK and BENZER 1988); however, it is not known whether the different rhodopsins are expressed in nonoverlapping sets of larval photoreceptor cells. Likewise little is known about how the two photoreceptor cell clusters modulate larval locomotion in response to light. The existence of two clusters suggests that modulation of locomotion may be triggered by the unequal stimulation of the two photosensitive organs (tropotaxis; FRAENKEL and GUNN 1961). Alterna-

tively, the regular swinging motions of the anterior of the larva from left to right before the onset of locomotion may suggest a mechanism by which orientation relative to the light source is possible by comparing the light intensity at different points in time (klinotaxis; FRAENKEL and GUNN 1961).

Here we report an investigation into larval photobehavior in Drosophila. A genetic screen was designed to identify mutations that disrupt the response of foraging third instar larva to light, from a collection of 64 second chromosome EMS-induced pupal lethals. The screen was based on a previously described population assay that we improved by supplementing the food substrate with vitamin A (LILLY and CARLSON 1990; SAWIN *et al.* 1994). We identified one mutant strain (*P183*), which showed reduction in the response to light of the foraging third instar larva in the population assay and no response in a single larva assay developed in our laboratory (HASSAN *et al.* 1999). Deficiency and meiotic recombination mapping demonstrated that this mutation is allelic to mutations in a previously identified lethal complementation group, *l(2)34Dc* (WOODRUFF and ASHBURNER 1979). The *P183* strain displays disruption in the pattern of compound eye development and failure to undergo the behavioral changes characteristic of the wandering third instar larva. Further characterization of the behavioral phenotype demonstrated that the failure to respond to light was likely due to a locomotory deficit. Analysis of the sequence made available by the Berkeley *Drosophila* Genome Project (BDGP) together with the genetic mapping of the region strongly suggested that this gene [*l(2)34Dc*] encodes for the catalytic subunit of the mitochondrial DNA (mtDNA) polymerase. Sequencing of this gene from four available mutant alleles revealed changes consistent with the notion that this gene encodes for the catalytic subunit of the mitochondrial DNA polymerase. The gene represented by the *l(2)34Dc* complementation group was renamed *tamas* (*tam*), which in Sanskrit means "dark inertia."

## MATERIALS AND METHODS

**Stocks:** The lethal mutations and chromosome aberrations used in this study are described in FlyBase (FLYBASE CONSORTIUM 1999) and listed in Table 1. We used an isogenized derivative of Oregon-R as a wild-type stock (kindly provided by Art Hilliker).

**Fly culture:** The flies were cultured in a medium that contained inactivated yeast, sucrose, 10% tegosept in ethanol, and acid mix (propionic acid and phosphoric acid) and was supplemented with β-carotene (1.25 g/liter). Crosses were set up with 5–10 pairs of flies in 100 × 25-mm glass vials and were scored for 9 days after the emergence of the first progeny. Prior to the behavioral screen, larvae were grown on media plates streaked with a thin layer of live yeast paste.

**Larval collection for behavioral assays:** The egg collection involved 2–3 precollections of 2 hr each on a fresh plate. The last 1-hr collection was retained and incubated for 80–85 hr at 25° before testing in the plate assay at between 80 and 90 hr after egg laying (AEL). For the pupal lethal screen we incubated the embryos for the first 36 hr at 30° so that the heterozygous flies carrying the *CyO, l(2)DTS513*$^{1}$ (*CyO, DTS*) chromosome would die. The plates with larvae were placed at 25° until 80–85 hr AEL. The balancer chromosomes in all stocks used for photobehavior experiments were exchanged for *CyO, Dp(1;2)y*$^{+}$ (*CyO-y*$^{+}$) and the X chromosome was substituted for one carrying the mutations $y^{1}$ and $w^{1}$, to facilitate selection of larvae based on the *y* (*yellow*) phenotype of the larval mouth hooks. For the individual larval assays, eggs were collected for 1 hr and incubated at 25°. At 20–22 hr AEL all newly hatched first instar larvae were cleared and after another 1-hr incubation period ~70 newly hatched first instar larvae were collected and transferred to a fresh food plate coated with yeast paste. Larvae were grown in a 12-hr L:D cycle. Third instar larvae were tested for photobehavior at 84 hr AEL, a minimum of 3 hr into the dark cycle.

**The plate assay:** The plate assay used in this study was similar to the one used by LILLY and CARLSON (1990). Approximately 100 larvae were picked with a size 1 brush under safelight (20-W lamp with Kodak GBX-2 filter) and washed well with distilled water two or three times. The water was completely drained, and the larvae were collected and placed in the middle of the test plate (Fisher Scientific, Pittsburgh; 100 × 15 mm) layered with 15 ml of 1% agar. This plate rested on a light box with a template of dark and light quadrants between the light box and the plate. The larvae were allowed to distribute themselves with respect to their preference for light or dark quadrants. After 5 min the larvae in each quadrant were counted and a response index [RI = (dark − light)/(dark + light)] was calculated. Since the *DTS* lethality is leaky the final response index of the lines was recalculated after subtracting the number of escapers (surviving adults) from each quadrant in all tests (Figure 1).

**Optimization of the population plate assay:** The following experiments were carried out to improve larval response in the plate assay originally described by LILLY and CARLSON (1990). Vitamin A deprivation in adult Drosophila has been shown to result in loss of mature opsin photopigments (HARRIS and STARK 1977). The lack of opsin reduces visual sensitivity probably due to a lack of functional opsin apoprotein or loss of opsin transcription itself (HARRIS and STARK 1977; STARK and WHITE 1996). Supplementing our medium with vitamin A (β-carotene at 1.25 g/liter; ASHBURNER 1989) significantly increased the response index of wild-type strains. These results were confirmed by using vitamin A supplementation of Sang's minimal medium (kindly provided by William Stark; data not shown).

The relationship between light intensity and the response index was investigated using a series of neutral density filters placed between the plate and the light source (HASSAN *et al.* 1999). We concluded that the Drosophila larva responds to different light intensities and that the light intensity used in our assays elicits maximum response.

**Checker assay:** This assay used a petri dish (100 × 15 mm; Fisher Scientific) containing 15 ml of 1% agarose. This dish is positioned over a checkered template of alternating 1-cm black squares. Dark squares blocked all light while the clear squares allowed transmission of light. The template and dish were positioned on a light box that had been modified to emit light only in a 11-cm-diameter area in the center of the box. During the test the template and dish were lit from below.

Individual larvae were removed from the culture dish with a moist paintbrush, rinsed with distilled water to remove any residual food particles, and placed in a pretest plate for a period of 1 min to allow them to acclimatize to the agar surface. They were then transferred to the center of the test dish. Larval movement was visualized using a Fujinon TV/

**TABLE 1**

**Fly stocks used in this study**

| Strains | Breakpoint/cytology | Genetic limits | Reference |
|---|---|---|---|
| | | 34D region | |
| *Df(2L)64j, $Adh^{n1}L^2$* | 34D-1-D2; 35B9-C1 | *l(2)34Db-l(2)35cF* | Ashburner *et al.* (1982) |
| *Df(2L)b87e25* | 34C1; 35C1 | *kuz-vas* | Alexandrov and Alexandrova (1991) |
| *Df(2L)b80c1,b80c1 $noc^{Sco}$* | 34D3;34E2 | *l(2)34Db-Ance* | Ashburner *et al.* (1982) |
| *In(2LR)b81a2* | 34D5;34D8;41D | *Sos+/−-tam* | Alexandrov and Alexandrova (1986) |
| *In(2L)b81l7* | 34D1-2;40F | *l(2)34Db-b* | Alexandrov and Alexandrova (1986) |
| *Df(2L)b81a2$^{l}$A80$^{R}$, cn bw* | 34D5;35A3.4;41D | *Sos+/−-pu* | This study |
| *Df(2L)b84a9, pr pk cn sp* | Not visible | *Sos-l(2)34Dg* | This study |
| *In(2L)b82c44* | 34D4-5;40h | *Sos-b* | Alexandrov and Alexandrova (1986) |
| *Df(2L)b85b2* | Not visible | *b-tam* | Alexandrov and Alexandrova (1986) |
| *Df(2L)b88b42* | Not visible | *b-tam* | Alexandrov and Alexandrova (1991) |
| *In(2L)b83b22* | 34D4-5;35C1-2 | *b-tam* | Alexandrov and Alexandrova (1986) |
| *In(2L)b79h1A* | 34D4;34D8;40E | *l(2)34Db-tam +/−* | Alexandrov and Alexandrova (1991) |
| *b $tam^2$ $Adh^{n4}$* | | | Woodruff and Ashburner (1979) |
| *b $tam^3$ $Adh^{n4}$* | | | Woodruff and Ashburner (1979) |
| *b $tam^4$ $Adh^{n2}$ pr cn* | | | Woodruff and Ashburner (1979) |
| *$tam^9$* | | | This study |
| *$kuz^3$* | | | Unpublished data |
| *l(2)34Db$^3$ b$^1$ $Adh^{n2}$ pr$^1$ cn$^1$* | | | Woodruff and Ashburner (1979) |
| *l(2)Sop2$^1$ $Adh^D$ pr$^1$ cn$^1$* | | | Gubb *et al.* (1984) |
| *In(2LR)Gla, Gla l(2)34De$^2$* | | | Woodruff and Ashburner (1979) |
| *b l(2)34Df$^2$ el $rd^s$ pr cn* | | | Alexandrov and Alexandrova (1996) |
| *b l(2)34Dg$^1$ $Adh^{n4}$* | | | Ashburner *et al.* (1982) |
| *b $Sos^{34Ea\text{-}6}$ $Adh^{n4}$* | | | Woodruff and Ashburner (1979) |
| | | 35B region | |
| *Df(2L)TE35BC-24, b pr pk cn sp* | 35b4-6;35E1-2 | | Gubb *et al.* (1984) |
| *In(2LR)Gla, Gla l(2)34De$^2$ l(2)35Bb$^6$* | | | Woodruff and Ashburner (1979) |
| *b $Adh^D$ l(2)35Bc$^2$ pr cn* | | | Woodruff and Ashburner (1979) |
| *b l(2)35Be$^1$ pr* | | | Woodruff and Ashburner (1979) |
| *b $Adh^{n4}$ l(2)35Bf$^5$* | | | Woodruff and Ashburner (1979) |
| *$Adh^D$ l(2)35Bg$^2$ pr cn* | | | O'Donnell *et al.* (1977) |
| *$Adh^{UF}$ Su(H)$^8$ cn* | | | Woodruff and Ashburner (1979) |
| | | Miscellaneous chromosomes | |
| *b pr c px sp* | | | |
| *Cyo, l(2)DTS513$^1$* | | | |
| *Cyo, Dp(1;2)y$^+$* | | | Mardahl *et al.* (1993) |
| *b $Adh^{n2}$ pr cn* | | | Grell *et al.* (1968) |
| *b $Adh^{n4}$ pr cn* | | | Grell *et al.* (1968) |

zoom lens (Fuji Optical Co.) attached to a CCD camera (Elmo Mfg. Co., TSE272S) and recorded on videotape (Fuji HQ-120, RCA VCR) until they reached the assay boundary or until 180 sec had elapsed. Larvae that failed to move out of the first square in 90 sec were not included in calculating the response index, as these animals may have been injured during preparation. Measurements of residence time were taken using the VCR timer and started 5 sec after the larva was placed in the center dark check. Response index [(time in dark square − time in clear square)/total time of test] was calculated on a per larva basis. The same assay was performed without the light stimulus (20-W lamp with Kodak GBX-2 filter) and a response index was calculated. Therefore two response indices were calculated per genotype. A response to light is represented by a significant effect of light on the response index (Hassan *et al.* 1999).

**Locomotory assay:** Locomotory assays were conducted under safelight (20-W lamp with Kodak GBX-2 filter). Larvae were rinsed and acclimated to the agar surface in a plate as described earlier and placed in the center of the test plate. After 5 sec recovery time, larval movement was videotaped for 30 sec. Tracings of larval path were obtained and scanned using a flatbed scanner (Apple Color OneScanner 600/27). Path length was measured using NIH-image software version 1.61b.

**Lethality mapping and complementation analysis:** One pupal lethal, *P183*, was identified from the screen. The lethality of this line was mapped by meiotic recombination using the multiply marked chromosome *black* (*b*), *purple* (*pr*), *curved* (*c*), *plexus* (*px*), *speck* (*sp*). Females of the genotype *P183/b pr c px sp* were crossed to $y^1$ $w^1$; *S/CyO-y*$^+$ and putative recombinant chromosomes were recovered over *CyO-y*$^+$. Out of 367 lines tested 103 retained the *P183* lethality and only 1 of these carried *b*, suggesting that the *P183* lethality mapped close to

*b*. This recombinant was later determined to have been the result of a crossover between *b* and the lethal mutation located in 35B. Deficiency mapping was conducted using a set of deficiencies spanning the *black* region (see Figure 4 and Table 1 for a map of the region and the breakpoints of the deficiency stocks used). All deficiency chromosomes were kept over a *Cy* balancer. We tested for complementation by crossing the *P183/CyO-y*$^+$ flies to deficiency stocks. The presence of straight wing flies among the progeny of the cross was indicative of complementation of the *P183* chromosome by the deficiency. A minimum of 100 flies were counted for each cross. We determined that two nonoverlapping deficiencies spanning the 34D and 35B regions did not complement *P183* suggesting that *P183* carried two lethal mutations. These were mapped more precisely by crossing to other deletions and to alleles of known lethal complementation groups in these regions.

**Wandering test:** Bromophenol blue (J. T. Baker Inc., Phillipsburg, NJ; D293-01) was dissolved in the regular fly medium to the final concentration of 0.05%. The final egg collection was conducted in the bromophenol blue supplemented medium and the larvae were allowed to grow in the bromophenol supplemented medium. The larvae were removed at specified time points and photographed under a stereomicroscope (Zeiss, Thornwood, NY).

**Immunohistochemistry of the larval central nervous system:** Larval brains with the eye-antenna imaginal discs were dissected from third instar larvae in phosphate-buffered saline (PBS) and fixed in 4% paraformaldehyde (pH 7.4) for 45 min at room temperature. This was followed by three or four PBS washes. Brains were incubated for 1 hr in a blocking solution that contained PBS with 0.3% Triton X-100 and 5% goat serum at room temperature, followed by addition of a fresh 100 μl of blocking solution containing 2 μl of 24B10 primary antibody. After 8–12 hr of incubation at 4° the samples were washed with PBT for 4 hr, with changes every 10–20 min, incubated in a blocking solution as described above, and finally incubated with a secondary antibody conjugated to horseradish peroxidase (HRP) for another 8–12 hr. Once again the specimens were washed thoroughly for 4 hr and stained with 0.5 ml of 3, 3′-diaminobenzidine (0.5 mg/ml; Sigma, St. Louis, 72H3614) in the presence of hydrogen peroxide. The reaction was stopped by washing several times with PBS. The samples were mounted in 70% glycerol in PBS and observed with a Zeiss axiophot microscope.

**Mitochondrial staining:** Staining to visualize mitochondrial mass was done using Mitotracker Red CMXRos (kindly provided by Molecular Probes Inc., Eugene, OR, M-7512) at 100 nM concentration made in PBS. The brains were dissected in PBS, incubated in the staining solution for 10 min at room temperature and mounted for observation using fluorescein filters.

**Environmental scanning electron microscopy of adult compound eyes:** We used environmental scanning electron microscope (ESEM) model 2020 manufactured by ElectroScan Corporation (now Philips ElectroScan). This technology does not require metal coating of the specimen that is to be visualized. Adult flies were etherized and placed on the ESEM mount. Flies were immobilized using water-based colloidal carbon glue for proper orientation. The electroscan was performed at 20.0 kV and 3.9 Torr.

**DNA sequencing:** Genomic DNA was extracted from 80–100 larvae of the appropriate genotype by selecting for the *yellow* mouth hook marker. The larvae were washed with distilled water and frozen in liquid nitrogen prior to grinding using a mortar and pestle. The powdered larvae were resuspended (10 μl/larvae) in homogenization buffer (0.1 M Tris HCl, pH 9.0; 0.1 M EDTA; 1% SDS) for 30 min at 70°. Fourteen microliters of 8 M KCl per 100 ml of homogenate was added and the homogenate was placed on ice for 30 min and then centrifuged at 15,000 rpm, at 4° for 15 min. The supernatant was precipitated with 0.5 volumes of isopropanol. The precipitate was centrifuged at room temperature for 5 min, washed with 500 μl of cold 70% absolute alcohol and again centrifuged at room temperature for 5 min at 15,000 rpm. The pellet was dried for 10 min at 37° and resuspended in 80–100 μl of sterile water for 8–10 hr at 37°. Templates for DNA sequencing were generated through PCR amplification using the following oligonucleotides: (A) 5′-CCCCACCAACTTCCATAATG-3′; 3′-GTTACTACTTCCCCTGGTCCA-5′; (B) 5′-GGTTGGA CTTCAGTTGCCTTA-3′; 3′-CGTGTGGTGCAACAAAGTACT-5′; (C) 5′-GAGGAGTTACTACTTCCCCTG-3′; 3′-CTGTGG AGCTTAAGGATTCTG-5′; (D) 5′-TGTGGGTTCATCATTTT CATG-3′; 3′-ATCCCTAACAGCTACAGC-5′; (E) 5′-GGGCG TAAGTAGTCACAAACC-3′; 3′-AAGGAGACTTGGAGGCTG TTA-5′; (F) 5′-TAGAGGATGACGAAGAGCCGT-3′; 3′-GATG GAACCCACATGGATGAC-5′; (G) 5′-CAGCGATATGCAACT CCATAAC-3′; 3′-GTGGACTTCCTTCATCTGATG-5′.

The fragments generated by PCR amplification [using Platinum Taq DNA polymerase (GIBCO BRL, Gaithersburg, MD) in a GeneAmp 2400 machine (Perkin-Elmer, Norwalk, CT)] covered the whole gene including introns, beginning 354 bp upstream of the open reading frame start site and terminating 75 bp after the stop codon. The DNA fragments generated in the PCR reactions were purified using the QIAquick gel extraction kit (cat. no. 28704). Automated sequencing was done using the cycle sequencing protocol with Taq-FS enzyme and BigDye terminator chemistry in a Perkin-Elmer-ABI 373A Stretch machine. Each fragment was sequenced from at least two different PCR reactions from both directions. The progenitor strains of three of the *tam* alleles were used as controls for sequence alignments: *b Adh*$^{n4}$ for *tam*$^2$ and *tam*$^3$ and *b Adh*$^{n2}$ *pr cn* for *tam*$^4$ (see Table 1). The *tam*$^9$ mutation was confirmed by amplification of DNA using primer set B and primer set F, which provide overlapping sequence data ($n$ = 6). The mutation in *tam*$^2$ was identified by overlapping sequence data obtained using the primer set D ($n$ = 4). The mutation in *tam*$^3$ was identified using primer set E which also provides overlapping PCR product ($n$ = 4). The lesion in *tam*$^4$ was identified using the primers in set E ($n$ = 6). The sequence alignments were conducted using Clustal_X (Thompson *et al.* 1997) on a Power Macintosh computer.

## RESULTS

**Screen of a set of pupal or late larval lethal strains for disruption in photobehavior using the population plate assay:** The 64 EMS-induced second chromosome recessive lethal lines were tested in the plate assay using the dominant temperature-sensitive balancer *CyO, DTS*. The scheme is presented in Figure 1. In the first screen all lines were tested and those that showed a response index above 0.6 (20% larvae in the light and 80% in the dark) were discarded. The 11 lines that showed a response index below 0.6 were screened again and 2 lines retained that showed a response index of less than 0.5 (Figure 2). These lines (*P183* and *E22*) were then tested in a different genetic background using a *CyO-y*$^+$ balancer. The *E22* line was found to be a second instar lethal in this genetic background and was discarded. The *P183* line continued to show a response index below 0.5 (data not shown) and was further studied.

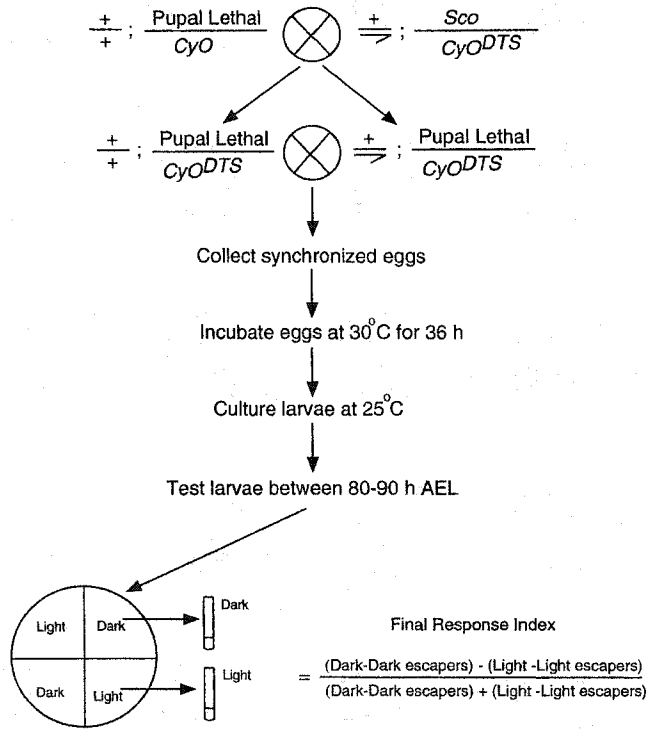


FIGURE 1.—The mutant screen.

**Genetic analysis of *P183*: a double hit in the *l(2)34Dc* and *Suppressor of Hairless* genes:** Meiotic recombination mapping of the *P183* lethality was conducted using the *b pr c sp px* chromosome (see MATERIALS AND METHODS for description). The results suggested that the lethality mapped very close to *b*. This region has been well characterized genetically and several lethal complementation groups have been identified (WOODRUFF and ASHBURNER 1979). We used a set of deficiencies that spanned the 34D-35C interval to map the *P183* lethality. A large deficiency in the region *Df(2L)64j* [Df(2L) 34D1-2;35B9-35C1] and two nonoverlapping deficiencies *Df(2L)b80c1* [Df(2L) 34D3;34D8-34E1] and *Df(2L)TE35BC-24* [Df(2L) 35B4-6;35E1-35E2] did not complement the *P183* lethality (Figure 3 and Table 2A). This suggested that *P183* carried at least two lethal hits in this region, one in the region 35B4;35C1 and the other located more distally at 34D. We crossed lethal alleles of the known complementation groups in these regions to *P183* (Figure 3; Table 2, B and C; WOODRUFF and ASHBURNER 1979). The lethality in the 35B region was found to be allelic to *Su(H)* mutations whose cytological map position is 35B9-10 (Figure 3; Table 2C; data not shown). The noncomplementing deficiency *Df(2L)b80c1* removes eight lethal complementation groups, *l(2)34Db-Ance* (ASHBURNER *et al.* 1982). All three available alleles of *l(2)34Dc* lethal complementation group did not complement the lethality of the *P183* strain, whereas alleles of the other lethals removed by *Df(2L)b80c1* complemented *P183* (Table 2B; data not shown).

Thus we concluded that the *P183* lethality was due to mutations in two genes, one in the 34D region [*l(2)34Dc*] and the other in the 35B region [*Su(H)*]. *Su(H)* alleles cause lethality during early pupal stages (SCHWEISGUTH and POSAKONY 1992). The gene represented by the lethal complementation group *l(2)34Dc* was renamed *tamas* (*tam*). Eight preexisting alleles of *l(2)34Dc* [$l(2)34Dc^{1\text{-}8}$] are listed by FlyBase (FLYBASE CONSORTIUM 1999) and so we named the new allele $tam^{9}$ (Table 3). Additionally, a chromosomal inversion [*In (2L)b79h1A*; Figure 4] behaves as a hypomorphic allele of *tam* when heterozygous with other mutant alleles and was henceforth named $tam^{10}$ (Table 3). We separated $tam^{9}$ mutant allele from the $Su(H)^{P183}$ allele by recombination with a wild-type chromosome and checked for lethality against all three available *tam* alleles and chromosomal aberrations that uncover the *tam* gene (Table 4).

The $tam^{9}$ mutation causes lethality at the late third instar larval stage when heterozygous with a 34D deletion [*e.g., Df(2L)b80c1*]. Two other alleles ($tam^{2}$ and $tam^{4}$) are early larval lethals when homozygous and one ($tam^{3}$) is a late embryonic lethal. $tam^{2}$, $tam^{3}$, and $tam^{4}$ lethalities are probably due to second-site mutations on these chromosomes because larvae carrying either one of these alleles and a deficiency also die at the late third instar stage (data not shown).

**The genetics of the 34D region:** The genetics of the 34D-35F region have been studied extensively by M. Ashburner and colleagues (*e.g.*, WOODRUFF and ASHBURNER 1979; ASHBURNER *et al.* 1982; Figure 3; Table 1). They have shown from deletion mapping that the lethal complementation groups in the immediate vicinity of *b* are *l(2)34Db, Son of sevenless* (*Sos*), *tam*, and *Sop2*: 75 out of 103 *b* deletions also remove these four loci (M. ASHBURNER and J. ROOTE, unpublished observations). That *l(2)34Db* is the most distal of these is shown by 4 proximally extending *b* deletions that remove *Sos*, *tam*, and *Sop2* but not *l(2)34Db* [*e.g., Df(2L)b84a9*]. Both *Sos* and *tam* are adjacent to *b* by the criterion that many aberrations are either $Sos^{-}$, $b^{-}$, $l(2)34Dc^{+}$ or $Sos^{+}$, $b^{-}$, $l(2)34Dc^{-}$ [*e.g., In(2L)b82c44* and *In(2L)b83b22*, respectively]. That *Sos* is distal and *tam* is proximal to *b* is confirmed by the aberration *In(2L)b81l7*, which is deleted for *l(2)34Db*, *Sos*, and *b*, but not *tam* or *Sop2*; therefore the genetic order is *l(2)34Db, Sos, b, tam, Sop2*.

**The *tam* gene product is required for the onset of wandering behavior in the third instar larva:** Drosophila larvae spend most of their time inside the food substrate (the foraging larval stage). During the third instar stage, in response to increased levels of ecdysone, they leave the food in search of an adequate site to pupariate and undergo metamorphosis (reviewed by TRUMAN *et al.* 1994). This behavioral pattern is called wandering behavior and one characteristic aspect of the wandering phase is emptying of the gut as seen by the disappearance of blue-colored food (MARONI and STAMEY 1983).

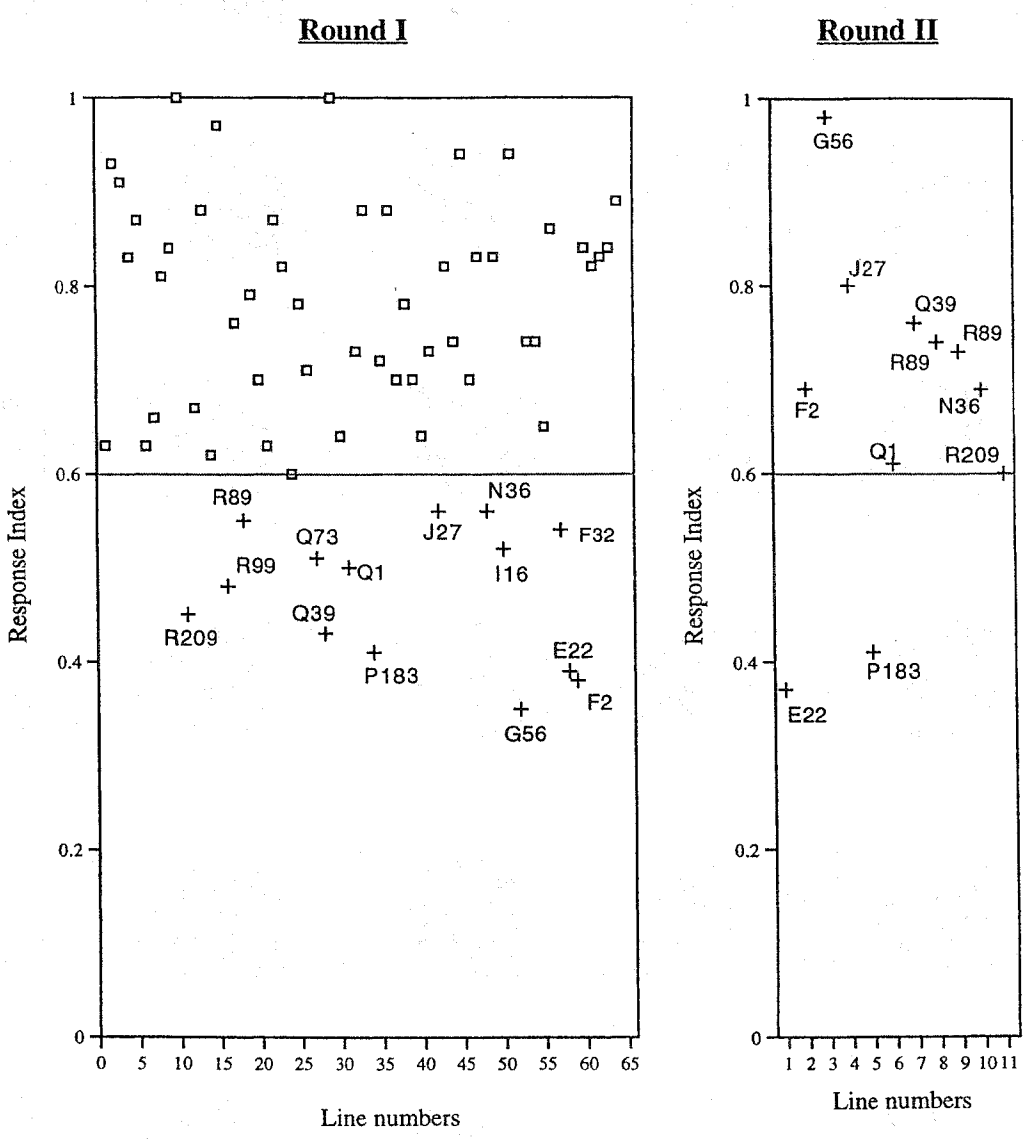


FIGURE 2.—Behavioral screen results. This is a scatterplot of the final response indices after the first round and the second round of screening. In the first round the lines that showed response index above 0.6 were discarded. Strains with response indices indicated by (+) were screened again. The second round resulted in two lines (*E22* and *P183*) considered to be putative behavior mutants.

Larvae homozygous for *P183* (double mutant) failed to wander out of the food substrate at the appropriate time. Consequently these larvae displayed a prolonged foraging phase that could last up to 20 days, after which they died. Prolonged foraging was visualized as larvae that retained bromophenol blue after the wild-type larvae had cleared their guts (Figure 4, A–D). This failure-to-wander phenotype was observed in larvae heterozygous for other alleles of *tam* and a deficiency of the 34D region (Figure 5, E and F and data not shown). Larvae homozygous for the recombinant $b^-$, $Su(H)^{P183}$ wander at the appropriate time and die at pupation (data not shown). Thus we conclude that the failure-to-wander phenotype is a consequence of loss of *tam* gene function.

**Mutations in the *tam* gene disrupt visual system development:** The isolation of mutations that affect photobehavior may also have important consequences for the study of pattern formation in the nervous system as mutations that ostensibly affect behavior may do so by disrupting developmental processes. To investigate the role of the *tam* gene in the larval response to light we analyzed the morphology of the visual system in *tam* mutant larvae with the 24B10 monoclonal antibody that labels a photoreceptor-specific antigen present in both the larval and developing adult visual systems in the third instar larva (Figure 5, A and B; ZIPURSKY *et al.* 1984).

The visual system of the original double mutant strain *P183* was characterized by overall reduction in the size of the eye-antenna imaginal disc (Figure 5B). While labeling with the 24B10 monoclonal was found in the posterior portion of the disc, it was not seen in the usual clustering pattern representing the developing ommatidia. Rather, the expression of the epitope recognized by this monoclonal antibody seemed to be continuous throughout the developing retina. These observations may indicate that all cells in the disc were taking a photoreceptor fate. Subsequent analysis using the *P183* chromosome heterozygous with chromosomal deficiencies that remove either the 35B [*Su(H)*] or the

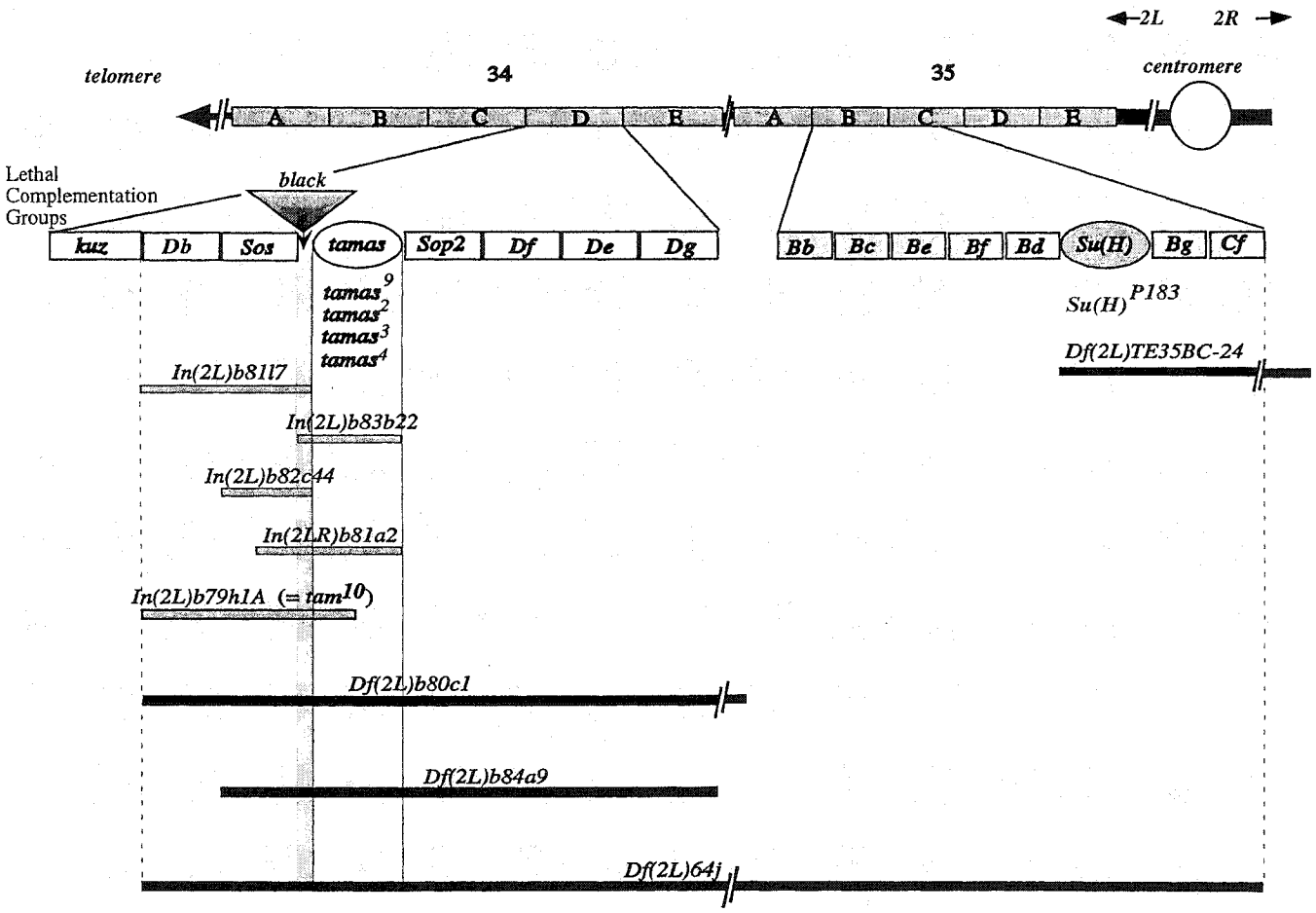


FIGURE 3.—Genetic analysis of *P183*. A diagram of the left arm of the second chromosome cytological regions, 34 and 35. The 34D and 35B regions are expanded to show the lethal complementation groups included in these subdivisions (WOODRUFF and ASHBURNER 1979). The rectangular boxes represent the lethal complementation groups, the oval-shaped boxes represent the lethal hits present in the *P183* line. The triangular insert in the 34D region is the nonvital gene *black*. Below the lethal complementation groups the chromosomal aberrations that were used in this study are shown. Solid bars depict the chromosomal segments that are deleted in the deficiency strains. In strains carrying chromosomal inversions the inverted segment is shown as a shaded bar.

34D (*tam*) regions and with mutant alleles of each gene demonstrated that this particular phenotype was due to disruption of the *Su(H)* gene (data not shown; SCHWEISGUTH and POSAKONY 1992).

Disruption of *tam* gene function led to less severe disruption in the pattern of the developing ommatidia by comparison with the original double mutant strain (Figure 5, C and D). The eye disc, while still reduced compared to a wild-type control, showed the usual pattern of clustering albeit somewhat disorganized. The projection of the photoreceptor axons into the optic lobes was also disrupted probably due to the abnormal differentiation of the retinal cells. Closer inspection of the eye disc under higher magnification suggested that older retinal cells were degenerating or losing the antigen recognized by the 24B10 monoclonal antibody (Figure 6F). The larval visual system was present; however, the projection defects observed in the developing adult visual system masked the terminus of the larval visual system, at that time in development. An interesting aspect of the phenotype of the visual system of *tam* mutant larvae was the delayed onset of retinal differentiation. 24B10 labeling could only be seen in *tam* mutant larvae several days after it was seen in wild-type larvae (Figure 5). The severity of these defects varies possibly due to the delayed onset of retinal differentiation.

The phenotype observed in the developing eye disc was reflected in the compound eye of adult escaper flies heterozygous for all lethal alleles of *tam* and a hypomorphic allele carried by *In(2L)b79h1A* (Table 3). These escapers have rough compound eyes that are significantly smaller than the control (Figure 6).

In *tam* mutant larvae there was an overall reduction in the volume of both the CNS and the imaginal discs reflected externally by the smaller than average larvae (Figure 4). The general morphology of the CNS as seen by labeling with the anti-ELAV monoclonal antibody was relatively normal (data not shown). The imaginal

**TABLE 2**

**Mapping lethality in the *P183* line**

| | | | | | | | | | | |
|---|---|---|---|---|---|---|---|---|---|---|
| A. | | *Df(2L)TE35BC-24* | | *Df(2L)b80c1* | | *Df(2L)64j* | | | | |
| | *P183* | −(0/180) | | −(0/129) | | −(0/182) | | | | |
| B. | | *kuz*$^{2}$ | *l(2)34Db*$^{2}$ | *Sos*$^{6}$ | *tam*$^{3}$ | *Sop2*$^{1}$ | *l(2)34De*$^{2}$ | *l(2)34Df*$^{2}$ | *l(2)34Dg*$^{1}$ |
| | *P183* | +(48/149) | +34/105) | +(38/120) | −(0/176) | +(47/132) | +(44/110) | +(32/123) | +(49/145) |
| C. | | *l(2)35Bb*$^{5}$ | *l(2)35Bc*$^{2}$ | *l(2)35Be*$^{1}$ | *l(2)35Bf*$^{5}$ | *l(2)35Bd*$^{4}$ | *Su(H)*$^{8}$ | *l(2)35Bg*$^{2}$ | |
| | *P183* | +(40/126) | +(65/209) | +(41/147) | +(38/117) | +(50/135) | −(0/262) | +(39/118) | |

Minus indicates lethality and plus indicates viability. Numerator indicates the number of viable adult flies that were heterozygous either for the chromosomal aberration or the alleles of lethal complementation groups, with the *P183* chromosome. The denominator indicates the number of flies with a marked balancer chromosome. (A) Indicates mapping lethality using deficiencies in the *black* region. (B and C) Results of complementation test using representative alleles of lethal complementation groups in the 34D region and 35B region, respectively.

discs, seen under Nomarski microscopy, were reduced by comparison to wild-type controls but the overall morphology was apparently normal (data not shown).

**The reduced response to light of *tam* mutant larvae is due to a locomotory deficit:** The disruption in the response to light was reevaluated using an individual larval assay (HASSAN *et al.* 1999). This assay measures the response to light in individual larvae as the relationship between residence time in light and dark squares with or without the light stimulus (see MATERIALS AND METHODS for details). Larvae homozygous for the original double mutant chromosome *P183* or for the recombinant strain carrying only the *tam*$^{9}$ mutation showed no response to light in the Checker assay (data not shown; Figure 7). Larvae heterozygous for *tam*$^{9}$ and other mutant alleles of the *tam* gene responded to light (*tam*$^{3}$, Figure 7; *tam*$^{2}$, data not shown) suggesting partial complementation of this phenotype.

Visual inspection of the larvae during the course of the Checker assay suggested that these organisms moved considerably less than the wild-type background strain. In fact, measurements of the distance traveled in 30 sec in the absence of a light stimulus confirmed these observations (Figure 8). *tam*$^{9}$*/Df(2L)b80c1* or *tam*$^{3}$*/Df(2L)b80c1* larvae could not be tested in the Checker assay because of a severe deficit in locomotion (Figures 7 and 8). This deficit in locomotion was not seen in *tam*$^{9}$/+, *tam*$^{3}$/+, or *Df(2L)b80c1*/+ larvae (Figure 8) and these mutant larvae responded to light in the Checker assay (Figure 7). Larvae carrying the heteroallelic combination *tam*$^{9}$*/tam*$^{3}$ moved significantly less than the control larvae *tam*$^{3}$/+ ($P = 0.005$) and appeared to show a similar trend when compared to *tam*$^{9}$/+ larvae ($P = 0.099$; Figure 8). The measure of locomotion of *tam*$^{3}$/+ and *tam*$^{9}$/+ showed no statistically significant difference (Figure 8). We concluded that lack of response to light seen in the *tam*$^{9}$ mutant larvae was due to a primary deficit in locomotion that is uncovered by *Df(2L)b80c1* and that this allele behaves as a hypomorph.

***tam* codes for the catalytic subunit of the mitochondrial DNA polymerase (*DNApol-γ125*):** The genetic location of *tam* suggested that this gene was included in the sequence recently released by the Berkeley *Drosophila* Genome Project (S. MISRA, personal communication). The superimposition of the genetic map onto the physical map showed that *tam* was located on the P1 DS00941 in a region tightly packed with open reading frames coding for known gene products (ASHBURNER *et al.* 1999; Figure 9). The region of interest was delimited distally by *Sos* (*BG:DS00941.4*), which codes for guanine nucleotide exchange factor (SIMON *et al.* 1991; BONFINI *et al.* 1992), and proximally by the profilin associated protein gene, *Sop2* (*BG:DS00941.7*), transformants of which have been shown to rescue the lethality of the *l(2)34Dd* complementation group (HUDSON and COOLEY 1998; Figure 9). Since the glutamate decarboxylase

**TABLE 3**

**Interallelic complementation among *tam* alleles**

| | $tam^9$ | $tam^2$ | $tam^3$ | $tam^4$ |
|---|---|---|---|---|
| $tam^2$ | −(0/154) | | | |
| $tam^3$ | −(0/396) | −(0/302) | | |
| $tam^4$ | −(0.171) | −(0/167) | −(0/295) | |
| $tam^{10}$ | −/+(121/412) | −/+(22/562) | −/+(69/427) | −/+(6/67) |

Minus indicates lethality and −/+ indicates reduced viability. Numerator indicates the number of viable adult flies that were heterozygous for *tam* alleles and the denominator indicates the number of flies with a marked balancer chromosome. New nomenclature of *tam* alleles: $tam^2$ corresponds to *l(2)34Dc*$^2$, $tam^3$ corresponds to *l(2)34Dc*$^3$, $tam^4$ corresponds to *l(2)34Dc*$^4$. *In(2L)b79h1A* is named $tam^{10}$, as it behaves like a hypomorphic *tam* allele, exhibiting low viability, reduced compound eyes, and missing head and thoracic bristles when heterozygous with other alleles of *tam*.

(*BG:DS00941.5*) and mitochondrial DNA polymerase (*BG:DS00941.6*) genes were the only open reading frames between *Sos* and *Sop2*, we hypothesized that *tam* was the more proximal of these, *DNApol-γ125*. To test this hypothesis we sequenced this gene from the genomic DNA of all available mutant alleles ($tam^2$, $tam^3$, $tam^4$, and $tam^9$).

In the $tam^9$ allele a single nucleotide change (A → C) was found in exon 1 that substitutes a glutamine for alanine (Figure 10). This change was not found in any of the wild-type strains sequenced thus far. A mutation in the polymerase domain X (Glu → Val) was found in $tam^2$ mutation. This glutamine residue has been reported to be essential for the *E. coli* DNA polymerase catalytic function (Polesky *et al.* 1990) and is conserved in Drosophila, Saccharomyces, and Xenopus (Lewis *et*

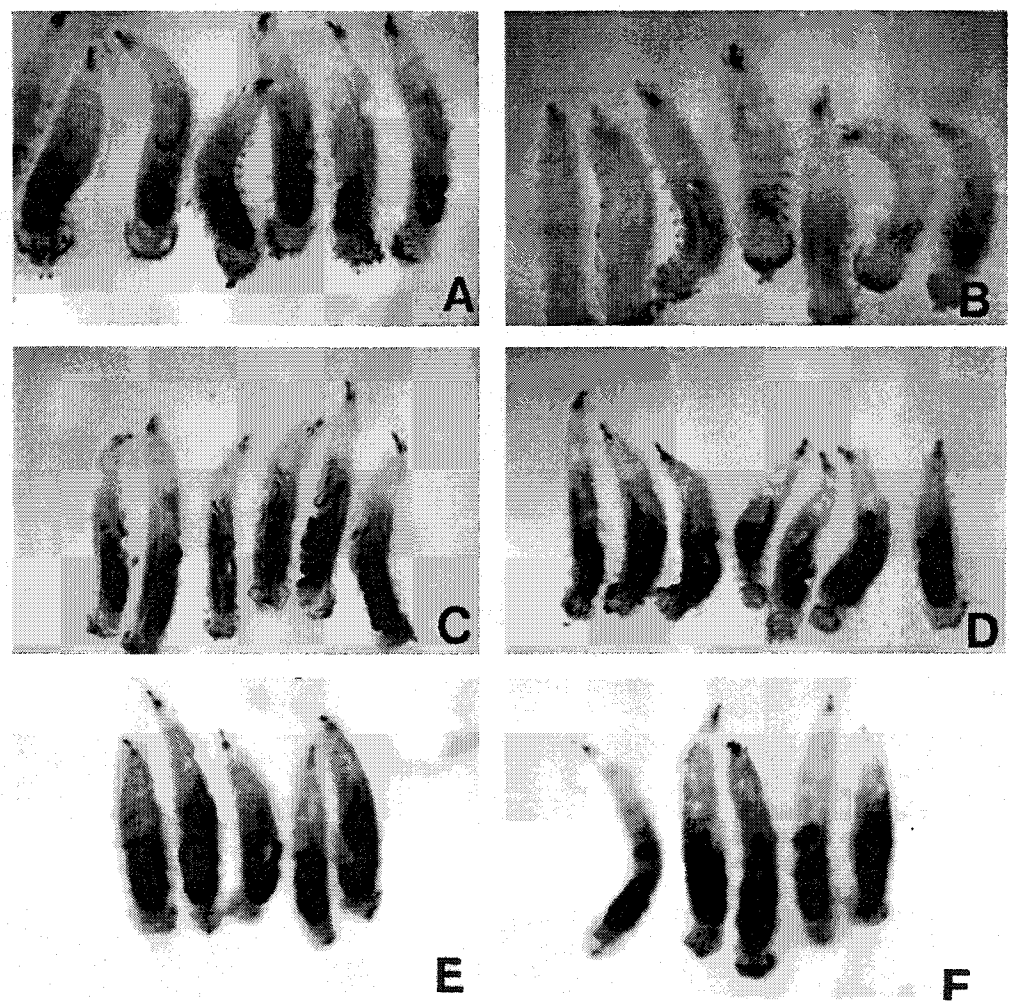


Figure 4.—Mutations in the *tam* gene resulted in prolonged foraging in third instar larvae. The larvae were grown in medium supplemented with bromophenol blue. Emptying of the guts as seen by the disappearance of blue coloration is a landmark of the transition from foraging to wandering stage. (A) Wild type (*P183/CyO-y*$^+$), 108 hr AEL. At this time larvae are at the wandering/foraging boundary. At this point in development wild-type larvae show blue coloration of the gut. (B) Wild type (*P183/CyO-y*$^+$), 117 hr AEL. Larvae at the wandering phase show reduced blue coloration in the gut. (C) *P183/P183* larvae at 108 hr AEL. (D) *P183/tam*$^3$ larvae at 108 hr AEL. (E) *P183/P183* larvae at 117 hr AEL. (F) *P183/tam*$^3$ larvae at 119 hr AEL. The retention of blue coloration at time points where the wild-type larvae show reduced coloration indicated that the mutant larvae did not wander on time.

**TABLE 4**

**Pattern of complementation of the recombined *tam*$^{9}$ is indistinguishable from a previously isolated allele (*tam*$^{3}$)**

| | *Df(2L)b80c1* | *In(2L)b82c44* | *In(2L)b83b22* | *In(2LR)b81a2* | *In(2L)b81l7* |
|---|---|---|---|---|---|
| *tam*$^{9}$ | −(0/289) | +(35/102) | −(0/105) | −(0/111) | +(45/146) |
| *tam*$^{3}$ | −(0/353) | +(40/101) | −(0/142) | −(0/164) | +(13/100) |

Minus indicates lethality and plus indicates viability. Numerator indicates the number of viable adult flies that were heterozygous for the chromosomal aberration and the *tam* alleles. The denominator indicates the number of flies with a marked balancer chromosome.

*al.* 1996). The mutation found in the *tam*$^{3}$ allele was a 5-bp deletion in exon 3 just outside the conserved DNA polymerase domain Z (Figure 10). The mutation identified in *tam*$^{4}$ was a single base pair deletion near the polymerase domain Z that results in a frameshift in the remainder of the coding region.

While the consequences of the change found in *tam*$^{9}$ for enzymatic activity are not known, the deletion found in *tam*$^{3}$ and *tam*$^{4}$ and the amino acid change found in *tam*$^{2}$ demonstrate that the catalytic subunit of the mitochondrial DNA polymerase is disrupted in *tam* mutants. Consistent with this notion we found that the pattern of distribution of mitochondria in the central nervous system as seen with the Mitotracker probe is

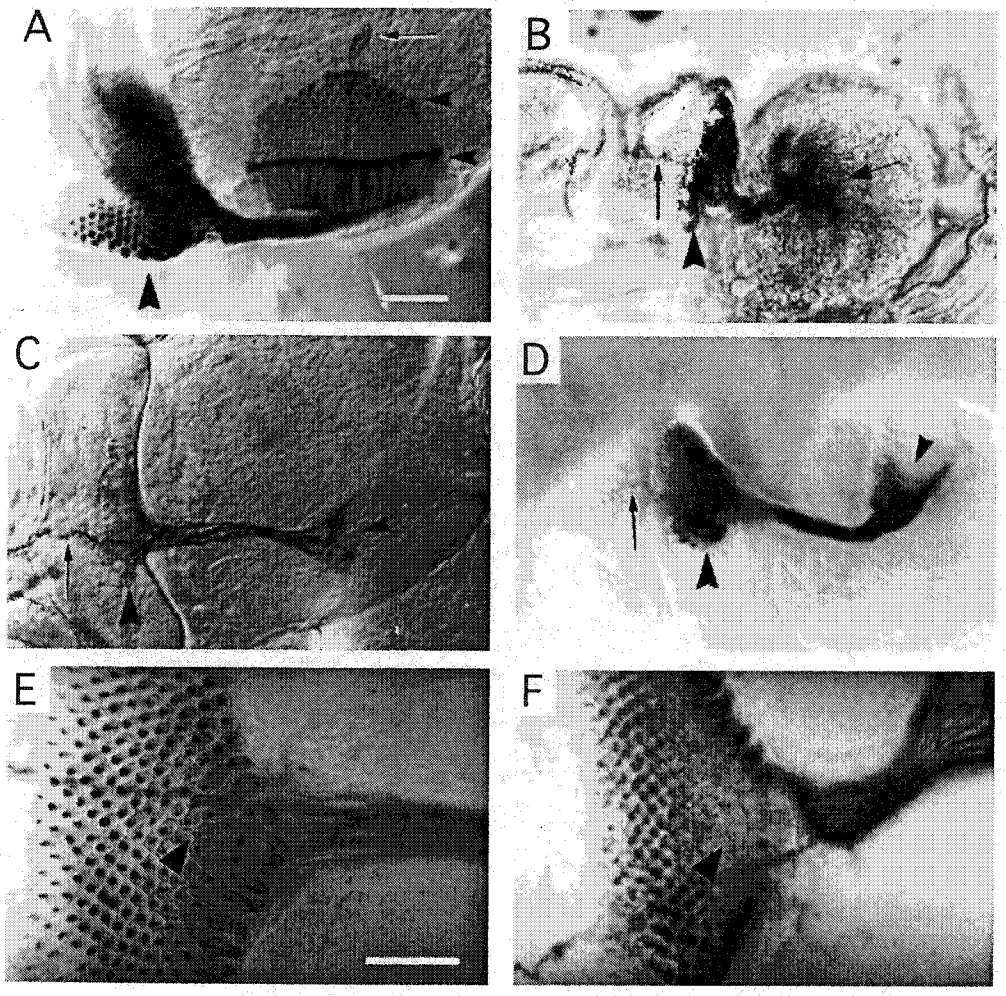


FIGURE 5.—Morphology of the developing adult visual system in *tam* mutants. The micrograph shows the developing adult visual system as seen by labeling with 24B10 primary antibody and HRP-conjugated secondary antibody. (A) Wild-type (Oregon-R) projection pattern viewed horizontally. In eye imaginal disc differentiating arrays of photoreceptors (large arrowhead) and the photoreceptor axonal projections of R1-R6 and R7-R8 into the optic lobe (small arrowheads) are seen. The larval optic nerve terminates deeper in the brain (arrow). (B) *P183/P183*. The photoreceptor differentiation is abnormal (arrowhead). Likewise photoreceptor axonal projection is disorganized (arrow). The larval optic nerve is present (thin arrow). (C) *P183/Df(2L)b80c1*. The defects in photoreceptor differentiation are apparent (large arrowhead). Abnormal projection pattern of photoreceptors in the optic lobe can also be seen (small arrowhead). The larval optic nerve is present (arrow). (D) *P183/tam*$^{3}$. As well as showing delayed photoreceptor differentiation, the eye disc is smaller and the area of differentiated photoreceptors is abnormal (large arrowhead). The projection pattern is also abnormal (small arrowhead). (E) Wild type. The older photoreceptor clusters located more posteriorly retain the clustered staining pattern as the differentiation proceeds more anteriorly. (F) *tam*$^{9}$/*tam*$^{9}$. The differentiating eye disc of the mutant larvae. In mutant eye discs a similar clustered staining pattern at the posterior regions of the eye disc appears not to be maintained. The scale bar in A represents 50 μm and is valid for B, C, and D. The scale bar in E represents 50 μm and is valid for F.

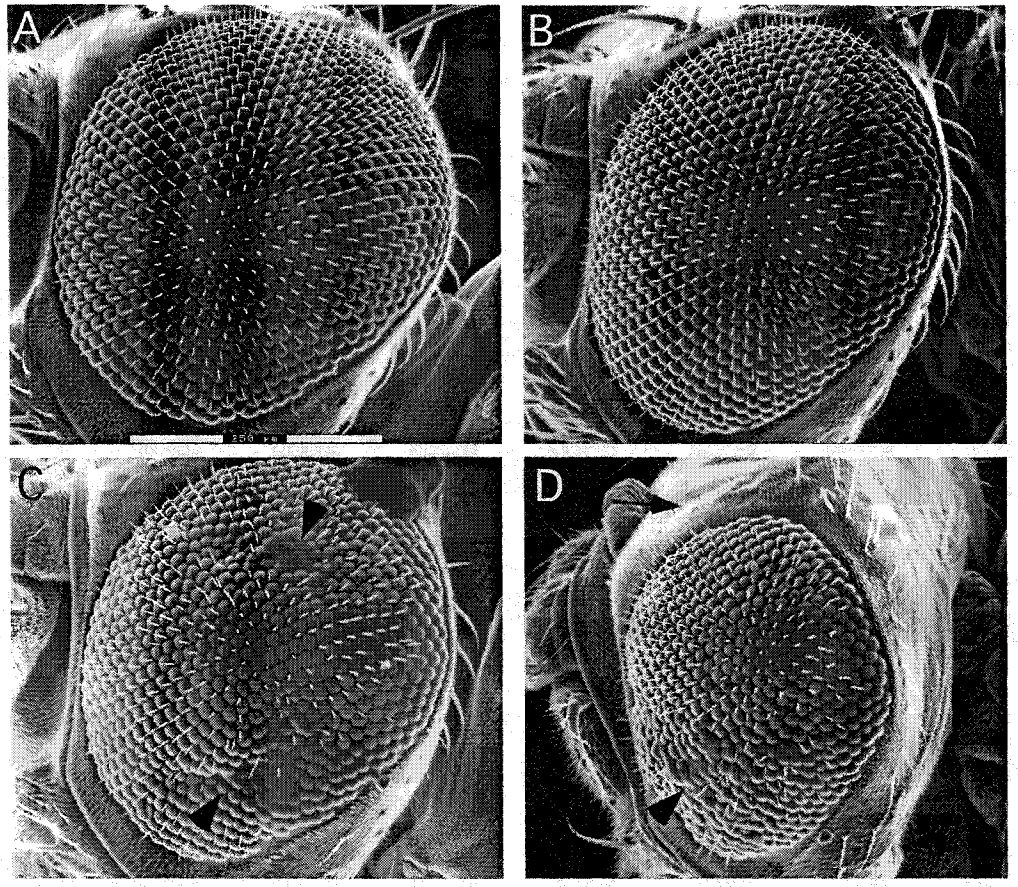


FIGURE 6.—ESEM scan of compound eye defects in *tam* escapers. (A) Wild-type control *In(2L)b79h1A/CyO-y*$^{+}$. (B) *In (2L)b79h1A/kuz*$^{3}$. *kuzbanian* (*kuz*) is the first known lethal complementation group to the left of *In(2L)b79h1A*; it is not disrupted by this inversion as seen by the wild-type pattern of the compound eye. (C) *In(2L) b79h1A/tam*$^{9}$. The compound eye is characterized by disorganized surface, fused ommatidia, and missing bristles (arrowheads). (D) *In(2L)b79h1A/ tam*$^{3}$. The arrowhead shows the rough surface, missing bristles, and fused ommatidia. These flies show a more severe disorganization of the eye than *In(2-L)b79h1A/tam*$^{9}$. The scale bar in A represents 250 μm and is valid for all panels.

severely disrupted by *tam* mutations (Figure 11). We concluded that the *tam* gene codes for the Drosophila DNA polymerase catalytic subunit (*DNApol-γ125*).

## DISCUSSION

To identify genes required for the larval response to light we screened a collection of pupal lethal lines using a population assay employed previously for the characterization of the wild-type response (SAWIN-MCCORMACK *et al.* 1995). The decision to use mutations that caused lethality at a later stage of development is supported by the observation that in Drosophila most of the genes required for visual system development are also required elsewhere for the viability of the organism (THAKER and KANKEL 1992; reviewed by MIKLOS and RUBIN 1996). This generalization was confirmed by BIER *et al.* (1989) who reported that the expression of most genes analyzed in enhancer trap strains was not restricted to one developmental stage. Investigations into the requirements of lethal mutations at different points in development by mosaic analysis yielded similar conclusions (reviewed by MIKLOS and RUBIN 1996).

The sequencing of the mitochondrial DNA polymerase gene in all available *tam* alleles confirms the hypothesis, drawn from the genetics and published BDGP sequence data, that the *tam* gene codes for the catalytic subunit of the mitochondrial DNA polymerase. This is the first report in metazoans of a mutation in the mitochondrial DNA polymerase catalytic subunit (*DNA-pol-γ125*). Mutations in *tam* cause noticeable defects in the development of the adult visual system. Homozygous *tam* mutants also failed to undergo the behavioral changes characteristic of the wandering stage and remained in the food as foraging third instar larvae for a prolonged period. A more detailed analysis of the larval response to light in individual assays revealed that the lack of response to light of *tam* mutant larvae is due to a defect in locomotion. This motor deficit may also contribute to this mutant's failure to undergo the behavioral changes characteristic of the wandering stage.

Homozygous *tam* mutants die as a late third instar larvae. This observation suggests that the perdurance of the maternal contribution of *tam* gene product as well as of maternal mitochondria are sufficient to overcome the zygotic deficit of *tam* gene function well into late larval development. The locomotory phenotype of *tam*$^{3}$ and *tam*$^{9}$ mutations does not apparently represent the phenotype of complete absence of gene function as it is considerably worse when *in trans* with a deficiency that deletes the *tam* gene. In fact the molecular lesions found in these alleles support the notion suggested by the genetic analysis that the *tam*$^{3}$ and *tam*$^{9}$ mutations are hypomorphs. The *tam*$^{2}$ mutation is at present the

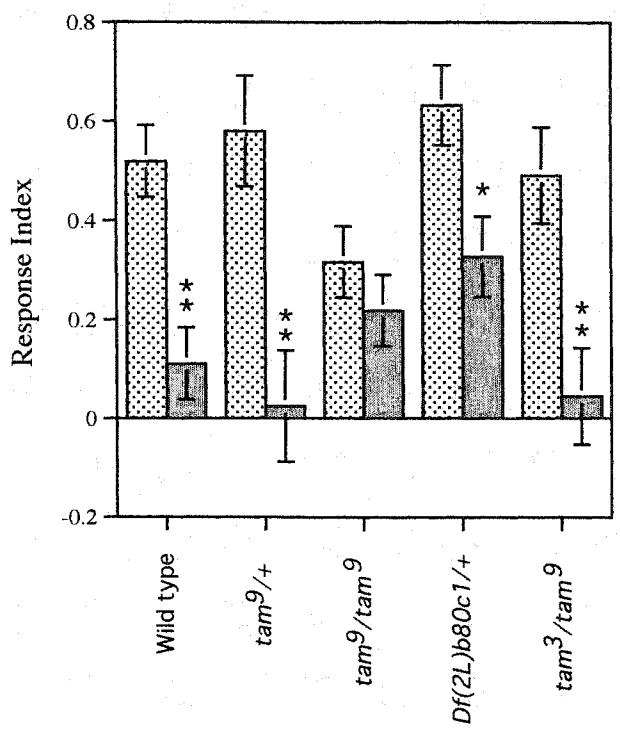


FIGURE 7.—Genetic analysis of photobehavior defect in *tam* mutants. In the Checker assay each genotype was assayed with lights on (test assay) and lights off (control assay). A response to light is present when the response index obtained with lights on (dotted bar) is significantly different from the response index obtained with lights off (shaded bar). The response index with lights on is not significantly different from that obtained with lights off in the homozygous *P183* (double mutant) and $tam^9$ (recombined) strains at any level of comparison, indicating a lack of response to light. In all other strains tested the response index obtained with lights on is significantly higher than that obtained with the lights off (**$P < 0.001$, *$P < 0.01$ by Student's *t*-test). Wild-type control, lights on $n = 17$, lights off $n = 19$; $tam^9/+$, lights on $n = 17$, lights off $n = 16$; $tam^9/tam^9$, lights on $n = 17$, lights off $n = 15$; *Df(2L)b80c1*/+, lights on $n = 12$, lights off $n = 13$; $tam^9/tam^3$, lights on $n = 22$, lights off $n = 16$.

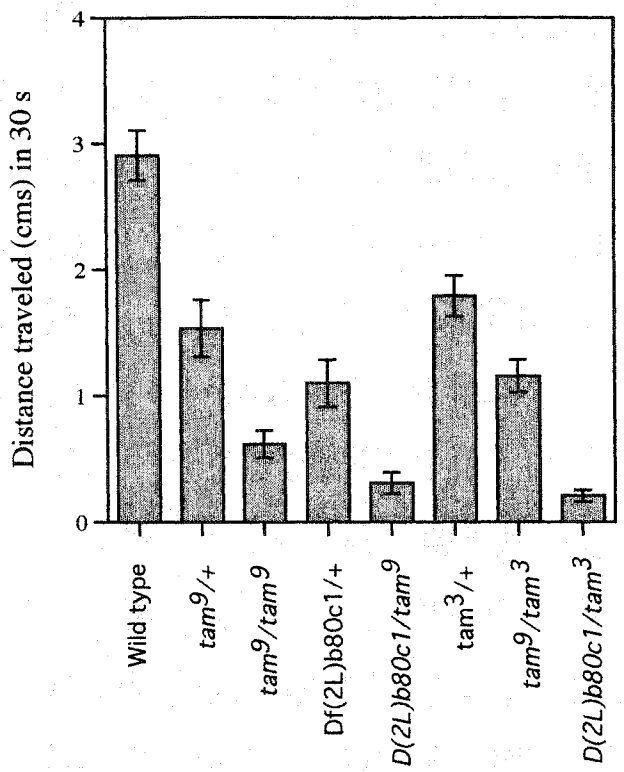


FIGURE 8.—Genetic analysis of locomotory defect in *tam* mutants. The graph depicts the mean distance traveled (SEM) in 30 sec on a nonnutritive substrate in the absence of light. The following comparisons were made using Student's *t*-test: $tam^9/tam^9$ *vs.* $tam^9/$*Df(2L)b80c1*, $T = 2.23$, $P = 0.033$; $tam^9/+$ *vs.* *Df(2L)b80c1*/+, $T = -1.71$, $P = 0.095$; *Df(2L)b80c1*/$tam^9$ *vs.* *Df(2L)b80c1*/+, $T = 3.89$, $P = 0.0006$; $tam^9/tam^9$ *vs.* $tam^9/tam^3$, $T = -3.10$, $P = 0.004$; $tam^3/+$ *vs.* $tam^9/tam^3$, $T = -2.97$, $P = 0.0052$; $tam^9/+$ *vs.* $tam^9/tam^3$, $T = 1.69$, $P = 0.099$; $tam^3/+$ *vs.* $tam^9/+$, $T = -1.08$, $P = 0.28$; *Df(2L)b80c1*/+ *vs.* *Df(2L)b80c1*/$tam^3$, $T = 4.67$, $P = 0.0001$. Wild-type control, $n = 19$; $tam^9/+$, $n = 22$; $tam^9/tam^9$, $n = 17$; *Df(2L)b80c1*/+, $n = 20$; *Df(2L)b80c1*/$tam^9$, $n = 18$; $tam^9/+$, $n = 22$; $tam^3/tam^9$, $n = 19$; *Df(2L)b80c1*/$tam^3$, $n = 19$.

best candidate for a null mutation. It presents a substitution in a glutamine residue of the DNA polymerase domain X essential for enzyme activity (POLESKY *et al.* 1990).

Three other genes encoding for mitochondrial proteins with at least one allele affecting behavior have been identified in *D. melanogaster.* One is the *sluggish-A* (*slgA*) gene (HAYWARD *et al.* 1993), which encodes proline oxidase, a mitochondrial enzyme required for glutamate synthesis. *slgA* mutants display a locomotory and phototactic deficit similar to that described for *tam* mutants. The other two genes belong to the class of "bang or stress sensitive" mutants. They are *technical knockout* (*tko*) and *stress sensitive B* (*sesB*) and they encode a mitochondrial ribosomal protein and the adenine nucleotide translocase of the inner mitochondrial membrane, respectively (ROYDEN *et al.* 1987; ZHANG *et al.* 1998). Mutations in these loci cause flies to become temporarily paralyzed in response to physical jolt or stress. Similarly to *tam* mutants, *tko* mutants are weak and uncoordinated and grow significantly more slowly than wild type. Thus the Drosophila mutations isolated so far that affect mitochondrial function display a variety of nervous system-related phenotypes, some of which are similar to those described for *tam* mutants. These mutant phenotypes probably reflect the particular metabolic requirement of the nervous system.

The Drosophila mitochondrial DNA polymerase (pol-γ) is a heterodimer of two subunits (125 and 35 kD). This heterodimer contains two enzyme activities, a 5′→3′ DNA polymerase and a 3′→5′ exonuclease and is the sole enzyme responsible for mtDNA synthesis (LEWIS *et al.* 1996). *In vitro* studies suggest that the 3′→5′ exonuclease activity proofreads errors during DNA synthesis and thus may play a role in the maintenance of the mitochondrial genetic integrity (LEWIS *et al.* 1996). The cloning and sequence analysis of the Drosophila 125-

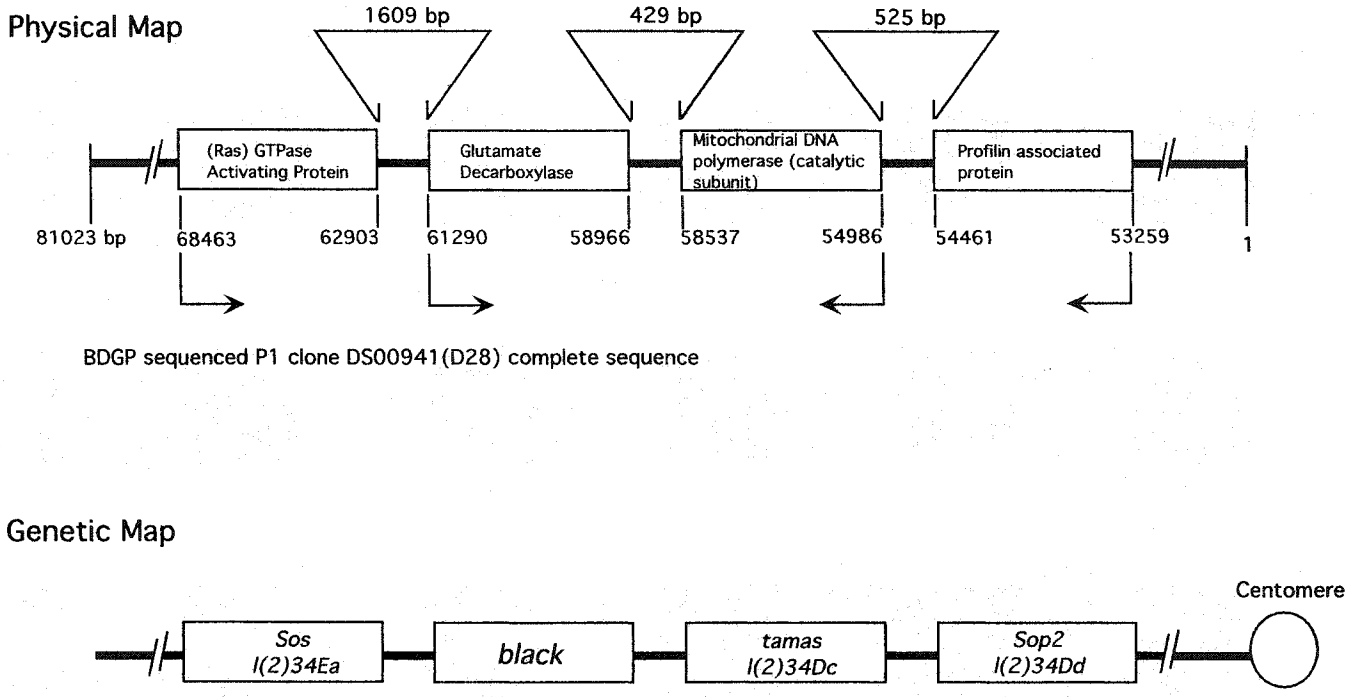


FIGURE 9.—Physical map of the vicinity of the *tam* locus. The map shows the nucleotide numbers of BDGP sequenced P1 clone DS00941, which starts at 1 and ends at 81023. Rectangular boxes indicate the transcriptional units. The direction of transcription is indicated by the arrows below the boxes. The distance between transcriptional units is indicated above and between the rectangular boxes. To aid comparison a genetic map is placed below the physical map. GenBank submitted sequences of guanine nucleotide exchange factor (*Sos*; GenBank accession no. L13173), *glutamate decarboxylase (black*; GenBank accession no. U01239), *mitochondrial DNA polymerase* (GenBank accession no. U60298), and profilin associated protein (*Sop2*; GenBank accession no. Y08999) were used to align the translational start and stop signal on the P1 DS00941 published sequence.

kD subunit demonstrated that this polypeptide contains both enzyme activities (LEWIS *et al.* 1996). The gene for the Drosophila 35-kD subunit has also been cloned and sequenced (WANG *et al.* 1997). Interestingly, its genetic location is only 3.8 kb proximal to that of the catalytic subunit gene. It has been suggested that the β-subunit is required for the enzymatic efficiency and structural integrity of the holoenzyme (LEWIS *et al.* 1996).

Mitochondrial diseases are a group of disorders caused by mitochondrial dysfunction. Most often the brain and/or muscle are affected, reflecting the energy requirement of these tissues. Several mtDNA mutations have been associated with specific clinical disorders (MORAES 1996). A smaller number of encephalomyopathies have been described that are likely due to mitochondrial DNA depletion caused by nuclear DNA mutations (MORAES *et al.* 1991; RICCI *et al.* 1992; SHANSKE 1992; MORAES 1996). Of those the most interesting is a fatal mitochondrial disease of infancy characterized by up to 95% mtDNA depletion in affected tissues. The pedigree of affected families suggested an autosomal recessive mode of inheritance (MARIOTTI *et al.* 1995). Two candidate genes tested in these studies were the mitochondrial single-stranded DNA-binding protein (*mtSSB*) required for strand displacement during mtDNA replication and the mitochondrial transcription factor A (*mtTFA*). Previous studies have indicated that *mtTFA* also plays a role in DNA replication as initiation of DNA synthesis requires an RNA primer (PARISI and CLAYTON 1991). The sequencing of *mtSSB* and *mtTFA* cDNAs isolated from probands showing mtDNA depletion did not show any difference from nonaffected individuals. It is possible that this early onset encephalomyopathy characterized by tissue-specific mtDNA depletion is caused by mutations that disrupt mtDNA replication and/or maintenance.

Mice lacking *mtTFA* die prior to embryonic day 10.5. The mutant embryos display growth retardation and delayed neural and cardiac development (LARSSON *et al.* 1998). Given the requirement for an RNA primer for mtDNA replication, the phenotype of *mtTFA* homozygous knockout mice is likely to be very similar to animals lacking mtDNA replication. In fact homozygous knockout mice exhibit severe mtDNA depletion while heterozygous animals show tissue-specific mtDNA depletion. As expected from the studies of humans showing mtDNA depletion, the affected tissues in these mutant mice displayed a large number of abnormal mitochondria (LARSSON *et al.* 1998).

Some aspects of the behavioral and morphological phenotype of *tam* mutant larvae are similar to that of *mtTFA* knockout mice and of humans showing an early onset encephalomyopathy associated with mtDNA depletion (MARIOTTI *et al.* 1995; LARSSON *et al.* 1998).

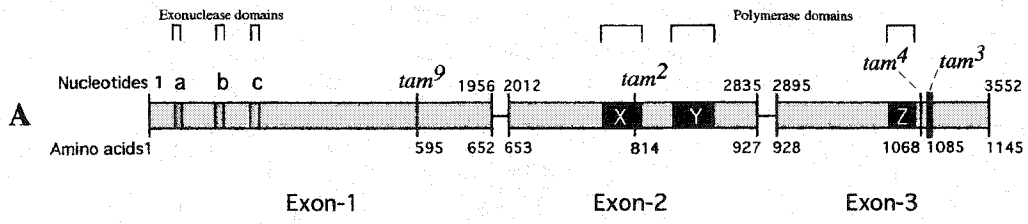


**B**

| | | |
|---|---|---|
| Wild type | 1770 | CGACTGCCCATGGAGCAACTTCTGGCG |
| | 591 | R L P M E Q L L A |
| *tam*$^9$ | | CGACTGCCCATGGCGCAACTTCTGGCG |
| | | R L P M A Q L L A |

**C**

| | | |
|---|---|---|
| Wild type | 2415 | GTTGGTGCCGATGTCGATTCGCAGGAGCTG |
| | 805 | V G A D V D S Q E L |
| *tam*$^2$ | | GTTGGTGCCGATGTCGATTCGCAGGTGCTG |
| | | V G A D V D S Q V L |

**D**

| | | |
|---|---|---|
| Wild type | 3354 | TCGGTGGCCTTCTTCTCGTCCGTGGAGGTAGACACT |
| | 1080 | S V A F F S S V E V D T |
| *tam*$^3$ | | TCGGTGGCCTTCTTCTC-----TGGAGGTAGACGCT |
| | | S V A F F |

**E**

| | | |
|---|---|---|
| Wild type | 3186 | ATGACGCGCTCCTTTTGTGTGTCCCGCATC |
| | 1062 | M T R S F C V S R I |
| *tam*$^4$ | | ATGACGCGCTCCTTT-GTGTGTCCCGCATC |
| | | M T R S F V C O A |

FIGURE 10.—Molecular lesions in *tam* mutant alleles. The genetic analysis and the BDGP sequencing project of the 34D region suggested that *DNApol-γ125* gene may represent the *tam* gene product. The sequence of the DNA polymerase catalytic subunit gene of all available *tam* mutant alleles was aligned to the respective sequence of the parental strains using Clustal X (see Table 1 for genotypes). The parental strain of the *tam*$^9$ allele was not available, hence it was aligned to sequence from an Oregon-R wild-type strain. (A) Schematic depiction of the structure of DNA*pol-γ125* gene (LEWIS *et al.* 1996). Boxes a, b, and c represent the conserved 3′→5′ exonuclease domains, and X, Y, and Z represent the conserved DNA polymerase domains. Numbers above the exon boxes indicate the nucleotides from 1 to 3552 and numbers below the exon boxes indicate amino acids from 1 to 1145. (B) Sequence alignment of *tam*$^9$ allele against the Oregon-R wild-type sequence. The shaded box shows the mutation at nucleotide 1783 in *tam*$^9$ (A→C); this causes an amino acid change (glutamine to alanine). (C) Sequence alignment of *tam*$^2$ allele against the corresponding parental sequence showing a 5-bp deletion at position 3370. (D) Sequence alignment of *tam*$^3$ against the corresponding parental strain. The alignment shows an amino acid change from glutamine to valine at position 813 in a highly conserved polymerase domain of the protein. (E) Shows the alignment of *tam*$^4$ against the corresponding parental sequence. The alignment resulted in identification of a single base pair deletion at position 3201; this causes a frameshift of the remaining coding region.

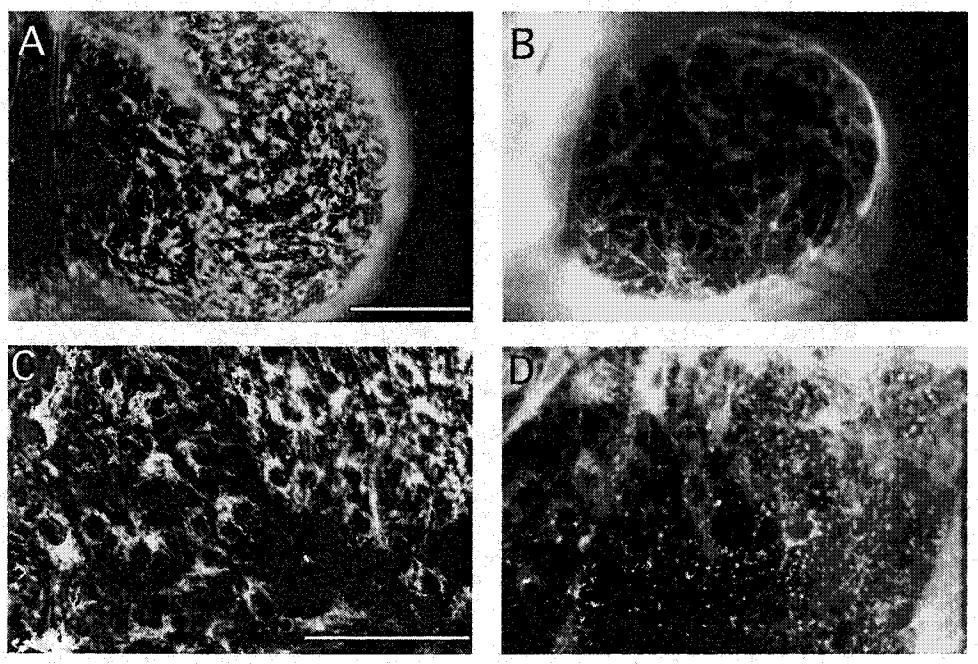


FIGURE 11.—Visualization of mitochondrial mass using Mitotracker probe. Third instar brain hemispheres stained with Mitotracker probe. (A) Wild-type brain hemisphere, 96 hr AEL. (B) *tam*$^9$/*tam*$^9$, 96 hr AEL. (C and D) Higher magnification of wild-type and mutant brain hemispheres, respectively. Scale bar in A represents 50 μm and is valid for B. Scale bar in E represents 50 μm and is valid for D.

*tam* mutant larvae and *mtTFA* mutant mice both display growth retardation and delayed neural development. The infant proband in this particular pedigree displayed severe motor delay during the first month of life and subsequent arrest of psychomotor development concomitant to mild global atrophy of the brain (MARIOTTI *et al.* 1995).

The control of mtDNA maintenance is an important issue not only in inherited encephalomyopathies but also in the treatment of AIDS. The mitochondrial myopathy seen in AIDS patients after prolonged exposure to AZT is due to the incorporation of this drug in mtDNA by mtDNA polymerase causing inhibition of mtDNA replication (DALAKAS *et al.* 1990; ARNAUDO *et al.* 1991; RICCI *et al.* 1992). Drosophila larvae mutant for the *tam* gene may provide a useful model system to study control of mtDNA replication. It provides the unique opportunity to screen for second-site mutations that modify the *tam* phenotype and hence allow us to identify genes that may be involved in the same pathway.

The authors are indebted to Drs. Art Hilliker and M. B. Sokolowski for the generous gift of the pupal lethal strains and for getting us started in this project and to Sima Misra and the Berkeley *Drosophila* Genome Project for sequencing data and analyses. We thank Dr. André Bedard and Dr. Richard Morton for comments on the manuscript and discussions on genetics and science in general. This research was supported by an operating grant from Medical Research Council of Canada (MRC) to A. R. Campos. J. Roote has been supported by an MRC program grant to M. Ashburner, S. Russell, and D. Gubb.

## LITERATURE CITED

ALEXANDROV, I. D., and M. V. ALEXANDROVA, 1986 Report of new mutants. Dros. Inf. Serv. **63:** 159–161.

ALEXANDROV, I. D., and M. V. ALEXANDROVA 1991 The genetic and cytogenetic boundaries of the radiation-induced chromosome rearrangements scored as lethal *black* mutations in *D. melanogaster*. Dros. Inf. Serv. **70:** 16–19.

ARNAUDO, E., M. DALAKAS, S. SHANSKE, C. T. MORAES, S. DIMAURO *et al.*, 1991 Depletion of muscle mitochondrial DNA in AIDS patients with zidovudine-induced myopathy. Lancet **337:** 508–510.

ASHBURNER, M., 1989 *Drosophila: A Laboratory Handbook*. Cold Spring Harbor Laboratory Press, Cold Spring Harbor, NY.

ASHBURNER, M., C. S. AARON and S. TSUBOTA, 1982 The genetics of a small autosomal region of *Drosophila melanogaster*, including the structural gene for alcohol dehydrogenase. Genetics **102:** 421–435.

ASHBURNER, M., S. MISRA, J. ROOTE, S. LEWIS, R. BLAZE *et al.*, 1999 An exploration of the sequence of a 2.9-Mb region of the genome of *Drosophila melanogaster*: The *Adh* region. Genetics **153:** 179–219.

BIER, E., H. VAESSIN, S. SHEPHERD, K. LEE, K. MCCALL *et al.*, 1989 Searching for pattern and mutation in the *Drosophila* genome with a *P-lacZ* vector. Genes Dev. **3:** 1273–1287.

BONFINI, L., C. A. KARLOVICH, C. DASGUPTA and U. BANERJEE, 1992 The *Son of sevenless* gene product: a putative activator of Ras. Science **255:** 603–606.

BOYNTON, S., and T. TULLY, 1992 *latheo*, a new gene involved in associative learning and memory in *Drosophila melanogaster* identified from P-element mutagenesis. Genetics **131:** 655–672.

CHALFIE, M., and J. SULSTON, 1981 Developmental genetics of the mechanosensory neurons of *Caenorhabditis elegans*. Dev. Biol. **82:** 358–370.

DALAKAS, M. C., I. ILLA, G. H. PEZESHKPOUR, J. P. LAUKAITIS, B. COHEN *et al.*, 1990 Mitochondrial myopathy caused by long-term zidovudine therapy [see comments]. N. Engl. J. Med. **322:** 1098–1105.

FLYBASE CONSORTIUM, 1999 FlyBase—The FlyBase Database of the *Drosophila* Genome Projects and community literature. Nucleic Acids Res. **26:** 85–88.

FRAENKEL, G. S., and D. L. GUNN, 1961 *The Orientation of Animals*. Dover Publications, New York.

GREEN, P., A. Y. HARTENSTEIN and V. HARTENSTEIN, 1993 The embryonic development of the *Drosophila* visual system. Cell Tissue Res. **273:** 583–598.

GRELL, E. H., K. B. JACOSON and J. B. MURPHY, 1968 Alterations of the genetic material for analysis of alcohol dehydrogenase isozymes of *Drosophila melanogaster*. Ann. NY Acad. Sci. **151:** 441–445.

GUBB, D., M. SHELTON, J. ROOTE, S. MCGILL and M. ASHBURNER 1984 The genetic analysis of a large transposing element of *Drosophila melanogaster*: the insertion of a $w^+$ $rst^+$ TE into the *ck* locus. Chromosoma **91:** 54–64.

HARRIS, W. A., and W. S. STARK, 1977 Hereditary retinal degeneration in *Drosophila melanogaster:* a mutant defect associated with the phototransduction process. J. Gen. Physiol. **69:** 261–291.

HASSAN, J., M. BUSTO, B. IYENGAR and A. R. CAMPOS, 2000 Behavioral characterization and genetic analysis of the *Drosophila melanogaster* response to light as revealed by a novel individual assay. Behav. Genet. (in press).

HAYWARD, D. C., S. J. DELANEY, H. D. CAMPBELL, A. GHYSEN, S. BENZER *et al.*, 1993 The sluggish-A gene of *Drosophila melanogaster* is expressed in the nervous system and encodes proline oxidase, a mitochondrial enzyme involved in glutamate biosynthesis. Proc. Natl. Acad. Sci. USA **90:** 2979–2983.

HEISENBERG, M., 1997 Genetic approaches to neuroethology. Bioessays **19:** 1065–1073.

HEISENBERG, M., and E. BUCHNER, 1977 The role of retinal cell types in visual behavior of *Drosophila melanogaster*. J. Comp. Physiol. **117:** 127–162.

HEISENBERG, M., and R. WOLF, 1984 The compound eye, pp. 1–32 in *Vision in Drosophila: Genetics of Microbehavior*, edited by V. BRAITENBERG. Springer-Verlag, Berlin.

HUDSON, A., and L. COOLEY, 1998 Analysis of the *Drosophila* Arp2/3 complex in oogenesis. A. Conf. Dros. Res. **39:** 289B.

KERNAN, M., D. COWAN and C. ZUKER, 1994 Genetic dissection of mechanosensory transduction: mechanoreception-defective mutations of *Drosophila*. Neuron **12:** 1195–1206.

KOENIG, J., and J. MERRIAM, 1977 Autosomal ERG mutants. Dros. Inf. Serv. **52:** 50–51.

LARSSON, N. G., J. WANG, H. WILHELMSSON, A. OLDFORS, P. RUSTIN *et al.*, 1998 Mitochondrial transcription factor A is necessary for mtDNA maintenance and embryogenesis in mice. Nature Genet. **18:** 231–236.

LEWIS, D. L., C. L. FARR, Y. WANG, A. T. R. LAGINA and L. S. KAGUNI, 1996 Catalytic subunit of mitochondrial DNA polymerase from *Drosophila* embryos: cloning, bacterial overexpression, and biochemical characterization. J. Biol. Chem. **271:** 23389–23394.

LILLY, M., and J. R. CARLSON, 1990 *smellblind:* a gene required for *Drosophila* olfaction. Genetics **124:** 293–302.

MARDAHL, M., R. M. CRIPPS, R. R. RINEHART, S. I. BERNSTEIN and G. L. HARRIS, 1993 Introduction of *y+* onto a CyO chromosome. Dros. Inf. Serv. **72:** 141.

MARIOTTI, C., G. UZIEL, F. CARRARA, M. MORA, A. PRELLE *et al.*, 1995 Early-onset encephalomyopathy associated with tissue-specific mitochondrial depletion: a morphological, biochemical and molecular-genetic study. J. Neurol. **242:** 547–556.

MARONI, G., and S. C. STAMEY, 1983 Use of blue food to select synchronous, late third-instar larvae. Dros. Inf. Serv. **59:** 142.

MIKLOS, G. L. G., and G. M. RUBIN, 1996 The role of genome projects in determining gene functions: insight from model organisms. Cell **86:** 521–589.

MORAES, C. T., 1996 Mitochondrial disorders. Curr. Opin. Neurol. **9:** 369–374.

MORAES, C. T., S. SHANSKE, H. J. TRITSCHLER, J. R. APRILLE, F. ANDREETTA *et al.*, 1991 mtDNA depletion with variable tissue expression: a novel genetic abnormality in mitochondrial diseases. Am. J. Hum. Genet. **48:** 492–501.

O'DONNELL, J. M., H. C. MANDEL, M. KRAUSS and W. SOFER, 1977 Genetic and cytogenetic analysis of the Adh region in *Drosophila melanogaster*. Genetics **86:** 553–566.

PAK, W. L., 1979 Study of photoreceptor function using *Drosophila* mutants, pp. 67–99 in *Neurogenetics: Genetic Approaches to the Nervous System*, edited by X. O. BREAKFIELD. Elsevier, New York.

PARISI, M. A., and D. A. CLAYTON, 1991 Similarity of human mitochondrial transcription factor 1 to high mobility group proteins. Science **252:** 965–969.

POLESKY, A. H., T. A. STEITZ, N. D. GRINDLEY and C. M. JOYCE, 1990 Identification of residues critical for the polymerase activity of the Klenow fragment of DNA polymerase I from *Escherichia coli*. J. Biol. Chem. **265:** 14579–14591.

POLLOCK, J. A., and S. BENZER, 1988 Transcript localization of four opsin genes in the three visual organs of *Drosophila*: RH2 is ocellus specific. Nature **333:** 779–782.

RICCI, E., C. T. MORAES, S. SERVIDEI, P. TONALI, E. BONILLA *et al.*, 1992 Disorders associated with depletion of mitochondrial DNA. Brain Pathol. **2:** 141–147.

ROYDEN, C. S., V. PIRROTTA and L. Y. JAN, 1987 The *tko* locus, site of a behavioral mutation in *Drosophila melanogaster*, codes for a protein homologous to prokaryotic ribosomal protein S12. Cell **51:** 165–173.

SAWIN, E. P., H. B. DOWSE, M. J. HAMBLEN-COYLE, J. C. HALL and M. B. SOKOLOWSKI, 1994 A lack of locomotor activity rhythms in *Drosophila melanogaster* larvae (Diptera: Drosophilidae). J. Insect. Behav. **7:** 249–262.

SAWIN-MCCORMACK, E., M. B. SOKOLOWSKI and A. R. CAMPOS, 1995 Characterization and genetic analysis of *Drosophila melanogaster* photobehavior during larval development. J. Neurogenet. **10:** 119–135.

SAYEED, O., and S. BENZER, 1996 Behavioral genetics of thermosensation and hygrosensation in *Drosophila*. Proc. Natl. Acad. Sci. USA **93:** 6079–6084.

SCHWEISGUTH, F., and J. W. POSAKONY, 1992 Suppressor of Hairless, the *Drosophila* homolog of the mouse recombination signal-binding protein gene, controls sensory organ cell fates. Cell **69:** 1199–1212.

SEHGAL, A., J. PRICE and W. YOUNG, 1992 Ontogeny of a biological clock in *Drosophila melanogaster*. Proc. Natl. Acad. Sci. USA **89:** 1423–1427.

SHANSKE, S., 1992 Mitochondrial encephalomyopathies: defects of nuclear DNA. Brain Pathol. **2:** 159–162.

SIMON, M. A., D. D. L. BOWTELL, G. S. DODSON, T. R. LAVERTY and G. M. RUBIN, 1991 Ras 1 and putative guanine nucleotide exchange factor perform crucial steps in signaling by the *sevenless* protein tyrosine kinase. Cell **67:** 701–716.

STARK, W. S., and R. H. WHITE, 1996 Carotenoid replacement in *Drosophila:* freeze-fracture electron microscopy. J. Neurocytol. **25:** 233–241.

THAKER, H. M., and D. K. KANKEL, 1992 Mosaic analysis gives an estimate of the extent of genomic involvement in the development of the visual system in *Drosophila melanogaster*. Genetics **131:** 883–894.

THOMPSON, J. D., T. J. GIBSON, F. PLEWNIAK, F. JEANMOUGIN and D. G. HIGGINS, 1997 The CLUSTAL_X windows interface: flexible strategies for multiple sequence alignment aided by quality analysis tools. Nucleic Acids Res. **25:** 4876–4882.

TRUMAN, J. W., W. S. TALBOT, S. E. FAHRBACH and D. S. HOGNESS, 1994 Ecdysone receptor expression in the CNS correlates with stage-specific responses to ecdysteroids during *Drosophila* and *Manduca* development. Development **120:** 219–234.

VITATERNA, M. H., D. P. KING, A.-M. CHANG, J. M. KORNAHAUSER, P. L. LOWREY *et al.*, 1994 Mutagenesis and mapping of a mouse gene, clock, essential for circadian behavior. Science **264:** 719–725.

WANG, Y., C. L. FARR and L. S. KAGUNI, 1997 Accessory subunit of mitochondrial DNA polymerase from *Drosophila* embryos: cloning, molecular analysis, and association in the native enzyme. J. Biol. Chem. **272:** 13640–13646.

WOODRUFF, R. C., and M. ASHBURNER, 1979 The genetics of a small autosomal region of *Drosophila melanogaster* containing the structural gene for alcohol dehydrogenase. II. Lethal mutations in the region. Genetics **92:** 133–149.

ZHANG, Y. Q., A. W. DAVIS, J. ROOTE and M. ASHBURNER, 1998 Stress sensitive B encodes the *Drosophila* ADP/ATP translocase. A. Conf. Dros. Res. **39:** 565A.

ZIPURSKY, S. L., T. R. VENKATESH, D. B. TEPLOW and S. BENZER, 1984 Neuronal development in the *Drosophila* retina: monoclonal antibodies as molecular probes. Cell **36:** 15–26.

ZUKER, C. S., A. F. COWMAN and G. M. RUBIN, 1985 Isolation and structure of a rhodopsin gene from *D. melanogaster*. Cell **40:** 851–858.

Communicating editor: M. J. SIMMONS

**D: Manuscript -** *Drosophila* Amphiphysin is a post-synaptic protein required for normal locomotion but not endocytosis

Traffic 2001; 2: 839–850
Munksgaard International Publishers


ISSN 1398-9219

# *Drosophila* Amphiphysin is a Post-Synaptic Protein Required for Normal Locomotion but Not Endocytosis

**Peter A. Leventis[1,3,*], Brenda M. Chow[2,3,*], Bryan A. Stewart[3,5], Balaji Iyengar[4], Ana Regina Campos[4] and Gabrielle L. Boulianne[1,2,3,**]**

*Departments of [1]Zoology and [2]Molecular and Medical Genetics, University of Toronto, Toronto, Canada*
*[3]Program in Developmental Biology, The Hospital for Sick Children, 555 University Avenue, Toronto, Ontario, Canada, M5G 1X8,*
*[4]Department of Biology, McMaster University, Hamilton, Ontario, Canada, L8S 4K1*
*[5]Current address: Division of Life Sciences, University of Toronto at Scarborough, 1265 Military Trail, Toronto, Ontario, Canada, M1C 1A4*
***Corresponding author: Dr Gabrielle L. Boulianne, gboul@sickkids.ca*

**Clathrin-mediated endocytosis is required to recycle synaptic vesicles for fast and efficient neurotransmission. Amphiphysins are thought to be multiprotein adaptors that may contribute to this process by bringing together many of the proteins required for endocytosis. Their *in vivo* function, however, has yet to be determined. Here, we show that the *Drosophila* genome encodes a single *amphiphysin* gene that is broadly expressed during development. We also show that, unlike its vertebrate counterparts, *Drosophila* Amphiphysin is enriched postsynaptically at the larval neuromuscular junction. To determine the role of *Drosophila* Amphiphysin, we also generated null mutants which are viable but give rise to larvae and adults with pronounced locomotory defects. Surprisingly, the locomotory defects cannot be accounted for by alterations in the morphology or physiology of the neuromuscular junction. Moreover, using stimulus protocols designed to test endocytosis under moderate and extreme vesicle cycling, we could not detect any defect in the neuromuscular junction of the *amphiphysin* mutant. Taken together, our findings suggest that Amphiphysin is not required for viability, nor is it absolutely required for clathrin-mediated endocytosis. However, *Drosophila* Amphiphysin function is required in both larvae and adults for normal locomotion.**

**Key words: actin, amphiphysin, endocytosis, synaptic vesicle recycling**

**Received 6 August 2001, revised and accepted for publication 27 August 2001**

*These authors contributed equally to the work described in this article.

Clathrin-mediated endocytosis has been widely implicated as a mechanism to regenerate and maintain pools of synaptic vesicles (SVs) during neurotransmission. It is thought to be initiated by the formation of clathrin-coated pits through a process involving clathrin and its adaptor proteins, AP180 and AP2 (1). 'Pinching off' of the vesicle is thought to require the function of the GTPase dynamin (2). Dynamin has been suggested to act as a 'popase' by wrapping around the neck of a budding vesicle and 'popping' the vesicle off the end of the neck (3), or as a regulator to ensure that a neck is the correct diameter (4).

Other cytosolic proteins are also believed to play a role in clathrin-mediated endocytosis. These include the inositol-5'-phosphatase, synaptojanin (5), the lysophosphatidic acid acyl transferase endophilin (6) and amphiphysin (7–10). In vertebrates, two amphiphysin homologs, amphiphysin 1 and 2, have been found to be highly concentrated in nerve terminals (7–9) and are composed of three domains. The amino terminal BAR domain (9) named after the original family members (Bin1/Amphiphysin 1/Rvs167), is predicted to form coiled-coil structures that are involved in dimerization and interaction with lipid membranes (11). Bin1 is an alternatively spliced product of the amphiphysin 2 gene in mammals, whereas Rvs167 is found in budding yeast. The central region binds, through distinct sites, to clathrin (8,12–14), endophilin (14), and the α-adaptin subunit of AP2 (10,15). Finally, the carboxy terminus contains an SH3 domain that binds both dynamin (16–18) and synaptojanin (19). The ability of amphiphysin to bind to several components of the endocytic machinery strongly suggests that amphiphysin may function as a multiprotein adaptor to assemble a number of proteins required for SV endocytosis.

To date, the function of amphiphysin has largely been studied using dominant-negative constructs or by injecting peptides into neuronal or non-neuronal cells. These studies have shown that overexpression of the clathrin/AP2 binding domain of amphiphysin can block transferrin receptor endocytosis in HeLa cells, presumably by blocking the interaction of amphiphysin with clathrin and AP2 (20). Similarly, overexpression of the SH3 domain that binds both dynamin and synaptojanin has been shown to block endocytosis in several different cell lines (10,17). Presynaptic injection of a GST-fusion protein consisting of the SH3 domain of human amphiphysin 1 into the lamprey giant reticulospinal synapse also results in the accumulation of coated pits and a large decrease in amplitude of excitatory postsynaptic potentials during prolonged stimulation, consistent with disruption of clathrin-mediated SV endocytosis (17). Interestingly, loss-of-

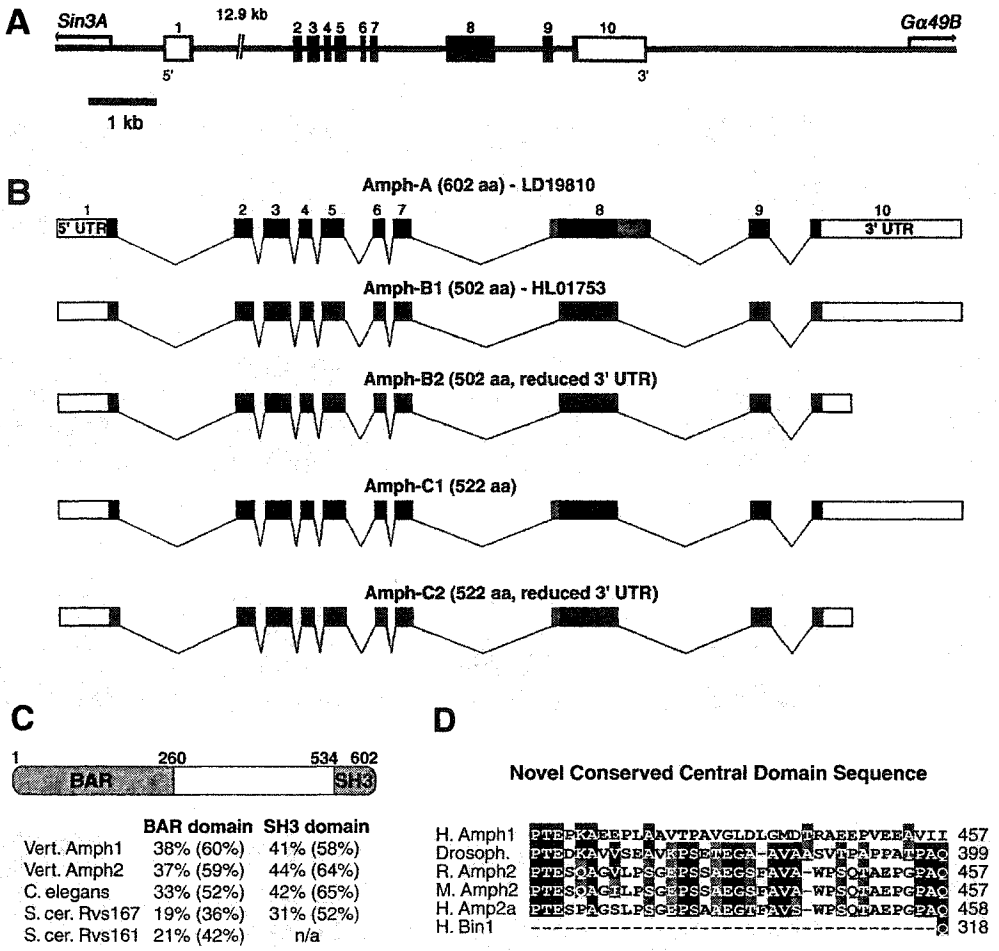


**Figure 1: (A) *amph* consists of 10 exons (boxes) over 18 425 bp, with a large intron of 12.9 kb separating the first two exons.** Exons 1 and 10 contain both untranslated sequence (open boxes) and parts of the ORF (filled boxes). The two genes flanking *amph*, *Sin3A* and *Gα49B*, are shown with their orientation. (B) The structure of the various *amph* cDNAs identified is shown. Amph-A represents the longest clone identified in our screens. The additional isoforms differ primarily within exon 8 which encodes part of the central domain and the 3′ UTR. Variably spliced parts of exons are shaded grey to highlight these regions. (C) The predicted three-domain structure of amphiphysin is shown. Below is indicated the percent identity and similarity (bracket) between amphiphysins from different species within the BAR and SH3 domain. (D) An additional domain was identified within the central portion of amphiphysin that is highly conserved between *Drosophila* Amph and vertebrate amphiphysin 2 isoforms. Amino acid identities are shaded in black, whereas conserved residues are shaded in grey. H = human; M = mouse; R = rat.

function mutations in the yeast orthologs of amphiphysin, RVS167p and a related protein RVS161p, not only exhibit defects in endocytosis (21,22) but also show reduced viability upon nutrient starvation (23,24), budding defects (24) and delocalized actin patches (22,24–26). This actin phenotype appears to be due to the inability of the yeast cdk5 homolog, Pho85, to signal via Rvs161p/Rvs167p to the cortical actin cytoskeleton. More recently, vertebrate amphiphysins have also been shown to play a role in cortical actin dynamics and to interact with cdk5 (27). Taken together, these data suggest that in addition to a role in SV endocytosis, amphiphysin may have additional cell biological roles. Therefore, to gain further insight into the *in vivo* roles of amphiphysin, we generated and characterized null mutations in the *Drosophila amphiphysin* gene (*amph*).

## Results

### *Molecular organization of the Drosophila amphiphysin gene*

As a first step to identify the *in vivo* function of amphiphysin, we characterized the *amphiphysin (amph)* gene from *Drosophila*. Unlike vertebrates, the *Drosophila* genome contains a single *amph* gene (28,29) that gives rise to multiple isoforms by alternative splicing. The entire gene is contained within 18.5 kb of genomic DNA and is flanked at the 5′ end by the *Sin3A* gene which encodes a transcription corepressor (30,31) and at the 3′ end by the *Gα49B* gene which encodes an eye-specific subunit of a heterotrimeric G-protein GTPase (32,33). The predicted intron/exon structure of *Drosophila amph* is illustrated in Figure 1(A).

Consistent with a previous report (28) we found that *amph* gives rise to a 3162 bp transcript. In addition, we have also identified four other predicted isoforms of *amph* (2922 bp, 2862 bp, 2117 bp, and 2057 bp) by sequencing another EST (HL01753) and several positive clones isolated from a cDNA library screen (Figure 1B). All isoforms identified arise from alternative splicing within exon 8. Additionally, the two shortest isoforms also contain a shorter 3′ UTR due to polyadenylation at a cryptic site 120 bp after the stop codon. The longest isoform encodes a predicted 602 amino acid product, whereas the shorter isoforms predict proteins of 522 and 502 aa, respectively.

Overall, the predicted full-length protein is approximately 30% identical to rat amphiphysins 1 and 2, and 24% identical to the predicted *C. elegans* amphiphysin. The highest degree of similarity is in the N-terminal BAR domain which shares ~38% identity and ~60% similarity with vertebrate amphiphysin 1 and 2 (Figure 1C). This domain is predicted to form coiled-coil structures that are involved in dimerization and interaction with lipid membranes and is encoded by exons 1–6 (11). Similarly, the C-terminal SH3 domain, which binds both dynamin and synaptojanin (34), is also highly conserved and is encoded by exons 9 and 10 (Figure 1C). In contrast, the central domain which binds clathrin, endophilin, and the α-adaptin subunit of AP2 is poorly conserved and the consensus sequences for binding these proteins are absent. However, within this central domain, we have identified another region that is conserved between *Drosophila* Amph and vertebrate amphiphysin 2 (but not Bin-1 splice variants). This region lies between amino acids 363 and 398 of *Drosophila* Amph and is encoded by the nonvariably spliced part of exon 8. This domain starts 2 amino acid residues after the second clathrin binding domain in some forms of amphiphys in 2 and is partially conserved in amphiphysin 1 (Figure 1D).

***Amph is broadly expressed during development***

To examine the temporal and spatial distribution of Amph during development, we generated rabbit polyclonal antibodies to a full-length (602 aa) $His_6$-tagged Amph protein. We found on Western blots that this antiserum recognized a single band corresponding to the recombinant Amph protein, while none were detected using the pre-immune serum, even after prolonged exposures (data not shown). We then performed Western blots on lysates from *Drosophila* at different stages of development. At all developmental stages examined, we observed an 85-kDa band, a cluster of bands at 80 kDa that may represent additional splice variants or different phospho-isoforms of Amph and a 45-kDa band that may be the product of an as-of-yet unidentified transcript, or a proteolytic degradation product (Figure 2A). However, all of the isoforms appear to be down-regulated in both first larval instars and pupae. Moreover, all 3 major isoforms are absent in null mutants (discussed below) and are not detected by the pre-immune serum. As with vertebrate amphiphysin (7), *Drosophila* Amph has a reduced mobility on SDS-PAGE gels compared to the predicted size of the protein (~85 kDa vs. 65.9 kDa predicted). We also examined the distribution of Amph in several tissues including body wall/muscle, central nervous system (CNS) and imaginal discs (Figure 2B). We found that all of the isoforms could be detected in whole larvae and in the body wall, which is comprised primarily of muscle. In contrast, the 45 kDa isoform appears to be absent or strongly down-regulated in both the CNS and imaginal discs (Figure 2B). Multiple isoforms of amphiphysin have also been observed in vertebrates, including brain-specific and ubiquitous forms. This suggests that in addition to a role in synaptic vesicle-mediated endocytosis, amphiphysins may also have additional cell biological functions within specific tissues.

to further investigate the distribution of Amph, we also per-

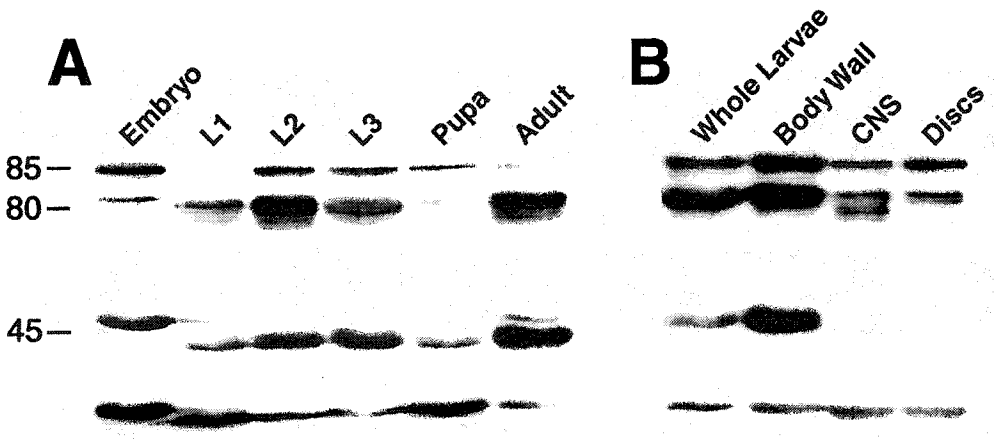


**Figure 2: Expression of Amph was examined using a rabbit polyclonal antibody raised against a full-length fusion protein.** (A) Western blot analysis of 20 μg total protein lysates made from different developmental stages (embryos, first, second and third instar larvae, early pupae, and adults) of a wildtype line (Oregon-R) separated by SDS-PAGE. Anti-Amph 9184 antiserum (1 : 1500) detects at least three different bands at 45, 80, and 85 kDa at all stages. (B) Western blot analysis of 20 μg total protein lysates made from wildtype whole larvae, dissected CNS, imaginal discs, and body wall of wandering third instar larvae separated by SDS-PAGE. Three major immunoreactive bands are seen in whole third instar larvae and in the body wall, which contains mostly muscle. Two are seen in the CNS and the imaginal discs. The bottom panel shows anti-β-tubulin which was used as a loading control.

formed immunohistochemical and immunofluorescence staining of embryos and third instar larval CNS and imaginal discs. We found that Amph was widely expressed in embryos and larvae (Figure 3). Specifically, we found that Amph is first detected in embryos at the onset of cellularization at the sites of developing membranes (Figure 3A,B). At later stages, we observed staining in epithelial tissues, the foregut and hindgut (Figure 3C,D). In contrast, we did not observe any Amph expression in either the embryonic nervous system or muscle. In third larval instars, Amph can be detected at high levels in both larval epithelial cells (Figure 3E) and muscles (Figure 3F), with intense staining at the neuromuscular junction (Figure 3F, arrow). In addition, and consistent with our Western blot analysis, we also observed ubiquitous expression of Amph in both imaginal discs and the CNS (data not shown). No staining was observed in either embryos or larvae from null mutants (described below).

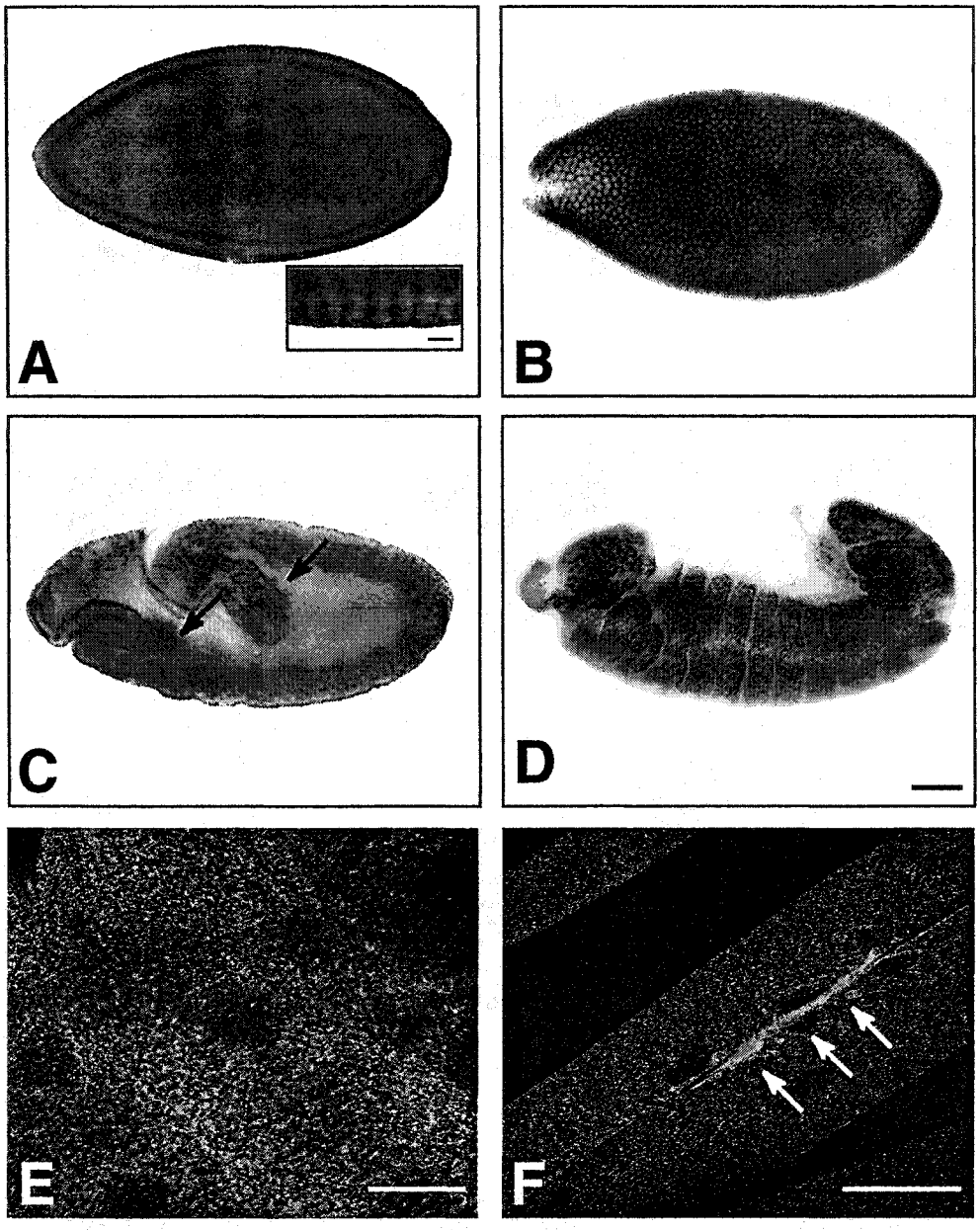


**Figure 3: Amph localization in embryos and third larval instar.** Amph is broadly distributed throughout early embryos. In cellular blastoderm embryos (A,B), it is localized to epithelial cells and appears to be concentrated at cellular membranes (A, inset and B). During later stages of embryogenesis, Amph is localized in the gut (C, arrows) and abdominal segments (D). Immunofluorescent staining of Amph in third larval instars demonstrates punctate cytoplasmic staining in epithelial cells (E) and muscle (F), with intense staining at the neuromuscular junction (F, arrows). Both images are from stacked confocal slices. Epithelial cells in E have also been stained with anti-crumbs (in red) to outline the plasma membrane. Scale bars are 50 μm in A–D (with inset in A, 8 μm), 20 μm in E and 50 μm in F.

### *Amphiphysin is localized postsynaptically at the larval neuromuscular junction*

Since amphiphysin has been widely implicated in synaptic vesicle endocytosis, we also examined the subcellular distribution of Amph at the larval neuromuscular junction (NMJ). Vertebrate amphiphysins have previously been shown to be highly enriched at nerve terminals and associated with SVs. To determine if *Drosophila* Amph was similarly found at sites of SV endocytosis, we used immunofluorescence techniques and confocal microscopy. We found that *Drosophila* Amph was highly expressed at the NMJ (Figure 4). To determine if synaptic Amph was localized pre- or postsynaptically, we performed co-immunolocalization studies with the presynaptic protein, cysteine string protein (CSP), and with UAS-CD8::Sh-GFP that is driven postsynaptically by MHC-GAL4. As expected, we found that CSP and CD8::Sh-GFP had discrete, nonoverlapping distributions (Figure 4A). Surprisingly, double labeling of wildtype NMJs demonstrated that CSP and Amph did not colocalize (Figure 4B). However, Amph and CD8::Sh-GFP showed a high degree of colocalization at the NMJ, although Amph was more diffusely localized (Figure 4C). Therefore, within the limits of our detection ability, Amph is not localized presynaptically, but is present at the synaptic surface of the muscle cell.

### *Generation and characterization of amph mutants*

The broad tissue distribution and postsynaptic localization of Amph was unexpected, based on prior results obtained in vertebrates. To further characterize the function of Amph, we therefore created a series of *amph* mutants by imprecise excision of a transposable P-element, *EP(2)2175*, inserted 39 bp 5′ to the *amph* transcription start site (Figure 5A; Berkeley Drosophila Genome Project (BDGP), unpublished). In total, we generated four independent deletions which removed various portions of the *amph* gene and failed to complement each other (Figure 5A). All of the *amph* mutants are homozygous viable, although the larvae and adults appeared sluggish (see below). Using a combination of Southern blot

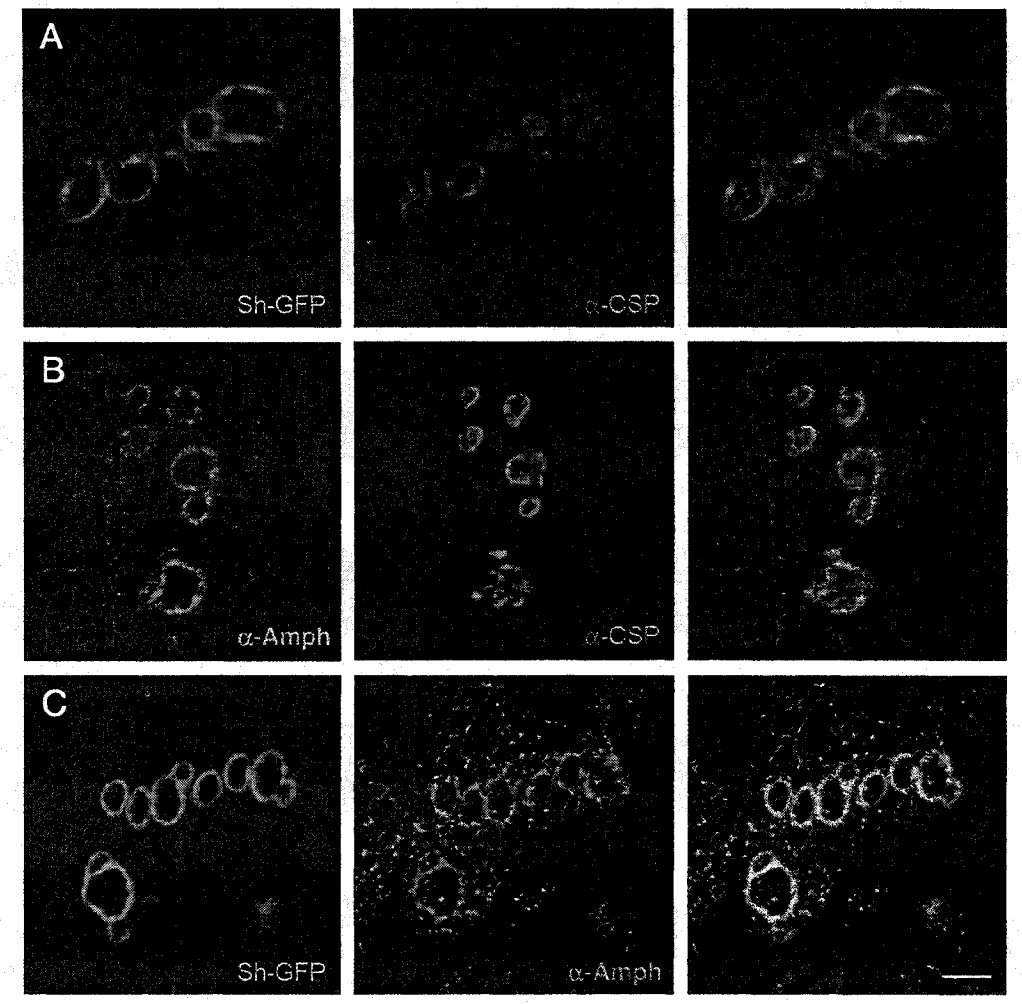


**Figure 4: Amph localizes to the post-, but not presynaptic membrane at the NMJ.** (A) The presynaptic marker cysteine string protein (CSP; red) and the postsynaptic marker CD8::Sh-GFP (green) do not colocalize at the NMJ. (B) Amph (green) and CSP (red) also do not colocalize. (C) Amph (red) and CD8::Sh-GFP (green) do colocalize at the NMJ, showing that Amph is found not at the presynaptic membrane, but at the postsynaptic membrane. Scale bar = 2.5 μm.

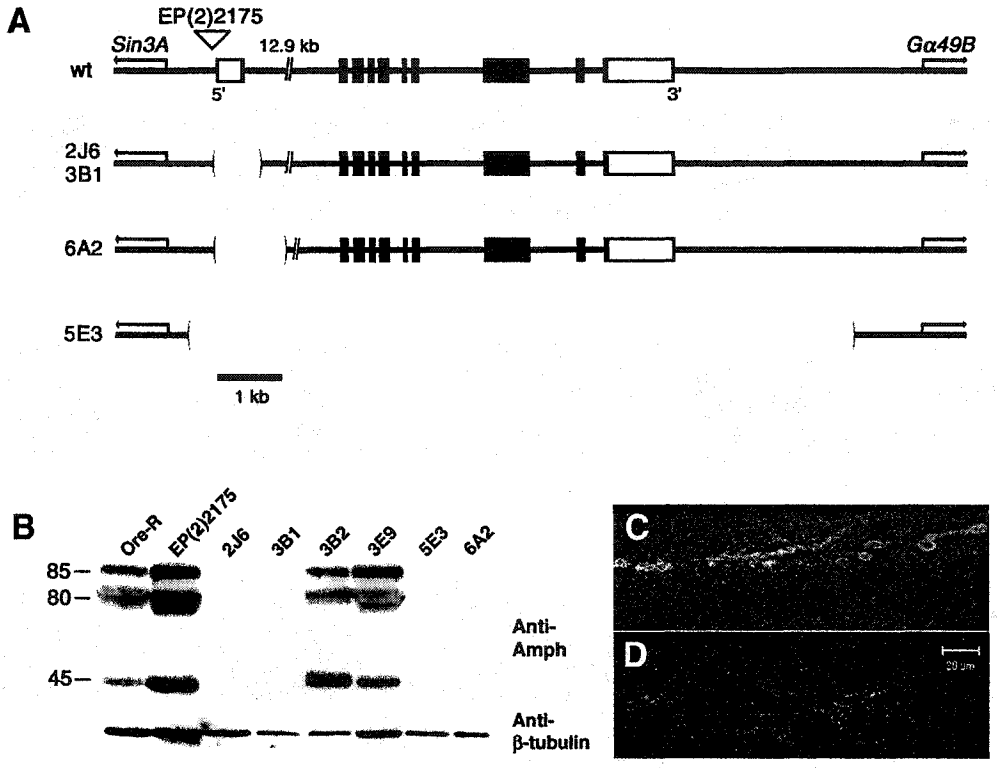


**Figure 5: amph mutants are protein null.** (A) *amph* mutants were generated by imprecise excision of the EP line EP(2)2175. The breakpoints of the four deletions analyzed are illustrated. The excision mutants $amph^{2J6}$ *and* $amph^{3B1}$ (733 bp deletion), *and* $amph^{6A2}$ (1109 bp deletion) are missing exon 1 along with parts of the first intron. $amph^{5E3}$ is an excision of the entire gene (~20 kb), but neither *Sin3A* nor *Gα49B* is disrupted. Scale bar = 1 kb (B) Anti-Amph recognizes three bands in wildtype (Ore-R), original P-element line (EP2175), and precise excision lines ($amph^{3B2}$ and $amph^{3E9}$), but does not recognize any bands in the excision lines $amph^{2J6}$, $amph^{3B1}$, $amph^{5E3}$, and $amph^{6A2}$. In all experiments, anti-β-tubulin was used to demonstrate equal loading. (C) Amph protein can be detected at the NMJ of wildtype larvae but is absent from mutants (D).

and PCR analyses, we found that three lines had deletions of the first exon ($amph^{2J6}$, $amph^{3B1}$, $amph^{6A2}$), whereas $amph^{5E3}$ represented a deletion of the entire gene. Importantly, none of the deletions disrupted either of the flanking genes, *Sin3A* and *Gα49B*, indicating that these mutations only affect *amph* (data not shown).

To determine if any of the mutants produced Amph protein, we performed Western blot analysis on lysates from control and mutant third instar larvae. Not surprisingly, the genetic null mutant $amph^{5E3}$ was also protein null (Figure 5B). Additionally, we found that the removal of exon 1 also led to a complete elimination of Amph protein expression. In contrast, Amph protein was detected from lysates generated from wildtype flies, the original EP insertion line and two precise excision lines ($amph^{3B2}$, $amph^{3E9}$). Consistent with these results, we also found that Amph was present at the NMJ of wildtype larvae and controls but not in mutants (Figure 5C).

### *amph mutants exhibit locomotion defects*

As mentioned above, all of the *amph* mutants identified were viable but gave rise to larvae and adults that appeared sluggish and slower in their movements. For example, while adult flies are capable of hopping they are essentially flightless. To further quantify any potential locomotory defects, we measured the total distance traveled by third instar larvae over 30 s (35). The genetic null $amph^{5E3}$ mutant larvae showed about a 70% reduction in movement (Figure 6). They moved (mean ± standard error of the mean) 51.1 ± 12.76 pixels (n = 17), compared with 167.4 ± 9.83 pixels (n = 16) for the precise excision line $amph^{3E9}$, and 161.1 ± 11.64 pixels (n = 16) for the original P-element line *EP(2)2175* (Figure 6A,B). This difference was significant in both cases ($p < 0.0001$).

### *amph mutants exhibit no defects in synaptic morphology, physiology or vesicle recycling*

Locomotory defects such as we have observed in our *amph* mutants could reflect defects in synaptic morphology or physiology. To determine if *amph* mutants exhibited any alterations in NMJ morphology, we compared anti-horseradish peroxidase (HRP)-FITC stained NMJs (36) from mutant and control third instar larvae and found no difference in either the number of boutons or the amount of branching (data not shown). Therefore, we concluded that Amph is not required for the normal morphogenesis of the NMJ. Since no

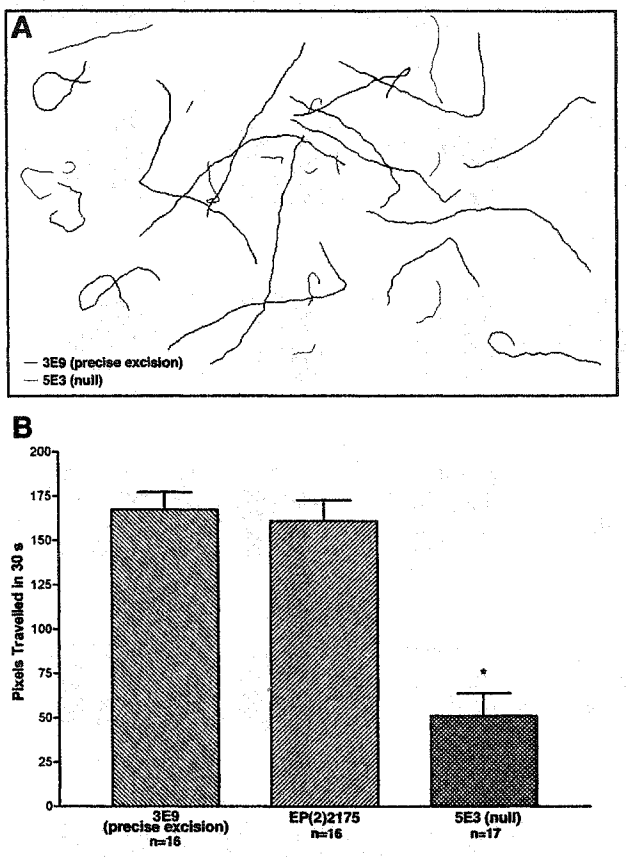


**Figure 6: *amph* mutant larvae have defects in locomotion.** A The distance traveled by 90-h-old third instar larvae was recorded in the dark over 30 s. Sample traces of 16 control larvae (blue) and 17 mutant larvae (red). (B) $amph^{5E3}$ larvae moved only 51.1 ± 12.76 pixels (n = 17; mean ± standard error of the mean), compared with 167.4 ± 9.83 pixels (n = 16) for the precise excision line $amph^{3E9}$, and 161.1 ± 11.64 pixels (n = 16) for the original P-element line *EP(2)2175*. This difference was significant ($p < 0.0001$).

phenotypic difference was detected in any of the mutants and they were all protein null, all subsequent experiments were performed with a single *amph* mutant line, $amph^{5E3}$Figure 7.

To determine whether the locomotory defects in *amph* mutants were due to impaired synaptic physiology, we then characterized synaptic currents from neuromuscular junctions of third instar larvae. Because Amph is predominantly localized postsynaptically, we first analyzed spontaneously occurring quantal events from both the precise excision line and the mutant $amph^{5E3}$ to determine if there were any effects on glutamate receptors (Figure 7). We found the amplitude of mEJCs (excitatory junctional current) from $amph^{5E3}$ was 0.68 ± 0.02 nA (305 mEJCs from 6 cells), while in $amph^{3E9}$ mEJCs were 0.62 ± 0.03 nA (395 mEJCs from 7 cells). We first conducted a single classification ANOVA on the individual cells within each genotype to determine if we could pool these raw data, but we found that there was significant variation ($p < 0.01$) within each genotype. Therefore, rather than pooling the data, we carried out a nested ANOVA on the mEJC amplitudes, as described in Sokal and Rohlf (37). This procedure enabled us to take into account the variation between cells within each genotype while testing for differences between the mutants and controls. When analyzed this way, we found that while there were significant differences ($p < 0.01$) within the genotypes, there was no significant difference in mEJC amplitude between the mutant and controls. Thus we conclude that the *amph* mutant does not alter the mEJC amplitude.

Although we found that Amph was predominantly localized postsynaptically at the NMJ, it remains possible that low levels are present presynaptically but undetectable using immunofluorescence microscopy. These low levels could then be required for SV endocytosis and contribute to the locomotory behavior observed in both larvae and adults. If the mutations re-

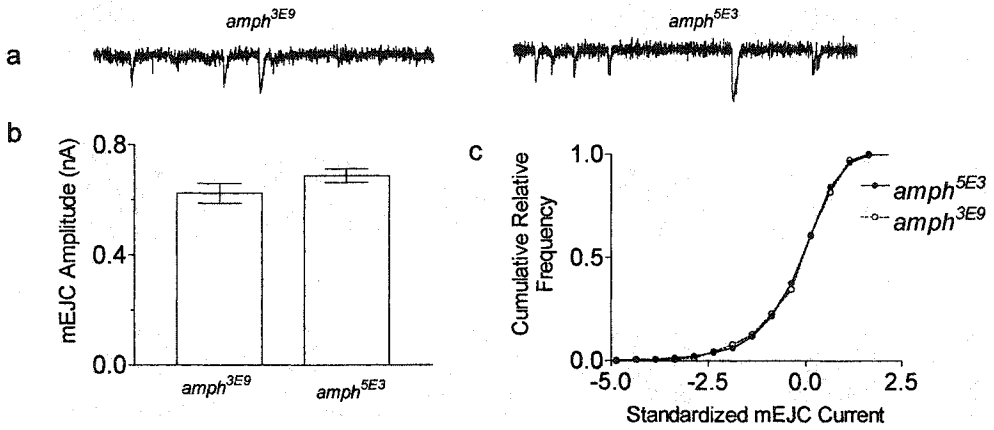


**Figure 7: Miniature excitatory junctional currents measured from *amph* mutants.** (A) Examples of mEJCs recorded from the mean mEJC amplitude measured from $amph^{3E9}$ and mutant $amph^{5E3}$ muscles. (B) Summary of mEJC amplitude data collected from $amph^{3E9}$ (n = 7 cells, 395 mEJCs) and $amph^{5E3}$ (n = 6 cells, 305 mEJCs). (C) The shape of the cumulative relative frequency distribution of standardized mEJC amplitudes was not different between the two genotypes. The data were standardized as described in Frerking et al. (46).

sulted in chronic suppression of vesicle endocytosis, we might expect there to be a reduction in basal transmitter release. However, we found that the mutant line had maximal synaptic currents of 132.2 ± 7.2 nA (n = 8), while the control line had currents of 140.0 ± 8.6 nA (n = 7) (p > 0.3) in 1.0 mM $Ca^{2+}$, HL3 physiological solution (Figure 8A).

To determine if the *amph* mutant affected SV endocytosis in a more dynamic manner, we challenged the synapses with long trains of stimuli. First, in a moderate challenge, we delivered stimuli at 3 Hz for 10 min. This protocol led to a rapid decline in synaptic currents in *shi*$^{1}$ larval synapses, confirming this protocol induced detectable SV endocytosis (Figure 8B). In the *amph* lines we found that both the controls and the mutants maintained synaptic transmission at about 40% of their initial value for the duration of the train (1800 stimuli, Figure 8C,D), whereas responses in the *shi*$^{1}$ larvae go below 40% of their initial value after ~150 stimuli. When we averaged the last 10 values of the 3 Hz train, we found synaptic transmission in the *amph* control line was 39.8 ± 0.03% (n = 5) and in the *amph* mutant it was 44.8 ± 0.05% (n = 5) of the initial value (p > 0.4). Recovery from synaptic fatigue was not altered in the *amph* mutant, as we found that when stimulation frequency was reduced to 0.1 Hz, immediately following the end of the 3 Hz train, synaptic currents returned to near their initial value within ~4 stimuli (40 s) (data not shown) in both lines. To induce the maximal rate of vesicle endocytosis (38), we maximized transmitter release by reducing [$Mg^{2+}$] (from 20 to 5 mM) and increasing [$Ca^{2+}$] (from 1 to 2 mM) of the HL3 medium and delivered 2000 or 4000 stimuli at 10 Hz to the synapses. After 2000 stimuli at 10 Hz, we found EJCs in the control line were 26.0 ± 0.01% (n = 11) and in the *amph* mutant were 23.7 ± 0.01% (n = 13) of the initial quantal content. After 4000 stimuli, we found quantal content in the controls to be 19.4 ± 0.02% (n = 6) and in the mutants it was 17.1 ± 0.03% (n = 6) of the initial values. The small differences between the two genotypes are not significant (p > 0.2). The fractional rates of quantal secretion corresponded to ~1000 quanta/s and at the end of 4000 stimuli the total number of quanta secreted in the mutant was >460 000. In a *shi* mutant background we have estimated the total vesicle pool size to be ~50 000 quanta (B.A.S. unpublished data), in agreement with the range of results previously reported (38). This suggests that in the present experiments the total vesicle pool is turned over ~9 times during the course of this stimulation protocol. Taken together, we could not find evidence for either a chronic or acute impairment of SV endocytosis at the neuromuscular junction in null alleles for *Drosophila amph*.

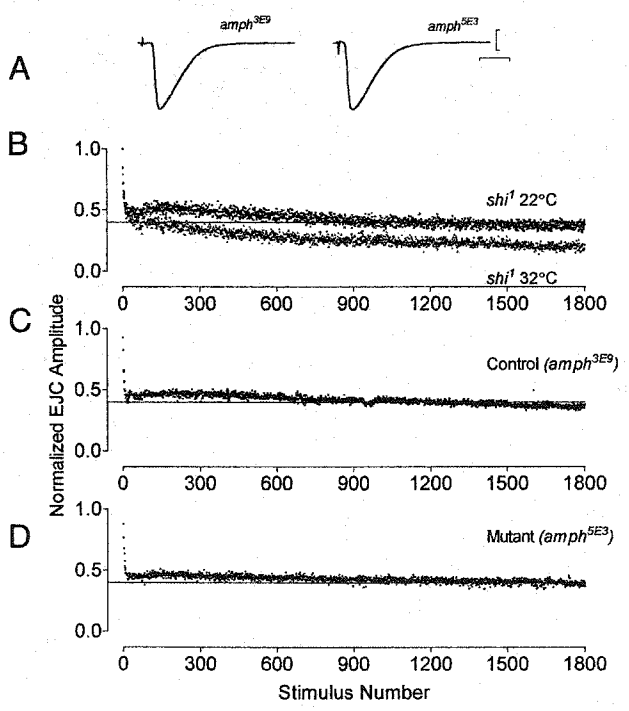


**Figure 8: Synaptic fatigue in *amph* mutants.** (A) Sample evoked traces from *amph*$^{3E9}$ *and amph*$^{5E3}$ cells. Each is the average of 20 individual traces obtained at 0.1 Hz in 1.0 mM $Ca^{2+}$ HL3 solution. Bars: 50 nA; 10 ms (B) 3 Hz stimulation resulted in a modest but clear decline in synaptic transmission of *shi*$^{1}$ synapses at restrictive temperature (32°) compared to the permissive temperature (22°). There was no difference in the responses measured from *amph*$^{5E3}$ (C) and *amph*$^{3E9}$ (D) synapses. Each point represents the mean data obtained from 3 cells of *shi*$^{1}$, 5 cells from each of *amph*$^{3E9}$ and *amph*$^{5E3}$. The solid line in each graph indicates the 40% level. The initial quantal content as determined from the average response to 20 stimuli delivered at 0.1 Hz.

Finally, to examine potential defects in CNS synapses that might account for the locomotory defects observed in mutants, we recorded endogenous motor output from the CNS by measuring the frequency and duration of synaptic activity from intact CNS–NMJ preparations. These experiments did not reveal a major difference in CNS-generated motor activity when *amph* mutants were compared to controls (data not shown).

## Discussion

Amphiphysin was first identified as a cytosolic protein which is highly enriched in nerve terminals and partially associated with synaptic vesicles. Since then, several additional amphiphysin isoforms have been identified in mammals, yeast and nematodes, where they have been implicated in clathrin-mediated endocytosis, actin function and signaling pathways. Amphiphysin is composed of three domains which mediate its interaction with a number of endocytic proteins, such as clathrin and dynamin, suggesting that it functions as a multiprotein adaptor during clathrin-mediated endocytosis. Consistent with this model, experimental manipulations in cells using peptides or dominant-negative constructs that can block the interaction of amphiphysin with either dynamin, or clathrin and AP2, markedly inhibit clathrin-mediated endocytosis.

To further elucidate the function of amphiphysin, we characterized Amphiphysin (Amph) in *Drosophila* and generated

loss-of-function mutations. *Drosophila*, unlike vertebrates, has a single *amphiphysin* gene that gives rise to multiple isoforms by alternative splicing. Alternative splicing has also been observed in vertebrate amphiphysins, particularly amphiphysin 2 (9,39,40). In vertebrates, the largest isoform is a brain-specific 95-kDa protein that is the major amphiphysin found in the brain. In addition, several smaller isoforms have been identified, some of which are cell-type specific while others are ubiquitously expressed. This suggests that in addition to its putative role in SV endocytosis, amphiphysin 2 may have a more general role during development.

Although *Drosophila* Amph shares an equal amount of overall amino acid identity (~30%) with both Amphiphysin 1 and 2 we have identified an additional domain within *Drosophila* Amph that is conserved with Amphiphysin 2 but not Amphiphysin 1, suggesting that *Drosophila* Amph may be an Amphiphysin 2 ortholog. Consistent with this model, we also find that like Amphiphysin 2, *Drosophila* Amph is expressed throughout development and present in several tissues including muscle, CNS and imaginal discs. In most cases, we observe three predominant immuno-reactive bands on Western blots corresponding to 85 kDa, 80 kDa and 45 kDa proteins that are not recognized with the pre-immune serum. The higher molecular weight bands likely correspond to several cDNAs that we have identified. To date, we have yet to identify any cDNAs that could correspond to the smaller 45-kDa band, and it remains possible that it represents a proteolytic product. At present, it is unclear if these represent additional splice variants or different phospho-isoforms of Amph. Several potential phosphorylation sites on *Drosophila* Amph have been identified (28) and Amphiphysin homologs are known to be phosphorylated *in vivo* (10,22,27).

To further characterize the distribution of Amph, we also performed immunohistochemical and immunofluorescence studies. Similar to what we observed using Western blot analysis, we found that Amph is broadly expressed throughout development in a variety of tissues. During early embryogenesis, Amph is found at the sites of developing membranes, epithelial cells as well as the foregut and hindgut. We did not, however, observe any Amph expression in either embryonic CNS or muscle. In contrast, Amph is expressed in both larval muscle and CNS as well as epithelial cells. Surprisingly, unlike its vertebrate counterparts, *Drosophila* Amph was predominantly found post- rather than presynaptically at the neuromuscular junction, suggesting alternative functions for the protein.

To directly assess the *in vivo* role of Amph, we characterized a series of *amph* null mutant lines that we generated by imprecise P-element mobilization. Surprisingly, all of the lines were homozygous viable although both the larvae and adults exhibited locomotory defects. This demonstrates that like yeast, Amph is not required for viability in *Drosophila*. To determine the basis of the locomotory defects in *amph* mutants, we then examined the distribution of Amph at the NMJ and determined if *amph* mutants had any defects in synaptic morphology, physiology or synaptic vesicle endocytosis. We found no evidence for any defects in either the number of synaptic boutons or branching in our *amph* mutants.

Since Amph is localized postsynaptically at the larval neuromuscular junction, Amph may be important for regulating endocytosis of postsynaptic elements such as the glutamate receptors. If this were true, we would have predicted an effect on the amplitude of mEJCs in *amph* mutants but found no differences. Despite the abundance of Amph at postsynaptic locations, it remained possible that a low level of Amph was located within the presynaptic nerve terminal that functions in SV endocytosis. However, our physiological assessment of synaptic physiology at larval neuromuscular junctions did not reveal any chronic or acute defect in neurotransmitter release that would indicate a role for Amph in SV endocytosis at this synapse. Even under stimulation conditions which result in a nine-fold turnover of the releasable pool of SVs, we did not detect a defect in *amph* null mutants. Therefore these data suggest that Amph is not required for the normal function of the larval neuromuscular synapse.

At present, the function of Amph in *Drosophila* remains unclear. The observation that Amph is expressed postsynaptically suggests that it might act to regulate the number of neurotransmitter receptors. However, changes in receptor number would have resulted in a change in the size or distribution of the mEJCs in the *amph* mutants, which we did not observe. Nor were we able to observe any defects in the subcellular localization of two postsynaptic proteins, discs large (Dlg) and Lethal giant larvae (Lgl), which might contribute to the locomotory defects. Discs large is the *Drosophila* ortholog of PSD-95 and is thought to act as a scaffolding molecule which organizes the postsynaptic density (41). Lgl is a tumor suppressor protein which is found in epithelial cells as well as at the NMJ (29), although its function at the NMJ is unclear. We found no evidence that postsynaptic localization of either protein was affected in the *amph* mutants (P.A.L., unpublished observation). However, it remains possible that other muscle defects are responsible for the abnormal locomotion we observed in both mutant larvae and adults.

Alternatively, although Amph is not required at NMJs, it could act within CNS neurons which typically have fewer vesicles available than at NMJs and may require higher rates of SV endocytosis. Consistent with this model, we did observe Amph expression in the CNS. According to this model, Amph would not be necessary for SV endocytosis but would act to promote efficient endocytosis at specific synapses. Although surprising, our data are in fact consistent with *in vitro* binding studies which clearly demonstrate that endocytic proteins thought to be recruited by amphiphysin can assemble in the absence of amphiphysin by binding directly to each other. This suggests that amphiphysin is not required for SV endocytosis but may have evolved to promote high efficiency endocytosis.

Finally, the function of Amph may also be revealed by analyzing the role of other BAR family members. Since *Droso-*

*phila* Amph does not contain the conserved central domain required for interaction with other endocytic proteins, this may suggest that Amph has alternative functions within the cell. For example, the homologs of amphiphysin in budding yeast, Rvs161p and Rvs167p, not only have defects in endocytosis but also exhibit a depolarized actin cytoskeleton, as well as defects in cell polarity and bud-site selection. Although we did not detect any defects in *Drosophila amph* mutants, these may be masked by redundant proteins which act together with Amph to mediate these cellular functions. Clearly, further genetic and biochemical studies will be required to determine if Amph in *Drosophila* can interact with the actin cytoskeleton and other components of the endocytic machinery.

## Materials and Methods

### *Fly stocks and generation of mutants*

All fly stocks were maintained at room temperature on standard cornmeal agar media. Wild-type flies were Oregon-R. Mobilization of the P{EP} transposable P-element (42) insertion in $w^{1118}$; *EP(2)2175* flies (43) was used to generate both the precise excision line $amph^{3E9}$, and the imprecise excision alleles $amph^{2J6}$, $amph^{3B1}$, $amph^{5E3}$, and $amph^{6A2}$. The deficiency *amph-4A10*, which was generated at the same time as the above P-element excision, was balanced with $w^*$; $L^2$ $Pin^1$/*CyO*, p{$w^{+mC}$ = *GAL4-Kr.C*}*DC3*, p{$w^{+mC}$ = *UAS-GFP.S65T*}*DC7* (BL-5194). *Df(2R)amph-4A10* complements *l(2)k08268* (BL-P2350, Bloomington), a P-element insertion in *Sin3A*, but fails to complement both the large deficiency *vg-C* (BL-754) and *l(2)k05316* (BL-P567, Bloomington), a P-element insertion 40 kb 3′ of the *EP(2)2175* insertion in the gene *spt4*. For polymerase chain reactions (PCR), genomic DNA was prepared using the single fly PCR protocol (44), with primers designed using Primer3 (S. Rozen and H.J. Skaletsky 1998, unpublished; http://www-genome.wi.mit.edu/cgi-bin/primer/primer3_www.cgi). The molecular breakpoints for all deletions were determined using a combination of Southern blot analysis and PCR with primers designed to *amph* or its two flanking genes, *Sin3A* and *Gα49B*. Additionally, all mutants complemented the lethality of the local deficiency *amph-4A10*, and *l(2)k08268*. The temperature-sensitive allele of *shibire*, $shi^1$, was obtained from Bloomington (BL-1328). The transgenic line *MHC-Gal4 UAS-CD8::Sh-GFP* (C. Goodman, University of California, Berkeley) contains the transmembrane domain of mouse CD8 fused to a small intracellular portion of the *Drosophila* Shaker $K^+$ channel and to green fluorescent protein (GFP). The transgene is expressed exclusively in muscle, where it localizes to the postsynaptic membrane of the NMJ.

### *Amph antibody generation*

The EST containing the full-length *amph* cDNA, LD19810, was subcloned into a modified pGEX-4T vector (Pharmacia) containing a C-terminal $(His)_6$ cassette. The sequence of the construct was verified by bi-directional sequencing. Protein expression in BSJ72 cells was induced with 1 mM IPTG, and the crude protein was purified using glutathione agarose beads (Sigma). The N-terminal GST tag was removed with thrombin protease (Sigma), and the Amph-$His_6$ protein was further purified with Talon cobalt resin (Clontech) and injected into rabbits for the generation of polyclonal antibodies.

### *Immunohistochemistry and immunoblotting*

For Western blot analysis of wildtype (Oregon-R) expression, protein lysates were made from either different developmental stages (embryos, first, second and third instar larvae, early pupae, and adults) or from different tissues of third instar larvae (whole larvae, body wall, CNS, and imaginal discs). To assess Amph protein expression in *amph* mutants, lysates were made from third instar larvae from each mutant line by homogenization of tissue in 20 µl of Ripa buffer separated by SDS-PAGE on a 10% polyacrylamide gel, transferred to a PVDF membrane, and probed with anti-Amph 9184. Equal loading was confirmed by stripping and reprobing the membrane with anti-β-tubulin antibody. Primary antibodies used were rabbit anti-Amph 9184, 1 : 1500, and mouse anti-β-tubulin, 1 : 1000. Secondary antibodies used were goat anti-rabbit IgG-HRP 1 : 10 000 (Bio-Rad) and goat anti-mouse-HRP 1 : 10 000 (Bio-Rad).

Immunofluorescence of wandering third instar larvae was performed as described (43). Primary antibodies used were crude or affinity-purified anti-Amph 9184, 1 : 1000 (preadsorbed with $amph^{5E3}$ embryos), mouse anti-cysteine string protein (CSP), 1 : 1000 (Konrad Zinsmaier), rat anti-crumbs, 1 : 500 (Ulrich Tepass), rabbit anti-gl, 1 : 200 (Fumio Matsuzaki) and rabbit anti-Dlg, 1 : 5000 (Vivian Budnik). Secondary antibodies used were goat anti-rabbit IgG-FITC, 1 : 200 (Bio-Rad), donkey anti-rabbit IgG-Cy3, 1 : 1000 and donkey anti-mouse IgG-Cy3, 1 : 1000 (Jackson Immunochemicals). Staining of the NMJs with goat anti-HRP-FITC, 1 : 500 (ICN Biomedicals, Costa Mesa, CA, USA) was performed without a secondary antibody.

### *Electrophysiology*

Synaptic junctional currents were measured from abdominal muscle 6 of segments 3–4 using the two-electrode voltage clamp mode of an Axoclamp 2B Amplifier (Axon Instruments, Inc., Foster City, CA). For nerve stimulated experiments the nerves were cut close to the CNS and the CNS removed. For measuring endogenous motor output, the CNS and nerves were left intact. Statistical analysis was performed with Prism3 (Graphpad Software, Inc). Physiological solutions and methodology for measurements of synaptic junctional currents and data analysis are described in (45). For long trains of stimuli, we first collected baseline data by evoking 20 EJCs at a frequency of 0.1 Hz. We then increased the stimulation frequency to 3 or 10 Hz for the duration of the train. The EJC amplitudes measured during the train were normalized to the mean value of the baseline data for each cell. Quantal content was estimated for the *amph* mutant and control lines by dividing the mean EJC amplitude by the mean mEJC amplitude collected for each genotype.

### *Locomotion assay*

Locomotion assays were performed as described in Iyengar et al. (35). One-hour embryo collections made on grape agar plates were aged 23 h and cleared of hatched larvae. After a further 1 h of aging, all hatched larvae were transferred to a 5-cm Petri dish containing fly food without cornmeal and aged to 90 h (late foraging third instar stage) at 25 °C. Individual larvae were rinsed in $dH_2O$, and transferred to a 10-cm plate containing 1% agar to dry off for 1 min. The larva was then transferred to another 1% agar plate and allowed to habituate for 30 s before tracking was initiated. The real-time movement tracking of the larva was recorded under darkroom safelight illumination (20 W incandescent lamp, Kodak GBX-2 filter) and a CCD camera (Model TSE272S, ELMO Mfg. Corp Plainview, NY) interfaced to a Scion AG-5 video rate frame grabber connected to a PowerMac 9500/200 computer. Track data were obtained using a semi-automated setup that involved a macro program written in NIH Image v1.61b (a public domain image analysis program developed at the US National Institutes of Health). The program was driven by a digitizing tablet–stylus setup (Intuos Tablet, Wacom Technology Co. WA, USA). The macro program recorded all the X–Y coordinates of the track. These data were used to create the locomotory track and to calculate the distance traveled by the larva in 30 s. The data were analyzed with Prism 3 (Graphpad Software, Inc.).

## Acknowledgments

We thank C. Goodman for providing the CD8:Sh-GFP flies and C.C. Hui for the GST-$His_6$ vector. We also thank the following individuals for kindly

providing us with antibodies to the following proteins: K. Zinsmaier (CSP), U. Tepass (crb); F. Matsuzaki (1(2)gl) and V. Budnik (dlg). We also thank U. Tepass and W.S. Trimble for useful discussions and W.S. Trimble for critical comments on the manuscript. Finally, we also wish to thank C. Doe for sharing information prior to publication. This work was supported by funds from the Canadian Institutes of Health Research to G.L.B. and Doctoral Research Awards to P.A.L. and B.M.C. G.L.B. is the recipient of a CIHR Investigator award and B.A.S. is the recipient of a Post-doctoral Fellowship from the Hospital for Sick Children Research Training Center.

## References

1. De Camilli P, Takei K. Molecular mechanisms in synaptic vesicle endocytosis and recycling. Neuron 1996;16:481–486.
2. De Camilli P, Takei K, McPherson PS. The function of dynamin in endocytosis. Curr Opin Neurobiol 1995;5:559–565.
3. Stowell MHB, Marks B, Wigge P, McMahon HT. Nucleotide-dependent conformational changes in dynamin: evidence for a mechanochemical molecular spring. Nat Cell Biol 1999;1:27–32.
4. Sever S, Muhlberg AB, Schmid SL. Impairment of dynamin's GAP domain stimulates receptor-mediated endocytosis. Nature 1999;398:481–486.
5. McPherson PS, Garcia EP, Slepnev VI, David C, Zhang X, Grabs D, Sossin WS, Bauerfeind R, Nemoto Y, De Camilli P. A presynaptic inositol-5-phosphatase. Nature 1996;379:353–357.
6. Schmidt A, Wolde M, Thiele C, Fest W, Kratzin H, Podtelejnikov AV, Witke W, Huttner WB, Soling HD. Endophilin I mediates synaptic vesicle formation by transfer of arachidonate to lysophosphatidic acid. Nature 1999;401:133–141.
7. Lichte B, Veh RW, Meyer HE, Kilimann MW. Amphiphysin, a novel protein associated with synaptic vesicles. EMBO J 1992;11:2521–2530.
8. Ramjaun AR, Micheva KD, Bouchelet I, McPherson PS. Identification and characterization of a nerve terminal-enriched amphiphysin isoform. J Biol Chem 1997;272:16700–16706.
9. Sakamuro D, Elliott KJ, Wechsler-Reya R, Prendergast GC. BIN1 is a novel Myc-interacting protein with features of a tumour suppressor. Nat Genet 1996;14:69–77.
10. Wigge P, Vallis Y, McMahon HT. Inhibition of receptor-mediated endocytosis by the amphiphysin SH3 domain. Curr Biol 1997;7:554–560.
11. Ramjaun AR, Philie J, de Heuvel E, McPherson PS. The N terminus of amphiphysin II mediates dimerization and plasma membrane targeting. J Biol Chem 1999;274:19785–19791.
12. McMahon HT, Wigge P, Smith C. Clathrin interacts specifically with amphiphysin and is displaced by dynamin. FEBS Lett 1997;413:319–322.
13. Slepnev VI, Ochoa G-C, Butler MH, Grabs D, De Camilli P. Role of phosphorylation in regulation of the assembly of endocytic coat complexes. Science 1998;281:821–824.
14. Ramjaun AR, McPherson PS. Multiple amphiphysin II splice variants display differential clathrin binding: identification of two distinct clathrin-binding sites. J Neurochem 1998;70:2369–2376.
15. Leprince P, Romero F, Cussac D, Vayssiere B, Berger R, Tavitian A, Camonis JH. A new member of the amphiphysin family connecting endocytosis and signal transduction pathways. J Biol Chem 1997;272:15101–15105.
16. David C, McPherson PS, Mundigl O, De Camilli P. A role of amphiphysin in synaptic vesicle endocytosis suggested by its binding to dynamin in nerve terminals. Proc Natl Acad Sci USA 1996;93:331–335.
17. Shupliakov O, Low P, Grabs D, Gad H, Chen H, David C, Takei K, De Camilli P, Brodin L. Synaptic vesicle endocytosis impaired by disruption of dynamin-SH3 domain interactions. Science 1997;276:259–263.
18. Volchuk A, Narine S, Foster LJ, Grabs D, De Camilli P, Klip A. Perturbation of dynamin II with an amphiphysin SH3 domain increases GLUT4 glucose transporters at the plasma membrane in 3T3-L1 adipocytes. Dynamin II participates in GLUT4 endocytosis. J Biol Chem 1998;273:8169–8176.
19. Cestra G, Castagnoli L, Dente L, Minenkova O, Petrilli A, Mignone N, Hoffmuller U, Schneider-Mergener J, Cesareni G. The SH3 domains of endophilin and amphiphysin bind to the proline-rich region of synaptojanin 1 at distinct sites that display an unconventional binding specificity. J Biol Chem 1999;274:32001–32007.
20. Slepnev VI, Ochoa GC, Butler MH, De Camilli P. Tandem arrangement of the clathrin and AP-2 binding domains in amphiphysin 1 and disruption of clathrin coat function by amphiphysin fragments comprising these sites. J Biol Chem 2000;275:17583–17589.
21. Munn AL, Stevenson BJ, Geli MI, Reizman H. end5, end6 and end7: mutations that cause actin delocalization and block the internalization step of endocytosis in *Saccharomyces cerevisiae*. Mol Biol Cell 1995;6:1721–1742.
22. Lee J, Colwill K, Aneliunas V, Tennyson C, Moore L, Ho Y, Andrews B. Interaction of yeast Rvs167 and Pho85 cyclin-dependent kinase complexes may link the cell cycle to the actin cytoskeleton. Curr Biol 1998;8:1310–1321.
23. Crouzet M, Urdaci M, Dulau L, Aigle M. Yeast mutant affected for viability upon nutrient starvation. characterization and cloning of the RVS161 gene. Yeast 1991;7:727–743.
24. Bauer F, Urdaci M, Aigle M, Crouzet M. Alteration of a yeast SH3 protein leads to conditional viability with defects in cytoskeletal and budding patterns. Mol Cell Biol 1993;13:5070–5084.
25. Sivadon P, Bauer F, Aigle M, Crouzet M. Actin cytoskeleton and budding pattern are altered in the yeast rvs161 mutant: the RVS161 protein shares common domains with the brain protein amphiphysin. Mol Gen Genet 1995;246:484–495.
26. Balguerie A, Sivadon P, Bonneu M, Aigle M. Rvs167p, the budding yeast homolog of amphiphysin, colocalizes with actin patches. J Cell Sci 1999;112:2529–2537.
27. Floyd SR, Porro EB, Slepnev VI, Ochoa GC, Tsai LH, De Camilli P. Amphiphysin binds the cdk5 regulatory subunit p35 and is phosphorylated by cdk5 and cdc2. J Biol Chem 2001;276:8104–8110.
28. Razzaq A, Su Y, Mehren JE, Mizuguchi K, Jackson AP, Gay NJ, O'Kane CJ. Characterization of the gene for *Drosophila* amphiphysin. Gene 2000;41:167–174.
29. Lloyd TE, Verstreken P, Ostrin EJ, Phillippi A, Lichtarge O, Bellen HJ. A genome-wide search for synaptic vesicle cycle proteins in *Drosophila*. Neuron 2000;26:25–50.
30. Neufeld TP, Tang AH, Rubin GM. A genetic screen to identify components of the sina signaling pathway in *Drosophila* eye development. Genetics 1998;148:277–286.
31. Penneta G, Pauli D. The *Drosophila* Sin3 gene encodes a widely distributed transcription factor essential for embryonic viability. Dev Genes Evol 1998;208:531–536.
32. Lee YJ, Dobbs MB, Verardi ML, Hyde DR. dgq: a *Drosophila* gene encoding a visual system-specific G alpha molecule. Neuron 1990;5:889–898.
33. Strathmann M, Simon MI. G protein diversity. a distinct class of alpha subunits is present in vertebrates and invertebrates. Proc Natl Acad Sci USA 1990;87:9113–9117.
34. Marsh M, McMahon HT. The structural era of endocytosis. Science 1999;285:215–220.
35. Iyengar B, Roote J, Campos AR. The tamas gene, identified as a mutation that disrupts larval behavior in *Drosophila melanogaster*, codes for the mitochondrial DNA polymerase catalytic subunit (DNApol-gamma125). Genetics 1999;153:1809–1824.
36. January LY, January YN. Properties of the larval neuromuscular junction in *Drosophila melanogaster*. J Physiol (London) 1976;262:189–214.

37. Sokal RR, Rohlf FJ. Biometry. San Francisco: W.H. Freeman; 1969.
38. Delgado R, Maureira C, Oliva C, Kidokoro Y, Labarca P. Size of vesicle pools, rates of mobilization, and recycling at neuromuscular synapses of a *Drosophila* mutant, shibire. Neuron 2000;28:941–953.
39. Butler MH, Ochoa DC, Freyberg Z, Daniell L, Grabs D, Cremona O, De Camilli P. Amphiphysin II (SH3P9;BIN1), a member of the amphiphysin/Rvs family, is concentrated in the cortical cytomatrix of axon initial segments and nodes of ranvier in brain and around T tubules in skeletal muscle. J Cell Biol 1997;137:1355–1367.
40. Wechsler-Reya R, Sakamura D, Zhang J, Duhadaway J, Prendergast GC. Structural analysis of the BIN1 gene. Evidence for tissue-specific transcriptional regulation and alternate RNA splicing. J Biol Chem 1997;272:31453–31458.
41. Lahey T, Gorczyca M, Jia XX, Budnik V. The *Drosophila* tumor suppressor gene dlg is required for normal synaptic bouton structure. Neuron 1994;13:823–835.
42. Rorth P. A modular misexpression screen in *Drosophila* detecting tissue-specific phenotypes. Proc Natl Acad Sci USA 1996;93:12418–12422.
43. Rorth P, Szabo K, Bailey A, Laverty T, Rehm J, Rubin GM, Weigmann K, Milan M, Benes V, Ansorge W, Cohen SM. Systemic gain-of-function genetics in *Drosophila*. Development 1998;125:1049–1057.
44. Gloor GB, Preston CR, Johnson-Schlitz DM, Nassif NA, Phillis RW, Benz WK, Robertson HM, Engels WR. Type I repressors of P element mobility. Genetics 1993;135:81–95.
45. Stewart BA, Mohtashami M, Trimble WS, Boulianne GL. SNARE Proteins contribute to calcium cooperativity of synaptic transmission. Proc Natl Acad Sci USA 2000;97:13955–13960.
46. Frerking M, Borges S, Wilson M. Variation in GABA mini amplitude is the consequence of variation in transmitter concentration.. Neuron 1995;15:885–895.

**E: Manuscript -** The accessory subunit of DNA polymerase γ is essential for mitochondrial DNA maintenance and development in *Drosophila melanogaster*

# The accessory subunit of DNA polymerase $\gamma$ is essential for mitochondrial DNA maintenance and development in *Drosophila melanogaster*

**Balaji Iyengar*, Ningguang Luo†, Carol L. Farr†, Laurie S. Kaguni†, and Ana Regina Campos*‡**

*Department of Biology, McMaster University, Hamilton, ON, Canada L8S 4K1; and †Department of Biochemistry and Molecular Biology, Michigan State University, East Lansing, MI 48824-1319

Edited by I. Robert Lehman, Stanford University School of Medicine, Stanford, CA, and approved February 5, 2002 (received for review December 12, 2001)

**DNA polymerase $\gamma$, Pol $\gamma$, is the key replicative enzyme in animal mitochondria. The *Drosophila* enzyme is a heterodimer comprising catalytic and accessory subunits of 125 kDa and 35 kDa, respectively. Both subunits have been cloned and characterized in a variety of model systems, and genetic mutants of the catalytic subunit were first identified in *Drosophila*, as chemically induced mutations that disrupt larval behavior (*tamas*). Mutations in the gene encoding the accessory subunit have not yet been described in any organism. Here, we report the consequences of null mutations upon mitochondrial DNA (mtDNA) replication and morphology, cell proliferation, and organismal viability. Mutations in the accessory subunit cause lethality during early pupation, concomitant with loss of mtDNA and mitochondrial mass, and reduced cell proliferation in the central nervous system. Surprisingly, the function of the central nervous system and muscle, as assessed in a locomotion assay, are only marginally affected. This finding is in contrast to our previous findings that disruption in the function of the catalytic subunit causes severe reduction in larval locomotion. We discuss our results in the context of current hypotheses for the function of the accessory subunit in mtDNA replication.**

The cellular requirement for energy varies during development and as a consequence of different physiological signals. The differential demand is met by changes in mitochondrial proliferation and function (1). In turn, modulation of mitochondrial biogenesis depends upon gene products encoded by the mitochondrial and nuclear genomes. One important aspect of mitochondrial proliferation is appropriate mitochondrial DNA (mtDNA) replication and expression, carried out by nuclear-encoded gene products. Therefore, mitochondrial biogenesis and maintenance requires the integrated expression of two distinct genomes as well as the coordinated replication of the mitochondrial genome. A link between the cell cycle and mitochondrial biogenesis has been demonstrated recently in *Drosophila*. Expression of the genes encoding the mitochondrial single-stranded DNA-binding protein (*lopo*), mitochondrial transcription factor A (*D-mtTFA*), and the accessory subunit of the mitochondrial DNA polymerase (*pol* $\gamma$-$\beta$) depend upon the presence of binding sites for the transcription factor DREF (2–4). This factor has been shown to play a role in the orchestrated expression of genes involved in cell cycle control and nuclear DNA replication (5, 6).

Recently, mitochondrial function has emerged as an essential component of different apoptotic pathways. Several signals that lead to cell death are integrated by the mitochondria and lead to the release of cytochrome *c* (7). Toxic insults of different origins including hypoxia may damage the mitochondria, triggering changes in mitochondrial permeability and, thereby, activating programmed cell death. Consistent with these findings, mitochondrial dysfunction has been reported as causing or contributing to a wide variety of neural degenerative diseases and encephalomyopathies (8). For example, expression of mutant superoxide dismutase in transgenic mice, an animal model for amyotrophic lateral sclerosis, causes massive mitochondrial degeneration and subsequent motoneuron death (9). Similarly, dopamine oxidation products have been shown to open the mitochondrial permeability transition pore, thereby implicating mitochondrial dysfunction in the neuronal cell death observed in Parkinson's disease (10).

Of particular interest among the various diseases caused by inherited mitochondrial dysfunctions are the encephalomyopathies characterized by mtDNA depletion that are caused by mutations in nuclear genes. The importance of mtDNA metabolism in this subgroup of mitochondrial disorders is underscored by the recent finding (11) that recessive and dominant forms of progressive external opthalmoplegia are associated with mutations in the catalytic subunit of mitochondrial DNA polymerase, Pol $\gamma$. Similar mutations were first reported in *Drosophila melanogaster*. These were recovered as chemically induced mutations that disrupt larval behavior (*tamas*) and were shown to have an overall cell proliferation, cell growth defect, and a marked reduction in the mitochondrial mass in the central nervous system (CNS; ref. 12). Amongst the lesions described in both humans and *Drosophila* were amino acid substitutions in the polymerase domain and in regions of the enzyme not yet associated with a specific biochemical function.

Another essential component of the mtDNA replication machinery that functions in helix destabilization is the mitochondrial single-stranded DNA-binding protein, mtSSB. Mutations in the mtSSB gene (*low power*, or *lopo*) were identified in *Drosophila* as a P element insertion that disrupts the development of the adult visual system. *lopo* mutants show a defect in cell proliferation concomitant with a drastic decrease in mitochondrial DNA content and loss of respiration (13). These studies substantiate the usefulness of *Drosophila* as a model for the study of mtDNA replication, in the context of the organismal requirement for mitochondrial DNA maintenance and biogenesis.

In animal mitochondria, Pol $\gamma$ is the sole polymerase responsible for mtDNA replication. It is a highly accurate and processive enzyme, comprising a catalytic subunit ($\alpha$) and an accessory subunit ($\beta$). Both subunits have been cloned and characterized in a variety of systems, including *Drosophila* (14, 15). The catalytic subunit contains both 5′→3′ DNA polymerase and 3′→5′ exonuclease activities. Biochemical studies have demonstrated that the accessory subunit is essential for the catalytic efficiency and the high processivity of the holoenzyme (16–20). Structural and functional studies support the hypothesis that the accessory subunit has an additional role as a primer recognition

This paper was submitted directly (Track II) to the PNAS office.

Abbreviations: mtDNA, mitochondrial DNA; CNS, central nervous system; Pol $\gamma$, mitochondrial DNA polymerase; BrdUrd, 5′-bromo-2′-deoxyuridine.

‡To whom reprint requests should be addressed at: Department of Biology, McMaster University, 1280 Main Street West, Hamilton, ON, Canada L8S 4K1. E-mail: camposa@mcmaster.ca.

The publication costs of this article were defrayed in part by page charge payment. This article must therefore be hereby marked "*advertisement*" in accordance with 18 U.S.C. §1734 solely to indicate this fact.

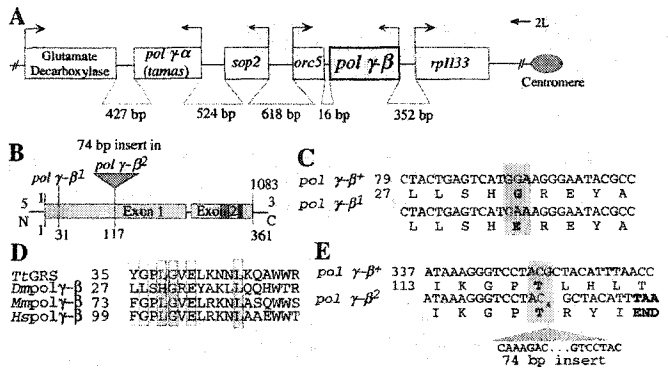


**Fig. 1.** Molecular characterization of mutations in the accessory subunit gene of *Drosophila* Pol γ. (*A*) Schematic representation of the ≈12-kb micro region that contains the tightly packed ORFs of six genes, including the mitochondrial DNA polymerase catalytic subunit *pol γ-α* and its accessory subunit *pol γ-β*. Arrows indicate the direction of transcription; distances between the ORFs are indicated below the schematic. (*B*) Key features in the *pol γ-β* ORF. The gene contains two exons; the positions of the sequenced mutations are indicated. (*C*) Nucleotide and amino acid sequence alignments of the parental strain with the *pol* $\gamma$-$\beta^1$ mutant allele. The base substitution at nucleotide 92 changes amino acid 31 from glycine, a highly conserved amino acid, to glutamic acid. (*D*) Amino acid sequence alignment within motif 1 of *Thermus thermophilus* Glycyl-tRNA synthetase with *D. melanogaster*, mouse, and human Pol γ-β. The asterisk denotes the residue that is mutated in the *pol* $\gamma$-$\beta^1$ allele. The unshaded box represents a similar amino acid, and the shaded boxes indicate conserved amino acids among all four proteins. (*E*) Nucleotide and amino acid sequence alignments of wild-type strain with the *pol* $\gamma$-$\beta^2$ mutant allele. The *pol* $\gamma$-$\beta^2$ allele contains a 74-bp insertion after nucleotide position 350, within the codon for threonine 117 within exon 1. This insertion results in premature termination of the translational product.

factor (21–23). A cellular requirement for the accessory subunit has not yet been demonstrated, because mutations in the gene encoding it have not been described in any organism.

The gene encoding the accessory subunit of Pol γ in *Drosophila* (*pol γ-β*) is located in the 34D subdivision of the left arm of the second chromosome, 3.8 kb distal from the gene encoding the catalytic subunit (*pol γ-α/tamas*; refs. 12 and 15). This chromosomal microregion has been mutagenized extensively and studied by Ashburner and coworkers (24) and represents the first sequenced 3-Mb segment of the *Drosophila* genome. It is characterized by a gene density considerably above the average for the whole genome (refs. 4 and 25; Fig. 1*A*).

To evaluate the role of the accessory subunit in mtDNA synthesis and in mitochondrial function *in vivo*, we sought to identify mutations in the gene encoding it. The superimposition of the physical map (represented by the DNA sequence) with the genetic map (represented by the ordered complementation groups as determined by classical genetic analysis) allowed the identification of candidate mutations in the *pol γ-β* gene. Here, we report the molecular and phenotypic characterization of these mutations that serve to demonstrate for the first time the essential function of the accessory subunit of DNA polymerase γ in animals.

## Materials and Methods

**Fly Stocks and Culture.** Alleles of the 34De complementation group and a deficiency stock *Df(2L)b80c1* were obtained from the Bloomington *Drosophila* Stock Center at Indiana University. The *34De*$^1$ parental stock was kindly provided by John Roote (Univ. of Cambridge, U.K.); the *tamas* (*pol γ-α*) alleles used in this study have been described earlier (12). The following are the genotypes of stocks that were used in this study: (*i*) *l(2)34De*$^1$ *Adh*$^{UF}$ *rds pr*$^1$ *cn*$^1$/*CyO*($y^+$); (*ii*) *In(2LR)Gla, wgGla-1 l(2)34De*$^2$/*CyO*($y^+$); (*iii*) yw; *tam*$^9$/*CyO*($y^+$); (*iv*) *b tam*$^2$ *Adh*$^{n4}$/*CyO*($y^+$); (*v*) Canton-S; (*vi*) *yw;Df(2L)b80c1/CyO*($y^+$); (*vii*) *yw;+/+;Hs-34De*$^+$; (*viii*) *yw;S/CyO*($y^+$); (*ix*) *+;Sp/Sm5;Ly/Tm3Sb*.

Culture medium was made of inactivated yeast, sucrose, 10% tegosept made in ethanol and 1 ml acid mix (10 parts of propionic acid:1 part of phosphoric acid per 100 ml of fly culture medium). For behavioral assays, the culture medium was supplemented with 1.25 g of β-carotene per liter of culture medium. Crosses were set with 5–10 pairs of male and virgin female flies in 100 × 25 mm vials; parents were allowed to lay eggs for 4–5 days.

**Complementation Analysis.** The genetic map of the 34D region (12) (John Roote, personal communication) suggested that alleles of 34De lethal complementation group were likely candidates for mutations in the *pol γ-β* subunit gene. The deficiency stock *Df(2L)b80c1* with breakpoints (34D3:34E2) removes genes *l(2)34Db-Ance* (24). The chromosomes containing the lethal alleles and the deficiency stocks were crossed into a *yw;CyO*($y^+$) background by using a *yw;S/CyO*($y^+$) stock followed by selection against *Star* phenotype.

To rescue the lethality associated with the mutation in *pol* $\gamma$-$\beta^1$ allele, we crossed a transgenic line containing HS-*pol* $\gamma$-$\beta^+$ (insert in the third chromosome) to the *34De*$^1$(*pol* $\gamma$-$\beta^1$) fly stock. This transgene contained a miniwhite gene that confers orange eye color in a mutant white eye color background. Thus, in the genetic cross *yw/yw; pol* $\gamma$-$\beta^1$/*CyO*; HS-*pol* $\gamma$-$\beta^+$ × *yw/Y*; *Df(2L)b80c1/CyO*($y^+$), we observed that of 115 flies that were scored, all straight-winged flies ($n = 31$) exhibited the orange eye color. A heat shock stimulus was not necessary.

**Larval Behavior Assay.** Eggs were collected overnight and larvae hatching in a 3-h window were picked after a 24-h incubation at 25°C. Larvae were allowed to grow in β-carotene-supplemented medium for 80–90 h in a 12 h light/12 h dark cycle. Locomotory tests were conducted on third instar larvae under safelight (20 watt lamp with Kodak GBX-2 filter). The larva was picked with a fine brush from the culture medium and was rinsed with distilled water. It was then placed on a 1% agar surface for 1 min to allow acclimation and to dislodge water. The locomotory behavior was assayed by measuring the distance traveled by the larva in 30 s. The distance traveled by the larva was measured in pixel units with a semiautomatic tracking system that was driven through a macro program written in NIH IMAGE (available on request).

**Fluorescence Staining for Mitochondria and Nucleus in the Larval Brain.** Staining was performed as described in (12) with the following modifications. After dissection in PBS, individual brains were immediately transferred to a glass tube containing Mitotracker CMX-Ros (M-7512, Molecular Probes) at 1 μg/ml concentration in PBS. After 10 min, the brains were transferred to a glass tube containing 100 ng/ml of 4′,6-diamidino-2-phenylindole (DAPI) in PBS for 3–4 min. The mitochondrial and nuclear profiles were visualized separately by using the Texas red and DAPI filters, respectively. The images were captured by using a SPOT charge-coupled device (CCD) camera, and the images were merged by using the SPOT imaging software (Diagnostic Instruments, Sterling Heights, MI).

**5′-Bromo-2′-Deoxyuridine (BrdUrd) Staining.** BrdUrd was dissolved in an injection buffer (1 mg/ml in 0.1 mM $NaPO_4$/5 mM KCl). Injection was carried out on late third instar larvae anesthetized on a $CO_2$ pad for a few minutes by using a micromanipulator setup and pulled glass needle. BrdUrd solution (≈1 μl) was injected into the thoracic region. The larva was then placed in a Petri dish with moist filter paper for 4 h to allow incorporation. The CNS was dissected and further processed as described (26). The preparations were viewed with Nomarski optics in a Zeiss

Axioskop microscope. Images were captured by using a SPOT CCD camera.

**DNA Sequencing.** Genomic DNA from appropriate genotypes were extracted from larvae as described in ref. 12. Templates for DNA sequencing were produced by PCR amplification by using the primer set 5′-GAG AAT GTT GCG TCT GTT CA-3′ and 5′-GAA GGT TCC GCT AGG CTG-3′. This primer set amplified a 1.638-kb product that included a 447-bp upstream sequence of the translational start site and 120 bp after the translational stop site. To sequence the whole 1.638-kb product, we used the above mentioned primers and 5′-GGA AGA CAA TAA ACT GGA GC-3′. This primer was designed from within the ORF. Automated sequencing was done by using the cycle-sequencing protocol with *Taq*-FS enzyme and BigDye terminator chemistry in a Perkin-Elmer ABI 373 stretch machine. Mutations were confirmed by sequencing two independent samples. The *pol* $\gamma$-$\beta^1$ mutation was further confirmed by sequencing the parental strain of this stock. Sequence alignments were performed by using CLUSTALX software (27).

**Larval Preparation for Southern and Immunoblot Analyses.** Embryos of wild-type and homozygous or heterozygous *pol* $\gamma$-$\beta$ flies were collected for 0–6 h on fly food plates. The embryos were incubated at 25°C for 24 h. All larvae that had already hatched at 24 h were discarded, and larvae that emerged in the next 3 h were collected and transferred to a fresh food plate. The heterozygous *CyO*($y^+$) larvae were separated from the homozygous *yellow* mouth-hook larvae before the transfer. Larvae were allowed to grow for 6–7 days at 25°C; they were harvested by washing several times with 0.01% Triton X-100/0.7% NaCl, frozen in liquid nitrogen, and stored at −80°C.

To prepare larval extracts for protein analysis, 150 larvae (≈0.25 g) were suspended in 0.5 ml of HB-0.28 (15 mM Hepes, pH 8.0/0.28 M sucrose/5 mM KCl/2 mM $CaCl_2$/0.5 mM EDTA/1 mM phenylmethylsulfonyl fluoride/10 mM sodium metabisulfite/2 $\mu$g per ml leupeptin/2 mM DTT). The larvae were homogenized by grinding 10 times with a microfuge pestle on ice. The homogenate was centrifuged at 1000 × *g* for 30 s at 3°C in a microcentrifuge, and the supernatant fraction was collected and saved. The pellet was reground in 0.1 ml of the same buffer and centrifuged as above, twice. The resulting supernatant fractions were combined and centrifuged at 8000 × *g* for 3 min to pellet mitochondria. The mitochondrial pellet was washed three times by resuspension in 0.5 ml HB-0.28 followed by recentrifugation and then frozen in liquid nitrogen and stored at −80°C. In the preparation of mitochondrial extracts, the mitochondrial pellets were thawed on ice for 10 min and resuspended in 0.5 ml/gm EB-mitos [25 mM Hepes, pH 8.0/10% (vol/vol) glycerol/2 mM EDTA/0.3 M NaCl/1 mM phenylmethylsulfonyl fluoride/10 mM sodium metabisulfite/2 mg/ml leupeptin/2 mM DTT]. Sodium cholate was added to 2% final concentration, and the mixture was incubated for 30 min on ice, with gentle flicking every 5 min. The extract was centrifuged at 13,000 × *g* for 30 min at 3°C in a microcentrifuge, and the supernatant was removed carefully and used as the soluble mitochondrial fraction.

## Results

**Identification and Molecular Characterization of Mutations in the Accessory-Subunit Gene of DNA Polymerase $\gamma$.** The ≈12-kb microregion containing the gene for the accessory subunit of DNA polymerase $\gamma$ is depicted in Fig. 1. Two mutant alleles isolated previously within the complementation group *l(2)34De* or *l(2)br16* were identified as candidate mutations in *pol* $\gamma$-$\beta$ (24). Sequence analysis demonstrated that these mutant strains indeed carried disruptions in the *pol* $\gamma$-$\beta$ gene (Fig. 1*B*). The mutant allele *pol* $\gamma$-$\beta^1$ is an EMS-induced mutation resulting in a glutamic acid substitution of a highly conserved glycine residue in the N-terminal domain of the accessory subunit (Fig. 1 *C* and *D*). The *pol* $\gamma$-$\beta^2$ allele is a spontaneous mutation caused by an in-frame 74-bp insertion in the N-terminal domain that creates a premature stop (Fig. 1*E*). The lethal complementation group *l(2)34De* is thus demonstrated as encoding the accessory subunit of DNA polymerase $\gamma$. This conclusion was further substantiated by the finding that one copy of the *pol* $\gamma$-$\beta$ gene under the control of the heat shock promoter *hsp70* partially complements the lethality caused by the *pol* $\gamma$-$\beta^1$ mutation (see *Materials and Methods*).

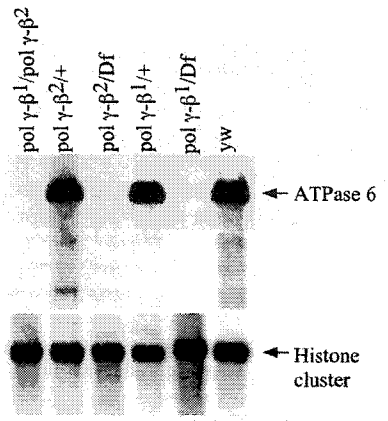


**Fig. 2.** Mitochondrial DNA is absent in mutants of the accessory subunit of *Drosophila* Pol $\gamma$. Three micrograms of total DNA that was isolated from third instar larvae was digested with *Xho*I, which cleaves mtDNA once; duplicate samples of the DNAs (1 $\mu$g) were electrophoresed in a 0.8% agarose gel, transferred to a nylon membrane, and hybridized with $^{32}$P-labeled DNA probes from the ATPase 6 gene of mtDNA and a repeated histone gene cluster as a nuclear DNA control.

**Loss of mtDNA Caused by Mutations in the Accessory Subunit Gene Disrupts Mitochondrial Morphology.** Biochemical studies have demonstrated that the accessory subunit of *Drosophila* Pol $\gamma$ is essential to maintaining the catalytic efficiency of the holoenzyme (17, 23). Additionally, the accessory subunit is likely involved in maintaining the structural integrity of the holoenzyme through contacts between its M and C regions, with multiple sites in the exonuclease (exo) region, and part of the spacer between the exo and DNA polymerase (pol) regions of the catalytic subunit (23). Furthermore, structural modeling predicted roles for the accessory subunit in both primer recognition and in processivity (21). Thus, it was important to evaluate mtDNA content and integrity in the *pol* $\gamma$-$\beta$ mutants. Fig. 2 shows a quantitative Southern blot of wild-type and *pol* $\gamma$-$\beta$ mutant DNA hybridized with a mtDNA probe and with a multiple-copy genomic probe as a control. Multiple analyses of mtDNA content of moribund larvae late in the 3rd instar reproducibly failed to detect any mtDNA, demonstrating severe mtDNA depletion in *pol* $\gamma$-$\beta$ mutants. The mechanism by which this depletion occurs is an important subject for further study, in comparison with other developmentally lethal mutants in the catalytic subunit gene, and in that for mitochondrial single-stranded DNA-binding protein.

We attempted to determine the level of Pol $\gamma$-$\beta$ protein in larvae by immunoblot analysis. Protein extracts were prepared from wild-type, heterozygous, and homozygous *pol* $\gamma$-$\beta$ mutant larvae at the end of the third instar stage and subjected to SDS/PAGE followed by immunoblot analysis with high-titer affinity-purified rabbit antiserum against native Pol $\gamma$ from *Drosophila* embryos and recombinant Pol $\gamma$-$\beta$ protein. Unfortunately, the relative abundance of endogenous Pol $\gamma$-$\beta$ is below

GENETICS

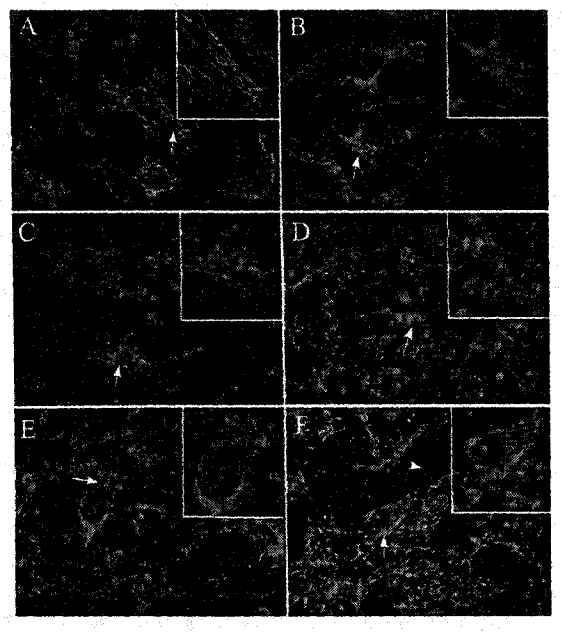


**Fig. 3.** Mitochondrial morphology and localization are altered in mutants of Pol γ. All panels depict photomicrographs of third instar larval brain hemispheres labeled with mitochondrial probe Mitotracker (red) and the nuclear stain DAPI (blue) photographed at the same magnification. The arrows point to the mitochondrial reticulum in all panels that are magnified in *Insets*. In wild-type cells, mitochondria are found in a reticulum tightly arranged in the periphery of the nucleus (arrow in *A*). Disruption of Pol γ function either by mutations in genes encoding the accessory subunit (*B*, *C*, and *D*) or the catalytic subunit (*E* and *F*) disrupt this reticulum similarly. Abnormal mitochondrial morphology is characterized by a vesicular staining pattern. (*A*) Wild-type CNS (*pol* γ-$\beta^1$/+). (*B*) *pol* γ-$\beta^1$ mutant CNS [*pol* γ-$\beta^1$/*Df(2L)b80c1*]. (*C*) Heteroallelic combination of two-accessory subunit mutant alleles (pol γ-$\beta^2$/*pol* γ-$\beta^1$). (*D*) *pol* γ-$\beta^2$ mutant CNS [*pol* γ-$\beta^2$/*Df(2L)b80c1*]. Catalytic subunit mutant CNS *tam*$^2$/*Df(2L)b80c1* (*E*) and *tam*$^9$/*Df(2L)b80c1* (*F*). The arrowhead indicates empty regions devoid of any staining.

the level of detection, even in an enhanced chemiluminescence analysis, so we were unable to show directly the level of the Pol γ-β protein in the *pol* γ-β mutants (data not shown). We do know, however, that recombinant proteins lacking the M and C region, such as what would be produced in the *pol* γ-$\beta^2$ mutant, fail to assemble into holoenzyme, and that the free Pol γ-β protein is largely insoluble (ref. 23 and unpublished data).

To analyze the consequences of mtDNA depletion on mitochondrial physiology and morphology, we labeled brains dissected from *pol* γ-β mutant larvae with the selective dye Mitotracker red concomitantly with the nuclear stain DAPI. The uptake and fluorescence of Mitotracker red depends upon the presence of a membrane potential and oxidative conditions within the mitochondria and, thus, can be used to assess mitochondrial integrity as well as morphology and abundance.

The organization of mitochondria in wild-type *Drosophila* neurons is similar to that described for live mammalian cells stained with the fluorescent dye JC-1 (28). Typically, mitochondria are found in a reticulum surrounding the nucleus (Fig. 3*A*). Reduction in *pol* γ-β gene function results in an overall disorganization of this reticular pattern. There is an expansion of areas showing no mitochondrial staining, together with the appearance of nuclei lacking a surrounding mitochondrial reticulum (Fig. 3 *B* and *C*). In a manner similar to that observed in mtDNA-depleted mammalian cells, the mitochondrial reticulum appears fragmented, as evidenced by the increased presence of vesicular profiles. These results also suggest, at least at this level of resolution, that mitochondrial number is not reduced drastically. Likewise, mutations that disrupt the function of the catalytic subunit of Pol γ (Pol γ-α) show a similar phenotype (Fig. 3 *E* and *F*).

**Table 1. Complementation analysis of accessor γ-subunit mutations**

| Subunit | *pol* γ-$\beta^1$ | *Df(2l)b80c1* | *tam*$^2$ |
|---|---|---|---|
| *pol* γ-$\beta^1$ | − (0/200) | − (0/147) | + (36/112) |
| *pol* γ-$\beta^2$ | − (0/183) | − (0/100) | + (43/120) |

Lethal mutations in the accessory subunit gene are complemented by a lethal mutation in the catalytic subunit gene of *Drosophila* Pol γ. Minus and plus signs indicate noncomplementation and complementation of lethality, respectively. Numerators indicate the number of viable adult flies that were heterozygous for the alleles of the *pol* γ-β (*pol* γ-$\beta^1$ and *pol* γ-$\beta^2$) and a deficiency chromosome (*Df(2L)b80cl*) or a mutation in the catalytic subunit gene (*tam* allele). Complete complementation is marked by heterozygous progeny constituting approximately 33% of the total.

**Mutations in the Accessory Subunit Gene Are Lethal to the Organism and Impair Cell Proliferation in the CNS.** Mutations in the *pol* γ-β gene are strict organismal lethals in transheterozygotes with a deficiency of the region and fail to complement each other (Table 1). In all cases, lethality occurs during the early pupal period. The *pol* γ-β mutants begin pupariation on average 2–3 days later than wild-type controls and die soon after. These results indicate that the two mutant alleles of the *pol* γ-β gene represent complete lack of gene function with regard to organismal lethality and suggest the presence of a maternal contribution sufficient for embryonic and larval development.

The two *pol* γ-β mutations complement completely null alleles of the *tamas* gene encoding the catalytic subunit (Table 1). Thus, a single copy of each of the genes encoding the two subunits of the Pol γ holoenzyme provides sufficient gene product for organismal viability. The external appearance of larvae lacking the accessory subunit of Pol γ is indistinguishable from wild type, whereas larvae mutant for the catalytic subunit gene are noticeably smaller (data not shown; ref. 12). Fig. 4 depicts a lateral view of brain hemispheres of these mutants seen under Nomarski optics. The CNS of larvae carrying mutations in the accessory subunit gene is smaller than that of wild-type controls but, in general, are not as small as that from catalytic-subunit gene mutants (compare Fig. 4 *B* to *C* and *F*; ref. 12). To assess cell proliferation, we labeled third instar larvae with BrdUrd. An overall reduction in BrdU incorporation in the CNS was observed in both mutant alleles of the *pol* γ-β gene (Fig. 4 *B*, *C*, and *D*). This finding is well illustrated by the aberrant BrdUrd labeling observed in the proliferation center of the optic lobes. Both the outer and inner proliferation centers appear to be equally affected. Mutations that disrupt the function of the catalytic subunit of Pol γ show a largely similar phenotype (Fig. 4 *E* and *F*).

**Larval Behavior Is Affected Moderately by Reduction in Accessory Subunit Function.** To evaluate the consequences of lack of accessory-subunit gene function for overall nervous system and muscle function, we measured larval locomotion in the absence of any light stimulus. The heteroallelic combination of the two alleles and the pol γ-$\beta^1$ allele heterozygous over a deficiency of the region, did not impair significantly larval locomotion; locomotion was affected only when the larvae carried the pol γ-$\beta^2$ allele over a deficiency of the region (Fig. 5). In contrast, null mutations in the catalytic-subunit gene reduced locomotion more severely and prevented the larval response to light (ref. 12 and data not shown).

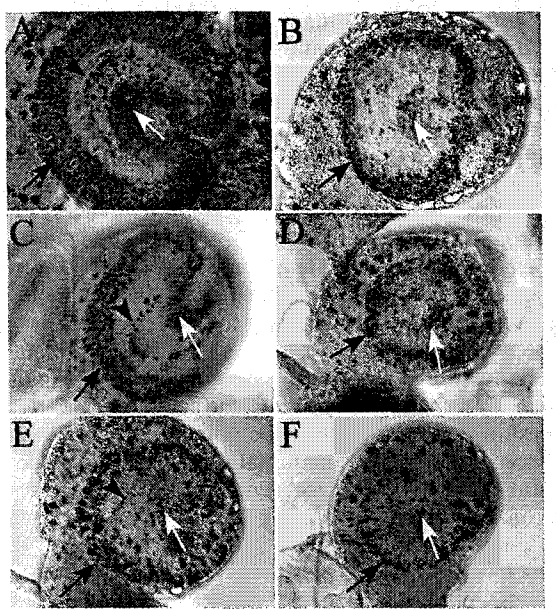


**Fig. 4.** DNA replication and cell proliferation are impaired in mutants of Pol γ. All panels depict photomicrographs of a lateral view of third instar larval brain hemispheres dissected from larvae that had incorporated BrdU to visualize mitotically active cells found in the developing adult optic lobes. All specimens were photographed at the same magnification. In all panels, the black arrow indicates the outer proliferation center, the arrowhead indicates the lamina precursor cells, and the white arrow indicates the inner proliferation center. Disruption of Pol γ function either by mutations in genes encoding the accessory subunit (*B*, *C*, and *D*) or the catalytic subunit (*E* and *F*) disrupts these proliferation centers to the same extent. (*A*) Wild-type CNS (*pol* $\gamma$-$\beta^1$/+). (*B*) *pol* $\gamma$-$\beta^1$ mutant CNS (*pol* $\gamma$-$\beta^1$/*Df(2L)b80c1*). (*C*) Heteroallelic combination of two accessory-subunit mutant alleles (*pol* $\gamma$-$\beta^2$/*pol* $\gamma$-$\beta^1$). (*D*) *pol* $\gamma$-$\beta^2$ mutant CNS (*pol* $\gamma$-$\beta^2$/*Df(2L)b80c1*). Catalytic-subunit mutant CNS. (*E*) *tam*$^2$/*Df(2L)b80c1*. (*F*) *tam*$^9$/*Df(2L)b80c1*.

## Discussion

Mutations that disrupt the function of the *pol* γ-β gene cause lethality in the early pupal stage. On the molecular and cellular levels, these mutations cause mtDNA depletion, aberrant mitochondrial morphology, and diminished cell proliferation in the CNS. We have not yet determined whether all tissues are affected equally. The quantitative Southern analysis was performed with DNA extracted from a total larval homogenate. Perdurance of mtDNA in the CNS, or in any other tissue that represents a small fraction of the total sample, would not likely have been detected. Moreover, different cell types have different energy requirements and, therefore, the maternal contribution of mitochondria, and/or of the *pol* γ-β transcript or polypeptide, will likely differ, as will their relative turnover rates. Thus, it will be of substantial interest to evaluate the temporal and spatial requirements for *pol* γ-β expression during zygotic development.

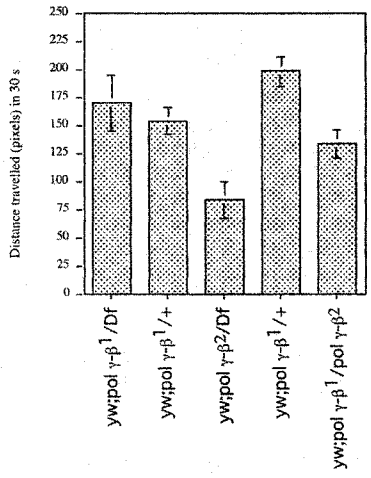


**Fig. 5.** Genetic analysis of larval locomotion. Mean distance traveled in 30 s on an agar surface under safelight conditions. The following statistical comparisons were made with Mann–Whitney *U* tests at a 95% confidence interval: *pol* $\gamma$-$\beta^1$/*Df(2L)b80c1* ($n$ = 14) vs. *pol* $\gamma$-$\beta^2$/*Df(2L)b80c1* ($n$ = 19), test statistic (W) = 315.0, $P$ = 0.0053; *pol* $\gamma$-$\beta^2$/+ ($n$ = 26) vs. *pol* $\gamma$-$\beta^2$/*Df(2L)b80c1* ($n$ = 19), test statistic (W) = 254.0, $P < 0.001$; *pol* $\gamma$-$\beta^2$/*Df(2L)b80c1* ($n$ = 19) vs. *pol* $\gamma$-$\beta^1$/*pol* $\gamma$-$\beta^2$ ($n$ = 14), test statistic (W) = 261.5, $P$ = 0.0263.

The two available *pol* γ-β mutations both map in its N-terminal region, an insertion that creates a premature stop codon and an amino acid substitution in a highly conserved glycine residue within the motif GPLGVEL in glycyl-tRNA synthetase and cause similar disruptions in *Drosophila* development. Both alleles, in combination with a chromosomal deficiency as well as the heteroallelic combination, cause organismal lethality at the same stage during metamorphosis. Such is also the case for nearly all other mutant phenotypes. It is reasonable to conclude that the truncated polypeptide resulting from the insertion in the N terminus will be largely or completely devoid of function and effectively represents a null mutation. That they exhibit similar phenotypes suggests that the *pol* $\gamma$-$\beta^1$ base-substitution allele also represents a nearly complete lack-of-function mutation. Thus, we demonstrate not only that the accessory subunit of Pol γ is essential *in vivo*, consistent with earlier biochemical studies, but also that Gly-31 is critical for its function in mtDNA synthesis.

The biochemical consequence of the G31E substitution in the accessory subunit has not yet been determined. *In vivo* reconstitution of recombinant forms of *Drosophila* Pol γ have demonstrated that much of the N-terminal region is not required for holoenzyme assembly, yet deletion mutants exhibit a substantial loss in DNA polymerase catalytic efficiency and reduced DNA binding (23). In contrast, large deletions in human Pol γ-β that include the conserved motif GPLGVEL lack activity and apparently do not associate with the catalytic subunit on template-primer DNA *in vitro* (19). A recent crystallographic study suggests that mouse Pol γ-β exists as a homodimer and that the M1 domain, as defined by sequence similarity with GlyRS and including the conserved GPLGVEL motif (19, 22), is part of the interface that participates in dimerization. Notably, the M1 domain as defined by sequence similarity outside the GPLGVEL motif is almost entirely absent in *Drosophila* Pol γ-β, highlighting important differences in the structure of two proteins that share highly similar biochemical properties. We anticipate that *Drosophila* will prove a valuable model to carry out *in vivo* structure–function analysis by means of genetic and phenotypic characterization of additional chemically induced mutations in the accessory subunit gene.

The accessory subunit of Pol γ was initially identified in *Drosophila* as a 35-kDa polypeptide of unknown function copurifying with the 125-kDa catalytic subunit (29, 30). Subsequent studies demonstrated that the accessory subunit contributes to both the catalytic efficiency and the structural integrity of *Drosophila* Pol γ (14, 17, 18, 21). Current data support a role for the accessory subunit as a processivity clamp and primer recognition factor (16, 18–23), supporting the expectation that it would be essential for animal mtDNA replication, and that lack-of-function mutations in either the catalytic or accessory-subunit genes would disrupt development and organismal homeostasis similarly. Surprisingly, mutations in the catalytic-subunit gene appear to have more drastic consequences for the organism than mutations in the accessory-subunit gene. *tamas* mutant larvae are considerably smaller, with a smaller CNS and

GENETICS

smaller, malformed imaginal discs than similarly aged larvae carrying mutations in the accessory-subunit gene. A similar disparity is found for the extent of the locomotory deficit. The difference in the stage of lethality may reflect a difference in the requirement for these gene products during development. *tamas* mutant larvae exhibit a significantly longer larval stage and die as third-instar foraging larvae while on the food substrate (12). These mutants rarely undergo pupariation or exhibit the behavioral and developmental changes that signal the end of larval stage and the beginning of pupal stage. In contrast, accessory-subunit mutants are able to wander and enter pupariation (2–3 days later than a wild type), dying soon after. This difference may be attributable to differences in cell growth and cell proliferation. In *Drosophila,* cells that will form the adult fly or imago, the so-called imaginal discs, are diploid and divide actively during the larval stages, whereas cells that form the larva never divide and are polytene (31, 32). Starvation or adverse nutritional conditions can delay larval development and the onset of pupariation, a phenocopy of mutations in the catalytic subunit gene (33). These starved larvae are, like the *tamas* mutant, noticeably reduced in size. Similarly, partial but not complete ablation of imaginal discs either using $\gamma$-irradiation or cell-lethal mutations delays the onset of pupariation (34, 35). These observations suggest that the developmental delay observed in larvae mutant for the catalytic-subunit gene may be caused largely by disruption of both cell growth and proliferation resulting from mitochondrial dysfunction. Recently, hypoxic conditions have been shown to induce cell-cycle arrest in *Drosophila* embryos, implicating a role for oxidative phosphorylation in driving cell proliferation (36).

Taken together, our observations suggest that accessory-subunit mutants sustain overall mitochondrial function sufficient for the larval transition into pupariation, whereas in catalytic-subunit mutants, mitochondrial function is disrupted such that transition into the pupal stage is prevented, presumably by the inability of the larva to reach the appropriate size and developmental stage. The observed differences between the phenotypes of the accessory and catalytic mutants may reflect a difference in the amount and/or the perdurance of the maternal contribution in tissues that are critical for the viability of the organism. Our observation that mtDNA is absent in the two mutant strains in the late third instar stage leaves open the possibility that mutations in the catalytic subunit gene actually cause mitochondrial dysfunction earlier than this point in development. Both differences in the relative maternal contribution and the developmental regulation of these genes (37) may account for an earlier onset of mitochondrial dysfunction.

We thank John Roote for pointing out the l (2)34De lethal complementation group as the most likely candidate for the gene encoding the accessory subunit of DNA polymerase $\gamma$ and the Bloomington Stock Center at Indiana University for the fly stocks. A.R.C. is indebted to Dr. R. A. Morton and Dr. G. Singh for comments on the manuscript. This work was supported by Grant MT12700 from Canadian Institutes of Health Research (to A.R.C.) and National Institutes of Health Grants GM45295 and HL59656 (to L.S.K.).

1. Garesse, R. & Vallejo, C. G. (2001) *Gene* **263,** 1–16.
2. Ruiz De Mena, I., Lefai, E., Garesse, R. & Kaguni, L. S. (2000) *J. Biol. Chem.* **275,** 13628–13636.
3. Takata, K., Yoshida, H., Hirose, F., Yamaguchi, M., Kai, M., Oshige, M., Sakimoto, I., Koiwai, O. & Sakaguchi, K. (2001) *Biochem. Biophys. Res. Commun.* **287,** 474–483.
4. Lefai, E., Fernandez-Moreno, M. A., Kaguni, L. S. & Garesse, R. (2000) *Insect Mol. Biol.* **9,** 315–322.
5. Hirose, F., Yamaguchi, M., Kuroda, K., Omori, A., Hachiya, T., Ikeda, M., Nishimoto, Y. & Matsukage, A. (1996) *J. Biol. Chem.* **271,** 3930–3937.
6. Yamaguchi, M., Hayashi, Y., Nishimoto, Y., Hirose, F. & Matsukage, A. (1995) *J. Biol. Chem.* **270,** 15808–15814.
7. Ferri, K. F. & Kroemer, G. (2001) *BioEssays* **23,** 111–115.
8. Goto, Y. (2000) *Neuropathology* **20,** Suppl., S82–S84.
9. Jaarsma, D., Haasdijk, E. D., Grashorn, J. A., Hawkins, R., van Duijn, W., Verspaget, H. W., London, J. & Holstege, J. C. (2000) *Neurobiol. Dis.* **7,** 623–643.
10. Berman, S. B. & Hastings, T. G. (1999) *J. Neurochem.* **73,** 1127–1137.
11. Van Goethem, G., Dermaut, B., Lofgren, A., Martin, J. J. & Van Broeckhoven, C. (2001) *Nat. Genet.* **28,** 211–212.
12. Iyengar, B., Roote, J. & Campos, A. R. (1999) *Genetics* **153,** 1809–1824.
13. Maier, D., Farr, C. L., Poeck, B., Alahari, A., Vogel, M., Fischer, S., Kaguni, L. S. & Schneuwly, S. (2001) *Mol. Biol. Cell* **12,** 821–830.
14. Lewis, D. L., Farr, C. L., Wang, Y., Lagina, A. T., 3rd, & Kaguni, L. S. (1996) *J. Biol. Chem.* **271,** 23389–23394.
15. Wang, Y., Farr, C. L. & Kaguni, L. S. (1997) *J. Biol. Chem.* **272,** 13640–13646.
16. Carrodeguas, J. A., Kobayashi, R., Lim, S. E., Copeland, W. C. & Bogenhagen, D. F. (1999) *Mol. Cell. Biol.* **19,** 4039–4046.
17. Wang, Y. & Kaguni, L. S. (1999) *J. Biol. Chem.* **274,** 28972–28977.
18. Lim, S. E., Longley, M. J. & Copeland, W. C. (1999) *J. Biol. Chem.* **274,** 38197–38203.
19. Carrodeguas, J. A. & Bogenhagen, D. F. (2000) *Nucleic Acids Res.* **28,** 1237–1244.
20. Johnson, A. A., Tsai, Y., Graves, S. W. & Johnson, K. A. (2000) *Biochemistry* **39,** 1702–1708.
21. Fan, L., Sanschagrin, P. C., Kaguni, L. S. & Kuhn, L. A. (1999) *Proc. Natl. Acad. Sci. USA* **96,** 9527–9532.
22. Carrodeguas, J. A., Theis, K., Bogenhagen, D. F. & Kisker, C. (2001) *Mol. Cell.* **7,** 43–54.
23. Fan, L. & Kaguni, L. S. (2001) *Biochemistry* **40,** 4780–4791.
24. Woodruff, R. C. & Ashburner, M. (1979) *Genetics* **92,** 133–149.
25. Adams, M. D., Celniker, S. E., Holt, R. A., Evans, C. A., Gocayne, J. D., Amanatides, P. G., Scherer, S. E., Li, P. W., Hoskins, R. A., Galle, R. F. *et al.* (2000) *Science* **287,** 2185–2195.
26. Winberg, M. L., Perez, S. E. & Steller H. (1992) *Development (Cambridge, U.K.)* **115,** 903–911.
27. Thompson, J. D., Gibson, T. J., Plewniak, F., Jeanmougin, F. & Higgins, D. G. (1997) *Nucleic Acids Res.* **25,** 4876–4882.
28. Gilkerson, R. W., Margineantu, D. H., Capaldi, R. A. & Selker, J. M. (2000) *FEBS Lett.* **474,** 1–4.
29. Wernette, C. M. & Kaguni, L. S. (1986) *J. Biol. Chem.* **261,** 14764–14770.
30. Olson, M. W., Wang, Y., Elder, R. H. & Kaguni, L. S. (1995) *J. Biol. Chem.* **270,** 28932–28937.
31. Madhavan, M. M. & Schneiderman, H. A. (1977) *Roux's Arch. Dev. Biol.* **183,** 269–305.
32. Smith, A. V. & Orr-Weaver, T. L. (1991) *Development (Cambridge, U.K.)* **112,** 997–1008.
33. Mensua, J. L. & Moya, A. (1983) *Heredity* **51,** 347–352.
34. Simpson, P., Berreur, P. & Berreur-Bonnenfant, J. (1980) *J. Embryol. Exp. Morphol.* **57,** 155–165.
35. Poodry, C. A. & Woods, D. F. (1990) *Roux's Arch. Dev. Biol.* **199,** 219–227.
36. DiGregorio, P. J., Ubersax, J. A. & O'Farrell, P. H. (2001) *J. Biol. Chem.* **276,** 1930–1937.
37. Lefai, E., Fernandez-Moreno, M. A., Alahari, A., Kaguni, L. S. & Garesse, R. (2000) *J. Biol. Chem.* **275,** 33123–33133.

## Appendix F. Sang's medium ingredients

| Ingredients | Amont (mg) |
|---|---|
| Agar | 3000 |
| Casein | 5500 |
| Fructose | 750 |
| Cholesterol | 30 |
| Lecithin | 400 |
| Yeast nucleic acid | 400 |
| Thiamin HCl | 0.2 |
| Riboflavin | 1.0 |
| Nicotinic acid | 1.2 |
| Ca pantothenate | 1.6 |
| Pyridoxine HCl | 0.25 |
| Biotin | 0.016 |
| Folic acid | 0.3 |
| NaHCO3 | 140 |
| KH2PO4 | 183 |
| Na2HPO4 | 189 |
| Carolina biological mold inhibitor | 320 |

(Methods in developmental biology ed. F.H. Wilt, N. K. Wessels, NY: Thomas Y. Crowell Co. 1967, p. 234).

## G: Plate assay setup

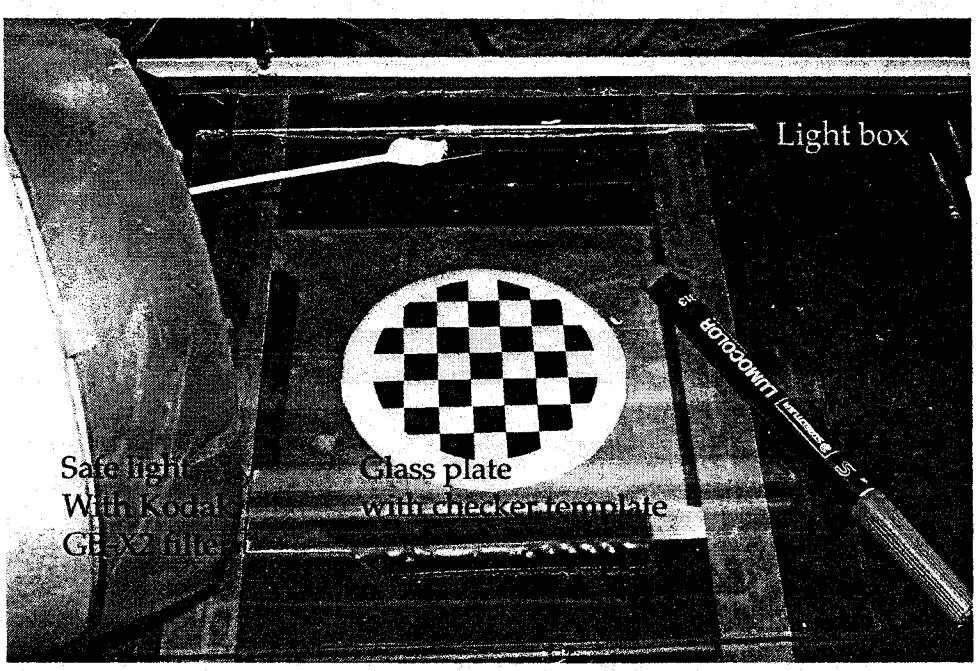
Light box
LUMOCOLOR
Safe light
With Kodak
GB-X2 filter
Glass plate
with checker template

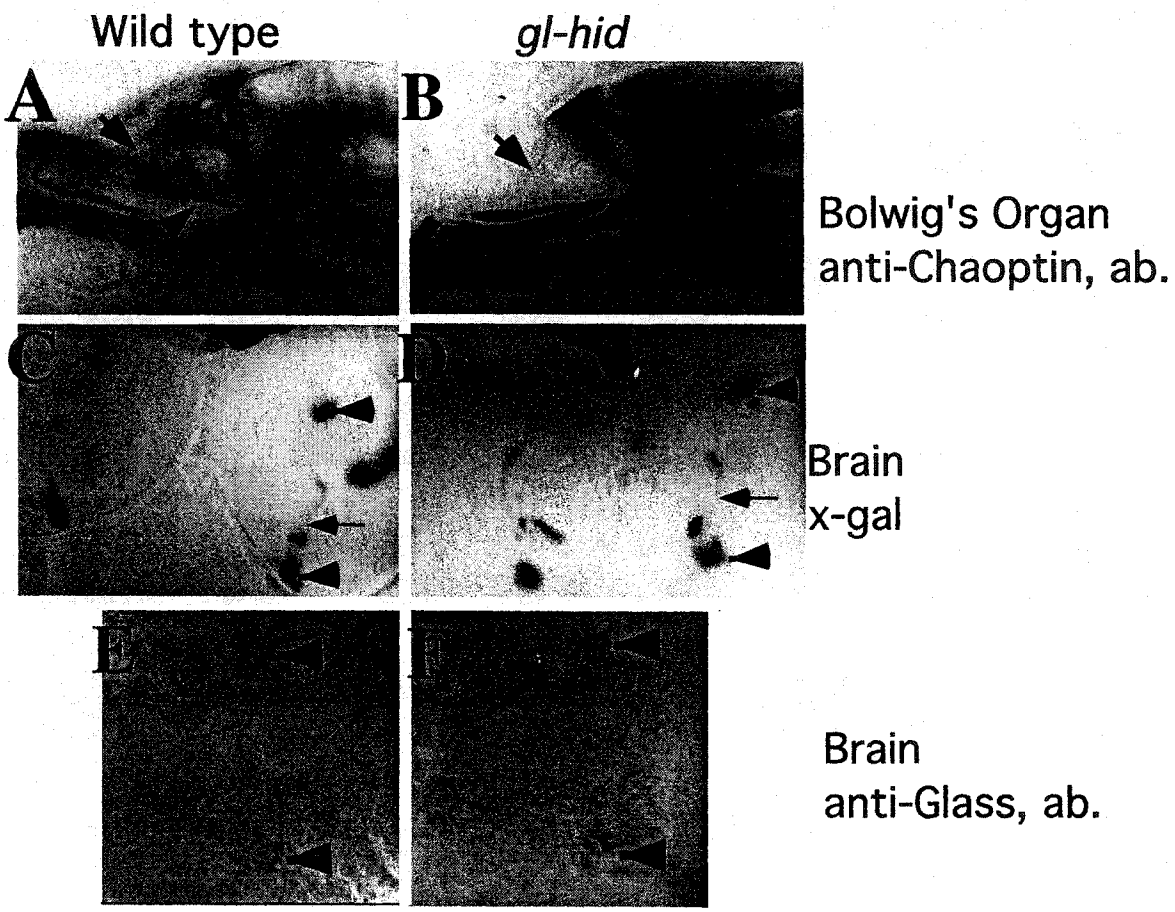
Wild type
gl-hid
A
B
C
D
E
F
Bolwig's Organ
anti-Chaoptin, ab.
Brain
x-gal
Brain
anti-Glass, ab.

## H: *gl-hid* mediated ablation of Bolwig's Organ

# I: Rh5 and Rh6 promoter driven Lac-Z expression in Bolwig's Organ

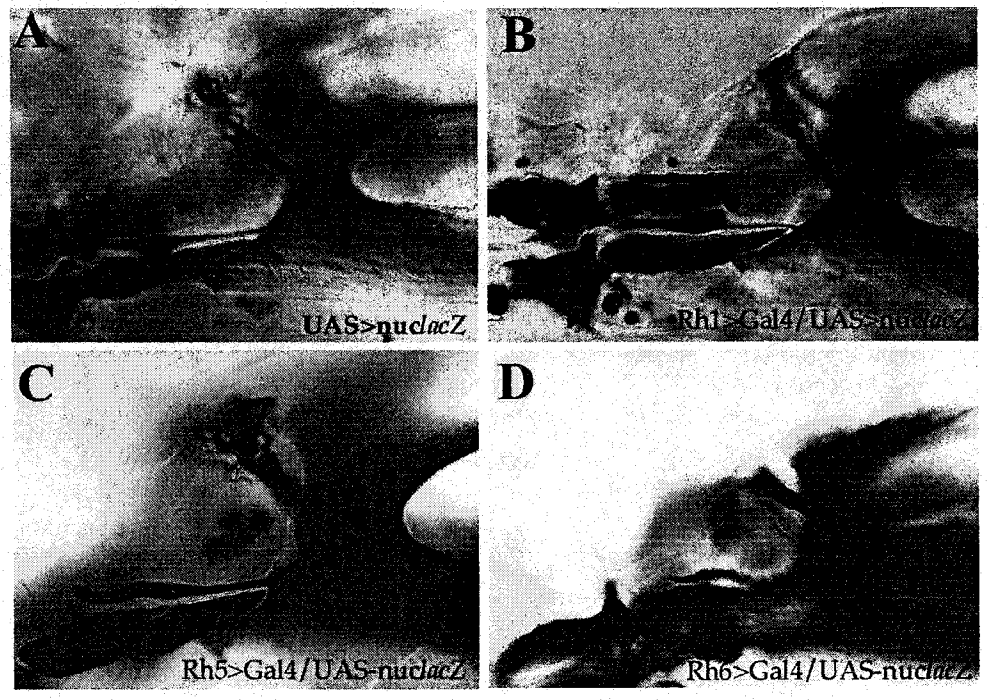
A
UAS>nuclacZ
B
Rh1>Gal4/UAS-nuclacZ
C
Rh5>Gal4/UAS-nuclacZ
D
Rh6>Gal4/UAS-nuclacZ

# J: NIH-Image macro programme

## NIH image macro for tracking larva during On/Off assay:

```
macro 'Light/Dark[F1]';
var
x1,y1,x2,y2,height,width,dist,tdist,ndist,rdist,adRI,odist
,time1,time2,time,time3,interval,startvalue,ldist,ddist,
idist,i, pulses,mind:integer;
ri:real;

begin
    OpenSerial('9600 baud, no parity, eight data, one
stop');
    NewTextWindow('Dist/10s',150,480);
    MoveWindow(730,40);
    writeln('<tDist>,<rDist>,<Pulse>');
    GetPicSize(width,height);
    SetUser1Label('<sec>');
    SetUser2Label('<pix>');
    setOptions('X-Y Center  User1 User2');
    resetCounter;
    getmouse(x1,y1);
    y1:=height-y1;
    resetCounter;
    interval:=600;
    time1:=TickCount;
    time3:=TickCount;
    startvalue:=0;
    SetCursor('cross');
    ndist:=0;
    rdist:=0;
    ddist:=0;
    ldist:=0;
    mind:=5;

    Begin
       repeat
          if TickCount>=time3 then

             Begin
            rdist:=tdist-ndist;
            writeln(tdist:9:0 ','  rdist:9:0 ','  i:9:0 );
            ndist:=tdist;
            time3:=time3+interval;

            if odd(i) then
            begin
               ldist:=rdist+ldist;
                        PutSerial('"MIOAG100"');
```

```
        end else
        begin
           ddist:=rdist+ddist;
           PutSerial('"MIOAG11:"');
        end;
beep;
i:=i+1;

end else

   GetPicSize(width,height);
   GetMouse(x2,y2);
   y2:=height-y2;
   dist:=sqrt(sqr(x2-x1)+sqr(y2-y1));

   if dist>mind then
      begin
        time2:=TickCount;
        time:=time2-time1;
        tdist:=dist+tdist;
        SetCounter(rCount+1);
        rX[rCount]:=x2;
        rY[rCount]:=y2;
        rUser1[rCount]:=time 60;
        rUser2[rCount]:=tdist;
        x1:=x2;
        y1:=y2;
      end;

until button;

Pulses:=i-1;

if odd(pulses) then
            begin
               odist:=ldist-rdist;
               adRI:=(ddist-odist)/(ddist+odist);
               writeln('');
               writeln('adL-dis,  D-dis');
               writeln(ldist-rdist:8:0,  ddist:9:0);
               writeln('');
               writeln( 'Observe odd # of pulses');
               writeln('Adjusted R.I');
               writeln('');
               writeln('adR.I, Pulses');
                           writeln(adRI:6:3,
      pulses:6:0);
                           writeln('');
```

```
                    end else

                    begin
                      ri:=(ddist-ldist)/(ddist+ldist);
                      writeln('');
                      writeln('     D-dis,  L-dis');
                      writeln(ddist:9:0, ldist:9:0);
                      writeln('');
                      writeln('     R.I,     Pulses');
                      writeln(ri:9:3,  pulses:6:0);
                      writeln('');

                    end;

        PutSerial('"MIOAG100"');

        showResults;
                end;
end;
```

**K: Recombination crossing scheme for *tamas***

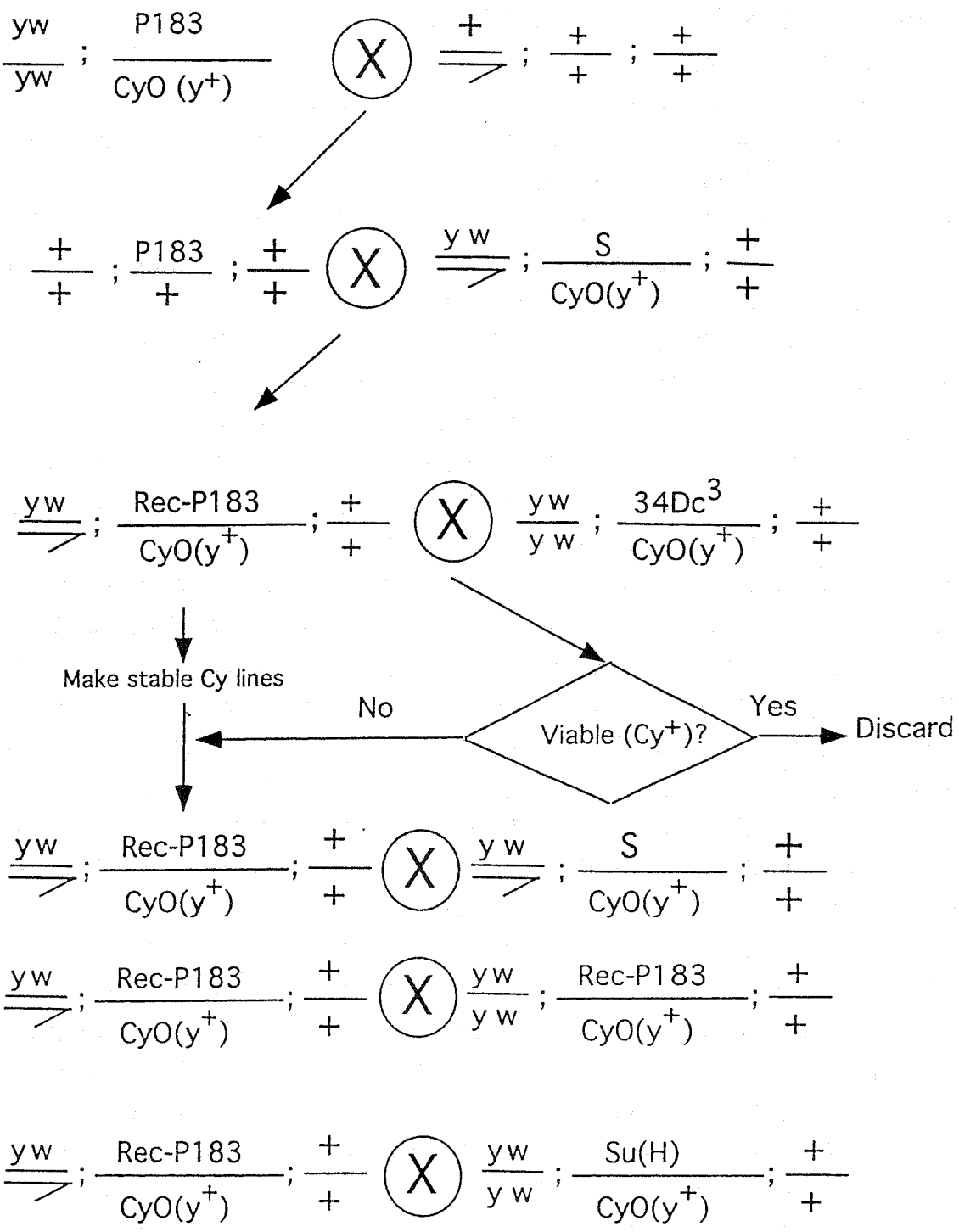

## L: *Twinkle* homologue in *Drosophila*

### Human TWINKLE Protein sequence:

MWVLLRSGYPLRILLPLRGEWMGRRGLPRNLAPGPPRRRYRKET
LQALDMPVLPVTATEIRQYLRGHGIPFQDGHSCLRALSPFAESSQLKGQTGVTTSFSL
FIDKTTGHFLCMTSLAEGSWEDFQASVEGRGDGAREGFLLSKAPEFEDSEEVRRIWNR
AIPLWELPDQEEVQLADTMFGLTKVTDDTLKRFSVRYLRPARSLVFPWFSPGGSGLRG
LKLLEAKCQGDGVSYEETTIPRPSAYHNLFGLPLISRRDAEVVLTSRELDSLALNQST
GLPTLTLPRGTTCLPPALLPYLEQFRRIVFWLGDDLRSWEAAKLFARKLNPKRCFLVR
PGDQQPRPLEALNGGFNLSRILRTALPAWHKSIVSFRQLREEVLGELSNVEQAAGLRW
SRFPDLNRILKGHRKGELTVFTGPTGSGKTTFISEYALDLCSQGVNTLWGSFEISNVR
LARVMLTQFAEGRLEDQLDKYDHWADRFEDLPLYFMTFHGQQSIRTVIDTMQHAVYVY
DICHVIIDNLQFMMGHEQLSTDRIAAQDYIIGVFRKFATDNNCHVTLVIHPRKEDDDK
ELQTASIFGSAKVSG

### A Drosophila Homologue?

BLAST Result using BDGP sequences:
>CG5924 | FBgn0032154 | pp-CT18608 | FBan0005924 GO:[] mol_weight=70069 located on:
2L 30E2-30E3; Length = 613

Score = 870 (311.3 bits), Expect = 1.7e-95, Sum P(2) = 1.7e-95
Identities = 160/287 (55%), Positives = 209/287 (72%)

```
Query:   295 LPYLEQFRRIVFWLGDDL-RSWEAAKLFARKLNPKRCFLVRPGDQQPRPLEALNGGFNLS 353
             LP LE+F+ ++FWL  D   SW+AA+ FA KL+ +RC L+RP + +P P  AL    NL
Sbjct:   261 LPALERFKELIFWLHYDASHSWDAARAFALKLDERRCLLIRPTETEPAPHLALRRRLNLR 320

Query:   354 RILRTALPAWHKSIVSFRQLREEVLGELSNVEQAAGLRWSRFPDLNRILKGHRKGELTVF 413
              IL  A P  HK+I +F  +R ++L EL N+E+  G++W RFP LN++LKGHR+GELT+
Sbjct:   321 HILAKATPVQHKAITTFGAMRNDILSELQNIEKVNGVKWKRFPVLNKLLKGHRRGELTIL 380

Query:   414 TGPTGSGKTTFISEYALDLCSQGVNTLWGSFEISNVRLARVMLTQFAEGRLEDQLDKYDH 473
             TGPTGSGKTTF+SEY+LDL  QGVNTLWGSFEI N RLA  +L Q+    L+D+L +++H
Sbjct:   381 TGPTGSGKTTFMSEYSLDLAMQGVNTLWGSFEIRNTRLAATLLRQYVGYPLDDRLHEFNH 440

Query:   474 WADRFEDLPLYFMTFHGQQSIRTVIDTMQHAVYVYDICHVIIDNLQFMMGHEQLSTDRIA 533
             WA  FE LPLYFMTFHGQQ ++ V++ ++HA YV+D+ HVIIDNLQFMMG      D+
Sbjct:   441 WAAEFERLPLYFMTFHGQQPLKPVLEAIEHASYVHDVMHVIIDNLQFMMGVSTFRGDKFF 500

Query:   534 AQDYIIGVFRKFATDNNCHVTLVIHPRKEDDDKELQTASIFGSAKVS 580
              QD II  FR FAT +N HVTLV+HPRKE  + EL T+S+FG+AK +
Sbjct:   501 EQDSIIAAFRSFATKHNVHVTLVMHPRKERQEDELTTSSVFGTAKAT 547

 Score = 86 (35.3 bits), Expect = 1.7e-95, Sum P(2) = 1.7e-95
 Identities = 20/81 (24%), Positives = 38/81 (46%)

Query:    37 RRRYRKETLQALDMPVL-PVTATEIRQYLRGHGIPFQDGHSCLRALSPFAESSQ---LKG 92
             R+ Y  + +  L+   L P    + ++ LR   +P +DGH+CL+       + ++
Sbjct:    22 RKNYATQVVSGLEECSLDPKEYVDFKRQLRQLNLPHKDGHTCLQLECRLCDRNRQPVTNA 81

Query:    93 QTGVTTSFSLFIDKTTGHFLC 113
             Q G       +++K TG F+C
```

## M: Rescue crosses to demonstrate rescue of lethality in *pol γ-β¹* allele

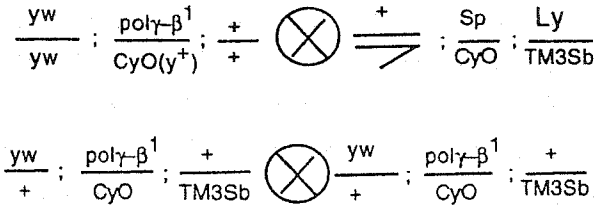

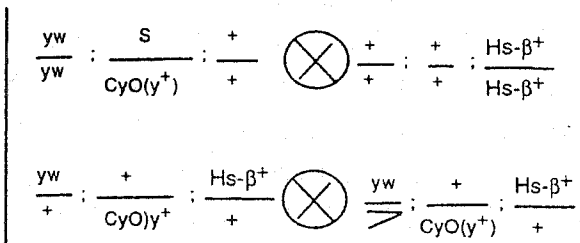

NB: Hs-β$^+$ also contains a white$^+$ gene in the construct

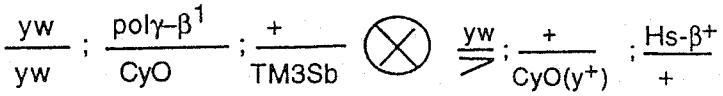

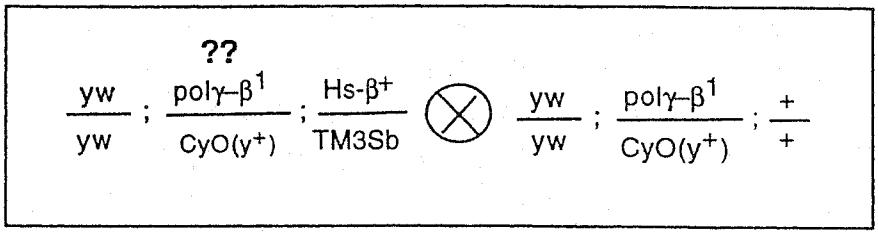

>>Screening for non-complementation. All Cy+ should be w$^+$ if the rescue element can already rescue homozygous pol γ-β$^1$ allele

>>Obtained one stock that already appeared to rescue homozygous pol γ-β$^1$

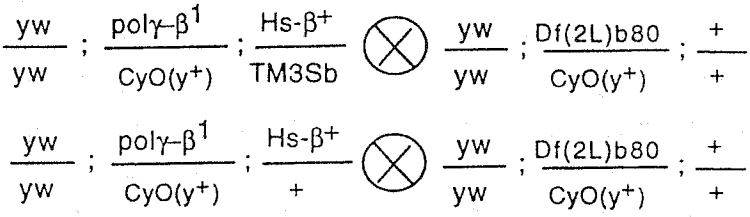

49-Cy$^-$, w$^+$, pol γ-β$^1$

31-Cy$^+$, w$^+$, pol γ-β$^1$/ Df(2L)b80

35-Cy$^-$, w$^-$, (15-Df's, 20-pol γ-β$^1$)

NB: Df(2L)b80c1 chromosome has a dominant bristle marker